HEI HEALTH EFFECTS INSTITUTE

Consequences of Prolonged Inhalation of Ozone on F344/N Rats: Collaborative Studies

Part VIII: Morphometric Analysis of Structural Alterations in Alveolar Regions

Ling-Yi Chang, Barbara L. Stockstill, Margaret G. Ménache, Robert R. Mercer, and James D. Crapo
Duke University Medical Center, Durham, NC

Part IX: Changes in the Tracheobronchial Epithelium, Pulmonary Acinus, and Lung Antioxidant Enzyme Activity

Kent E. Pinkerton, Margaret G. Ménache, and Charles G. Plopper
Department of Anatomy, Physiology, and Cell Biology, School of Veterinary Medicine, and California Regional Primate Research Center, University of California, Davis, CA, Duke University Medical Center, Durham, NC

Includes the Commentary of the Institute's Health Review Committee

Research Report Number 65
March 1995

HEI HEALTH EFFECTS INSTITUTE

The Health Effects Institute, established in 1980, is an independent and unbiased source of information on the health effects of motor vehicle emissions. HEI studies all major pollutants, including regulated pollutants (such as carbon monoxide, ozone, nitrogen dioxide, and particulate materials) and unregulated pollutants (such as diesel engine exhaust, methanol, and aldehydes). To date, HEI has supported more than 120 projects at institutions in North America and Europe.

Typically, HEI receives half its funds from the U.S. Environmental Protection Agency and half from 28 manufacturers and marketers of motor vehicles and engines iu the United States. Occasionally, revenues from other public or private organizations either support special projects or provide resources for a portion of an HEI study. For this study, the Institute acknowledges the cooperation and support of the National Toxicology Program (NTP), whicb consists of four charter agencies of the U.S. Department of Health and Human Services. The NTP sponsored the inhalation component of this project as part of its studies on the toxicologic and carcinogenic effects of ozone. However, in all cases HEI exercises complete autonomy in setting its research priorities and in disbursing its funds. An independent Board of Directors governs the Iustitute. The Research Committee and the Review Committee serve complementary scientific purposes and draw distinguished scientists as members. The results of HEI-funded studies are made available as Research Reports, which contain both the Investigators' Report and the Review Committee's evaluation of the work's scientific and regulatory relevance.

HEI Statement

Synopsis of Research Report Number 65 Parts VIII and IX

Studies of Changes in Lung Structure and Enzyme Activities in Rats After Prolonged Exposure to Ozone

BACKGROUND

Ozone is a major pollutant in smog. It is formed by complex photochemical reactions between nitrogen oxides and volatile organic compounds in the presence of sunlight. Motor vehicle and industrial emissions are prominent sources of these compounds. Peak atmospheric ozone concentrations generally occur during the summer months because the photochemical reactions that produce ozone are enhanced by sunlight and high temperature. The standard currently set by the U.S. Environmental Protection Agency for ozone exposure is 0.12 parts per million (ppm), a level that is not to be exceeded for more than one hour once a year.

Exposure to ozone as part of photochemical smog is known to have acute health effects in humans. There is also concern that prolonged exposure may lead to chronic lung damage. The National Toxicology Program (NTP) conducted a series of tests to evaluate ozone's carcinogenicity in rats and mice after prolonged exposure to this pollutant. The NTP study presented a unique opportunity to study ozone's noncancerous effects as well; therefore, the NTP and the HEI entered into a collaboration. The studies discussed in this Commentary, which were two of eight studies and a biostatistical analysis in the NTP/HEI Collaborative Ozone Project, were conducted to determine whether prolonged inhalation of ozone produces lasting effects on lung structure, potentially contributing to or aggravating chronic lung disease.

APPROACH

Healthy male and female F344/N rats were exposed to either 0.12, 0.5, or 1.0 ppm ozone for six hours/day, five days/week, for 20 months; control animals breathed filtered air. In two independent studies, Drs. Chang and Pinkerton and their colleagues investigated the effects of this prolonged ozone exposure on respiratory tract structure. They used light and electron microscopy to measure site-specific changes in cell and tissue characteristics. The Pinkerton group also studied the activity levels of antioxidant enzymes, which protect tissues against the potentially harmful effects of oxidants such as ozone. The investigators' goals were to characterize the nature and magnitude of the alterations in the tissue and cellular structure in the respiratory tract and the changes in enzyme activities.

RESULTS AND IMPLICATIONS

The investigators focused most of their analyses on the regions of the lung that are known to be targets for damage induced by ozone. Dr. Chang and colleagues found that in rats exposed to 0.5 or 1.0 ppm ozone, cellular reorganization occurred in the smallest airways of the lungs, known as bronchioles and alveolar ducts, when compared with control animals. All changes observed were localized to the centriacinar region, which is the anatomical site that is the junction of the conducting airways and the gas-exchange region of the lung. In a process known as bronchiolarization, the thinner cells normally lining these regions were replaced by thicker cells that are more characteristic of the small bronchioles. Thickening of the interstitium, which is the supporting tissue for cells, also was seen in the alveolar ducts of rats exposed to 0.5 or 1.0 ppm ozone. These changes were specific to the centriacinar region and were not seen in randomly chosen sections from other regions of the lung. In this study, no structural effects were observed in rats exposed to 0.12 ppm ozone.

Dr. Pinkerton and colleagues did not find any cellular reorganization in the trachea and bronchi (the larger airways of the lung), but did report some changes in the amount of mucus and an increase in the activities of antioxidant enzymes. In agreement with Dr. Chang's findings, Dr. Pinkerton and colleagues observed cellular reorganization and bronchiolarization in the centriacinar region of the lungs of rats exposed to 0.5 or 1.0 ppm ozone. Dr. Pinkerton also reported increases in some indices of bronchiolarization at the exposure level of 0.12 ppm ozone. However, these latter results may not be statistically significant. Also, both the cellular reorganization and the bronchiolarization varied by region, depended on gender, and have weak statistical support. Thus, the question of whether prolonged exposure to 0.12 ppm ozone affects the structure of rat lungs requires further study.

Overall, the results of these studies confirm earlier reports that cellular reorganization occurs in specific regions of the small airways of rats exposed to concentrations of ozone equal to or greater than 0.5 ppm. The cellular reorganization observed in these two studies was confined to the centriacinar region of the lungs and consisted of cells that are sensitive to ozone being replaced by types of cells that are more resistant. The protective response of the lung is also illustrated by the fact that antioxidant enzyme activities increased in response to ozone exposure in these small airways. There were no signs of airway inflammation in rats exposed to ozone in either study. Because the structural changes observed in these studies, even at the highest ozone exposure concentrations, were relatively mild and did not cause changes in lung function, the implications of these studies for human health must be evaluated with caution.

This Statement, prepared by the Health Effects Institute and approved by its Board of Directors, is a summary of two research studies sponsored by HEI from 1991 to 1994. The inhalation component of this Project was supported by the National Toxicology Program as part of its studies on the toxicologic and carcinogenic effects of ozone. Dr. Ling-Yi Chang and colleagues of Duke University Medical Center in Durham, NC, conducted the first study, Morphometric Analysis of Structural Alterations in Alveolar Regions; and Dr. Kent E. Pinkerton and associates of the University of California at Davis, CA, conducted the second study, Changes in the Tracheobronchial Epithelium, Pulmonary Acinus, and Lung Antioxidant Enzyme Activity. The following Research Report contains an Introduction to the NTP/HEI Collaborative Ozone Project, the two Investigators' Reports, and a Commentary on both studies prepared by the Institute's Health Review Committee.

Library of Congress Catalog Number for the HEI Research Report Series: WA 754 R432.

The paper in this HEI Research Report (Number 65 Parts VIII and IX), and in Reports 1 through 20, 25, 26, 32, 51, and 65 Part IV is acid-free coated paper. The paper in all other publications in this series meets the minimum standard requirements of the ANSI Standard Z39.48-1984 (Permanence of Paper).

TABLE OF CONTENTS

Research Report Number 65

Consequences of Prolonged Inhalation of Ozone on F344/N Rats: Collaborative Studies

(continued on next page)

INTRODUCTION

The National Toxicology Program and Health Effects Institute Collaborative Ozone Project

The NTP/HEI Collaborative Ozone Project was a four-year project that was organized to evaluate the effects of prolonged ozone exposure on lung injury in animals. The ozone exposures were conducted by the National Toxicology Program (NTP) at Battelle Pacific Northwest Laboratories. Eight groups of investigators addressed the pathologic and physiologic consequences of prolonged ozone exposure, supported by the Health Effects Institute (HEI). A full description of the NTP/HEI Collaborative Ozone Project and the exposure protocol can be found in the Introduction and Supplement to Research Report Number 65 Part I. This information also will be published in Part VI of Research Report Number 65.

Briefly, in 1987, the Health Effects Institute entered into a partnership with the National Toxicology Program to evaluate the effects of chronic ozone exposure in rats. The NTP, consisting of four agencies of the U.S. Department of Health and Human Services, coordinates the nation's testing of potentially toxic and hazardous chemicals. The Health Effects Institute, an independent research organization supported by both government and industry, provides unbiased information on the health effects of motor vehicle emissions.

Because of the widespread exposure to ozone and concerns about its potential health effects, HEI and the California Department of Health and Human Services nominated ozone for carcinogenicity and toxicity testing by the NTP. The NTP, recognizing that cancer was only one of the chronic diseases of concern, included additional animals for HEI-supported studies of the pathologic and physiologic consequences of prolonged ozone exposures. The HEI animals were housed in cages that would otherwise have been empty. By developing a partnership, the HEI and NTP were able to leverage their funds to develop a comprehensive research program that extended beyond carcinogenicity endpoints; the HEI-sponsored research focused on the relation between long-term ozone exposure and the pathogenesis of chronic lung diseases, such as asthma, emphysema, and fibrosis. The Health Effects Institute would not have been able to undertake such an expensive project, which requires special facilities and trained personnel, without the NTP's support of the inhalation component and the cooperation of the NTP's contractor, Battelle Pacific Northwest Laboratories.

For the HEI component of the Project, eight studies were selected for funding from proposals submitted in response to the Request for Applications (RFA) 90-1, Health Effects of Chronic Ozone Inhalation: Collaborative National Toxicology Program–Health Effects Institute Studies, Part A: Respiratory Function Studies, and Part B: Structural, Biochemical, and Other Alterations. Because of the complexity of a project with many investigators and many endpoints, the HEI Health Research Committee also funded a Biostatistical Advisory Group to provide assistance with experimental design, animal allocation, and data analyses. Figure 1 presents a diagram of the studies in the NTP/HEI Collaborative Ozone Project and their relations to each other. They include those studies that were part of the NTP bioassay, the eight HEI-funded studies, and the biostatistical study. In addition, HEI engaged Battelle Pacific Northwest Laboratories to provide support services for the HEI-sponsored investigators.

Starting at six to seven weeks of age, male and female F344/N rats were exposed to 0, 0.12, 0.5, or 1.0 parts per million (ppm) ozone, six hours per day, five days per week. These concentrations were selected to include the maximum concentration the animals would tolerate (1.0 ppm), the current National Ambient Air Quality Standard (NAAQS) for ozone (0.12 ppm), and an intermediate concentration. The NTP's carcinogenicity bioassay consisted of a two-year study and a lifetime study in rats and mice, and a study of male rats exposed to 0.5 ppm ozone and two levels of a human pulmonary carcinogen, 4-(*N*-methyl-*N*-nitrosamino)-1-(3-pyridyl)-1-butanone (NNK). The design of the HEI studies was directed, to some extent, by the constraints of the NTP protocol. These included ozone exposure concentrations that were set by the NTP, a limit on the sample size (164 rats) to the number of available exposure chambers, and quarantine restrictions that did not allow reentry of animals into the exposure chambers once they had been removed, thus eliminating the possibility of conducting serial tests.

The Biostatistical Advisory Group developed a sample allocation scheme that allowed several researchers to obtain measurements on tissue samples from the same subset of study animals, providing the maximum overlap of animals and tissues among the eight studies while ensuring balance with respect to dose, gender, and time of death. When the ozone exposure of the HEI animals ended (at 20 months), several investigators traveled to Battelle Pacific

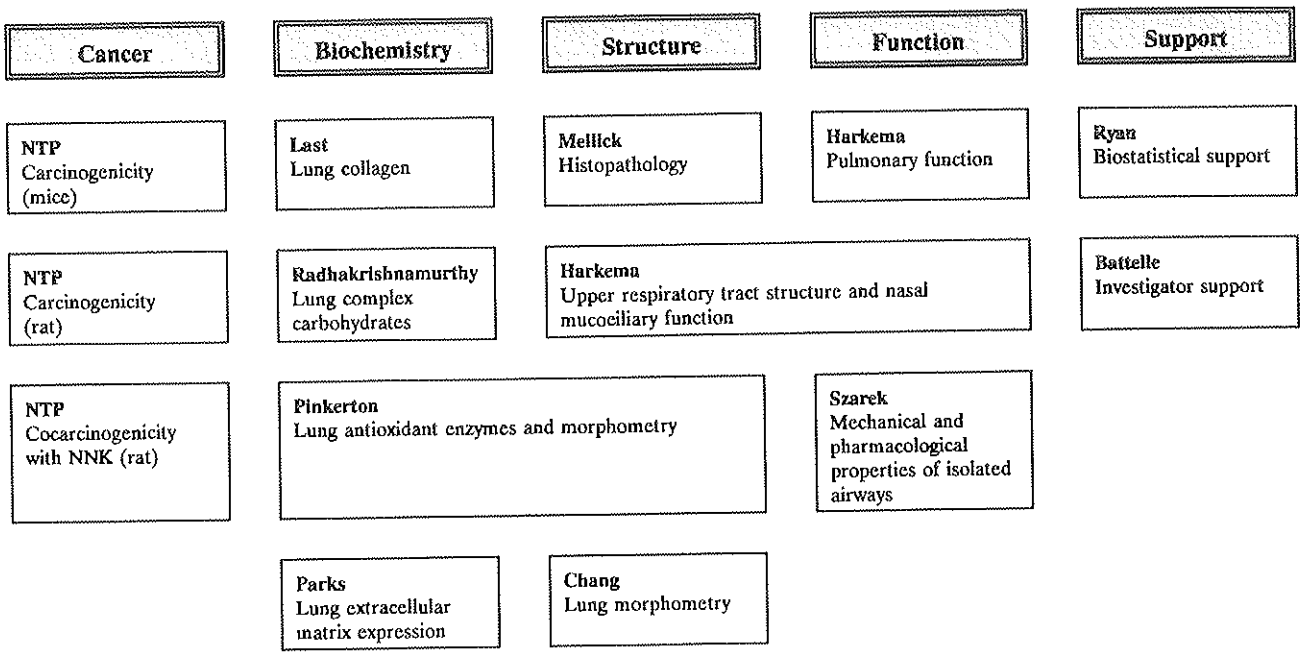

Figure 1. The NTP/HEI Collaborative Ozone Project: individual studies.

Northwest Laboratories to conduct their assays or to obtain samples on site. Battelle personnel prepared the tissues for off-site investigators and shipped them directly to their laboratories.

Because the studies varied in duration from six months to two years, HEI is publishing the reports for each individual study after the Institute's review process for each study is complete. Each Investigator's Report and a forthcoming Integrative Summary Report will be Parts of Report Number 65 of the HEI Research Report series.

This report contains the results of two studies designed to investigate morphometric alterations in different regions of the respiratory tract. In Part VIII, Dr. Chang and colleagues describe structural alterations in the alveolar regions of the lung induced by ozone. In Part IX, Dr. Pinkerton and associates present the results of morphometric and biochemical studies of the tracheobronchial and alveolar responses to ozone. The impact of these structural changes on airway smooth muscle contractility and pulmonary function are discussed in detail in Part II (Szarek), Part V (Harkema and Mauderly), and Part XI (the Integrative Summary).

The importance of the collaborative NTP and HEI chronic ozone exposure studies is that they provide an unparalleled opportunity to examine the effects of prolonged ozone exposure using a variety of scientific approaches. The interaction of a number of methods to analyze the pathologic and physiologic consequences of chronic ozone exposure is one of this project's unique features. The results of these studies will provide new information about the threshold effects of ozone exposure on lung injury and the type and extent of damage in a well-established animal model. These results may be helpful for evaluating current standards of ozone exposure as they apply to human health and for designing future animal and human studies.

Consequences of Prolonged Inhalation of Ozone on F344/N Rats: Collaborative Studies

Part VIII: Morphometric Analysis of Structural Alterations in Alveolar Regions

Ling-Yi Chang, Barbara L. Stockstill, Margaret G. Ménache, Robert R. Mercer, and James D. Crapo

ABSTRACT

Morphometric techniques were used to examine cellular and tissue changes occurring in male and female rat lungs exposed to ozone for a prolonged time. F344/N rats were exposed to 0.0, 0.12, 0.5, or 1.0 parts per million (ppm)* ozone for six hours per day, five days per week, for 20 months. Changes in cell volume, cell surface ratios, and cellular characteristics were studied in the terminal bronchioles and in the proximal alveolar regions of the lungs. Animals exposed for 20 months to 0.5 or 1.0 ppm ozone demonstrated dramatic increases in the volume of interstitium and epithelium along the alveolar ducts. The thickening of the epithelium was caused by an epithelial metaplasia in which the normal squamous epithelium was modified to a cuboidal epithelium similar, hut not identical, to the type found in terminal bronchioles. This bronchiolar epithelial metaplasia was directly related to dose of ozone, and was characterized by differentiated ciliated cells and Clara cells similar to those found in terminal bronchioles; undifferentiated cuhoidal cells also were found in the animals exposed to 0.5 and 1.0 ppm ozone. A mild fibrotic response was seen in the animals exposed to 1.0 ppm ozone, with increases in both the interstitial matrix and cellular interstitium. The individual components of the interstitial matrix, including collagen, elastin, basement membrane, and acellular spaces, all were increased. The increase in cellular interstitium was due to an increase in the volume of interstitial fibroblasts. A slight inflammatory response, identified by an increase in alveolar macrophages, was observed in the animals exposed to 1.0 ppm. The terminal bronchioles were less affected than the proximal alveolar region by the ozone exposures, which may indicate a resistance of this tissue to ozone damage. The changes in the terminal bronchioles mainly consisted of a shift in cell type from ciliated to Clara cells in the animals exposed to 1.0 ppm ozone. The bronchiolar epithelial metaplasia observed in the proximal alveolar ducts may indicate that a protective mechanism develops in response to prolonged exposure to high concentrations of ozone.

INTRODUCTION

Ozone is a major component of smog. The ubiquitous nature of ozone and its known health effects are sufficient for it to be classified as a criteria pollutant, and a National Ambient Air Quality Standard has been established under the Clean Air Act. Unlike other pollutants that are emitted directly into the air, ozone is formed by atmospheric photochemical reactions between volatile organic compounds and nitrogen oxides, both of which are emitted from stationary and mobile combustion sources. The chemical reactions that form ozone can occur far from the site at which the precursor emissions originate. As a result, populations in wide geographical areas are exposed to ozone and are subject to its effects.

PHYSIOLOGIC EFFECTS OF OZONE

Short-term exposure to ozone via inhalation alters the breathing patterns of both animals and humans. Ozone exposure causes an increase in respiratory frequency and a decrease in tidal volume (Folinsbee et al. 1977; McDonnell et al. 1983, 1985; Avol et al. 1985; Kulle et al. 1985; Kreit et al. 1989). Acute ozone exposure has been demonstrated to cause airway constriction and air flow limitation in humans, guinea pigs, and cats (reviewed by Mauderly 1984). Inhaled ozone also has been shown to temporarily increase airway reactivity to aerosolized bronchoactive agents in both humans and animals (Golden et al. 1978; Abraham et

* A list of abbreviations appears at the end of the Investigators' Report.

This Investigators' Report is Part VIII of Health Effects Institute Research Report Number 65, Parts VIII and IX, which also includes an Introduction to the NTP/HEI Collaborative Ozone Project, a Commentary by the Health Review Committee on the two Investigators' Reports included in this monograph, and an HEI Statement about the research studies. Correspondence concerning this Investigators' Report may be addressed to Dr. Ling-Yi Chang, Duke University Medical Center, Department of Medicine, Center for Extrapolation Modeling, Box 3177, Durham, NC 27710.

This study was supported by HEI funds from the U.S. Environmental Protection Agency and the motor vehicle industry. The inhalation component of this project was sponsored by the National Toxicology Program as part of its studies on the toxicologic and carcinogenic effects of ozone.

Although this document was produced with partial funding by the U.S. Environmental Protection Agency under Assistance Agreement 816285 to the Health Effects Institute, it has not been subjected to the Agency's peer and administrative review and therefore may not necessarily reflect the view of the Agency, and no official endorsement should be inferred. The contents of this document also have not been reviewed by private party institutions, including those that support the Health Effects Institute; therefore, it may not reflect the views or policies of these parties, and no endorsement by them should be inferred.

al. 1980; Mauderly 1984). A recent review of studies in which human lung function had been measured after chamber exposure to ozone showed a strong correlation between an increase in ozone concentration and a decrease in lung function, and a threshold level for this response was not apparent (Hazucha 1987). Prolonged exposures of animals have revealed small but discernable changes in some measurements of respiratory function. Rats exposed to 0.5 ppm ozone for 52 weeks showed increased functional residual capacity and decreased carbon monoxide diffusing capacity (D_{CO}) (Gross and White 1987). Rats exposed to a simulated urban pattern of ozone (a nine-hour ramped spike, equal to an integrated concentration of 0.19 ppm ozone) for 78 weeks showed increased expiratory resistance. This increase in resistance most likely accounted for the rats' reduced ability to increase ventilation during carbon dioxide challenge (Tepper et al. 1991).

MORPHOLOGIC EFFECTS OF OZONE

At concentrations of ozone below 1 ppm, injury to the lung is concentrated primarily at the junction between the terminal bronchioles and the alveolar regions. Due to anatomical differences among species, the exact location of the lesions may differ (Dungworth et al. 1975; Castleman et al. 1977, 1980; Plopper et al. 1979; Eustis et al. 1981). In dogs and primates, the respiratory bronchioles are the major site of lung injury, whereas in rodents, the proximal alveolar regions are more sensitive to ozone damage. The alveolar type I epithelial cells are the most susceptible cells in these regions of the lung (Stephens et al. 1974; Evans et al. 1976; Mellick et al. 1977; Castleman et al. 1980; Eustis et al. 1981). Detachment of type I epithelial cells can be observed after exposure for as short as two hours to 0.5 to 0.8 ppm ozone (Evans et al. 1976a,b; Boorman et al. 1980). In the airways, ciliated cells appear to be the most sensitive cell type. Loss of cilia from the apical surface of the cell and swollen or fused cilia have been reported to occur after 8- to 24-hour exposures to 0.2 to 0.5 ppm ozone for seven days (Dungworth et al. 1975; Schwartz et al. 1976; Castleman et al. 1977; Mellick et al. 1977; Ibrahim et al. 1980).

The effects of ozone concentrations more relevant to ambient levels are subtle. Changes can be illustrated, however, by studying tissues using morphometric techniques (Plopper et al. 1979; Barry et al. 1985, 1988; Barr et al. 1988). These techniques confirm that the type I epithelium is the cell type most sensitive to ozone exposure. Type I epithelial cells frequently become smaller and cover less alveolar surface area; as a result of the type I cell injury, type II epithelial cells proliferate. Other morphologic changes include invasion of alveolar macrophages and increased volume of interstitial matrix. Another sensitive target of ozone injury is the ciliary surface on the terminal bronchioles. Loss of cilia after ozone exposure has been reported in a number of studies (Plopper et al. 1979; Barry et al. 1988; Chang et al. 1992). Furthermore, the Clara cell dome is flattened (Plopper et al. 1979; Barry et al. 1988).

Prolonged exposure of rats to ozone in a simulated ambient pattern for up to 78 weeks revealed a biphasic response (Chang et al. 1992). Acute tissue reaction after one week of exposure included epithelial inflammation, interstitial edema, interstitial cell hypertrophy, and an influx of macrophages. These responses subsided after three weeks of exposure. Progressive epithelial and interstitial tissue responses that developed with prolonged exposure included epithelial hyperplasia (involving both type I and II cells), fibroblast proliferation, and accumulation of interstitial matrix, which involved thickening of the basement membrane and deposition of collagen fibers.

OZONE AS A POSSIBLE CAUSE OF CHRONIC LUNG DISEASE

An important question is whether ozone causes irreversible changes in the lung that lead to chronic lung diseases such as fibrosis or emphysema. Short-term exposures to more than 0.5 ppm ozone induced collagen synthesis, as indicated by increased incorporation of hydroxyproline (Last and Greenberg 1980; Last et al. 1983). Prolonged synthesis and accumulation of collagen fibers could result in interstitial fibrosis. Subacute and prolonged exposures to ambient levels of ozone increased the volume of noncellular interstitium. Quantitative and qualitative morphologic examination of collagen fibers in the interstitium of exposed animals has suggested an increase in the number of collagen bundles (Vincent et al. 1992) and the abnormal reorganization of collagen fibers. However, increased collagen deposition was at least partially resolved after recovery in clean air. Nevertheless, one element of the interstitial matrix, the basement membrane, definitely was thickened even after recovery in clean air, indicating that some irreversible changes of the matrix do occur (Chang et al. 1992; Vincent et al. 1992). Human exposures to ozone typically span a person's entire life. A large fraction of the world population is exposed daily to ozone levels that exceed the National Ambient Air Quality Standard of 0.12 ppm ozone, and, in some highly polluted urban environments, to levels of 0.4 ppm or greater (Calderon-Garcidenañas et al. 1992). Given the known potential of ozone to cause changes in lung structure and function and the large numbers of people at risk, more study is needed on the long-term effects of ozone on the tissues of the lung.

SPECIFIC AIMS

Two main goals were established for the morphometric studies using electron microscopy: (1) to define the lowest exposure concentration that would result in histologic lung injury significantly different from control measurements; and (2) to characterize the remodeling of interstitial connective tissue. We analyzed tissues from the proximal alveolar regions, where we expected to see the most changes, and from other alveolar tissues chosen at random, where we expected to see few changes. Because the effects of ozone are concentrated in the proximal alveolar region, measurable structural changes are normally not detectable in the tissues from the random alveolar regions, which consist mainly of the unaffected distal alveolar tissue. However, it is not known if extension of lung injury into the distal lung occurs at the high ozone concentrations used in this study. We used the following approach to accomplish our aims:

1. Measure tissue volume, surface area, and number of cells in various alveolar tissues (for example, epithelium, interstitium, and endothelium), and measure cell types in the proximal alveolar region.
2. Measure volume and surface area for various tissues and types of cells in random alveolar regions.
3. Measure the thickness of the epithelium in the terminal bronchioles, and determine the characteristics of terminal bronchiolar cells.
4. Measure changes in the volumes of elastin, collagen, and basement membrane in the interstitium of the proximal alveolar region.

Because both male and female rats were included in the study, gender differences in responses to ozone exposure also were analyzed.

METHODS AND STUDY DESIGN

EXPOSURE OF ANIMALS

Exposures to ozone were performed at Battelle Pacific Northwest Laboratories (Richland, WA) as part of a collaborative, multilevel study of the effects of prolonged ozone exposure performed by the National Toxicology Program (NTP) and the Health Effects Institute (HEI). Male and female F344/N rats were purchased from Simonsen Laboratories (Gilroy, CA) at three weeks of age. After a quarantine period of 14 days, rats were randomly assigned to air or ozone exposure groups, and individually housed in stainless-steel wire-bottom cages. Rats were given NIH-07 open formula pellets (Zeigler Bros., Gardner, PA) and softened tap water ad libitum, except during exposure periods. Relative humidity (55% ± 15%), temperature (24° ± 0.7°C), and lighting (12 hours light/12 hours dark) were maintained automatically.

Rats were exposed in modified Hazelton-2000 (Aberdeen, MD) inhalation chambers. Animals were exposed for six hours per day, five days per week, for 20 months to 0.00, 0.12, 0.50, or 1.00 ppm ozone. Ozone was generated from pure oxygen using a silent arc (corona) discharge ozonator (OREC Model 03V5-0, Ozone Research and Equipment Corp., Phoenix, AZ), and was monitored by a multiplexed Dasibi Model 1003-AH (Dasibi Environmental Corporation, Glendale, CA) ultraviolet spectrophotometric analyzer. The monitor was calibrated by comparing it with a chemical-specific, calibrated monitor (neutral-buffered potassium iodide method) that simultaneously sampled the exposure chambers. Chamber measurements were taken at 12 locations in each chamber to assure uniformity, which was enhanced by use of a recirculation device; airflow in the chambers was maintained at 15 air changes per hour. Ambient ozone was removed from the air entering all chambers using a potassinm permanganate filter. Charcoal and HEPA filters were used to further filter the air. The animals were killed and their lungs were removed one week after the exposnres were terminated.

TISSUE FIXATION AND PROCESSING

A total of 38 rats, equally divided between males and females, were used for this study; the group size from each ozone exposure concentration was 10 from 0.0 ppm, 12 from 0.12 ppm, 8 from 0.5 ppm, and 8 from 1.0 ppm. One male rat in the control group died, and one female rat from the control group was not studied due to massive lung thickening from monocellular leukemia. Animals were killed by anaesthesia with sodium pentobarbital, and the tracheas were cannulated. The diaphragms were punctured to deflate the lungs, and the lungs were fixed by instillation at 30 cm of water pressure with 2% glutaraldehyde in 0.85 M sodium cacodylate buffer (350 mOsm; pH 7.4). After fixing the lungs in the chest for 15 minutes, they were removed and stored in fixative until processed. Lung volumes were measured by fluid displacement. Three 2-mm slices of the left lung were cubed into 4-mm × 4-mm pieces. To enhance the visibility of the interstitial matrix components, tissues were stained en bloc in 1% osmium tetroxide for four hours, 1% tannic acid for 2.5 hours, and in 2% uranyl acetate for 2.5 hours (Mercer et al. 1991). Longer staining times caused the tissue to become excessively brittle, and shorter staining times reduced the staining quality of the matrix components. The en bloc staining also resulted in increased staining of the epithelium when compared to other tissue components. The tissue was extensively washed in 8% sucrose after each

step, dehydrated in an ethanol series, and embedded in epoxy resin with standard procedures. To assure adequate infiltration of the resin, the tissue blocks were allowed to incubate a long time (approximately 1 hour) in the propylene oxide–resin solution.

MICRODISSECTION

The microdissection technique described here was used to isolate terminal bronchioles and proximal alveolar regions (Chang et al. 1988). Tissue blocks selected arbitrarily were cut in a random orientation into slices 0.5 mm thick. They were examined sequentially with a dissecting microscope. Small airways, identified by their smooth circumference and thicker epithelium, were followed to the bronchiole–alveolar duct junction. Alveolar ducts that extend from the bronchiole–alveolar duct junction were clearly distinguishable from bronchioles by the thinness of the duct wall and by the holes (which open into the alveoli) that line the bronchiolar walls. Exposures to 0.5 ppm and 1.0 ppm ozone caused thickening of the alveolar duct wall due to bronchiolarization of the alveolar ducts and alveoli; however, even though the thinness of the wall was thus eliminated as a means of identification, the punctured appearance of the alveolar duct wall had not been altered by the ozone exposure, and was sufficient to identify the alveoli. Therefore, our microdissecting technique could be used consistently for tissues from all exposure groups.

As shown in Figures 1A and 1B, terminal bronchioles were cut in cross sections to facilitate morphometric analysis of their tubular and oriented structure. The alveolar tissue surrounding the first alveolar duct bifurcation, designated as the proximal alveolar region, also was studied in cross section on sections that presented a distinct alveolar duct at each side of the first alveolar duct bifurcation (Figure 1A). This orientation of the proximal alveolar region was selected to provide a definite boundary for the morphometric analysis of the proximal alveolar regions (Figure 1C). Because the plane of slicing was chosen at random with respect to the orientation of terminal bronchioles and alveolar ducts, samples in cross section occurred randomly within the tissue block. Three blocks of each anatomic location were selected randomly, and mounted on blank epoxy blocks. Since the orientation of the terminal bronchioles or proximal alveolar regions in the selected blocks were predetermined, thin sections of the blocks were cut by aligning the diamond knife to the block faces. Sections were placed on 200-mesh copper grids, poststained in uranyl acetate and lead, and examined on a Zeiss 10C electron microscope (Carl Zeiss Inc., Germany).

ELECTRON MICROSCOPIC MORPHOMETRY

Electron microscopic morphometric analysis was used to determine tissue volume, surface area, and cell characteristics in the proximal alveolar regions, random alveolar regions, and terminal bronchioles. A total of 177 morphologic parameters were calculated for each animal (2 related to the whole animal, 94 in the proximal alveolar region, 47 in the random alveolar regions, and 34 in the terminal bronchioles). The major morphometric measurements, locations, and cell types are illustrated in Figures 2 and 3.

Proximal Alveolar Regions

Three sites in the proximal alveolar region isolated by microdissection were randomly selected from each animal. Thin sections from each of these sites were stained and examined with an electron microscope. Two photomicrographs were taken of each grid square, one in the upper left corner and one in the lower right corner. Incomplete grid squares or grid squares containing large blood vessels were ignored. All nuclear profiles in each grid square used for

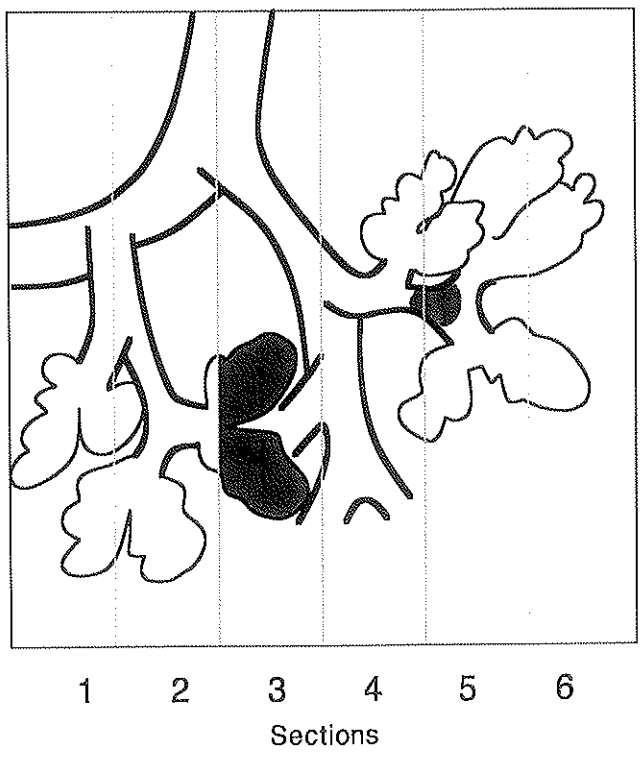

Figure 1A. Diagram showing terminal bronchioles and alveolar ducts. Diagram illustrating consecutive tissue slices of terminal bronchioles and alveolar ducts chosen at random. Section 5 contains a cross-sectioned terminal bronchiole (shaded area; made visible by light microscopy in Figure 1B). Section 3 contains a cross-sectioned proximal alveolar region (shaded area; made visible through light microscopy in Figure 1C).

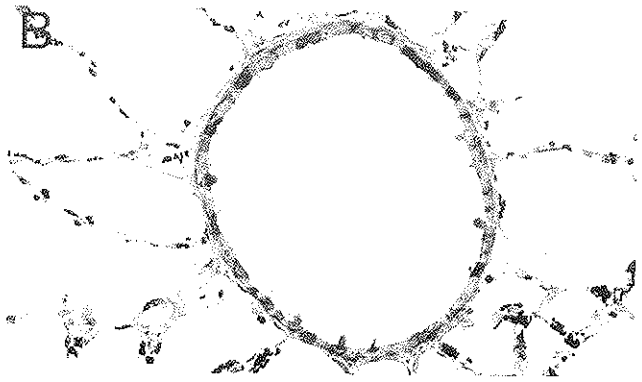

Figure 1B. Micrograph showing terminal bronchioles and alveolar ducts. Micrograph showing the cross section of a terminal bronchiole (section 5 in Figure 1A). (C) Micrograph showing the cross section of a proximal alveolar region with one alveolar duct (AD) at each side of the bifurcation (section 3 in Figure 1A). The block face was trimmed to just outside the duct wall for morphometric analysis of the proximal alveolar region.

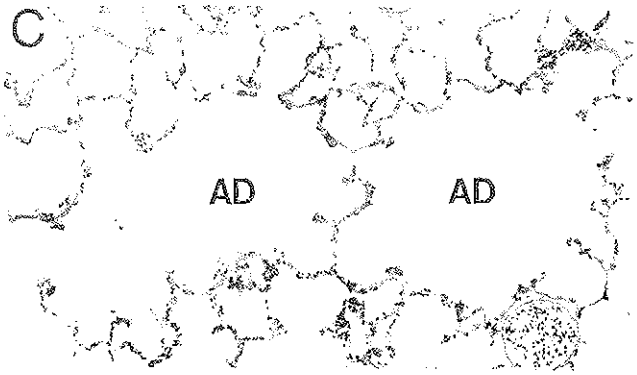

Figure 1C. Micrograph showing the cross section of a proximal alveolar region with one alveolar duct (AD) at each side of the bifurcation (section 3 in Figure 1A). The block face was trimmed to just outside the duct wall for morphometric analysis of the proximal alveolar region.

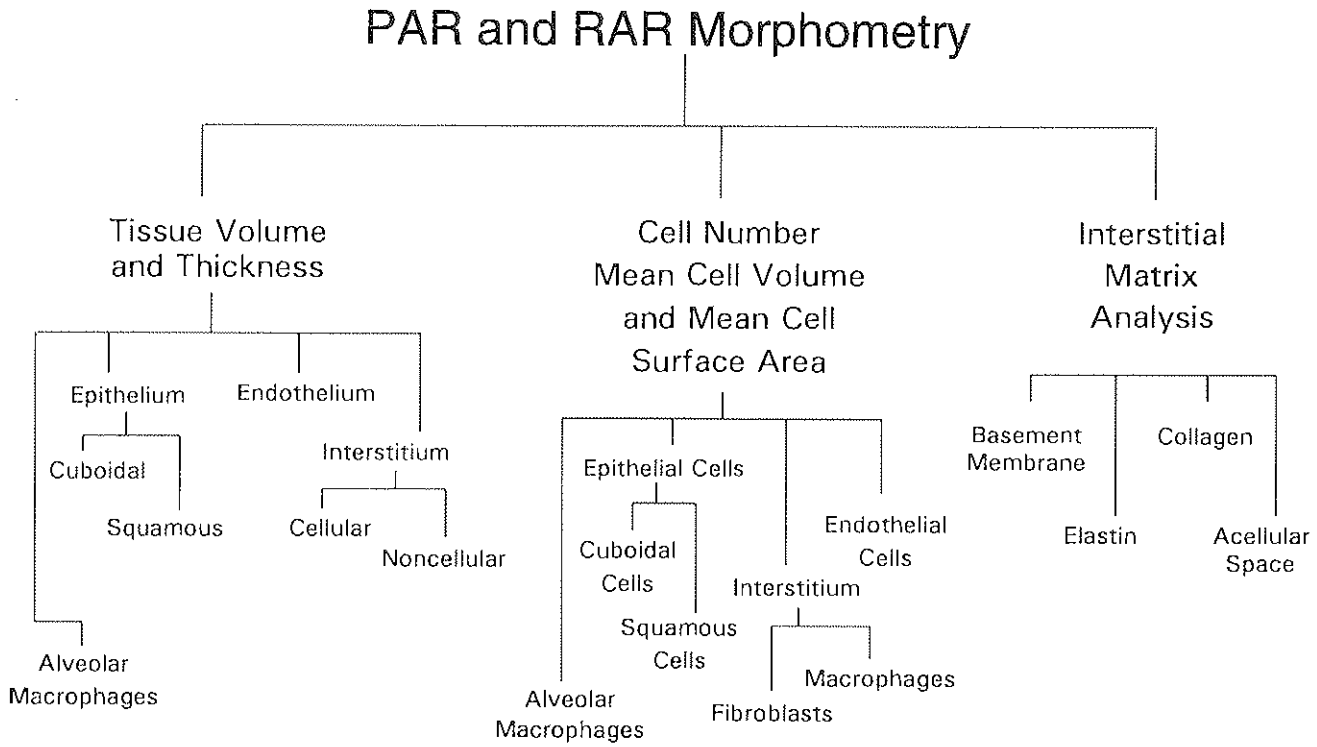

Figure 2. Major parameters of the morphometric study of the proximal and random alveolar regions. Note that cell characteristics (cell number, mean cell volume, and mean cell surface area) were not measured for the random alveolar regions.

photography were counted on the electron microscope using Gundersen's rule of forbidden lines (Gundersen 1977). Micrographs were enlarged to × 8500 on 11- by 19-inch photographic paper that previously had been printed with a point-counting lattice of 448 lines, each 1.37 cm long.

Points, intercepts, and nuclear profiles were counted to determine cell volume and cell surface densities. The formula used in the morphometric analysis has been described in detail (Barry and Crapo 1985; Chang and Crapo 1990). Briefly, volume density of structure a (V_{va}) was derived by the equation $V_{va} = P_a/P_T$, where P_a is the number of points

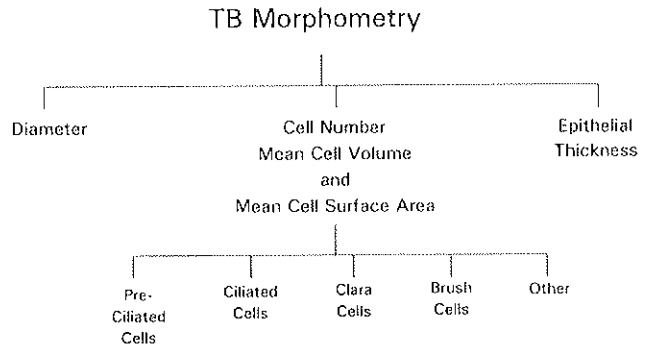

Figure 3. Major parameters of the morphometric study of terminal bronchioles.

falling on tissue a, and P_T is the total number of points. Surface density (S_V) was calculated by the equation $S_V = 2I_a/L_T$, where I_a is the number of intercepts with surface a, and L_T is the length of the test line. Numerical density (N_V) was derived by the equation $N_V = N_A/\overline{D}$, where NA is the number of nuclear profiles counted in an area of size A (connted directly on the electron microscope), and $\overline{D}$ is the mean caliper diameter of a cell nucleus. Mean caliper diameter values for the alveolar cells were taken from data on normal rats (Woody et al. 1979; Pinkerton et al. 1982). This derivation of $\overline{D}$ values depends on a lack of ozone exposure effects on the size or shape of tbe nuclei. Therefore, we analyzed the profiles and measured the size of 50 of each of type I epithelial cells, type II epithelial cells, endothelial cells, and fibroblasts from both control rats and rats exposed to 1 ppm ozone. The average diameters of the cell profiles for each cell type were calculated for control rats and rats exposed to ozone. Stndent t tests showed that the sizes of the nuclei from rats exposed to ozone were not statistically different from those from control rats. We accepted therefore, that the use of $\overline{D}$ values from normal rats was justified.

Usually, absolute volumes, surface area, and cell numbers in the lung can be calculated by mnltiplying the density measnrements by lung volume. However, the margins of the proximal alveolar region were difficult to define rigorously. Because of this difficulty, volume, surface, and numerical densities of cells cannot be easily expressed as absolute values. Instead, volume, surface, and nnmerical densities of cells were divided by the surface density nf alveolar epithelial basement membrane in the same sample. Variance that might result from different degrees of lung inflation would be eliminated by this normalization procedure. Because the surface density of basement membrane does not change in response to ozone exposure, the normalized data from the various groups can be compared in an unbiased manner. The morphometric analysis described above was applied to a variety of alveolar tissues and their subcomponents (Figure 2). Detailed definitions of the components for each category of tissue and the measurements performed are described below.

Epithelium. The epithelium is subdivided into alveolar (type I and type II) and bronchiolar-like (ciliated, Clara, and other) cells. The volume of total epithelium and of each of the components of the epithelium were determined. The cell characteristics measured were the numbers of cells per unit area (numerical density), mean cell volume, and, for epithelial and endothelial cells only, mean cell surface area.

Interstitial Matrix. Morphometric analysis of the interstitial matrix followed procedures designed by Vincent and associates (1992). The interstitial matrix was subdivided into four compartments: collagen fibers, elastin, basement membranes, and acellular space. Collagen fibers were defined as any arrangement of fibrils that can be delineated by an estimated perimeter and distinguished, according to the density of fibrils in the fibers, from other neighboring components. A point falling on a single fibril and a point falling between fibrils but within the perimeter of a fiber were both tallied as points on collagen. Elastin was recognized as amorphous material uniformly stained by tannic acid and uranyl acetate. A basement membrane was juxtaposed to both epithelial and endothelial cells and was easily recognized. Any point falling on a structure that could not be ascribed to collagen fibers, elastin, basement membrane, or interstitial cells was automatically tallied as a point on the acellular space. The volume of each interstitial matrix component was calculated and normalized to basement membrane surface area in the same manner described for tissues and cells in the proximal alveolar regions.

Endothelium and Capillaries. The volume of capillary endothelium normalized to the surface area of the basement membrane and the characteristics of the capillary endothelial cells were measured. The volume of the capillary bed was subdivided into red blood cells and plasma. The plasma component included all white blood cells. Because the results of numerous earlier studies of ozone exposure fail to show changes in white blood cells in the pulmonary vasculature, volume and cell characteristics of white blood cells were not measured as a separate category.

Evidence of Inflammation. Inflammatory cells (macrophages and neutrophils) in the alveolar spaces and in the interstitium were used as indicators of inflammation. The volumes and the cell characteristics of both were measnred.

Random Alveolar Regions

Tissue and cell volumes were measured morphometrically as indices of the responses to ozone exposure in the

total gas exchange region, referred to as the random alveolar region. Three blocks of tissue from each animal were randomly selected from the embedded tissue blocks without prior examination under the dissection microscope and without knowledge of the presence or absence of bronchiole–alveolar duct junctions. Fifteen micrographs, taken from the upper left corner of 15 consecutive grid squares, were obtained. Photographs were printed and analyzed in a manner similar to those from the proximal alveolar regions. Only total cell volume, matrix volume, and surface area were measured. Cell characteristics and matrix components were not analyzed.

Terminal Bronchioles

The terminal bronchioles were examined using morphometric techniques described by Barry and associates (1988) and Chang and associates (1988). The complete epithelium of each terminal bronchiole examined was photographed by 25 to 30 overlapping micrographs taken at a magnification of × 2000. Pictures were enlarged to × 8500 and printed on 11- by a 14-inch photographic paper. A montage of each terminal bronchiole was constructed and the portion contributed by each micrograph was marked on the composite. The pictures were then placed under a Merz overlay sheet marked with 224 points. Points falling on each cell type and intercept between test lines and a luminal surface, a basal surface, or a cilium were counted. The number of nuclei of each type of cell in the montage was recorded. The area of the bronchiolar epithelium and the lengths of the luminal surface and the basement membrane were measured by a digitizer. The thickness of the epithelium was derived from these measurements by assuming that the cross section of a bronchiole was a circle. The volume density of each cell type and the surface densities of the luminal and basement membrane surface areas for each type of cell in relation to the total volume of the terminal bronchiolar epithelium (the reference space) were calculated using point and intercept counts. The major morphometric measurements for the terminal bronchioles are shown in Figure 3.

For each terminal bronchiole, the number of cells is expressed in relation to the surface area of the bronchiolar epithelial basement membrane. These values were determined with the equation $N_{SA} = N_L/\overline{H}$ where N_{SA} is the number of cells per unit of surface area (in this case the surface area of the basement membrane), N_L is the number of nuclear profiles counted along the total length of basement membrane of a terminal bronchiole (measured with a digitizer), and $\overline{H}$ is the mean caliper height of the cell nucleus. The values of $\overline{H}$ for major bronchiolar cells and the methods for determining those values were reported by Barry and associates (1988). The mean caliper height of the cell nucleus ($\overline{H}$), instead of $\overline{H}$, was used for the morphometric analysis of terminal bronchioles because the sections of bronchioles were oriented perpendicularly to their long axes.

The volume of a certain cell type per unit area of epithelial basement membrane was calculated by multiplying its volume density by the surface density of the epithelial basement membrane. The latter was determined by the ratio of the basement membrane length to the epithelial area, both measured by digitizer. Cell surface area per unit area of epithelial basement membrane was derived in a similar manner. The reference space for all volume and surface densities was the bronchiolar epithelium. Cell characteristics then were calculated by dividing the volume or surface area per unit of surface area of basement membrane by the number of cells per unit area of basement membrane.

STATISTICAL METHODS

For the purposes of statistical analysis, we developed an analytical approach that would use all information most efficiently. We established five categories of injury and identified one or two of the 177 measured parameters as the most sensitive indicators for each kind of injury. These we called primary variables. The statistical analysis began with a multivariate analysis of variance (MANOVA) to test for statistical significance in this vector of primary variables. When the MANOVA revealed a significant relationship, univariate analysis of variance (ANOVA) was performed. If the MANOVA did not demonstrate significance, the variable was not tested further. In this study, six primary variables were established in the proximal and randomly selected alveolar regions, and seven primary variables in the terminal bronchioles were established; they, and the category of injury with which they are associated, are listed in Table 1 (proximal alveolar regions) and Table 2 (terminal bronchioles). If a primary variable showed statistical significance in the first MANOVA, then a second MANOVA was performed. The second vector for multivariate analysis consisted of 1 to 5 key variables that provided more information than the primary variable alone about the category of injury. The key variables also are listed in Table 1. In this study, 15 key variables were identified in the proximal alveolar region and 11 in the random alveolar regions. No key variables were counted in the terminal bronchioles. As for the primary variables, multivariate significance was required for each of the five (corresponding to the five injury categories) key variable MANOVAs before examining univariate significance and comparisons among exposure concentrations. This analysis provides the statistical basis for the statements of significant effects given in this report. We

Table 1. Primary and Key Variables for the Proximal and Random Alveolar Gas Exchange Regions

Class of Injury	Primary Variables[a]	Key Variables That Indicate Specific Injury[a]
Bronchiolarization	Percentage of Bronchiolarization	Volume of Clara cells Volume of ciliated cells[b] Volume of other epithelial cells[b]
Epithelial	Volume of type I epithelium	Volume of type I cells Volume of type II cells Number of type I cells Number of type II cells
Interstitial	Volume of interstitium	Volume of acellular space[b] Volume of elastin[b] Volume of interstitial cells[b] Volume of collagen[b] Volume of basement membrane[b]
Inflammation	Volume of the total inflammatory cells[c]	Volume of alveolar macrophages Volume of interstitial macrophages
Vascular	Surface area of capillaries Volume of endothelium	Volume of plasma Volume red blood cells

[a] Normalized volumes and surface areas were used.

[b] Not analyzed for the random alveolar regions.

[c] Total inflammatory cell volume includes macrophages and neutrophils in both alveolar spaces and the interstitium.

Table 2. Primary Variables for the Terminal Bronchioles

Site of Injury	Primary Variables
Epithelium	Total volume
Ciliated cells	Number Mean cell volume Mean cell surface area
Clara cells	Number Mean cell volume Mean cell surface area

have included, however, additional information on 125 uncontrolled parameters. These are called the confirmatory variables. They were analyzed without multivariate control; that is, using ANOVA without first performing a MANOVA. The rigor of the full step-down strategy is not applied because statistical significance in these variables does not carry the same weight as statistical significance in the identified primary and key variables, although it might be important to learn of effects in these variables. The *t* tests for the confirmatory variable analyses, however, are performed with a Bonferroni adjustment. In this study, the outcomes of these tests are presented in the Results section, and all of the data are presented in Appendices B through E. However, these results are not relied upon in presenting the interpretations and conclusions in the Discussion section.

SAMPLE SIZE

A total of 48 rats were originally assigned to the morphometric studies: 38 rats were included in the final analyses for the proximal alveolar region and the terminal bronchioles; and 33 rats were included in the final analyses for random alveolar regions. Table A.1 identifies the specific animals used for this study and the concentration of ozone to which each was exposed. In the control group, one male rat died before the end of the exposure, and one female rat was excluded from all statistical analyses because of marked incidence of leukemia in the lung. Of the rats used for pulmonary function testing after they were exposured to 0.5 or 1.0 ppm ozone, seven were not used in the morphometric studies of the proximal alveolar region and terminal bronchioles. To assess ozone effects on random alveolar regions, animals that had undergone pulmonary function tests were studied (expect for one male rat exposed to 1.0 ppm ozone

that died during pulmonary function tests), but rats exposed to 0.12 ppm ozone were not used in the morphometric study of random alveolar regions. The subset of rats used for pulmonary function tests before they were killed had been chosen randomly from each of the ozone exposure groups by the Biostatistical Advisory Group. When we received tissues from those rats, we assigned tissues from the groups exposed to 0 or 0.12 ppm ozone to our analysis of proximal alveolar regions, and tissues from groups exposed to 0, 0.5, or 1.0 ppm ozone to our analysis of random alveolar regions. Therefore, because tissues from all ozone exposure groups were not used for our studies of either proximal or random alveolar regions, this subset of animals could not be analyzed as a source of statistical variability.

Furthermore, evidence of leukemia with pulmonary involvement was found in a percentage of rats in the portion of this project performed under the auspices of the NTP. All animals identified with lung leukemia also had advanced spleen and liver involvement. Although the tissues examined morphometrically in our laboratory indicated lung lukemia with substantial pulmonary involvement in only one animal, several rats were found to have advanced leukemia in their spleens and livers. As a result, all of our data were analyzed twice: once excluding only the one animal with lung leukemia (n = 38), and once excluding that rat, all rats with advanced spleen and liver leukemia (as identified by other investigators funded by HEI), and the subset of animals on which pulmonary function tests had been performed (n = 27).

RESULTS

Statistical analyses were performed twice. The first time, the animal with marked lung leukemia was excluded (n = 38). The second time, that animal and all animals with liver and spleen leukemia and those animals that had undergone pulmonary function testing were excluded (n = 27). If the leukemic rats and rats tested for pulmonary function contributed greatly to the variability of the responses, eliminating the data from those rats from the statistical analyses might produce more statistically significant results. On the other hand, excluding 11 animals results in a loss of more than 25% of the sample and a substantial loss of statistical power. We compared the results of the statistical analyses (multivariate and univariate ANOVA for all variables) from the two sets of animals. Few significant differences, particularly with respect to the effects of the ozone concentrations, were found between the two sets of analyses. With the smaller sample size, two additional variables showed significant effects from the concentration of ozone. Neither of these variables changed the overall interpretation of the results, however. On the other hand, the loss of power from the smaller sample size was much more noticeable when examining the patterns of significance in the t tests performed with the Bonferroni correction factor. We concluded that the presence of leukemia in these animals was not a confounding factor for the study of ozone effects. Therefore, we report here the results obtained from analyzing the group of 38 rats that excludes the rat identified as having lung leukemia. Because no significant interactions between gender and ozone were identified, data from male and female rats were pooled to derive the mean values for effects of ozone concentrations. Effects of gender have been described separately. Table 3 shows that body weights and lung volumes were not different among exposure groups. The alveolar surface density, which was used to normalize tissue volumes in the proximal and random alveolar regions, also was not changed by the ozone exposures.

EFFECTS OF OZONE CONCENTRATION AND GENDER ON THE PROXIMAL ALVEOLAR REGION

The MANOVA applied to the primary variables in the first stage of the statistical analysis revealed an effect due to ozone exposure concentration in the following injury classes: bronchiolarization, interstitial, vascular, and inflammation (Table 4). No significant effects were attributable either to gender or to an interaction between gender and concentration. Therefore, effects from gender were not considered in subsequent stages of the statistical analysis. Significant effects due to ozone concentration were indicated by changes in the following primary variables: the percentage of bronchiolarization, the volume of interstitium, the volume of alveolar macrophages, and the surface area of capillaries. The volume of type I epithelium did not change following ozone exposure.

An uncontrolled ANOVA indicated that ozone concentration had a effect on a confirmatory variable, the total volume of tissue (epithelium, interstitium, and endothelium) due to increases in the volumes of both epithelium and interstitium. Table 5 presents the morphometric measurements of the primary variables and the results of the statistical analysis.

Epithelium

The epithelium in the proximal alveolar regions was not significantly altered by exposure to 0.12 ppm ozone, but major changes were found in the epithelium of rats exposed to either 0.5 or 1.0 ppm ozone. The higher concentrations of ozone induced epithelial metaplasia (a change of the squamous alveolar epithelium to cuboidal bronchiolar epithelium, also referred to as bronchiolarization) in the proximal alveolar regions. Normally, only a small number of bronchiolar epi-

Table 3. Body Weight, Lung Volume, and Alveolar Basement Membrane Surface Densities[a]

Variable	Ozone Concentration (ppm)			
	0.0 ($n = 10$)	0.12 ($n = 12$)	0.5 ($n = 8$[b] or 12[c])	1.0 ($n = 8$[b] or 11[c])
Body weight (g)	448 ± 30	444 ± 26	426 ± 32	427 ± 35
Lung volume (cm^3)	11.9 ± 0.7	11.8 ± 0.6	12.0 ± 0.8	12.6 ± 0.8
Alveolar basement membrane surface density (cm^2/cm^3)				
Proximal alveolar region	412 ± 28	432 ± 33	394 ± 43	430 ± 23
Random alveolar regions	485 ± 34	ND[d]	528 ± 26	474 ± 20
Total tissue volume ($\mu m^3/\mu m^2$)[e]				
Proximal alveolar region	1.18 ± 0.07	1.18 ± 0.05	1.75 ± 0.15	2.11 ± 0.12[f]
Random alveolar regions	1.12 ± 0.07	ND	0.97 ± 0.06	1.12 ± 0.23

[a] All values are given as means ± SE.

[b] n value for the proximal alveolar region.

[c] n value for random alveolar regions.

[d] ND = not determined.

[e] Tissue volumes were normalized to the surface area of the epithelial basement membrane.

[f] $p < 0.05$. Bonferroni-corrected t test on concentration factor means compared control to ozone exposure concentrations.

Table 4. Summary of Statistical Analyses Effects of Ozone Concentration in the Proximal Alveolar Region

Class of Injury	Significance of Ozone Concentration by MANOVA for Class of Injury[a]	Key Variable	Significance of Ozone Concentration by ANOVA for Key Variable[a]
Bronchiolarization	*	Volume of Clara cells	*
		Volume of ciliated cells	*
		Volume of other epithelial cells	*
Epithelial		Volume of type I cells	
		Volume of type II cells	
		Number of type I cells	
		Number of type II cells	
Interstitial	*	Volume of acellular space	*
		Volume of elastin	*
		Volume of interstitial cells	*
		Volume of collagen	*
		Volume of basement membrane	*
Inflammation	*	Volume of alveolar macrophages	
		Volume of interstitial macropbages	
Vascular	*	Volume of plasma	
		Volume of red blood cells	*

[a] An asterisk (*) in this column indicates a statistically significant result ($p < 0.05$).

Table 5. Morphometric Measurements for the Primary Variables of Lung Injury in the Proximal Alveolar Region[a]

Variable	Ozone Concentration (ppm)			
	0.0 (n = 10)	0.12 (n = 12)	0.5 (n = 8)	1.0 (n = 8)
Percentage of bronchiolarization	2.3 ± 0.8	1.4 ± 0.4	7.1 ± 2.2	12.1 ± 2.6[b]
Tissue volumes ($\mu m^3/\mu m^2$)[c]				
Type I epithelial cells	0.21 ± 0.01	0.22 ± 0.01	0.21 ± 0.01	0.21 ± 0.01
Interstitium	0.50 ± 0.04	0.50 ± 0.02	0.77 ± 0.07[b]	0.86 ± 0.04[b]
Total inflammatory cells	0.05 ± 0.01	0.05 ± 0.01	0.08 ± 0.02	0.15 ± 0.03[b]
Endothelium	0.24 ± 0.01	0.26 ± 0.01	0.25 ± 0.02	0.24 ± 0.01
Surface area of capillaries ($\mu m^2/\mu m^2$)[c]	90 ± 2	92 ± 1	98 ± 3	85 ± 2

[a] All values are given as means ± SE.

[b] $p < 0.05$. Bonferroni-corrected t test on concentration factor means compared control to ozone exposure concentrations. Significant effects of concentration were revealed by MANOVA. Significant effects were revealed by ANOVA for concentration with percentage of bronchiolarization, interstitial volume, inflammatory cells, and with capillary surface area.

[c] Measurements of volume and surface area were normalized to the surface area of epithelial basement membrane.

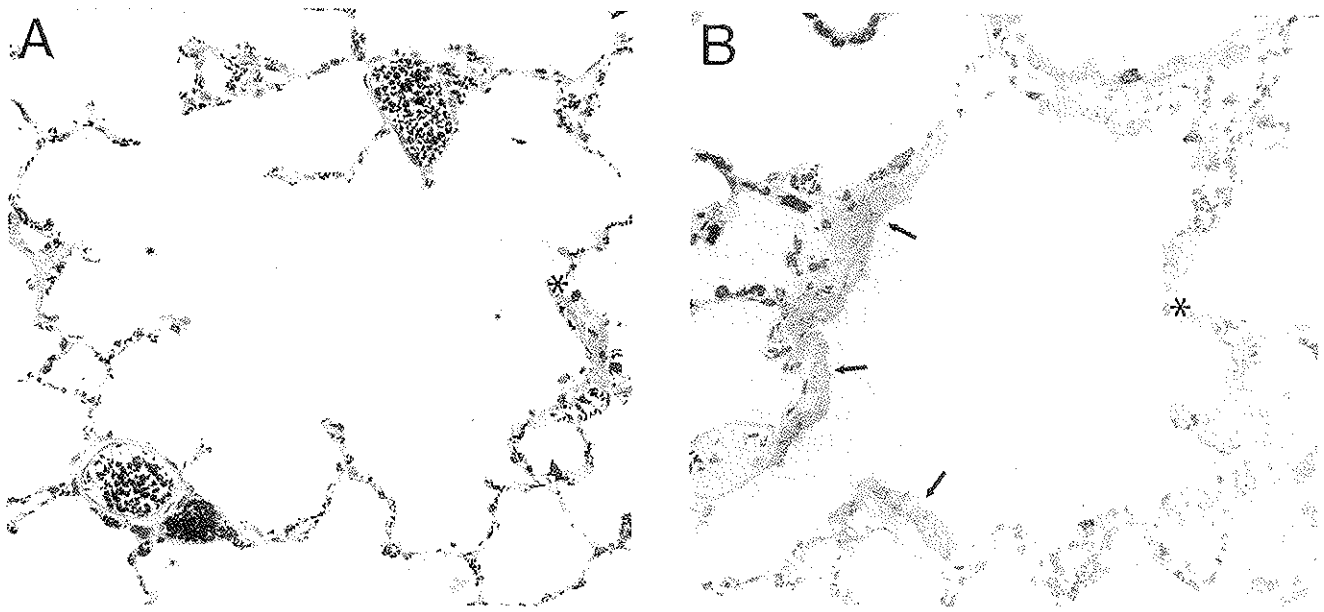

Figure 4. Low magnification electron micrographs of the proximal alveolar ducts. A first-generation alveolar duct from A: a rat exposed to 0.0 ppm O_3, and B: a rat exposed to 0.5 ppm O_3 for 20 months. A few cuboidal epithelial cells are present on the first alveolar duct bifurcation (in both panels A and B) and along the duct wall in the control rat lung. A large portion of the duct wall is covered by cuboidal epithelial cells or bronchiolarized epithelium after O_3 exposure (arrows in panel B). In contrast, no cuboidal terminal bronchiolar epithelial cells can be found lining the alveolar duct wall in panel A.

thelial cells, if any, can be found extending from terminal bronchioles into the proximal alveolar region (Figure 4A). In control rats, less than 2% (not significantly different from 0%) of the surface area in the proximal alveolar region was covered by bronchiolar cells. After exposure to either 0.5 or 1.0 ppm ozone, 7% or 12%, respectively, of basement membrane surface was covered by bronchiolar epithelium (Figure 4B and Figure 5), and the volume of bronchiolar epithelium in the proximal alveolar region increased 2.5-fold or 4.5-fold, respectively. The extent of bronchiolarization induced by ozone, therefore, is dependent on dose, although only the effect at 1.0 ppm ozone was statistically

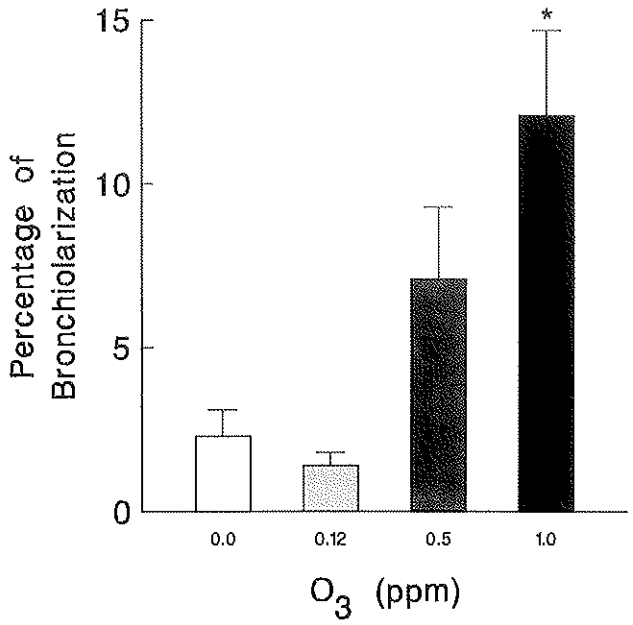

Figure 5. Changes in the percentage of alveolar basement membrane surface area covered by bronchiolar epithelium (percentage of bronchiolarization) in response to prolonged O_3 exposure. An asterisk (*) indicates statistical significance at the level of $p < 0.05$ when compared with the mean of the control group.

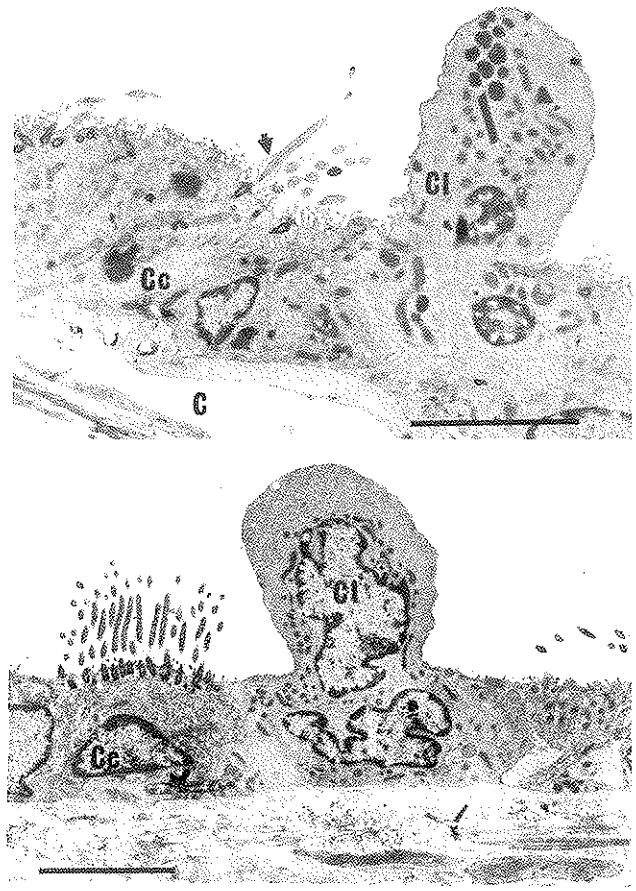

Figure 6. Bronchiolar epithelial metaplasia of a rat septum exposed for 20 months to 1.0 ppm ozone. Top: The metaplasia consists of ciliated (Cc) and Clara (Cl) cells. Abnormal swollen cilia were seen (arrow points to one example). A capillary (C) also is shown. Bottom: Epithelium from the terminal bronchiole of a control rat lung. Ciliated (Cc) and Clara (Cl) cells in terminal bronchioles were similar in structure to the ciliated and Clara cells observed in bronchiolar metaplasia of the alveolar ducts. Bars = 5 μm.

significant. The bronchiolar cells lining the alveolar ducts and the alveoli consisted mainly of fully differentiated ciliated cells and Clara cells that were structurally identical to those found in terminal bronchioles (Figure 6). Both types of cells increased in number and volume hy the prolonged ozone exposures (Figure 7). Unlike the terminal bronchiolar epithelium in normal proximal alveolar regions, in which the volume of ciliated cells is approximately twice as large as the volume of Clara cells, the metaplastic epithelium in the proximal alveolar regions contained approximately equal volumes of ciliated and Clara cells. There was also a large increase in the volume of unidentified cells (referred to as "other cuhoidal cells"). These cells were observed only in the metaplastic proximal alveolar region, and typically contained differentiated features of both ciliated cells and Clara cells, including fiber bundles, secretory granules, basal bodies, and glycogen granules (Figure 8). Preciliated cells and brush cells that are normally found in the terminal bronchioles were not observed in the metaplastic cuboidal epithelium in the proximal alveolar regions. Morphometric analysis of the characteristics of the ciliated and Clara cells in the metaplastic epithelium indicated that there was no effect of ozone exposure on mean cell size or on mean cell surface area.

Although the total epithelial volume increased, due to the metaplasia of the normal squamous epithelium to a cuboidal type of epithelium, in rats exposed to 0.5 or 1.0 ppm ozone, the total volumes of type I and type II epithelium were not changed by the exposures. Univariate ANOVA, however, showed an effect of ozone concentration on the characteristics of type I epithelial cells. The number of type I cells increased 64% to 74% after exposnre to 0.5 or 1.0 ppm ozone, respectively. The size of the type I cells decreased approximately 40%, and the luminal and hasal cell surface areas of alveolar type I cells decreased to approximately 50% of the control values (Figure 9). Few structural abnormalities were noted, except for focal thickening of type I epithelium (Figure 10) and small areas of cell necrosis. The characteristics of alveolar type II cells were not altered by the ozone exposures.

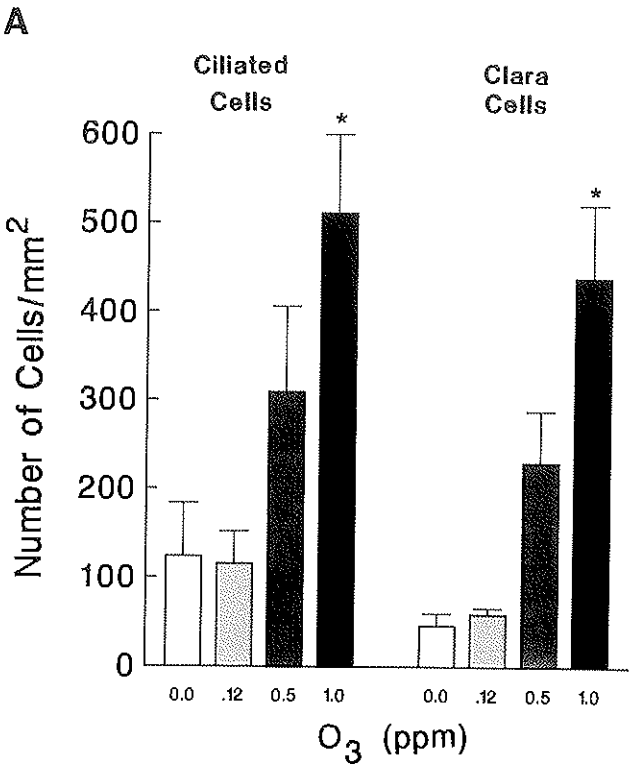

Figure 8. Cuboidal cells with some characteristics of several differentiated cell types were found in alveolar ducts of animals exposed to 0.5 or 1.0 ppm O_3. Fiber bundles (two filled arrowheads point to examples), basal bodies (one filled arrow points to an example), secretory granules (two open arrows point to examples), and numerous golgi apparatuses (g) were seen in these cells. Nu = nucleus. Bar = 5 μm.

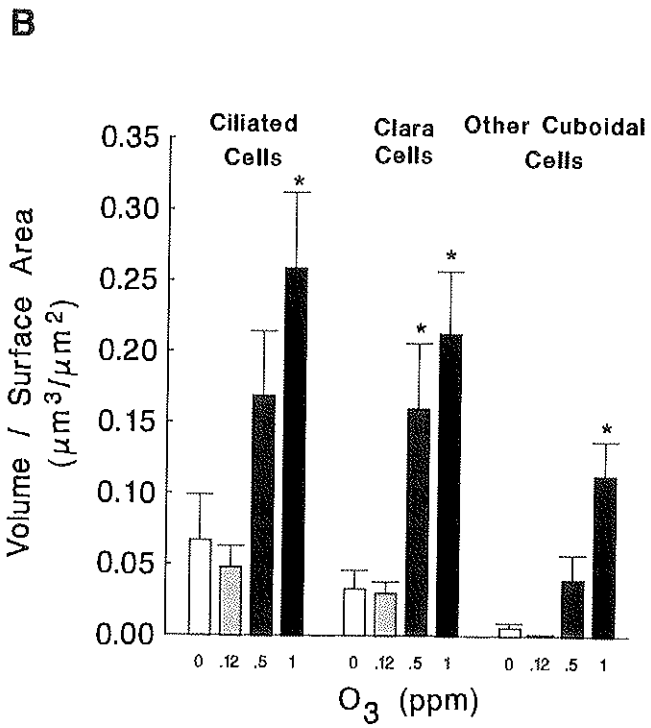

Figure 7. Changes in A: the number, and B: the volume of cuboidal cell types in the proximal alveolar region after prolonged exposure to ozone. An asterisk (*) indicates statistical significance at the level of $p < 0.05$ when compared with the mean of the control group.

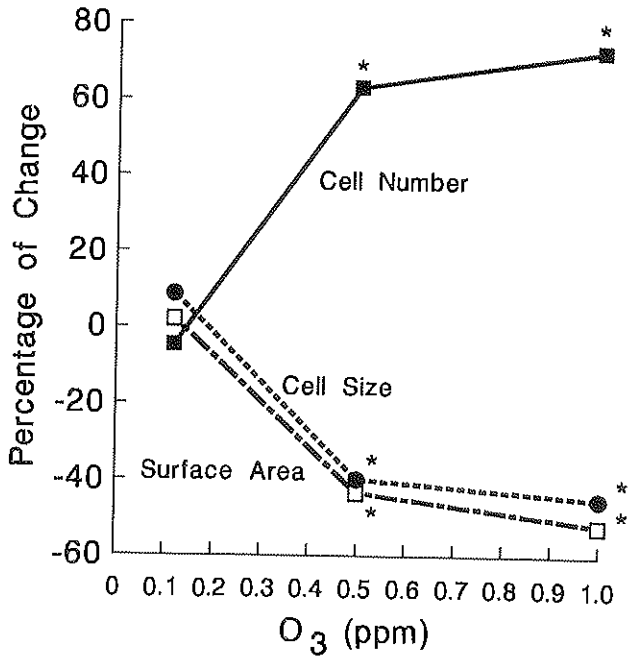

Figure 9. Percentage of change in the number, mean cell size (volume), and mean cell surface area of alveolar type I epithelial cells with increasing doses of ozone. An asterisk (*) indicates statistical significance at the level of $p < 0.05$ when compared with the mean of the control group.

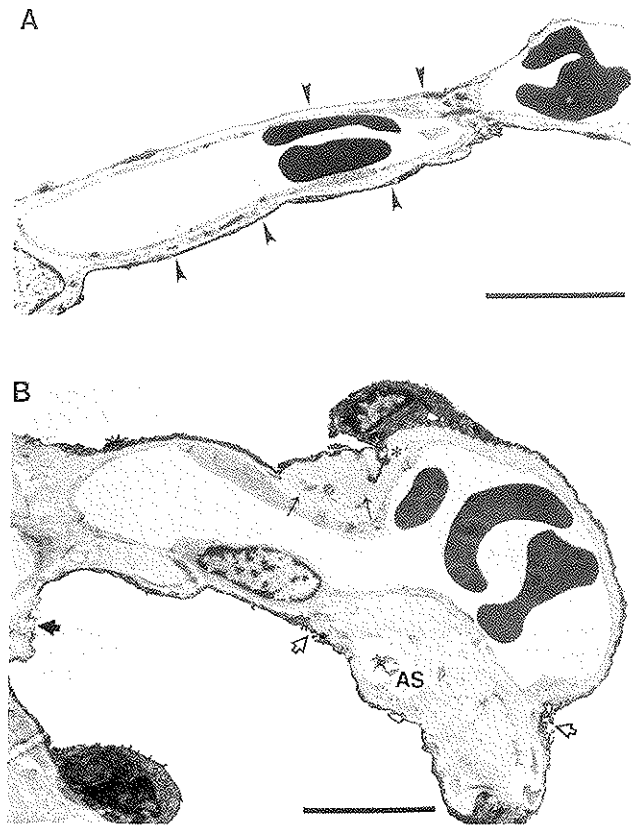

Figure 10. Comparison of type I epithelial cells. A: The septa from a control rat lung with thin flattened type I epithelial cells (filled arrowheads). B: Type I epithelial cells in the septa of a rat lung after prolonged exposure to 1.0 ppm ozone. Epithelial surface ruffling (open arrows show examples) and a small area of cellular necrosis (filled arrow) were observed. The basement membrane (*)was greatly thickened, and contained inclusions (small thin arrows). AS = acelluar space. Bar = 5 μm.

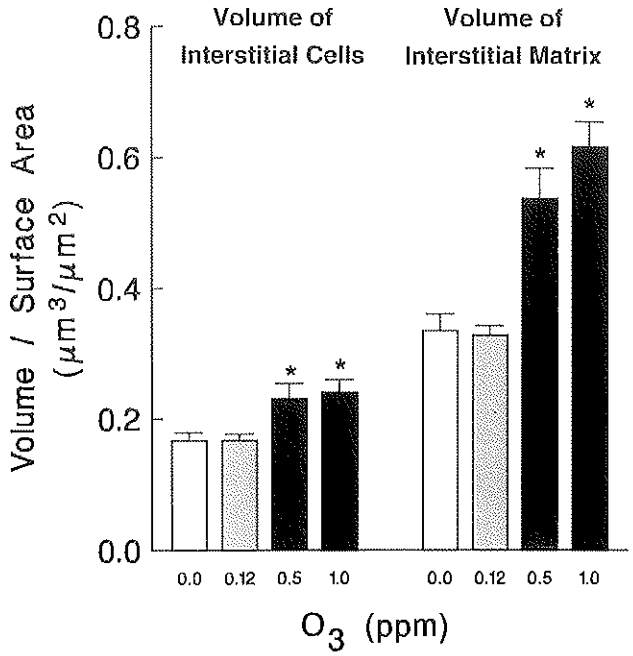

Figure 11. Changes in the volumes of interstitial cells and matrix components in the proximal alveolar region with exposure to ozone. An asterisk (*) indicates statistical significance at the level of $p < 0.05$, when compared with the mean value for the control group.

Interstitium

The volume of the interstitium increased as a function of ozone concentration. No difference in interstitial volume was noted between control rats and those exposed to 0.12 ppm ozone; however, the volume of interstitium was significantly increased after exposure to 0.5 or 1.0 ppm ozone (Figure 11). The vector of key variables for interstitial injury consisted of the cellular components and the compartments making up the interstitial matrix: acellular space, basement membrane, collagen, and elastin (Figure 12). Exposure to ozone had a significant effect on the volume of each of these variables. Elastin and acellular space were significantly elevated after exposure to 1.0 ppm ozone, and the volumes of cellular interstitial components, collagen, and the basement membrane were significantly increased after exposure to 0.5 or 1.0 ppm ozone.

The total interstitial volume increased 53% after exposure to 0.5 ppm ozone, with a 40% increase in the cellular component and a 60% increase of the noncellular component (Figure 11). After 1.0 ppm exposure to ozone, total interstitial volume increased 71%, with a 44% increase of the cellular component and an 84% increase of the noncellular components (Figure 11). The increase in the volume of cellular interstitium was due mainly to an increase in interstitial fibroblasts (Figure 13) that constituted approximately 80% of all interstitial cells. The increase of interstitial volume after exposure to 0.5 ppm ozone arises from small increases of both the number of fibroblasts and their mean cell size. Exposure to 1.0 ppm ozone, on the other hand, resulted in a significant increase in the number (Figure 13), but no increase in the mean cell volume, of interstitial fibroblasts. Furthermore, neither the number or volume of interstitial cells was changed after ozone exposure.

Of the total noncellular interstitium, 40% to 50% is occupied by collagen (Figure 12). After 20 months of exposure to 0.5 ppm ozone, the volume of collagen increased 64%, and after exposure to 1.0 ppm ozone, the volume increased 78% (Figure 12). Figure 14 shows an example of increased deposition of collagen fibers in the interstitium of rats exposed to 1.0 ppm ozone for 20 months. Basement membrane accounts for 22% to 26% of the noncellular interstitium. Exposure to 0.5 or 1.0 ppm ozone induced thickening of the basement membrane. The magnitude of changes were similar to those observed with collagen (Figure

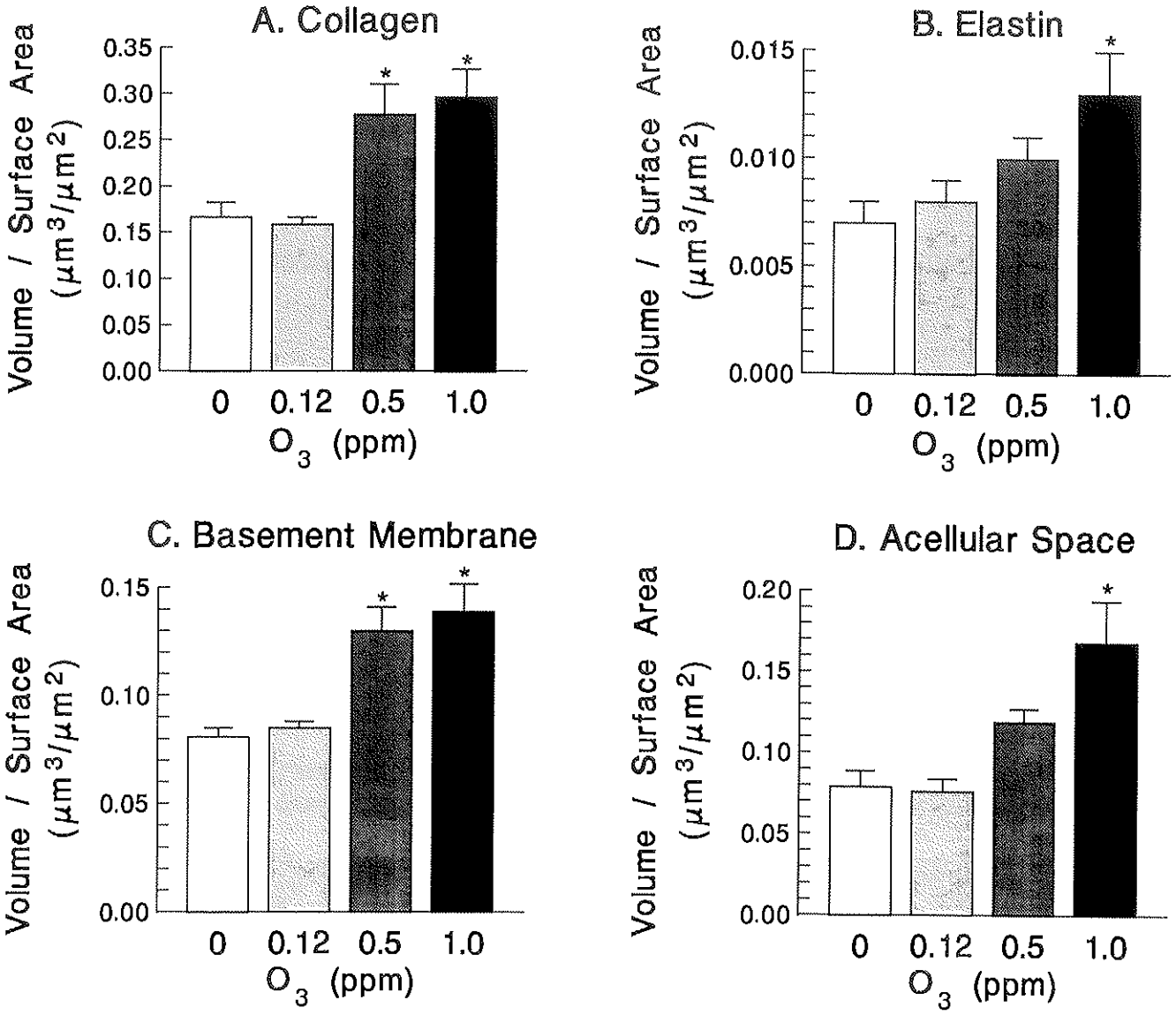

Figure 12. Changes in volumes of alveolar interstitial matrix components in rats exposed to 0, 0.12, 0.5 or 1.0 ppm O_3. Volumes are expressed as the ratios of volume to surface area of epithelial basement membrane (volume/surface area). An asterisk (*) indicates statistical significance at the level of $p < 0.05$ when compared with the mean value for the control group.

13). The thickened basement membranes contained inclusion bodies (Figure 15), the origin of which is not known. Elastin makes up only 2% of the total noncellular interstitium, and is mainly localized at septal tips. Exposure to 1.0 ppm ozone for 20 months caused an 80% increase in the volume of elastin (Figure 12). Acellular space made up 22% to 27% of the noncellular interstitium, and its volume increased 113% by exposure to 1.0 ppm ozone (Figure 12).

Endothelium and Capillaries

The vectors of primary variables for vascular injury were the volume of endothelium and the surface area of capillaries. No significant change in the volume of endothelium was observed in this study. The mean cell volume and the mean cell surface area of capillary endothelial cells remained unaltered after 20 months of exposure to either 0.12, 0.5, or 1.0 ppm ozone. The number of endothelial cells

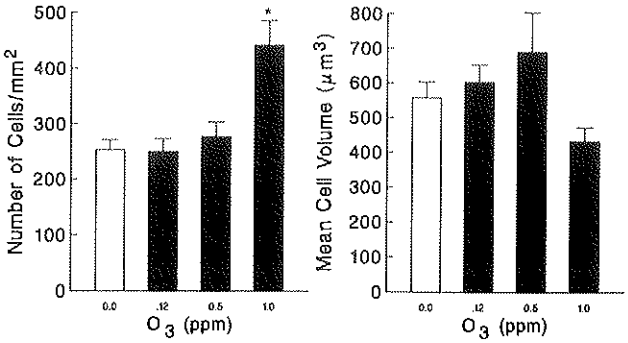

Figure 13. Changes in number and mean cell volume of interstitial fibroblasts after prolonged O_3 exposure. An asterisk (*) indicates statistical significance at the level of $p < 0.05$ when compared with the mean value for the control group.

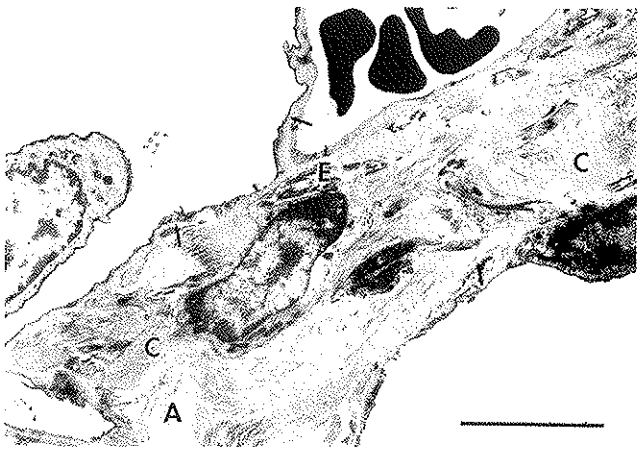

Figure 14. An alveolar septum of a rat lung exposed for 20 months to 1.0 ppm ozone. Increased deposition of collagen (C) was noted. Elastin (E), acellular spaces (A), and basement membrane (arrows) are shown. Bar = 5 μm.

increased slightly after exposure to 1.0 ppm ozone. A concentration effect was observed and found to be due to a significant increase in the capillary surface area after exposure to 0.5 ppm ozone. However, exposure to 0.12 or 1.0 ppm ozone did not cause significant change in the parameter of capillary surfaces. The inconsistency of the trend of ozone effect on capillary surface suggests that the change found after 0.5 ppm ozone may not be biologically significant.

Evidence of Inflammation

The primary variable used for analyzing inflammation was the volume of the inflammatory cells (the sum of the alveolar and interstitial macrophages). An ozone concentration effect was found for inflammatory cells by MANOVA. Exposure to 0.12 or 0.5 ppm ozone for 20 months did not change either the number or the size of alveolar macrophages. However, rats exposed to 1.0 ppm ozone exhibited

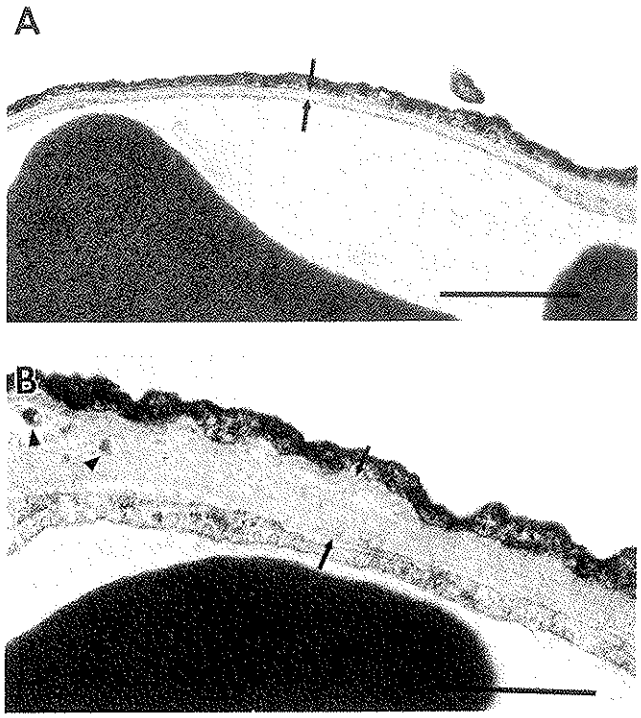

Figure 15. Comparison of epithelial basement membranes. A: Thin epithelial basement membrane (between the arrows) from a control rat lung. B: Thickened epithelial basement membrane (between the arrows) from a rat lung exposed to 1.0 ppm O_3 for 20 months. Inclusion bodies (filled triangles) are found in the basement membrane. Bar = 1 μm.

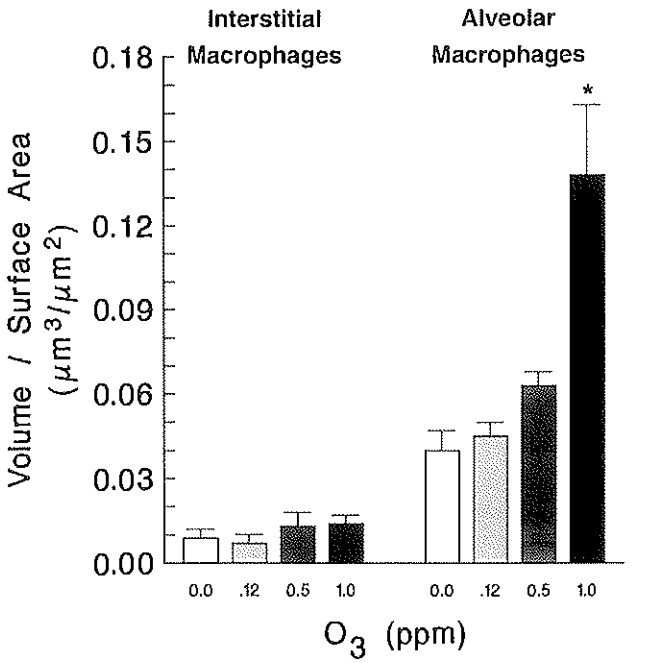

Figure 16. Changes in the volumes of alveolar and interstitial macrophages after prolonged exposure to O_3. An asterisk (*) indicates statistical significance at the level of $p < 0.05$ when compared with the mean of the control group.

a 113% increase in alveolar macrophages in the proximal alveolar region (Figure 16). Interstitial macrophages were rare in all exposure groups, and no significant changes in the volume of interstitial macrophages were noted after ozone exposure. Other inflammatory cells such as neutrophils and monocytes were not included in the quantitative analysis because previous studies with subchronic and prolonged exposures to ozone had shown little or no involvement of these cells. Qualitative examination of the sections in this study confirmed the near absence of neutrophils and monocytes in the proximal alveolar regions of rats exposed to 0.12, 0.5 or 1.0 ppm ozone for 20 months.

EFFECTS OF OZONE EXPOSURE ON RANDOM ALVEOLAR REGIONS

Because previous studies have shown that the effects of 0.12 ppm ozone are strictly confined to the proximal alveolar regions, the morphometric study of random alveolar regions was carried out only with animals exposed to 0.5 or 1.0 ppm ozone. The set of primary variables listed in Table 1 was assessed with MANOVA. No statistically significant ozone concentration effect was found. Table 6 lists the means and standard deviations of the primary variables studied from control rats and rats exposed to ozone. Because the epithelium of the distal alveolar regions, which constitute the great majority of the gas exchange region from which the alveolar region blocks were randomly selected, is composed completely of alveolar type I and type II epithelial cells, the percentage of bronchiolarization measured in all exposure groups was not significantly different from the control group. Type I and type II epithelial volumes were not altered by the exposures. The volumes of cellular interstitium and interstitial matrix and the volumes of the components of the interstitial matrix also were not changed by exposure to any concentration of ozone. The ultrastructure of the alveolar epithelial cells, interstitial fibroblasts, and capillary endothelial cells was normal. No significant increase of inflammatory cells was noted in either the alveolar spaces or in the interstitium. Further studies of the group exposed to 0.12 ppm ozone were not performed because no effect was found for the higher ozone doses.

EFFECTS OF OZONE EXPOSURE ON TERMINAL BRONCHIOLES

Multivariate analysis was carried out using the primary variables listed in Table 2. Statistically significant effects of exposure to 1.0 ppm ozone were observed in the number of ciliated cells, the number of Clara cells (Figure 17), and the mean cell volume of Clara cells. In addition, no effect was found for the thickness of the terminal bronchiole epithelium (Table 7), the mean cell volume of ciliated cells, the mean luminal surface areas of both ciliated and Clara cells, and the average diameter of terminal bronchioles.

Five types of cells were studied from the terminal bronchioles, ciliated cells, Clara cells, brush cells, preciliated cells, and unidentified cells. Exposure to 1.0 ppm ozone for 20 months was found to cause a 13% reduction in the total number of cells per unit of basement membrane (mm^2) in terminal bronchioles (Table 7). This reflects the combined result of a cell population shift with loss of ciliated cells but an increase in Clara cells. The total number of ciliated cells reduced 37% from 11,508 cells/mm^2 to 7,255 cells/mm^2 of basement membrane surface area. The percentage of cili-

Table 6. Measurements for the Primary Variables of Lung Injury in the Random Alveolar Regions[a]

Variable	Ozone Concentration[b] (ppm) 0.0 ($n = 10$)	0.5 ($n = 12$)	1.0 ($n = 11$)
Percentage of bronchiolarization	0	0	0.34 ± 0.23
Tissue volume ($\mu m^3/\mu m^2$)[c]			
Type I epithelial cells	0.24 ± 0.01	0.21 ± 0.01	0.22 ± 0.01
Interstitium	0.49 ± 0.03	0.45 ± 0.03	0.53 ± 0.03
Endothelium	0.23 ± 0.02	0.21 ± 0.01	0.23 ± 0.01
Total inflammatory cells	0.05 ± 0.01	0.02 ± 0.01	0.03 ± 0.01
Surface area of capillaries ($\mu m^2/\mu m^2$)[c]	88 ± 3	93 ± 2	91 ± 2

[a] All values are given as means ± SE. No significant differences were found between the means.

[b] Data for 0.12 ppm O_3 were not analyzed for random alveolar regions.

[c] Measurements of volume and surface area were normalized to the surface area of epithelial basement membrane.

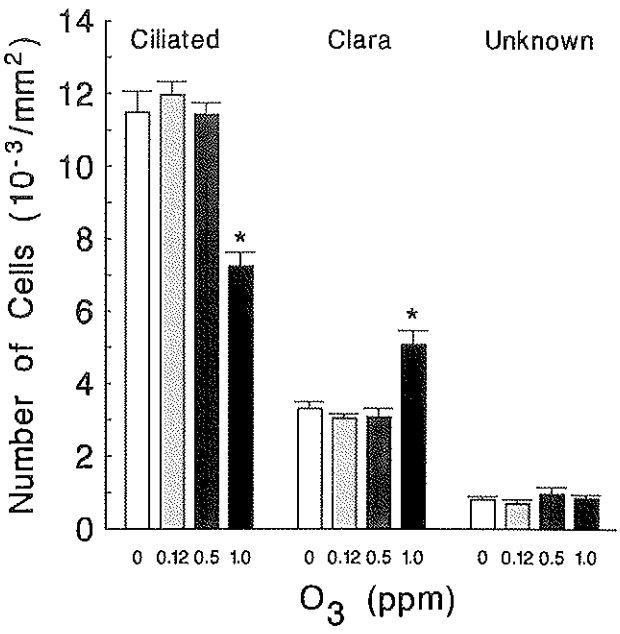

Figure 17. Changes in the numbers of the major cell types in the terminal bronchioles with prolonged exposure to ozone. An asterisk (*) indicates statistical significance at the level of $p < 0.05$ when compared with the mean of the control group.

ated cells in terminal bronchioles decreased from 71% in control rats to 51% in rats exposed to 1.0 ppm ozone. Despite the loss of ciliated cells from terminal bronchioles, the characteristics of these cells remained normal except for a 20% increase of their basement membrane surface area. The surface area of cilia per cell was not changed. However, due to the reduced number of ciliated cells (Figure 17), the total density of ciliated surface (or cilia) in terminal bronchioles was reduced (Table 7). In contrast to ciliated cells, the number of Clara cells in terminal bronchioles increased 54% after exposure to 1.0 ppm ozone, and the volume fraction of Clara cells increased from 21% to 36% of terminal bronchiolar cells. The size of the dome or luminal surface of Clara cells was not affected, but the average size of Clara cells decreased 13%. Aside from swollen cilia, the ultrastructure of ciliated cells and Clara cells was normal.

Brush cells were identified by their brush borders and filament bundles. They consisted of only 2% (by number) of the terminal bronchiolar cells in rats exposed to 0.0 ppm, 0.12 ppm, and 0.5 ppm ozone. Exposure to 1.0 ppm ozone increased the percentage of brush cells in terminal bronchioles to approximately 3%. Preciliated cells, a percussor of ciliated cells containing basal bodies and fibrinogen granules, were found to become smaller after exposure to 0.5 ppm ozone, and had a reduced basal surface area. These minor changes did not follow dose patterns and are probably random variability resulting from the small number of both cell types found in the terminal bronchioles.

DISCUSSION

The major findings of our morphometric studies of rats exposed to 0.0, 0.12, 0.5, or 1.0 ppm ozone for 20 months are summarized here.

1. Exposure to 0.12 ppm ozone had no effect on the anatomical regions we examined.
2. Extensive epithelial metaplasia occurred in the proximal alveolar ducts of rats exposed to 0.5 or 1.0 ppm

Table 7. Morphometric Measurements of Terminal Bronchioles[a]

Variable	Ozone Concentration (ppm)			
	0.0 ($n = 10$)	0.12 ($n = 12$)	0.5 ($n = 8$)	1.0 ($n = 8$)
Diameter (μm)	233 ± 5	243 ± 8	227 ± 12	218 ± 9
Thickness of Epithelium (μm)	7.2 ± 0.3	7.2 ± 0.2	6.7 ± 0.2	6.5 ± 0.2
Number of cells (cells/mm^2)	16,258 ± 529	16,309 ± 370	16,452 ± 646	14,099 ± 410[b]
Surface density of cilia (mm^2/mm^2)[c]	5.32 ± 0.47	5.52 ± 0.38	4.62 ± 0.31	3.43 ± 0.35[b]

[a] All values are given as means ± SE.

[b] $p < 0.05$. Bonferroni-corrected t test on concentration factor means compared control to ozone exposure concentrations. Significant effects of concentration were revealed by MANOVA. Significant effects were revealed by ANOVA for concentration with number of ciliated cells, number of Clara cells, and surface density of cilia.

[c] Expressed as total ciliated surface area on a unit (mm^2) surface of epithelium basement membrane.

ozone. Cuboidal epithelial cells identical to those in normal terminal bronchioles were found in the proximal alveolar region.

3. Exposure to 0.5 or 1.0 ppm ozone resulted in significant thickening of the interstitium. The volumes of the interstitial matrix components (collagen, basement membrane, elastin, and acellular spaces) increased.
4. The number of ciliated cells decreased in the terminal bronchioles of rats exposed to 1.0 ppm ozone, and the number of Clara cells increased.
5. The effects of ozone exposure were restricted to the central acinar regions. No exposure effect was detected by morphometric analysis of tissues from random alveolar regions.

The F344/N rats have been noted to have a predilection for developing leukemia after two years of age. Up to 25% of the animals we studied manifested clinical evidence of leukemia, although only one animal had substantial lung involvement, and that animal was found in the control group. Nevertheless, the incidence of leukemia for the entire NTP/HEI Collaborative Ozone Project animals did not differ among exposure groups (NTP 1994; Boorman et al. 1995) Because of the prevalence of spleen and liver leukemia in our group of rats, we examined the possibility that the changes induced by leukemia might mask the effects of ozone exposure (due to increased variability) by performing the statistical analysis twice, once including and once excluding animals with leukemia. The results of these analyses suggest that the possible effects of leukemia did not significantly affect the results of this study.

No previous animal studies have rigorously evaluated a possible gender-related sensitivity or resistance to ozone. The inclusion of both genders of rats in the present exposure provided an opportunity to address possible effects of gender on ozone toxicity. Our analysis found few interactions between gender and ozone exposure that were biologically significant. A previous study of the effects of ozone on human lung function has found that females are more sensitive to acute ozone exposure than males and that these changes are not related to body size alone (Messineo and Adams 1990). The lack of a gender-related effect on ozone toxicity in our study does not preclude the possibility that such a result could have occurred if the male and female rats had received different doses of ozone. The female rats had significantly smaller body weights and total lung volumes than the male rats, and yet the epithelial basement membrane surface density in the proximal alveolar region of male and female rats was similar. The effects of smaller lungs and, therefore, different ventilatory rates and tidal volumes on the site-specific dose of inhaled ozone on female rats cannot yet be accurately determined. Ventilatory unit volume in male rats has been shown to vary greatly, and larger ventilatory units are predicted to have a greater uptake of a reactive gas such as ozone (Mercer et al. 1991). The average size and number of ventilatory units also may differ between genders.

A dramatic increase in total epithelial volume occurred (Tables 1 and 2) and was due to metaplasia of the normal squamous epithelium to cuboidal epithelium in rats exposed for 20 months to 0.5 or 1.0 ppm ozone. Furthermore, an increase in bronchiolar metaplasia was noted in the animals exposed to 0.5 or 1.0 ppm ozone, and the increase was larger with the higher dose. The exposure to 0.12 ppm did not result in bronchiolar metaplasia of the epithelium. Bronchiolar epithelial metaplasia is a well documented result of longer exposure to higher doses of ozone (Fujinaka 1985; Barr et al. 1988; Hiroshimo et al. 1989; Pinkerton et al. 1993). Pinkerton and coworkers (1993) examined tissues from the same animals that we used in this study and, using light microscopy, found extensive bronchiolar metaplasia of the alveolar ducts extending into alveolar outpockets and into the ventilatory unit to 1,000 μm from the bronchiole–alveolar duct junction. This metaplasia was observed to be heterogenous in nature and contained cells with full-length cilia and cells that expressed Clara-cell secretory protein, a unique marker for Clara cells. We found the bronchiolar metaplasia to be composed mainly of ciliated and Clara cells that were structurally identical to those found in terminal bronchioles. The ciliated cells in the metaplastic epithelium showed signs of injury to the cilia. The swollen and abnormal cilia were similar to those noted in previous studies (Chang et al. 1988).

Despite the presence of ciliated and Clara cells that were structurally identical to those in terminal bronchioles, the metaplasia was not simply a continuation of the terminal bronchiolar epithelium. In contrast to the terminal bronchioles that contained a small number of preciliated cells, no preciliated cells could be identified in the bronchiolar metaplastic tissue. Instead, we found a cuboidal cell type that was not present in terminal bronchioles from any of the rats, but was observed only in the proximal alveolar region of rats exposed to 0.5 or 1.0 ppm ozone and had increased greatly at the higher level of exposure. These cuboidal cells had structural characteristics similar to many different cell types; for example, fiber bundles found in brush cells, granules found in Clara cells, and basal bodies found in ciliated cells. These cells may serve as stem cells, or may be transformed epithelial cells.

The origin of the stem cells responsible for the bronchiolarized epithelial metaplasia in lung injury is not known. The two cell types with known stem-cell functions in the area of the bronchiole–alveolar duct junction are type II

epithelial cells (Adamson and Bowden 1975) and Clara cells (Nettesheim et al. 1990). Clara cells have been found to have a limited range of differentiation in culture and produce only Clara and ciliated cells (Brody et al. 1987). The metaplastic epithelium in our study was composed mainly of Clara and ciliated cells, but also contained a population of cuboidal cells having diffuse structural characteristics. An alternative theory of bronchiolar metaplasia resulting from a common stem cell for both Clara and type II cells is controversial. Some investigators reject this theory (Kawanami 1982), although there is a growing body of evidence to support the presence of a common stem cell for both bronchiolar and alveolar cell types in a number of models describing cell development and injury. Bronchiolarization, including cells containing cilia, has been found to result from proliferation of type II cells in models of injnry that involve oxygen (Kapanci et al. 1969) or bleomycin (Adamson and Bowden 1979). A model of experimental pneumonia that progresses to fibrosis uses animals that contain cells that are structurally intermediate between Clara and type II cells, and that also produce protein associated with surfactant (Rhodes et al. 1990). Clara and type II cells appear to have a common ancestry in developing lungs (McDougall and Smith 1974) and these cells have been found to share common antigens (Erlinger et al. 1991). Examining the pattern of bronchiolar metaplasia in the animals exposed to 0.5 or 1.0 ppm ozone using scanning electron microscopy revealed patches of ciliated cells deep in alveolar outpockets, apparently completely surrounded by unbronchiolarized epithelium. Because these isolated groups of ciliated cells were apparently not connected to the epithelium of the terminal bronchioles, it would be difficult to explain their presence on the basis of down-growth from terminal bronchioles. If de novo production of bronchiolar tissue from an alveolar type II stem cell does not explain this phenomenon, the only other source of cells that could be responsible for this bronchiolarization is the presence of pores in the alveolar septa through which these areas may be connected to adjacent terminal bronchiolar tissue. Alveolar pores are known to increase in aged animals (Martin 1963; Boatman et al. 1983; Shimura et al. 1986).

Tbe exposure to ozone for 20 months did not cause substantial changes in the squamous epithelium normally present in the proximal alveolar region. The type II epithelium did not show a hyperplastic response, and the type I epithelium was only slightly thickened. In animals exposed to 0.5 or 1.0 ppm ozone, a significant increase was apparent in the number of type I cells, and a decrease in their average size and surface area. The change in the composition of the type I epithelium evidenced by increased numbers of smaller cells is consistent with previous findings after prolonged exposure to low levels of ozone (Chang et al. 1992), and may indicate an increase in cell turnover rates in response to ozone exposure. Although type II cells are the progenitors of type I cells, increased turn over in type I cells does not necessarily demand an increase in the type II cell population. In response to a chronic injury, a balance may be reached between the rate of proliferation of type II cells and the rate of differentiation of type II cells into type I cells.

Previous exposures of rats to an ambient level of ozone for 18 months have resulted in a thickening of the type I epithelium and in proliferation of type II epithelial cells (Chang et al. 1992). In the present study, however, exposure to 0.12 ppm ozone had no effect on the alveolar epithelium. One possible explanation for this variation in epithelial response is the difference in exposure regimen between the two studies. The ambient pattern used consisted of a 0.06-ppm background concentration for 13 hours, and a ramped nine-hour spike to a maximum concentration of 0.25 ppm (integrated concentration, 0.19 ppm); this regimen was followed seven days a week. A continuous background ozone concentration (including weekends) may be important in inducing the thickening of type I epithelial cells. The 0.12-ppm exposure in the present study did not involve a background level, and the exposure was broken at weekends. It should be noted that the exposure to 0.12 ppm ozone for six hours per day was found to affect the proximal alveolar tissue in these animals (Pinkerton et al. 1993). Thickened alveolar septal tips were found within 300 µm from the bronchiole–alveolar duct junction (Pinkerton et al. 1995). In our study, tissue was analyzed from around the first alveolar duct bifurcation, typically between 500 µm and 600 µm from the junction. The ozone concentration at tbis distance may have been too diluted to cause cell injury. Rats exposed to 0.5 or 1.0 ppm ozone also did not show significantly thickened type I epithelium. Again, the absence of any background exposure may be a factor. However, the metaplasia that we found to be characteristic in response to the higher ozone concentrations may have modified the overall response of type I and type II epithelium.

In addition to epitbelial changes, 0.5 and 1.0 ppm ozone induced structural alterations in the alveolar interstitium. Prolonged exposure of rats to ozone has been found to result in alveolar septal fibrosis (Chang et al. 1992). We found an increased volume of both cellular and noncellular interstitium in rats exposed for 20 months to 0.5 or 1.0 ppm ozone. This response was related to dose, in that a greater dose of ozone resulted in an increased volume of total interstitial matrix components. The increase in cellular interstitium was due mainly to an increase in interstitial fibroblasts. Furthermore, collagen synthesis rates have been observed

to increase in animals exposed to ozone (Last and Greenberg 1980), and collagen crosslinking has been found to be abnormal during ozone exposure and to be characteristic of collagen in fibrotic lungs (Reiser et al. 1987). We found an increase in all noncellular components of the interstitium, including collagen, elastin, basement membrane, and the acellular spaces. The noncellular matrix was mainly composed of collagen, but the acellular space, the volume of which correlates with the amount of edema in the tissue, and represents the deposition of other matrix proteins such as fibronectin, had the greatest percentage of change. The increase in collagen with prolonged exposure also may be enhanced by a reduction in the rates of collagen degradation. Also, abnormal collagen has been found after six months of recovery from prolonged ozone exposure, but it is not clear if this is due to irreversible deposition of collagen or a continued alteration in collagen metabolism (Reiser et al. 1987). The surface density of the epithelial basement membrane did not change with exposure to ozone, but the basement membrane greatly increased in volume with exposure.

Interstitial thickening may be important for the bronchiolar metaplasia that occurred with exposure to 0.5 or 1.0 ppm ozone. The extracellular matrix serves as a scaffolding for the epithelial cells, and also has been shown to modulate cell phenotypes. The thickened basement membrane found as a result of ozone exposure may play an important role in this respect. Previous studies suggest that the basement membrane is continuously remodeled during development (Grant et al. 1983). The basement membrane components, fibronectin and laminin, have been shown to affect type II cell differentiation. Type II cells have been found to maintain differentiation when cultured on laminin-rich matrices, and to lose differentiated characteristics when cnltured on fibronectin-rich matrices (Rannels and Rannels 1989a). Treatment with antifibronectin antibodies also causes a rapid loss of type II cell differentiation in culture (Rannels and Rannels 1989b). Increased production of fibronectin has been found in patients with idiopathic pulmonary fibrosis, a disease that causes bronchiolar metaplasia and pulmonary fibrosis (Kuhn et al. 1989; Limper et al. 1991). Thickening of the basement membrane or changes in its components alone may not be sufficient to trigger bronchiolar metaplasia. A similar degree of basement membrane thickening was observed after the 18-month ambient pattern of ozone exposure, but no bronchiolarization was found (Chang et al. 1992). Studies of basement membrane components and their effects on differentiation have sbown that antilaminin antibodies do not prevent the differentiation of mouse type II cells in culture (Zimmerman et al. 1985), and that basement membrane components alone will not maintain rat type II cells in culture, nor allow complete differentiation of type I cells from type II to occur (Adamson et al. 1989). Transforming growth factor–β (β-TGF) has been shown to stimulate bronchiolar epithelial cells to undergo squamous metaplasia (Jetten et al. 1986; Masui et al. 1986). It is possible that basement membrane changes are needed in concert with induced cytokine or growth factor release by the high-dose ozone exposures to trigger type II cells or another stem cell to form bronchiolarized metaplasia.

The role of alveolar epithelial cells in producing the interstitial fibrosis that results from prolonged ozone exposure is unknown. Type II cells and Clara cells have been shown to produce β-TGF in patients with idiopathic pulmonary fibrosis (Khalil et al. 1991). Transforming growth factor–β also has been identified in alveolar macrophages and bronchiolar epithelium in a model of fibrotic injury in rats (Khalil et al. 1989). Transforming growth factor–β is known to increase the rate of collagen synthesis (Khalil et al. 1989) and to activate extracellular collagen accumulation (Fine and Goldstein 1987). Another source of cytokines is inflammatory cells. Alveolar macrophages have been reported to release a number of growth factors that may stimulate epithelial and fibroblast proliferation. Previous studies of prolonged exposure to low levels of ozone found no increase in alveolar macropbages (Chang et al. 1992). We noted a significant increase in alveolar macrophage volume only in the animals exposed to 1.0 ppm ozone. Although alveolar macrophages may contribute to the fibrosis observed, other factors are likely to be equally important. Collagen increased in response to exposure to 0.5 ppm ozone without an increase in alveolar macrophages.

The role of bronchiolar epithelial metaplasia in the tbickening of the basement membrane also is not known, and it is not known whether the basement membrane changes proceed or follow the epithelial metaplasia. Thickened basement membranes have been observed in rats exposed chronically to low levels of ozone during which bronchiolar metaplasia does not occnr (Chang et al. 1992). Type II cells are known to synthesize basement membrane in culture (Zimmermann et al. 1985) and to remodel the basement membrane surface (Rannels et al. 1992). Fetal cell lines derived from type II cells have been found to produce collagen in culture (Federspiel et al. 1990). Increased synthesis and deposition of extracellular matrix by the alveolar epithelium is likely to have been responsible for the thickened basement membrane.

Dosimetry modeling predicts that the intrapulmonary ozone concentration of inhaled ozone decreases drastically within a few generations of alveolar ducts beyond the bronchiole–alveolar duct junction because of the tremendous expansion of surface area in the gas exchange region

(Miller et al. 1985; Overton et al. 1987). The concentration of ozone decreases in the conducting airways at a relatively slow rate because air flow is fast and the proportional surface area for absorption is smaller. The higher concentrations of ozone used in this study may cause injury to the more distal areas of the lung. This effect of dose could not be evaluated in our study because the samples were taken from a fixed position in the centriacinar region of rats in all exposure groups. Pinkerton and coworkers (1993) examined tissues from the same animals in a longitudinal fashion (whereas we studied tissues cut in cross sections) to correlate tissue response with distance from the bronchiole–alveolar duct junction. It may be possible to define the area affected with respect to ozone concentration on longitudinal sections.

Barry and associates (1985, 1988) found that 0.25 ppm ozone caused epithelial and interstitial changes in the proximal alveolar regions but not in terminal bronchioles. We found that exposure only to 1.0 ppm ozone resulted in significant structural alterations in terminal bronchioles. In addition, the changes in terminal bronchioles were less pronounced than were the changes in the proximal alveolar regions, which indicates that terminal bronchioles are somewhat resistant to ozone damage. Given this reduced response of the bronchiolar tissue to ozone damage, the extensive bronchiolar metaplasia seen in response to exposures to higher doses of ozone may indicate that a mechanism operates to protect bronchiolar tissue from the continued ozone insult. The major effect of ozone on terminal bronchioles was a loss of the number of ciliated cells. Despite a normal mean ciliated surface area in ciliated cells, the total ciliated surface in terminal bronchioles was significantly reduced by the exposure to 1.0 ppm ozone.

When the effect of ozone on the gas exchange region as a whole was analyzed using randomly selected alveolar regions as samples, no change was detected with the ozone concentrations studied. This observation is consistent with previous reports that injury from exposure to ozone is limited to the central acinar regions of the lung.

The critical question that the NTP/HEI Collaborative Ozone Project set out to examine was whether exposure to ozone caused development of chronic lung diseases such as fibrosis or emphysema. Prolonged exposures to 0.5 and 1.0 ppm ozone induced extensive remodeling of the proximal alveolar tissues that are known to be most vulnerable to ozone. Epithelial metaplasia and interstitial fibrosis were found in these regions. However, no evidence of emphysematous changes followed ozone exposures. The levels of ozone exposure studied here did not cause fibrosis or epithelial injury beyond the proximal alveolar regions. The observed changes may not be severe enough to cause clinically significant lung disease. It is not known whether prolonged exposures (for example, exposures as long as humans encounter), may cause extension of the tissue changes into the distal gas exchange regions. Although the terminal bronchioles were more resistant to ozone exposure, other scientists and we have shown that both low and high doses of ozone cause either loss of cilia or loss of ciliated cells that culminates in a decrease of total cilia in the airways. The loss of cilia is likely to impair clearance of particles in terminal airways. Harkema and coworkers studied the transport of mucus in the nasal epithelium from rats in the NTP/HEI Collaborative Ozone Project and found drastically reduced movement of cilia (Harkema et al. 1994). Loss of cilia function can further aggravate transport and clearance in the terminal bronchioles. In addition, ozone may act synergistically with other airborne pollutants and modify or enhance the development of other chronic lung diseases such as asbestosis or idiopathic pulmonary fibrosis. Although the present study did not find significant effects of ozone on the lungs of rats, the possibility of harmful effect by 0.12 ppm of ozone cannot be readily dismissed. Rodent and primate lungs differ greatly in structure. The actual dose that is delivered to cells in the lung parenchyma is likely to be different in rats and humans. The toxicity of an ambient concentration of ozone administrated to rats cannot be extrapolated to its toxicity to humans until the cellular doses in the two species can be determined. Finally, increasing evidence suggests that environmental pollutants including ozone increase morbidity (Bates 1991). Increased atmospheric concentrations of ozone are likely to affect sensitive populations such as people with asthma or pulmonary disease (Krzyzanowski et al. 1992; Molfino et al. 1992). The impact of prolonged exposure to ambient concentrations of ozone cannot, therefore, be fully evaluated until further studies on the effects of ozone on particle clearance, its synergistic effects on sensitive populations, and issues of dosimetry have been examined.

ACKNOWLEDGMENTS

The authors would like to express their appreciation for the skillful assistance of Ann Blinkhouse, Barbara Bell, Katharine McIntyre, and Robert Nielsen.

REFERENCES

Abraham WM, Januszkiewicz AJ, Mingle WM, Wanner A, Sackner MA. 1980. Sensitivity of bronchoprovocation and tracheal mucous velocity in detecting airway response to

ozone. J Appl Physiol: Respirat Environ Exercise Physiol 48:789–793.

Adamson IYR, Bowden DH. 1975. Derivation of type I epithelium from type II cells in the developing rat lung. Lab Invest 32:736–745.

Adamson IYR, Bowden DH. 1979. Bleomycin-induced injury and metaplasia of alveolar type II cells. Am J Pathol 96:531–538.

Adamson IYR, King GM, Young L. 1989. Influence of extracellular matrix and collagen components on alveolar type II cell morphology and function. In Vitro 25:494–502.

Avol EL, Linn WS, Shamoo DA, Valencia LM, Anzar UT, Venet TG, Hackney JD. 1985. Respiratory effects of photochemical oxidant air pollution in exercising adolescents. Am Rev Respir Dis 132:619–622.

Barr BC, Hyde DM, Plopper CG, Dungworth DL. 1988. Distal airway remodeling in rats chronically exposed to ozone. Am Rev Respir Dis 137:924–938.

Barry BE, Crapo JD. 1985. Application of morphometric methods to study diffuse and focal injury in the lung caused by toxic agents. CRC Crit Rev Toxicol 13:1–32.

Barry BE, Mercer RR, Miller FJ, Crapo JD. 1988. Effects of inhalation of 0.25 ppm ozone on the terminal bronchioles of juvenile and adult rats. Exp Lung Res 14:225–245.

Barry BE, Miller FJ, Crapo JD. 1985. Effects of 0.12 and 0.25 parts per million ozone on the proximal alveolar region of juvenile and adult rats. Lab Invest 53:692–704.

Bates DV. 1991. Unanswered questions about asthma. Health Environ 5:1–2.

Boatman ES, Ward G, Martin CJ. 1983. Morphometric changes in rabbit lungs before and after pneumonectomy and exposure to ozone. J Appl Physiol 54:778–784.

Boorman GA, Schwartz LW, Dungworth DL. 1980. Pulmonary effects of prolonged ozone insult in rats: Morphometric evaluation of the central acinus. Lab Invest 63:108–115.

Brody AR, Hook GER, Cameron GS, Jetten AM, Butterick CJ, Nettesheim P. 1987. The differentiation capacity of Clara cells isolated from the lungs of rabbits. Lab Invest 57:219–229.

Calderon-Garcidueñas L, Osorno-Velasquez A, Bravo-Alvarez H, Delgado-Chavez R, Barrios-Marquez R. 1992. Histopathologic changes of the nasal mucosa in Southwest Metropolitan Mexico City inhabitants. Am J Pathol 140:225–232.

Castleman WL, Dungworth DL, Schwartz LW, Tyler WS. 1980. Acute respiratory bronchiolitis: An ultrastructural and autoradiographic study of epithelial cell injury and renewal in rhesus monkeys exposed to ozone. Am J Pathol 98:811–840.

Castleman WL, Tyler WS, Dungworth D. 1977. Lesions in respiratory bronchioles and conducting airways of monkeys exposed to ambient levels of ozone. Exp Mol Pathol 26:384–400.

Chang LY, Crapo JD. 1990. Quantitative evaluation of minimal injuries. In: Models of Lung Disease: Microscopy and Structural Methods (Gil JG, ed.) pp. 597–640. Marcel Dekker, New York, NY.

Chang LY, Huang Y, Stockstill BL, Graham JA, Grose EC, Ménache MG, Miller FJ, Costa DL, Crapo JD. 1992. Epithelial injury and interstitial fibrosis in the proximal alveolar regions of rats chronically exposed to a simulated pattern of urban ambient ozone. Toxicol Appl Pharmacol 115:241–252.

Chang LY, Mercer RR, Stockstill BL, Miller FJ, Graham JA, Ospital JJ, Crapo JD. 1988. Effects of low levels of NO_2 on terminal bronchiolar cells and its relative toxicity compared to ozone. Toxicol Appl Pharmacol 96:451–464.

Dungworth DL, Cross CE, Gillespie JR, Plopper CG. 1975. The effect of ozone on animals. In: Ozone Chemistry and Technology: A review of the literature, 1961–1974 (Murphy JS, Orr JR, eds.) pp. 29–54. Franklin Institute, Philadelphia, PA.

Erlinger R, Rauh G, Schumacher U, Welsch U, Zöllner N. 1991. Similar frequency of autoantibodies against pneumocytes type II and Clara cells in patients with interstitial lung disease and healthy persons. Klin Wochenschr 69:297–302.

Eustis SL, Schwartz LW, Kosch PC, Dungworth DL. 1981. Chronic bronchiolitis in nonhuman primates after prolonged ozone exposure. Am J Pathol 105:121–137.

Evans MJ, Johnson LV, Stephens RJ, Freeman GT. 1976a. Cell renewal in the lungs of rats exposed to low levels of ozone. Exp Mol Pathol 24:70–83.

Evans MJ, Johnson LV, Stephens RJ, Freeman GT. 1976b. Renewal of the terminal bronchiolar epithelium in one rat following exposure of NO_2 or O_3. Lab Invest 35:246–257.

Federspiel SJ, DiMari SJ, Guerry–Force ML, Haralson MA. 1990. Extracellular matrix biosynthesis by cultured fetal rat lung epithelial cells: II. Effects of acute exposure to epidermal growth factor and retinoic acid on collagen biosynthesis. Lab Invest 63:455–466.

Fine A, Goldstein RH. 1987. The effect of transforming growth factor–β on cell proliferation and collagen formation by lung fibroblasts. J Biol Chem 262:3897–3902.

Folinsbee LJ, Horvath SM, Raven PB, Bedi JF, Morton AR, Drinkwater BL, Bolduan NW, Gliner JA. 1977. Influence of exercise and heat stress on pulmonary function during ozone exposure. J Appl Physiol 43:409–413.

Fujinaka LG, Hyde DM, Plopper CG, Tyler WS, Dungworth DL, Lollini LO. 1985. Respiratory bronchiolitis following long-term ozone exposure in Bonnet monkeys: A morphometric study. Exp Lung Res 8:167–190.

Golden JA, Nadel JA, Boushey HA. 1978. Bronchial hyperirritability in healthy subjects after exposure to ozone. Am Rev Respir Dis 118:287–294.

Grant MM, Cutts NR, Brody JS. 1983. Alterations in lung basement membrane during fetal growth and type II cell development. Dev Biol 97:173–183.

Gross KB, White HJ. 1987. Functional and pathological consequences of a 52-week exposure to 0.5 ppm ozone followed by a clean air recovery period. Lung 165:283–295.

Gundersen HJG. 1977. Notes on the estimation of the numerical density of arbitrary profiles: The edge effect. J Microsc Biol Cell 111:219–223.

Harkema JR, Morgan KT, Gross, EA, Catalano, PJ, Griffith, WC. 1994. Consequences of Prolonged Inhalation of Ozone on F344/N Rats: Collaborative Studies, Part VII, Effects on the Nasal Mucociliary Apparatus. Research Report Number 65. Health Effects Institute, Cambridge, MA

Hazucha MJ. 1987. Relationship between ozone exposure and pulmonary function changes. J Appl Physiol 62:1671–1680.

Ibrahim AL, Zee YC, Osebold JW. 1980. The effects of ozone on the respiratory epithelium of mice: II. Ultrastructural alterations. J Environ Pathol Toxicol 3:251–158.

Jetten AM, Shirley JE, Stoner G. 1986. Regulation of proliferation and differentiation of respiratory tract epithelial cells by TGF. Exp Cell Res 167:539–549.

Kapanci Y, Weibel ER, Kaplan HP, Robinson FR. 1969. Pathogenesis and irreversibility of pulmonary lesions of oxygen toxicity in monkeys: II. Ultrastructural and morphometric studies. Lab Invest 20:101–118.

Kawanami O, Ferrans VJ, Crystal RC. 1982. Structure of alveolar epithelial cells in patients with fibrotic lung disorders. Lab Invest 46:39–53.

Khalil N, Bereznay O, Sporn M, Greenberg AH. 1989. Macrophage production of transforming growth factor-β and fibroblast collagen synthesis in chronic pulmonary inflammation. J Exp Med 170:727–737.

Khalil N, O'Connor RN, Unruh HW, Warren PW, Flanders KC, Kemp A, Bereznay OH, Greenberg AH. 1991. Increased production and immunolocalization of transforming growth factor –β in idiopathic pulmonary fibrosis. Am J Respir Cell Mol Biol 5:155–162.

Kreit JW, Gross KB, Moore TB, Lorenzen TJ, D'Arcy J, Eschenbacher WL. 1989. Ozone-induced changes in pulmonary function and bronchial responsiveness in asthmatics. J Appl Physiol 66:217–222.

Krzyzanowski M, Quackenboss JJ, Lobewitz MD. 1992. Relationship of peak expiratory flow rates and symptoms of ambient ozone. Arch Environ Health 47:107–115.

Kuhn C, Boldt J, King T, Crouch E, McDonald JA. 1989. Immunohistochemical detection of architectural changes and fibroblast phenotype in human pulmonary fibrosis. Am Rev Respir Dis 140:1693–1703.

Kulle TJ, Sauder LR, Hebel JR, Chatham MD. 1985. Ozone response relationships in healthy nonsmokers. Am Rev Respir Dis 132:36–41.

Last JA, Gerriets JE, Hyde DM. 1983. Synergistic effects on rat lungs of mixtures of oxidant air pollutant (ozone or nitrogen dioxide) and respirable aerosols. Am Rev Respir Dis 128:539–544.

Last JA, Greenberg DB. 1980. Ozone-induced alterations in collagen metabolism of rat lungs: II. Long-term exposures. Toxicol Appl Pharmacol 55:108–114.

Limper AH, Broekelmann TJ, Colby TV, Malizia G, McDonald JA. 1991. Analysis of local mRNA expression for extracellular matrix proteins and growth factors using in situ hybridization in fibro-proliferative lung disorders. Chest 99:55S–56S.

Martin HB. 1963. The effects of ageing on the alveolar pores of Kohn in the dog. Am Rev Respir Dis 88:773–778.

Masui T, Wakefield LM, Lechner JF, LaVeck MA, Sporn MB, Harris CC. 1986. Type beta transforming growth factor is the primary differentiation-inducing serum factor for normal human bronchial epithelial cells. Proc Natl Acad Sci USA 83:2438–2442.

Mauderly JL. 1984. Respiratory function responses of animals and man to oxidant gases and to pulmonary emphysema. J Toxicol Environ Health 13:345–361.

McDonnell WF, Chapman RS, Leigh MW, Strope GL, Collier AM. 1985. Respiratory responses of vigorously exercising children to 0.12 ppm ozone exposure. Am Rev Respir Dis 132:875–879.

McDonnell WF, Horstman DH, Hazucha MJ, Seal E Jr, Haak ED, Salaam SA, House DE. 1983. Pulmonary effects of ozone exposure during exercise: Dose-response characteristics. J Appl Physiol 54:1345–1352.

McDougall J, Smith JF. 1974. The development of the human type II pneumocyte. J Pathol 115:245–251.

Mellick PW, Dungworth DL, Schwartz LW, Tyler WS. 1977. Short term morphologic effects of high ambient levels of ozone on lungs of rhesus monkeys. Lab Invest 36:82–90.

Mercer RR, Anjilvel S, Miller FJ, Crapo JD. 1991. Inhomogeneity of ventilatory unit volume and its effects on reactive gas uptake. J Appl Physiol 70:2193–2205.

Messineo TD, Adams WC. 1990. Ozone inhalation effects in females varying widely in lung size: Comparison with males. J Appl Physiol 69:96–103.

Miller FJ, Overton JH, Jaskot RH, Menzel DB. 1985. A model of the regional uptake of gaseous pollutants in the lung: I. The sensitivity of the uptake of ozone in the human lung to lower respiratory tract secretions and exercise. Toxicol Appl Pharmacol 79:11–27.

Molfino NA, Wright SL, Katz I, Tarlo S, Silverman F, McClean PA, Szalai JP, Raizenne M, Slutsky AS, Zamel N. 1992. Effects of low concentration of ozone on inhaled allergen responses in asthmatic subjects. Lancet 338:199–203.

National Toxicology Program. 1994. Toxicology and Carcinogenesis Studies of Ozone and Ozone/NNK in F344/N Rats and B6C3F$_1$ Mice: Inhalation Studies. NTP Technical Reports CAS 10028-15-6 and CAS 10028-15-6/64091-91-4; NIH Publication 94-3371. National Technical Information Service (NTIS), Springfield, VA.

Nettesheim P, Jetten AM, Inayama Y, Brody AR, George MA, Gilmore LB, Gray T, Hook GER. 1990. Pathways of differentiation of airway epithelial cells. Environ Health Perspect 85:317–329.

Overton JH, Graham RC, Miller FJ. 1987. A model of the regional uptake of gaseous pollutants in the lung: II. The sensitivity of ozone uptake in laboratory animal lungs to anatomical and ventilatory parameters. Toxicol Appl Pharmacol 88:418–432.

Pinkerton KE, Barry BE, O'Neil JJ, Raub JA, Pratt PC, Crapo JD. 1982. Morphometric changes in the lung during the lifespan of Fischer 344 rats. Am J Anat 164:155–174.

Pinkerton KE, Dodge DE, Cederdahl–Demmler J, Wong VJ, Peake J, Haselton CJ, Mellick PW, Singh G, Plopper CG. 1993. Differentiated bronchiolar epithelium in alveolar ducts of rats exposed to ozone for 20 months. Am J Pathol 142:947–956.

Pinkerton KE, Ménache MG, Plopper CG. 1995. Consequences of Prolonged Inhalation of Ozone on F344/N Rats: Collaborative Studies, Part IX, Changes in the Tracheobronchial Epithelium, Pulmonary Acinus, and Lung Antioxidant Enzyme Activity. Research Report Number 65, Health Effects Institute, Cambridge, MA.

Plopper CG, Dungworth DL, Tyler WS, Chow CK. 1979. Pulmonary alterations in rats exposed to 0.2 and 0.1 ppm ozone: A correlated morphological and biochemical study. Arch Environ Health 34:390–395.

Rannels DE, Dunsmore SE, Grove RN. 1992. Extracellular matrix synthesis and turnover by type II pulmonary epithelial cells. Am J Physiol: Lung Cell Mol Physiol 262(6):L582–L589.

Rannels SR, Rannels DE. 1989a. The type II pneumocyte as a model of lung cell interaction with the extracellular matrix. J Mol Cell Cardiol 21:151–159.

Rannels DE, Rannels SR. 1989b. Influence of extracellular matrix on type II cell differentiation. Chest 96:165–173.

Reiser KM, Tyler WS, Hennessy SM, Dominguez JJ, Last JA. 1987. Long-term consequences of exposure to ozone: II. Structural alterations in lung collagen of monkeys. Toxicol Appl Pharmacol 89:314–322.

Rhodes GC, Kumar RK, Lykke AWJ, Tapsall JW. 1990. Atypical differentiation of bronchiolar epithelial cells following experimental pneumonia. Virchows Arch [B] 59:343–347.

Schwartz LW, Dungworth DL, Mustafa MG, Tarkington BK, Tyler WS. 1976. Pulmonary responses of rats to ambient levels of ozone: Effects of 7-day intermittent or continuous exposure. Lab Invest 34:565–578.

Shimura S, Boatman ES, Martin CJ. 1986. Effects of ageing on the alveolar pores of Kohn and on the cytoplasmic components of alveolar type II cells in monkey lungs. J Pathol 148:1–11.

Stephens RJ, Evans MJ, Freeman G. 1974. Alveolar type I cell response to exposure to 0.5 ppm ozone for short periods. Exp Mol Pathol 20:11–23.

Tepper JS, Wiester MJ, Weber MF, Fitzgerald S, Costa DL. 1991. Chronic exposure to a simulated urban profile of ozone alters ventilatory responses to carbon dioxide challenge in rats. Fundam Appl Toxicol 17:52–50.

Vincent R, Mercer RR, Chang L, Miller FJ, Costa DL, Crapo JD. 1992. Quantitative ultrastructural analysis of connective tissue in the lungs. In: New Methods in Ozone Toxicology: Abstracts of Six Pilot Studies, pp. 24–27. HEI Communications Number 1. Health Effects Institute, Cambridge, MA.

Woody DM, Woody EZ, Crapo JD. 1979. Determination of the mean caliper diameter of lung nuclei by a method which is independent of shape assumptions. J Microsc Biol Cell 118:421–477.

Zimmermann B, Barrach H-J, Merker H-J, Hinz H. 1985. Basement membrane formation and lung cell differentiation in vivo. Eur J Cell Biol 36:66–73.

APPENDIX A. Identification of Specific Animals in Exposure Groups

Table A.1. Specific Animals Studied

Exposure Groups (ppm O_3)	Gender	Identification Numbers
0	M	H37, H45, H61[a], H117, H125
	F	H41, H49, H53[b], H57[a], H65[a], H121, H129[c]
0.12[d]	M	H38, H46, H54[a], H62[a], H118, H126
	F	H42, H50, H58[a], H66[a], H122, H130
0.5	M	H39, H47, H55[a,e], H63[a,e], H119, H127
	F	H43, H51, H59[a,e], H67[a,e], H123, H131
1.0	M	H40, H48, H56[a,e], H64[a,f], H120, H128
	F	H44, H52, H60[a,e], H68[a,e], H124, H132

[a] Animals that had pulmonary function tests performed on them before they were killed.

[b] Animal H53 in this group died before the end of the exposure. Its lungs were not processed for morphometric analysis. Therefore, this group had five animals (see footnote c).

[c] Animal H129 in this group had marked lung involvement of leukemia. It was excluded from the final statistical analysis. Therefore, this group had five animals (see footnote b).

[d] No animals in this group were studied in the morphometric analysis of the proximal alveolar region.

[e] Animals not used in the morphometric studies of the proximal alveolar region and terminal bronchioles.

[f] This animal died during pulmonary function testing and was not available for further analysis. Therefore, this group had five animals.

APPENDIX B. Morphometric Characteristics of Tissues in the Proximal Alveolar Region of Rat Lungs

Table B.1. Tissue Volumes Normalized to Epithelial Basement Membrane Surface Area in the Proximal Alveolar Region of Rat Lungs[a]

Type of Tissue or Cell	Ozone Concentration (ppm)			
	0.0 ($n = 10$)	0.12 ($n = 12$)	0.5 ($n = 8$)	1.0 ($n = 8$)
Total Tissue	1.177 ± 0.075	1.178 ± 0.053	1.746 ± 0.154[b]	2.105 ± 0.120[b]
Epithelium	0.395 ± 0.048	0.381 ± 0.032	0.659 ± 0.093[b]	0.870 ± 0.086[b]
Alveolar	0.289 ± 0.013	0.301 ± 0.017	0.291 ± 0.019	0.285 ± 0.020
Type I cells	0.209 ± 0.007	0.224 ± 0.010	0.212 ± 0.013	0.210 ± 0.014
Type II cells	0.073 ± 0.012	0.072 ± 0.011	0.071 ± 0.009	0.071 ± 0.009
Bronchiolar	0.106 ± 0.043	0.080 ± 0.022	0.369 ± 0.106[b]	0.585 ± 0.104[b]
Ciliated cells	0.067 ± 0.032	0.048 ± 0.015	0.169 ± 0.045	0.259 ± 0.053[b]
Clara cells	0.033 ± 0.013	0.030 ± 0.008	0.160 ± 0.046[b]	0.213 ± 0.044[b]
Other cells	0.006 ± 0.003	0.001 ± 0.001	0 040 ± 0.017	0.113 ± 0.024[b]
Interstitium	0.501 ± 0.036	0.496 ± 0.020	0.768 ± 0.066[b]	0.858 ± 0.044[b]
Cellular	0.167 ± 0.012	0.168 ± 0.009	0.231 ± 0.023[b]	0.241 ± 0.019[b]
Fibroblasts	0.136 ± 0.009	0.141 ± 0.007	0.175 ± 0.014	0.185 ± 0.007[b]
Macrophages	0.009 ± 0.003	0.007 ± 0.003	0.013 ± 0.005	0.014 ± 0.003
Matrix	0.335 ± 0.025	0.328 ± 0.014	0.537 ± 0.046[b]	0.617 ± 0.038[b]
Collagen	0.167 ± 0.016	0.159 ± 0.008	0.278 ± 0.033[b]	0.297 ± 0.030[b]
Elastin	0.007 ± 0.001	0.008 ± 0.001	0.010 ± 0.001	0.013 ± 0.002[b]
Basement membrane	0.081 ± 0.004	0.085 ± 0.003	0.130 ± 0.011[b]	0.139 ± 0.013[b]
Acellular space	0.079 ± 0.010	0.076 ± 0.008	0.119 ± 0.008	0.168 ± 0.026[b]
Endothelium	0.240 ± 0.015	0.256 ± 0.014	0.255 ± 0.016	0.239 ± 0.008
Capillaries	1.340 ± 0.096	1.413 ± 0.062	1.510 ± 0.079	1.144 ± 0.034
Plasma	0.885 ± 0.085	0.897 ± 0.062	0.931 ± 0.068	0.731 ± 0.011
Red blood cells	0.455 ± 0.019	0.516 ± 0.021	0.578 ± 0.047	0.413 ± 0.029
Alveolar macrophages	0.040 ± 0.007	0.045 ± 0.005	0.063 ± 0.012	0.138 ± 0.025[b]

[a] All values are given as means ± SE for surface area dimensions in $\mu m^3/\mu m^2$.

[b] $p < 0.05$ when compared with control values.

Table B.2. Surface Areas Normalized to Epithelial Basement Membrane Surface Area in the Proximal Alveolar Region of Rat Lungs[a]

Type of Tissue or Cell	Ozone Concentration (ppm)			
	0.0 ($n = 10$)	0.12 ($n = 12$)	0.5 ($n = 8$)	1.0 ($n = 8$)
Epithelium				
Alveolar				
Type I cells	96.2 ± 0.9	97.2 ± 0.4	90.8 ± 2.2[b]	86.4 ± 2.4[b]
Type II cells	1.3 ± 0.2	1.3 ± 0.2	2.0 ± 0.4	1.5 ± 0.2
Bronchiolar				
Ciliated cells	1.8 ± 0.8	1.0 ± 0.3	3.9 ± 1.2	5.9 ± 1.4[b]
Clara cells	0.4 ± 0.1	0.4 ± 0.1	2.2 ± 0.6	3.0 ± 0.7
Other	0.2 ± 0.1	0.0 ± 0.0	1.1 ± 0.6	3.2 ± 1.0
Capillaries	90.4 ± 1.8	92.4 ± 1.4	97.6 ± 2.6	85.4 ± 1.8[b]

[a] All values are given as means ± SE for surface area dimensions in $\mu m^3/\mu m^2$.

[b] $p < 0.05$ when compared with control values.

Table B.3. Tissue Thickness in the Proximal Alveolar Region of Rat Lungs[a]

Type of Tissue or Cell	Ozone Concentration (ppm)			
	0.0 ($n = 10$)	0.12 ($n = 12$)	0.5 ($n = 8$)	1.0 ($n = 8$)
Epithelium				
Alveolar	0.30 ± 0.01	0.31 ± 0.02	0.31 ± 0.02	0.32 ± 0.02
Type I cells	0.22 ± 0.01	0.23 ± 0.01	0.23 ± 0.01	0.24 ± 0.01
Type II cells	5.98 ± 0.59	5.92 ± 0.54	4.47 ± 0.75	4.96 ± 0.35
Bronchiolar	4.52 ± 0.67	5.89 ± 1.40	6.48 ± 1.53	5.26 ± 0.64
Ciliated cells	3.64 ± 0.55	5.65 ± 1.69	5.65 ± 1.19	4.57 ± 0.75
Clara cells	7.36 ± 2.61	11.88 ± 3.64	9.04 ± 1.94	7.97 ± 0.87
Interstitium	0.54 ± 0.04	0.52 ± 0.02	0.82 ± 0.09[b]	1.00 ± 0.06[b]
Endothelium	0.27 ± 0.02	0.28 ± 0.01	0.26 ± 0.01	0.28 ± 0.01

[a] All values are given as means ± SE for surface area dimensions in $\mu m^3/\mu m^2$.

[b] $p < 0.05$ when compared with control values.

Table B.4. Characteristics of Cells in the Proximal Alveolar Region of Rat Lungs[a]

Type of Tissue or Cell	Ozone Concentration (ppm) 0.0 ($n = 10$)	0.12 ($n = 12$)	0.5 ($n = 8$)	1.0 ($n = 8$)
Epithelium				
Alveolar				
Type I cells				
Number (cells/mm^2)	107 ± 11	102 ± 8	175 ± 20[b]	187 ± 16[b]
Average volume (μm^3)	2,170 ± 262	2,325 ± 205	1,299 ± 139[b]	1,183 ± 130[b]
Average cell surface area (μm^2)	10,210 ± 1,232	10,742 ± 1,046	5,825 ± 561[b]	4,938 ± 417[b]
Average basement membrane surface area (μm^2)	9,960 ± 1,187	10,200 ± 987	5,600 ± 561[b]	4,938 ± 417[b]
Type II cells				
Number (cells/mm^2)	119 ± 8	115 ± 12	131 ± 14	41 ± 25
Average volume (μm^3)	607 ± 91	637 ± 66	596 ± 124	596 ± 100
Average cell surface area: Total (μm^2)	258 ± 63	275 ± 37	351 ± 73	259 ± 63
Average cell surface area: Without microvilli (μm^2)	112 ± 20	115 ± 12	162 ± 38	130 ± 29
Bronchiolar				
Ciliated Cells				
Number (cells/mm^2)	124 ± 60	116 ± 36	310 ± 96	512 ± 88[b]
Average volume (μm^3)	617 ± 88	547 ± 180	612 ± 173	490 ± 109
Average cell surface area: Without cilia (μm^2)	160 ± 40	116 ± 38	133 ± 43	95 ± 27
Average cell surface area: Cilia only (μm^2)	571 ± 116	627 ± 272	458 ± 160	428 ± 85
Average basement membrane surface area (μm^2)	186 ± 40	141 ± 59	136 ± 49	114 ± 27
Clara cells				
Number (cells/mm^2)	46 ± 14	59 ± 7	230 ± 58[b]	439 ± 82[b]
Average volume (μm^3)	831 ± 337	886 ± 273	708 ± 200	489 ± 87
Average cell surface area (μm^2)	249 ± 79	184 ± 59	192 ± 80	155 ± 17
Average basement membrane surface area (μm^2)	86 ± 29	137 ± 59	80 ± 25	71 ± 17
Interstitium				
Fibroblasts				
Number (cells/mm^2)	253 ± 18	250 ± 23	277 ± 26	442 ± 41[b]
Average volume (μm^3)	588 ± 45	603 ± 49	690 ± 113	433 ± 39
Interstitial macrophages				
Number (cells/mm^2)	24 ± 5	27 ± 6	30 ± 4	50 ± 11
Average volume (μm^3)	780 ± 261	593 ± 318	447 ± 160	339 ± 100
Alveolar macrophages				
Number (cells/mm^2)	35 ± 6	37 ± 7	47 ± 11	92 ± 21
Average volume (μm^3)	2,778 ± 1,312	1,308 ± 234	1,646 ± 317	2,389 ± 820
Endothelium cells				
Number (cells/mm^2)	512 ± 325	551 ± 49	576 ± 55	608 ± 57[b]
Average volume (μm^3)	475 ± 29	486 ± 31	646 ± 45	418 ± 39
Average cell surface area (μm^2)	1,820 ± 93	1,800 ± 132	1,788 ± 173	1,495 ± 143

[a] Values are given as means ± SE. All numbers of cells (except for alveolar macrophages) are normalized to the epithelial basement membrane surface area.

[b] $p < 0.05$ when compared with control values.

APPENDIX C. Morphometric Characteristics of Tissues in Random Alveolar Regions of Rat Lungs

Table C.1. Morphometrically Determined Characteristics of Tissues in the Random Alveolar Regions[a]

Type of Tissue or Cell	0.0 (n = 10)	0.5 (n = 11)	1.0 (n = 10)
Normalized Tissue Volume (μm)			
Total Tissue	1.123 ± 0.066	0.970 ± 0.060	1.122 ± 0.052
Epithelium			
Alveolar	0.348 ± 0.034	0.286 ± 0.018	0.334 ± 0.026
Type I cells	0.241 ± 0.014	0.207 ± 0.018	0.225 ± 0.008
Type II cells	0.075 ± 0.014	0.073 ± 0.010	0.076 ± 0.013
Interstitium	0.494 ± 0.027	0.445 ± 0.034	0.532 ± 0.025
Cellular	0.156 ± 0.012	0.135 ± 0.014	0.174 ± 0.012
Fibroblasts	0.142 ± 0.012	0.122 ± 0.010	0.161 ± 0.010
Other	0.013 ± 0.004	0.013 ± 0.006	0.012 ± 0.004
Matrix	0.338 ± 0.019	0.310 ± 0.021	0.358 ± 0.018
Collagen	0.108 ± 0009	0.099 ± 0.008	0.118 ± 0.013
Basement membrane	0.049 ± 0.006	0.050 ± 0.004	0.063 ± 0.006
Acellular space	0.181 ± 0.014	0.160 ± 0.014	0.177 ± 0.009
Endothelium	0.228 ± 0.016	0.214 ± 0.014	0.226 ± 0.006
Capillaries	1.463 ± 0.125	1.442 ± 0.079	1.349 ± 0.042
Plasma	0.972 ± 0.098	0.876 ± 0.069	0.819 ± 0.034
Red blood cells	0.492 ± 0.034	0.566 ± 0.040	0.530 ± 0.030
Alveolar macrophages	0 053 ± 0.014	0.024 ± 0.006	0.030 ± 0.009
Surface Area ($\mu m^3/\mu m^2$)			
Epithelium			
Alveolar			
Type I cells	98.6 ± 0.2	98.6 ± 0.3	93.0 ± 0.3
Type II cells	1.1 ± 0.2	1.4 ± 0.3	1.0 ± 0.3
Capillaries	88.0 ± 2.9	93.0 ± 1.9	91.0 ± 1.9
Tissue Thickness (μm)			
Epithelium			
Alveolar			
Type I cells	0.24 ± 0.01	0.21 ± 0.01	0.23 ± 0.01
Type II cells	7.19 ± 0.79	6.17 ± 0.69	7.62 ± 0.87
Interstitium	0.53 ± 0.03	0.46 ± 0.04	0.56 ± 0.03
Endothelium	0.27 ± 0.03	0.23 ± 0.02	0.25 ± 0.01

[a] All values are given as means ± SE.

APPENDIX D. Morphometric Characteristics of Terminal Bronchiolar Cells in Rat Lungs

Table D.1. Morphometrically Determined Characteristics of Cells in the Terminal Bronchioles[a]

Characteristic	0.0 ($n = 10$)	0.12 ($n = 12$)	0.5 ($n = 8$)	1.0 ($n = 8$)
Ciliated cells				
Number (cells/mm^2)	11,507 ± 568	11,976 ± 356	11,427 ± 329	7,255 ± 380[b]
Average volume (μm^3)	363 ± 14	373 ± 11	357 ± 13	390 ± 20
Average basement membrane surface area (μm^2)	62 ± 2	62 ± 1	64 ± 3	75 ± 3[b]
Average luminal surface area (μm^2)				
Total	507 ± 31	512 ± 28	457 ± 25	533 ± 52
Without cilia	49 ± 2	50 ± 1	52 ± 1	58 ± 2[b]
Cilia only	458 ± 31	463 ± 28	405 ± 25	475 ± 51
Percentage of total number (cells/mm^2)	72%	73%	69%	51%
Percentage of volume of epithelium	69%	64%	62%	44%
Nonciliated bronchiolar cells (Clara cells)				
Number (cells/mm^2)	3,311 ± 193	3,048 ± 116	3,079 ± 233	5,092 ± 380[b]
Average volume (μm^3)	681 ± 18	726 ± 29	678 ± 39	591 ± 33
Average basement membrane surface area (μm^2)	60 ± 4	58 ± 3	58 ± 3	65 ± 3
Average luminal surface area (μm^2)	169 ± 9	161 ± 9	157 ± 11	133 ± 8[b]
Percentage of total number (cells/mm^2)	20%	19%	19%	36%
Percentage of volume of epithelium	33%	31%	31%	47%
Brush cells				
Number (cells/mm^2)	273 ± 39	266 ± 47	315 ± 66	391 ± 42
Average volume (μm^3)	307 ± 23	218 ± 25	262 ± 40	317 ± 64
Average basement membrane surface area (μm^2)	44 ± 6	39 ± 8	38 ± 14	59 ± 17
Average luminal surface area (μm^2)	29 ± 6	30 ± 8	21 ± 5	23 ± 5
Percentage of total number (cells/mm^2)	2%	2%	2%	3%
Percentage of volume of epithelium	1%	1%	1%	2%
Unknown cells				
Number (cells/mm^2)	822 ± 83	715 ± 108	973 ± 183	862 ± 90
Average volume (μm^3)	237 ± 24	234 ± 20	213 ± 7	263 ± 14
Average basement membrane surface area (μm^2)	72 ± 5	74 ± 4	69 ± 5	82 ± 5
Average luminal surface area (μm^2)	29 ± 6	30 ± 8	21 ± 5	23 ± 5
Percentage of total number (cells/mm^2)	5%	4%	6%	6%
Percentage of volume of epithelium	3%	2%	3%	4%
Preciliated cells				
Number (cells/mm^2)	344 ± 110	304 ± 120	660 ± 303	499 ± 121
Average volume (μm^3)	467 ± 124	244 ± 80	216 ± 66	530 ± 52
Average basement membrane surface area (μm^2)	58 ± 18	31 ± 9	28 ± 7	114 ± 22[b]
Average luminal surface area (μm^2)	67 ± 20	37 ± 14	27 ± 10	66 ± 6
Percentage of total number (cells/mm^2)	2%	2%	4%	3%
Percentage of volume of epithelium	3%	2%	2%	4%

[a] All values are given as means ± SE.

[b] $p < 0.05$ when compared with control values.

APPENDIX E. Morphometric Characteristics of Proximal Alveolar Tissues in Male and Female Rat Lungs

Table E.1. Morphometric Characteristics of Tissue in the Proximal Alveolar Region of Male Rat Lungs[a]

Characteristic	0.0 ($n = 5$)	0.12 ($n = 6$)	0.5 ($n = 4$)	1.0 ($n = 4$)
Body weight (g)	531.86 ± 20.41	529.30 ± 9.95	508.60 ± 10.11	515.53 ± 19.96
Lung volume (mL)	14.10 ± 0.26	13.67 ± 0.31	13.91 ± 0.55	14.66 ± 0.62
Basement membrane surface density (cm^2/cm^3)	432.60 ± 50.42	452.12 ± 44.31	439.24 ± 69.84	419.87 ± 31.77
Tissue Volume ($\mu m^3/\mu m^2$)				
Total tissue	1.237 ± 0.141	1.188 ± 0.081	1.801 ± 0.282	2.232 ± 0.088[b]
Epithelium (total)	0.426 ± 0.089	0.390 ± 0.042	0.645 ± 0.184	0.982 ± 0.048[b]
Alveolar	0.284 ± 0.018	0.279 ± 0.019	0.297 ± 0.039	0.255 ± 0.023
Type I cells	0.209 ± 0.015	0.222 ± 0.018	0.208 ± 0.026	0.193 ± 0.010
Type II cells	0.065 ± 0.011	0.051 ± 0.008	0.084 ± 0.017	0.057 ± 0.015
Bronchiolar	0.142 ± 0.081	0.111 ± 0.033	0.348 ± 0.209	0.726 ± 0.069[b]
Ciliated cells	0.097 ± 0.060	0.062 ± 0.021	0.151 ± 0.084	0.337 ± 0.057[b]
Clara cells	0.040 ± 0.022	0.046 ± 0.012	0.147 ± 0.091	0.234 ± 0.023[b]
Other	0.005 ± 0.002	0.001 ± 0.001	0-050 ± 0.036	0.156 ± 0.023[b]
Interstitium	0.520 ± 0.072	0.497 ± 0.029	0.826 ± 0.106[b]	0.902 ± 0.036[b]
Cellular	0.161 ± 0.023	0.162 ± 0.013	0.239 ± 0.029	0.233 ± 0.016
Fibroblasts	0.130 ± 0.019	0.135 ± 0.014	0.172 ± 0.015	0.184 ± 0.010
Macrophages	0.010 ± 0.004	0.004 ± 0.001	0.019 ± 0.009	0.011 ± 0.004
Matrix	0.360 ± 0.049	0.335 ± 0.019	0.587 ± 0.077[b]	0.669 ± 0.028[b]
Collagen	0.184 ± 0.032	0.173 ± 0.012	0.306 ± 0.059	0.308 ± 0.041
Elastin	0.008 ± 0.002	0.007 ± 0.001	0.011 ± 0.001	0.011 ± 0.002
Basement membrane	0.078 ± 0.007	0.084 ± 0.004	0.143 ± 0.018[b]	0.148 ± 0.017[b]
Acellular space	0 090 ± 0.016	0.071 ± 0.007	0.128 ± 0.008	0.201 ± 0.033[b]
Endothelium	0.252 ± 0.029	0.251 ± 0.012	0.256 ± 0.023	0.231 ± 0.004
Capillaries	1.585 ± 0.105	1.557 ± 0.069	1.570 ± 0.116	0.164 ± 0.066
Plasma	1.103 ± 0.090	1.018 ± 0.075	0.971 ± 0.049	0.742 ± 0.020
Red blood cells	0.482 ± 0.035	0.540 ± 0.020	0.600 ± 0.072	0.422 ± 0.053
Alveolar macrophages	0.038 ± 0.013	0.050 ± 0.009	0.074 ± 0.019	0.117 ± 0.043

(Table continues next page.)

[a] All values are given as means ± SE for surface area dimensions in $\mu m^3/\mu m^2$. All volumes and surface areas are normalized to the surface density of epithelial basement membranes.

[b] $p < 0.05$ when compared with control values.

Table E.1. Morphometric Characteristics of Tissue in the Proximal Alveolar Region of Male Rat Lungs[a] *(continued)*

Characteristic	0.0 ($n = 5$)	0.12 ($n = 6$)	0.5 ($n = 4$)	1.0 ($n = 4$)
Surface Area ($\mu m^2/\mu m^2$)				
Epithelium				
Alveolar				
Type I cells	95.82 ± 1.68	96.83 ± 0.61	90.69 ± 3 95	83.56 ± 3.21[b]
Type II cells	1.05 ± 0.18	0.97 ± 0.24	1.48 ± 0.42	1.16 ± 0.27
Bronchiolar				
Ciliated cells	2.39 ± 1.41	1.41 ± 0.59	3.62 ± 2.05	6.91 ± 1.69
Clara cells	0.43 ± 0.20	0.72 ± 0.21	2.71 ± 1.11[b]	3.57 ± 0.77[b]
Other cuboidal cells	0.13 ± 0.09	0	1.43 ± 1.14	4.77 ± 1.74[b]
Capillaries	91.45 ± 3.47	93.96 ± 1.57	97.83 ± 5.67	87.28 ± 3.38
Cell Characteristics				
Epithelium				
Alveolar				
Type I cells				
Number (cells/mm^2)	111 ± 17	110 ± 14	165 ± 37	207 ± 28
Average volume (μm^3)	2,080 ± 365	2,217 ± 378	1,195 ± 151	990 ± 137
Average cell surface area (μm^2)	9,600 ± 1,168	10,567 ± 2,015	5,650 ± 764[b]	4,500 ± 668[b]
Average basement membrane surface area (μm)	9,460 ± 1,281	9,950 ± 1,912	5,350 ± 758[b]	4,300 ± 667[b]
Type II cells				
Number (cells/mm^2)	112 ± 13	98 ± 14	124 ± 28	123 ± 44
Average volume (μm^3)	572 ± 43	568 ± 87	753 ± 219	618 ± 199
Average cell surface area: With microvilli (μm^2)	189 ± 39	240 ± 44	295 ± 61	303 ± 113
Average cell surface area: Without microvilli (μm^2)	100 ± 26	103 ± 23	133 ± 50	126 ± 45
Bronchiolar				
Ciliated cells				
Number (cells/mm^2)	174 ± 119	134 ± 63	166 ± 59	645 ± 71
Average volume (μm^3)	675 ± 59	767 ± 305	915 ± 485	575 ± 175
Average basement membrane surface area (μm^2)	200 ± 70	205 ± 102	225 ± 125	119 ± 43
Average luminal cell surface area (μm^2)				
Average lumina cell surface area: Without cilia	201 ± 56	172 ± 60	212 ± 119	117 ± 46
Average luminal cell surface area: Cilia only	768 ± 96	1031 ± 445	580 ± 400	525 ± 109

(Table continues next page.)

[a] All values are given as means ± SE for surface area dimensions in $\mu m^3/\mu m^2$. All volumes and surface areas are normalized to the surface density of epithelial basement membranes.

[b] $p < 0.05$ when compared with control values.

Table E.1. Morphometric Characteristics of Tissue in the Proximal Alveolar Region of Male Rat Lungs[a] *(continued)*

Characteristic	0.0 ($n = 5$)	0.12 ($n = 6$)	0.5 ($n = 4$)	1.0 ($n = 4$)
Clara cells				
Number (cells/mm^2)	57 ± 25	74 ± 32	146 ± 67	543 ± 95[b]
Average volume (μm^3)	660 ± 146	1230 ± 403	976 ± 625	500 ± 144
Average basement membrane surface area (μm^2)	84 ± 35	201 ± 89	140 ± 60	77 ± 26
Average luminal cell surface area (μm^2)	247 ± 71	261 ± 74	305 ± 155	185 ± 69
Interstitium				
Cellular				
Fibroblasts				
Number (cells/mm^2)	240 ± 26	230 ± 27	257 ± 31	440 ± 73
Average volume (μm^3)	552 ± 72	615 ± 81	720 ± 162	450 ± 67
Macrophages				
Number (cells/mm^2)	25 ± 8	31 ± 10	29 ± 6	49 ± 18
Average volume (μm^3)	745 ± 300	218 ± 50	665 ± 264	321 ± 166
Endothelium				
Number (cells/mm^2)	561 ± 24	575 ± 38	556 ± 77	646 ± 104
Average volume (μm^3)	446 ± 35	445 ± 36	485 ± 80	390 ± 65
Average cell surface area (μm^2)	1,640 ± 75	1,683 ± 98	1,850 ± 290	1,465 ± 249
Alveolar macrophages				
Number (cells/mm^2)	39 ± 12	43 ± 11	40 ± 13	100 ± 37
Average volume (μm^3)	4,228 ± 2,963	1,350 ± 343	2,025 ± 330	1,813 ± 1,111

[a] All values are given as means ± SE for surface area dimensions in μm^3/μm^2. All volumes and surface areas are normalized to the surface density of epithelial basement membranes.

[b] $p < 0.05$ when compared with control values.

Table E.2. Morphometric Characteristics of Tissue in the Proximal Alveolar Region of Female Rat Lungs[a]

Characteristic	0.0 ($n = 5$)	0.12 ($n = 6$)	0.5 ($n = 4$)	1.0 ($n = 4$)
Body weight (g)	363.50 ± 10.87	359.58 ± 9.91	342.78 ± 14.38	337.75 ± 7.28
Lung volume (mL)	9.79 ± 0.27	9.99 ± 0.31	10.16 ± 0.62	10.57 ± 0.42
Tissue Volume (μm^3/μm^2)				
Total tissue	1.116 ± 0.058	1.168 ± 0.077	1.691 ± 0.172[b]	1.978 ± 0.222[b]

(Table continues next page.)

[a] All values are given as means ± SE for surface area dimensions in μm^3/μm^2. All volumes and surface areas are normalized to the surface density of epithelial basement membranes.

[b] $p < 0.05$ when compared with control values.

Table E.2. Morphometric Characteristics of Tissue in the Proximal Alveolar Region of Female Rat Lungs[a] *(continued)*

Characteristic	0.0 (n = 5)	0.12 (n = 6)	0.5 (n = 4)	1.0 (n = 4)
Epithelium	0.363 ± 0.046	0.373 ± 0.052	0.674 ± 0.082	0.758 ± 0.155[b]
Alveolar	0.293 ± 0.021	0.323 ± 0.026	0.284 ± 0.007	0.314 ± 0.029
Type I cells	0.208 ± 0.005	0.226 ± 0.011	0.216 ± 0.012	0.228 ± 0.024
Type II cells	0.081 ± 0.021	0.093 ± 0.016	0.058 ± 0.003	0.085 ± 0.005
Bronchiolar	0.070 ± 0.036	0.049 ± 0.028	0.389 ± 0.089[b]	0.444 ± 0.179[b]
Ciliated cells	0.036 ± 0.023	0.034 ± 0.022	0.187 ± 0.048	0.182 ± 0.076
Clara cells	0.026 ± 0.015	0.014 ± 0.006	0.172 ± 0.041	0.193 ± 0.092[b]
Other cells	0.008 ± 0.005	0.001 ± 0.001	0.030 ± 0.007	0.069 ± 0.028[b]
Interstitium	0.482 ± 0.019	0.495 ± 0.030	0.711 ± 0.085[b]	0.815 ± 0.082[b]
Cellular	0.173 ± 0.006	0.174 ± 0.012	0.224 ± 0 040	0.249 ± 0.038
Fibroblasts	0.143 ± 0.005	0.148 ± 0.007	0.179 ± 0.027	0.186 ± 0.035
Macrophages	0.008 ± 0.004	0.010 ± 0.005	0.006 ± 0 003	0.016 ± 0.006
Matrix	0.310 ± 0.014	0.321 ± 0.020	0.487 ± 0.046	0.565 ± 0.065[b]
Collagen	0.150 ± 0.008	0.144 ± 0.008	0.251 ± 0.034[b]	0.285 ± 0.048[b]
Elastin	0.007 ± 0.001	0.010 ± 0.002	0.009 ± 0.003	0.015 ± 0.003
Basement membrane	0.084 ± 0.004	0.087 ± 0.006	0.118 ± 0.009	0.130 ± 0.020[b]
Acellular space	0.068 ± 0.010	0.080 ± 0.015	0.109 ± 0.014	0.135 ± 0.037
Endothelium	0.228 ± 0.010	0.260 ± 0.026	0.255 ± 0.027	0.247 ± 0.016
Capillaries	1.094 ± 0.022	1.269 ± 0.063	1.449 ± 0.116	1.124 ± 0.026
Plasma	0.667 ± 0.028	0.776 ± 0.075	0.892 ± 0.136	0.720 ± 0.009
Red blood cells	0.428 ± 0.008	0.493 ± 0.037	0.557 ± 0.069	0.404 ± 0.032
Alveolar macrophages	0.042 ± 0.009	0.041 ± 0.006	0.051 ± 0.016	0.158 ± 0.026[b]
Surface Area ($\mu m^3/\mu m^2$)				
Basement membrane surface density (cm^2/cm^3)	391.65 ± 28.53	412.57 ± 50.45	349.63 ± 47.20	440.85 ± 37.62
Epithelium				
Alveolar				
Type I cells	96.67 ± 1.02	97.63 ± 0.32	90.98 ± 2.60	89.22 ± 3.49[b]
Type II cells	1.56 ± 0.41	1.61 ± 0.16	2.45 ± 0.62	1.77 ± 0.18
Bronchiolar				
Ciliated cells	1.13 ± 0.61	0.54 ± 0.20	4.13 ± 1.55	4.84 ± 2.30
Clara cells	0.32 ± 0.21	0.13 ± 0 09	1.59 ± 0.48	2.50 ± 1.18[b]
Other cuboidal cells	0.24 ± 0.15	0.04 ± 0.04	0.70 ± 0.27	1.62 ± 0.57[b]
Capillaries	89.28 ± 1.21	90.75 ± 2.29	97.28 ± 0.28	83.61 ± 0.85

(Table continues next page.)

[a] All values are given as means ± SE for surface area dimensions in $\mu m^3/\mu m^2$. All volumes and surface areas are normalized to the surface density of epithelial basement membranes.

[b] $p < 0.05$ when compared with control values.

Table E.2. Morphometric Characteristics of Tissue in the Proximal Alveolar Region of Female Rat Lungs[a] *(continued)*

Characteristic	0.0 ($n = 5$)	0.12 ($n = 6$)	0.5 ($n = 4$)	1.0 ($n = 4$)
Cell Characteristics				
Epithelium				
Alveolar				
Type I cells				
Number (cells/mm^2)	104 ± 14	95 ± 7	166 ± 21	166 ± 11
Average volume (μm^3)	2,260 ± 413	2,433 ± 191	1,403 ± 247	1,375 ± 189
Average cell surface area (μm^2)	10,620 ± 2,296	10,917 ± 860	6,000 ± 928[b]	5,375 ± 487
Average basement membrane surface area (μm^2)	10,460 ± 2,139	10,450 ± 780	5,850 ± 896[b]	5,425 ± 390
Type II cells				
Number (cells/mm^2)	127 ± 11	133 ± 16	138 ± 11	159 ± 28
Average volume (μm^3)	642 ± 187	715 ± 102	430 ± 53	585 ± 104
Average cell surface area (μm^2)	328 ± 119	310 ± 61	408 ± 138	215 ± 68
Average cell surface area: Without microvilli (μm^2)	123 ± 34	126 ± 11	191 ± 61	134 ± 43
Bronchiolar				
Ciliated cells				
Number (cells/mm^2)	73 ± 27	98 ± 40	455 ± 161	380 ± 139
Average volume (μm^3)	540 ± 205	284 ± 88	460 ± 113	406 ± 142
Average cell surface area (μm^2)	167 ± 35	65 ± 23	91 ± 36	109 ± 43
Average cell surface area: Without cilia (μm^2)	106 ± 49	49 ± 20	94 ± 27	73 ± 29
Average cell surface area: Cilia only (μm^2)	310 ± 129	142 ± 58	398 ± 184	330 ± 123
Clara cells				
Number (cells/mm^2)	35 ± 11	44 ± 12	315 ± 80	335 ± 121[b]
Average volume (μm^3)	1,003 ± 699	370 ± 79	575 ± 130	478 ± 121
Average basement membrane surface area (μm^2)	88 ± 52	41 ± 30	50 ± 10	65 ± 24
Average luminal cell surface area (μm^2)	247 ± 156	70 ± 26	136 ± 42	126 ± 46
Interstitium				
Cellular				
Fibroblasts				
Number (cells/mm^2)	265 ± 27	270 ± 38	297 ± 44	443 ± 52
Average volume (μm^3)	564 ± 63	590 ± 63	660 ± 180	415 ± 47
Macrophages				
Number (cells/mm^2)	24 ± 6	23 ± 8	32 ± 7	52 ± 14
Average volume (μm^3)	827 ± 543	1,063 ± 686	229 ± 139	357 ± 136
Endothelium				
Number (cells/mm^2)	463 ± 32	527 ± 93	595 ± 89	569 ± 56
Average volume (μm^3)	504 ± 41	527 ± 47	443 ± 51	445 ± 48
Average cell surface area (μm^2)	2,000 ± 145	1,917 ± 248	1,725 ± 229	1,525 ± 180
Alveolar macrophages				
Number (cells/mm^2)	30 ± 6	31 ± 10	54 ± 20	85 ± 27
Average volume (μm^3)	1,618 ± 413	1,302 ± 351	1,268 ± 515	2,965 ± 1,297

[a] All values are given as means ± SE for surface area dimensions in μm^3/μm^2. All volumes and surface areas are normalized to the surface density of epithelial basement membranes.

[b] $p < 0.05$ when compared with control values.

ABOUT THE AUTHORS

Ling-Yi Chang received a Ph.D. in physiology in 1982 from North Carolina State University. She then joined the Pulmonary, and Critical Care Medicine, Department of Medicine, at Duke University as a Research Associate. She is currently Associate Research Professor of Medicine and Cell Biology. Her main research interests are pulmonary cell interactions with oxidants and their responses to oxidant stress, the effects on lung cell function and structure of air pollutants that generate free radicals, and the regulation of lung inflammation by molecules that adhere to alveolar epithelial cell surfaces.

Barbara L. Stockstill began her employment as a Senior Electron Microscopy Technician at Duke University Medical Center in 1984, after receiving a degree in botany from Texas A&M University in 1983. She returned to graduate school in 1989 and received her Ph.D. in pathology from the Duke University Graduate School in 1994. The work presented in this report is part of her Ph.D. dissertation.

Margaret Ménache is a Senior Statistician in the Division of Pulmonary and Critical Care Medicine at Duke University Medical Center. She holds an M.S. in biostatistics (1991) and an M.A. in economics (1983) from the School of Public Health at the University of North Carolina. Her research interests are biomedical statistics and modeling as applied to delivered dose and lung injury after exposures to airborne toxicants. Ms. Ménache is currently working toward a Ph.D. in the Duke University Graduate School of the Environment.

Robert R. Mercer received his Ph.D. from the Department of Biomedical Mathematics and Engineering at the University of North Carolina in 1982. Bob has been a faculty member in the Division of Pulmonary and Critical Care Medicine, Department of Medicine, at Duke University Medical Center since 1983, and has been an Associate Research Professor of Medicine since 1992. Dr. Mercer's primary research interests are in environmental toxicology. He has developed methods for reconstructing the lung architecture in three dimensions and has used the unique data collected in this manner to determine the essential parameters necessary to model the distribution of inhaled toxic particles and gases.

James D. Crapo received his M.D. from the University of Rochester in 1971. He is currently Professor of Medicine and Pathology and Chief of the Division of Pulmonary and Critical Care Medicine at Duke University. Dr. Crapo served as President of the American Thoracic Association from 1992-1993. His research interests are inhalation toxicology and the study of in vivo cell biology of the lung, with emphasis on evaluating the role of free radicals in pulmonary oxidant injury and on evaluating changes in pulmonary structure and function caused by inhaling environmental pollutants.

PUBLICATIONS RESULTING FROM THIS RESEARCH

Stockstill BL, Crapo JD, Mercer RR, Chang L-Y. 1993. Lung fibrosis and bronchiolar metaplasia after chronic exposure to ozone (abstract). Am Rev Respir Dis 147:A638.

ABBREVIATIONS

ANOVA	analysis of variance
β-TGF	transforming growth factor–β
D_{CO}	carbon monoxide diffusing capacity
MANOVA	multivariate analysis of variance
NTP	National Toxicology Program
ppm	parts per million

Consequences of Prolonged Inhalation of Ozone on F344/N Rats: Collaborative Studies

Part IX: Changes in the Tracheobronchial Epithelium, Pulmonary Acinus, and Lung Antioxidant Enzyme Activity

Kent E. Pinkerton, Margaret G. Ménache, and Charles G. Plopper

ABSTRACT

The effect of ozone on the respiratory system is not confined to a single region or a specific cell type. Ozone-induced injury can occur at all levels of the respiratory system. However, the effects of this oxidant gas throughout the tracheobronchial tree and the lung parenchyma can be highly variable. The doses of ozone delivered to the various regions may also be different, and these differences may have a significant effect on the extent of injury. To examine the effects of chronic exposure to ozone on the lungs, we used a systematic sampling approach to perform morphometric, histochemical, and enzymatic analyses of selected airway generations and pulmonary acini arising from short and long airway paths of the tracheobronchial tree. The objectives of this study were to define compositional, cytochemical, and architectural changes that occur in epithelial cells of the airways and major tissue components of the pulmonary acini after 20 months of exposure to 0.0, 0.12, 0.5, or 1.0 parts per million (ppm)* ozone in male and female F344/N rats. We found in the trachea and bronchi significant alterations in stored secretory product following exposure to ozone, but no changes in epithelial thickness or the volume density of nonciliated cells. The volume density of nonciliated cells was significantly increased in terminal bronchioles arising from a long airway path (caudal region) of the left lung. The predominant change within the pulmonary acini was the extension of bronchiolar epithelium beyond the bronchiole–alveolar duct junction into alveoli. This change was concentration-dependent and site-specific, with ventilatory units arising from a short path (cranial region) of the left lung in male rats being most affected. The antioxidant enzymes superoxide dismutase, glutathione peroxidase, and glutathione S-transferase were significantly elevated in the distal bronchiole to central acinus following 20 months of exposure to 0.5 or 1.0 ppm ozone. Changes in antioxidant enzyme levels were more variable in other airway generations. We conclude that the effects of long-term (20-month) exposure to ozone are dose-dependent and site-specific along the tracheobronchial tree and pulmonary acini of the lungs. With the tissue sampling strategies used in this study, for the first time microdosimetric relations between ozone concentrations and biological changes in precisely delineated regions of the lungs can be defined along the entire lower respiratory tract.

INTRODUCTION

Modeling studies predict that the major sites of ozone uptake and reactivity ("target sites") are the anterior nasal cavity, trachea, and central acinus (Miller et al. 1985; Patra et al. 1986). The nature of the resulting epithelial lesion appears to be related to the species, anatomic site, preexposure epithelial composition, concentration of ozone inhaled, and duration of exposure. Experimental work at ambient concentrations of ozone defined three stages of epithelial response based on the duration of exposure: short-term (3 days or less), intermediate (7 to 10 days), and long-term (60 days or longer). The reaction to short-term exposures in all three sites is ciliated cell necrosis, deciliation, degranulation of secretory cells, and hyperplasia of intermediate cells (in the rat), small mucous granule cells (in the macaque), or Clara cells (in the rat and macaque) (Stephens et al. 1974; Castleman et al. 1980; Wilson et al. 1984; Harkema et al. 1987a,b). In zones that lack ciliated cells, there is necrosis of mucous cells (Harkema et al. 1987b) and of serous or Clara cells (Castleman et al. 1980). By seven days of ozone exposure, ciliated cell necrosis is

* A list of abbreviations appears at the end of the Investigators' Report.

This Investigators' Report is Part IX of Health Effects Institute Research Report Number 65, Parts VIII and IX, which also includes an Introduction to the NTP/HEI Collaborative Ozone Project, a Commentary by the Health Review Committee on the two Investigators' Reports included in this monograph, and an HEI Statement about the research studies. Correspondence concerning this Investigators' Report may be addressed to Dr. Kent E. Pinkerton, Institute of Toxicology and Environmental Health, University of California at Davis, Old Davis Road, Davis, CA 95616.

This study was supported by HEI funds from the U.S. Environmental Protection Agency and the motor vehicle industry. The inhalation component of this project was sponsored by the National Toxicology Program as part of its studies on the toxicologic and carcinogenic effects of ozone.

Although this document was produced with partial funding by the U.S. Environmental Protection Agency under Assistance Agreement 816285 to the Health Effects Institute, it has not been subjected to the Agency's peer and administrative review and therefore may not necessarily reflect the view of the Agency, and no official endorsement should be inferred. The contents of this document also have not been reviewed by private party institutions, including those that support the Health Effects Institute; therefore, it may not reflect the views or policies of these parties, and no endorsement by them should be inferred.

markedly decreased and the major change is hyperplasia and metaplasia of nonciliated secretory and intermediate cells (Stephens et al. 1974; Mellick et al. 1977; Lum et al. 1978; Chow et al. 1981; Eustis et al. 1981; Wilson et al. 1984; Harkema et al. 1987a,b). After 90 days of ozone exposure, the macaque nasal epithelium is hyperplastic and hypertrophied, with reduced ciliated cell necrosis and secretory cell metaplasia (Harkema et al. 1987a,b). The principal epithelial changes in the macaque respiratory bronchioles are Clara cell hyperplasia and hypertrophy (Fujinaka et al. 1985; Moffatt et al. 1987). After 90 days of ozone exposure, the rat tracheal epithelium has a few shortened cilia, but no necrosis, hyperplasia, or metaplasia (Nikula et al. 1988). The rat bronchiolar epithelium invades the alveolar duct matrix and forms respiratory bronchioles (Tyler et al. 1987). There is no detectable necrosis of bronchiolar epithelial cells. These centriacinar epithelial changes persist in the rat up to 42 days after exposure ceases (Tyler et al. 1987). In summary, short-term ozone exposure disrupts the homeostasis of tracheobronchial epithelium by cell injury, necrosis, and hypersecretion, but after long-term exposure animals reestablish homeostasis by developing a cell population resistant to further injury by ozone. Between these two reactions is a phase of rapid cell repopulation under oxidant stress conditions that continue to produce cell injury and necrosis. The primary objective of the NTP/HEI Collaborative Ozone Project was to define the dose-related changes in the sites most sensitive to ozone exposure after a very long (near-lifetime) exposure.

This particular study addresses questions regarding tbe response of the lower respiratory system to long-term exposnre to ozone. After acute exposure, the pattern of injury within the lower respiratory tract is very site-specific. The principal sites of injury are the epithelium of the trachea, the epithelium of the most distal bronchioles, and the most proximal portion of the acinus, that is, the centriacinar region. By ultrastructural assessment, little or no injury has been detected in any of the intrapulmonary bronchi between the trachea and the distal broncbioles, nor in 90% or more of the pulmonary acinns more distal to the centriacinar region. The principal alteration in the centriacinar region in rats chronically exposed (for 60 to 90 days) to ozone is bronchiolarization of centriacinar alveolar ducts (Boorman et al. 1980; Barr et al. 1988).

The chronic response that follows the acute response is alteration of the storage capabilities of secretory epithelial cells. Whether or not these storage capabilities are permanently altered with long-term exposure has not been addressed. We used histochemical methods for analyzing stainable secretory material to assess changes in secretory products in epithelial cells and morphometric procedures to assess epithelial storage function.

A major characteristic of the pulmonary response to ozone is that continued exposure for periods of 60 to 90 days changes epithelial cell populations in target zones to ones that are no longer injured by concentrations of ozone that produce injury acutely. The mechanism behind the cell's ability to resist further injury is not understood. We tested the hypothesis that the target cell populations become resistant because they develop higher levels of antioxidant enzymes and are better able to maintain and regulate their glutathione pools. Our study was designed to assess antioxidant enzyme activity and regulation of the glutathione pool in defined anatomic sites. We can effectively measure antioxidant enzyme levels in different compartments of the lung. These activity levels are quite variable compared with the activity that is measured in whole-lung homogenates.

This study addressed two issues: (1) whether the hyperplastic bronchiolar centriacinar remodeling persists with continued exposure for 20 months; and (2) the extent of this remodeling within the pulmonary acinus. This study assessed injury throughout the airway tree of the rat, with samples selected specifically from different airway generations, and evaluated alterations in defined portions of the pulmonary acinus. Rigorous sampling strategies for examining centriacinar alterations allowed assessment of epithelial change and remodeling as a function of distance along the alveolar duct. In fact, site-specific sampling of the tracheobronchial tree and lung parenchyma offered a unique opportunity to define the overall response of the respiratory tract to ozone.

SPECIFIC AIMS

The overall objective of this study was to define quantitatively the effects of chronic ozone exposure on target and nontarget sites of the tracheobronchial tree and pulmonary acini using morphometric, histochemical, and enzymatic assays. The three specific aims were as follows:

1. To define quantitatively the changes in cell type, epithelial composition, and abundance of stored secretory product in epithelial cell populations of target and nontarget sites in airway generations of the tracheobronchial tree including the trachea, three intermediate bronchi, and the proximal and terminal bronchioles of two regions (representing short- and long-path lengths relative to the carina, which is the branching of the trachea into left and right bronchi).
2. To define qnantitatively the architectural remodeling of pulmonary acini arising from short and long airway

paths and changes in the epithelial, interstitial, and vascular (capillary) compartments of alveolar septa as a function of distance from the bronchiole–alveolar duct junction (BADJ) of each acinus.

3. To determine changes in levels of antioxidant enzyme activity for superoxide dismutase (SOD), glutathione S–transferase (GST), and glutathione peroxidase (GPx) within selected airway generations, pulmonary acini, and the lung parenchyma.

METHODS AND STUDY DESIGN

The effects of long-term exposure to ozone on the rat lower respiratory tract, in terms of changes in cell type, thickness, and volume of stored secretory product, were identified along with alterations in levels of antioxidant enzymes in these same populations of cells. Each level of the respiratory tract was isolated by microdissection techniques to allow for the selection of identical sites for morphometric, histochemical, and enzymatic studies within regions of the lung considered to be target and nontarget sites for the effects of ozone.

Male and female F344/N rats were obtained from Simonsen Laboratories (Gilroy, CA) at four to five weeks of age. Animals were randomly assigned to ozone exposure or control groups after a 10- to 14-day quarantine period. Animals were housed in modified (Hazelton 2000) inhalation chambers (Hazelton Systems, Aberdeen, MD) and exposed to either ozone or filtered air for six hours per day (between 0730 and 1730 hours), five days per week, for 20 months. Exposure to ozone was performed at Battelle Pacific Northwest Laboratories (Richland, WA) as part of a collaborative, multilevel study by the NTP and HEI to examine the long-term effects of ozone. Owing to the scope of the NTP/HEI Collaborative Ozone Project and the large number of animals involved, the animals that formed the basis of this study were received from a total of three different exposure chambers for each ozone concentration and from three chambers for filtered air. Animals were chosen by a strictly randomized scheme. (See Appendix B for the identification numbers of animals used in this study.) The animals were free of respiratory disease, as judged by the testing of sentinel animals from each chamber throughout the exposure period and at the end of the study. Animals with leukemia were also identified and examined as a potential confounding factor in morphometric measurements of tissue compartments. The average temperature range (± SD) within the exposure chambers over the course of the study was 23.9° C to 24.4° C (± 0.7°C); the relative humidity range was 57.1% to 60.2% (± 7.3%).

Ozone was generated by corona discharge using an ozonator (OREC Model 03V5-0, Ozone Research and Equipment Corporation, Phoenix, AZ) with 100% oxygen. The ozone concentration in each chamber was monitored by a multiplexed ultraviolet spectrophotometric analyzer (Model 1003-AH, Dasibi Environmental Corporation, Glendale, CA). The monitor was calibrated by comparison with a chemical-specific monitor (neutral-buffered potassium iodide method) simultaneously sampling the exposure chambers. The target concentrations for ozone were 0.0 ppm for the control chambers and 0.12, 0.5, and 1.0 ppm for the ozone chambers. The actual ozone exposure concentration over the course of the study in the control chambers was less than 0.002 ppm (below the limit of detection), and the mean concentration (± SD) was 0.12 (± 0.01), 0.51 (± 0.02), and 1.01 (± 0.05) ppm in the ozone chambers. To determine concentration uniformity, measurements were periodically made at 12 locations in each chamber. Ambient ozone was removed from all chambers using a potassium permanganate filter. Charcoal and high-efficiency particulate air (HEPA) filters were used to further filter air entering the chambers. At the end of the 20-month exposure, all animals were held for one week before being killed to emphasize permanent, nontransient changes in the lungs.

TRACHEOBRONCHIAL EPITHELIUM

METHODS

The analysis of the tracheobronchial epithelium is based on the assumption that the response of the respiratory tract to ozone will be highly heterogeneous and site-specific. We compared the same morphometric parameters for each site examined in the lungs: trachea; cranial, central, and caudal bronchi of the left lung lobe; and the proximal and terminal bronchioles arising from these cranial and caudal bronchi.

Lung Fixation and Processing for Microscopy

For this phase of the study, four male and four female animals from the control gronp and four male and four female animals from each of the ozone exposure groups were randomly selected for evaluation. Animals were killed with an overdose of sodium pentobarbital. The lungs were collapsed by diaphragmatic puncture and fixed in situ by intratracheal instillation of 2% glutaraldehyde in cacodylate buffer (pH 7.4, 350 mOsm) for 15 minutes at 30 cm of fixative pressure (Plopper 1990). The fixed lungs were removed by thoracotomy and stored in the same fixative until processing for analysis by histochemistry, light microscopy, and scanning electron microscopy. The fixed lungs were trimmed of all mediastinal contents, and the

lung volumes were measured by fluid displacement. Regions of the left lung lobe were selected for complementary studies by histochemistry and high-resolution light microscopy.

Beginning with the trachea, airways were dissected along their long axes to approximately the level of the terminal bronchiole (Plopper 1990). The dissections were done with the aid of a dissecting microscope (M8, Wild Heerbrngg Instruments, Farmingdale, NY) and fiber-optic illumination. The areas selected for study are illustrated in Figure 1 and are identified as the cranial, central, and caudal regions. As summarized in Table 1, the cranial region included a medium-sized conducting airway with a short path length, a large cumulative branch angle (change in the path direction), and a relatively small diameter. The cranial centriacinar regions were selected from the acini supplied by this bronchial pathway. The conducting airway selected from the central region had the same number of generations of branching as that from the cranial region, but was much larger in diameter and was part of the axial pathway for conducting airways in the left lobe. The airway selected from the caudal region had a much greater path length and approximately the same diameter as that of the cranial bronchus; however, the angle of deviation was much smaller in the caudal airway. The caudal centriacinar regions were selected from the acini supplied by this airway.

Identifying airway location during dissection was facilitated by using silicone casts prepared from the lungs of three male F344/N rats, four to five months old. Each cast was prepared according to a modified saline displacement casting procedure in which silicone rubber (Silastic 734 RTV, Dow Corning Corp., Midland, MI) is injected into the trachea at 25-mPa (cm of water) positive pressure. After being cured for two days, the silicone-filled lungs were

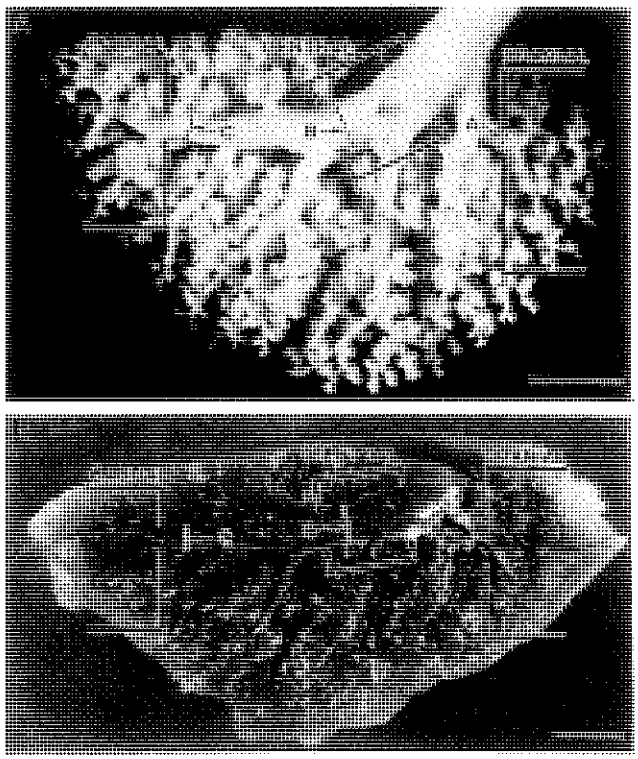

Figure 1. Location of tissue samples taken from the rat lung. A: Silicone cast of the tracheobronchial airway tree from the left lobe of a rat. Lung casts served to standardize sampling. Samples of terminal bronchiole–alveolar duct junctions were taken from the three regions (cranial, central, and caudal) indicated. The letters and arrows within the figure indicate the precise locations from which samples of intrapulmonary conducting airways were taken. Bar = 4 mm. B: Mediastinal half of a fixed, microdissected rat lung. Note how closely the pathways and sampling regions match the silicone cast shown above. Bar = 4 mm.

snrgically removed from the thorax and boiled in 1 N sodium hydroxide to remove the lnng tissne. Casts were trimmed to reveal airways from the major bronchus to the level of the terminal bronchioles. The path length and

Table 1. Characteristics of Airway Samples

Airway	Generation Number	Path Length (mm)	Cumulative Branch Angle (°)	Diameter (mm)
Distal trachea	0	NA[a]	NA	3.3 ± 0.1
Lobar bronchus	1	6.7 ± 0.1	15 ± 0.0	2.8 ± 0.1
Cranial region bronchus	4–5	11.7 ± 0.9	140 ± 15	0.7 ± 0.0
Cranial region central acinus	8–10	14.0 ± 1.2	225 ± 21.8	–
Central region bronchus	4–5	11.2 ± 0.3	8.3 ± 5.8	2.4 ± 0.1
Central region central acinus	6–7	13.7 ± 1.1	50 ± 8.7	–
Caudal region bronchus	10–12	20.2 ± 0.4	30.0 ± 8.6	1.0 ± 0.1
Caudal region central acinus	15–16	22.3 ± 0.3	30.0 ± 8.6	–

[a] NA = not applicable.

cumulative branch angle of each airway were measured directly from the casts.

The rat lung has a monopodial form of airway branching in which a major and minor daughter airway arise from each parent airway. A labeling system devised by Phalen and coworkers (Phalen et al. 1978; Phalen and Oldham 1983) exploits this unique arrangement and uses a binary numbering scheme to label all sequential major airways as "1" and all minor airways as "0." Beginning at the trachea (designated as 1), each new airway generation is classified to give a unique branching history for each pathway. These branching histories were easily and reliably determined from the lung casts and were used as guides to ensure that dissections in the fixed, wet lungs followed identical pathways to each region in every lung. Table 1 summarizes the branching history by generation number, path length, cumulative branch angle, and diameter for each airway followed. The most distal airways revealed by microdissection were usually two to four generations from the terminal bronchioles. Blocks of tissue approximately 1.5 × 1.5 × 0.4 mm in size were cut in a plane perpendicular to the axis of the most distal dissected airway to isolate parenchymal tissue arising from each dissected pathway.

Portions of the dissected left lung were embedded in glycolmethacrylate. Sections of 1 μm were cut with glass knives on a JB4 microtome. Serial and serial-step sections were stained with Alcian blue/periodic acid–Schiff (AB/PAS) (pH 2.5) or toluidine blue (0.5% in 1% borate buffer).

For the cranial, central, and caudal regions, blocks were removed and embedded as larger blocks, and the BADJs were isolated by the methods of Pinkerton and colleagues (1993). Briefly, tissue slices (approximately 2 × 4 × 6 mm in size) were postfixed in 1% osmium tetroxide in Zetterquist's buffer, followed sequentially by 1% tannic acid and 1% uranyl acetate in maleate buffer, dehydrated in ethanol and propylene oxide, and embedded in either Epon 812 or Araldite 502. Centriacinar sites from the cranial and caudal regions were isolated by cutting the entire tissue block into slices approximately 0.3 to 0.4 mm thick. Each slice was examined under a dissecting microscope to identify BADJs in longitudinal profile. The criterion for selection was a symmetrical pair of alveolar ducts arising from a single terminal bronchiole. Isolations meeting this selection criterion consistently contained alveolar duct paths in longitudinal profile that extended two to four generations beyond the BADJ. Selected isolations were remounted on beem blanks and sectioned at a thickness of 0.5 μm with glass knives. Sections were stained with toluidine blue (0.5% in 1% borate buffer). Centriacinar sites from the central region were analyzed by Chang and associates (1995).

Morphometry

The thickness and relative abundance (volume fraction) of conducting airway epithelial cells were evaluated by procedures that are discussed in detail elsewhere (Hyde et al. 1990, 1992b; Plopper et al. 1992). All measurements were made using high-resolution light microscopy (40 × objective and 0.5 to 1.0-μm sections). Measurements were made from video images captured with a video camera (DAGE MTI, Michigan City, IN) mounted on an Olympus BH-2 microscope, which was interfaced with a Macintosh IIci computer running National Institutes of Health IMAGE software. The analysis was performed using a cycloid grid overlay and software for counting points and intercepts (Stereology Toolbox, Davis, CA). (See Hyde et al. 1990 and 1992b for detailed descriptions of grids and counting procedures.) The volume fractions (V_v) of three categories of cells (nonciliated, ciliated, and basal) were determined by point counting and were calculated using the formula

$$V_v = P_p = P_n / P_t,$$

where P_p is the point fraction of P_n, the number of test points hitting the structure of interest, divided by P_t, the total points hitting the reference space (epithelium). The surface area of epithelial basement membrane per reference volume (S_v) was determined by point and intercept counting and was calculated using the formula

$$S_v = 2\ I_O / L_r,$$

where I_O is the number of intercepts with the object (epithelial basal lamina) and L_r is the total length of test line in the reference volume (epithelium). The thickness of the epithelium was calculated using the formula for arithmetic mean thickness (t):

$$t = V_v / S_v.$$

The abundance of stored secretory product was estimated using the threshholding and particle-counting function of the IMAGE software to measnre the area of AB/PAS-positive material in a defined area of the epithelial profile, and the percentage of the epithelium occupied by AB/PAS-positive material was calculated. The volume density of AB/PAS-positive material (per unit area of basal lamina) was determined by multiplying the percentage of AB/PAS-positive material in the epithelium by the thickness of epithelium determined at the site (Hyde et al. 1990, 1992b).

For each bronchus and the trachea, four fields were evaluated. Fields were selected at random by dividing the cross section of the airway into four quadrants, choosing a random angle (between 0° and 90°) from a random number table, and centering the field for evaluation on that angle.

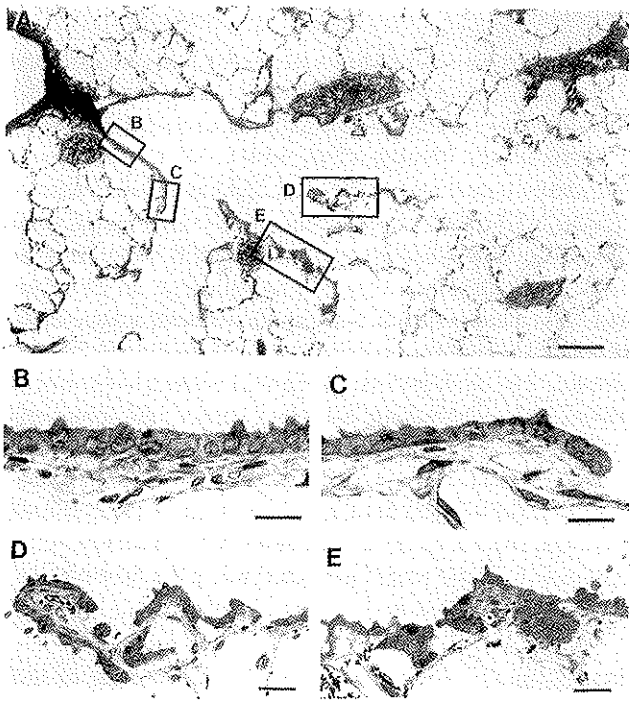

Figure 2. Position and composition of regions analyzed within the terminal bronchiole–alveolar duct junction. A: Centriacinar region from a rat exposed to 1.0 ppm ozone for 20 months. Epithelial samples of distal bronchioles one generation proximal to the terminal bronchiole were taken approximately 0.5 to 1.0 mm from the junction (box B). Epithelial samples of the terminal bronchiole were taken at the junction with the first alveolar duct (box C). Epithelial samples of the bronchiolarized alveolar duct were taken from bronchiolar epithelium clearly identified within the alveolar duct (boxes D and E). Bar = 150 μm. B: Epithelial composition of the area in box B. Bar = 15 μm. C: Epithelial composition of the area in box C. Bar = 15 μm. D: Epithelial composition of the area in box D. The epithelium in alveolar ducts lined both sides of interalveolar septa and, in many cases, appeared to be hyperplastic and metaplastic. Bar = 30 μm. E: Epithelial composition of the area in box E. Bar = 30 μm.

In the centriacinar region, at least five centriacinar areas were used for each analysis. Figure 2 illustrates the positions of the areas sampled. Epithelium evaluated for the terminal bronchiole was defined as the epithelium just proximal to the first alveolar outpocketing. Epithelium evaluated for the proximal bronchiole was obtained from a site contiguous with the terminal bronchiole, but 0.5 to 1 mm more proximal.

Statistical Analysis

To examine biological effects in the tracheobronchial airways, three primary variables were identified: stored secretory product, epithelial thickness, and volume fraction (%) of nonciliated cells. Ozone-induced change to the airway epithelium occurs in the forms of cellular injury and changes in cell populations. For each primary variable, a multivariate vector of the analyzed sites (trachea and cranial, central, and caudal bronchi) was constructed. The independent variables were ozone exposure concentration, gender, and the interaction between concentration and gender. Multivariate analysis of variance (MANOVA), with significance determined by a Hotelling-Lawley trace value of $p < 0.05$, was required before we examined effects using univariate analysis of variance (ANOVA). Significant ANOVA effects associated with concentration or with the concentration-gender interaction were subtested using t tests with a Bonferroni adjustment. The least-squares mean is the expected value for that mean in a balanced design with all covariates at their mean value.

Other confirmatory variables that were measured were ciliated cell and basal cell density. These also were analyzed in a step-down strategy as outlined for the primary variables; however, because they are simply alternative ways of looking at the primary variables, these results should be interpreted with caution especially if they are not in agreement with the primary variables.

A similar strategy was used to analyze the centriacinar bronchiole data. A single multivariate vector was constructed that included the cranial and caudal sites as well as the proximal and terminal bronchioles. These vectors were analyzed using a multivariate repeated measures analysis. With this design it was possible to test for differences between the two sites. As for the airway data, multivariate significance was required before examining univariate ANOVA effects. Significant ANOVA effects were subtested with t tests with the Bonferroni adjustment. The primary variables for this analysis were total epithelial thickness and the volume fraction of nonciliated cells.

Sample Size

A number of the rats identified for morphometric analysis underwent pulmonary function testing under anesthesia immediately before being killed. Because of the possibility of an effect on the stored secretory product and the antioxidant enzymes discussed in Specific Aim 3, none of these animals were used in the analyses performed as part of Specific Aim 1.

Evidence of lenkemia with pulmonary involvement was found in a number of the rats in the NTP/HEI Collaborative Ozone Project. Analyses by the Battelle pathologist indicated that in leukemic rats with advanced spleen and liver involvement, there was always advanced pulmonary involvement. The Battelle pathologist was not able to examine for leukemia the lung tissue of the rats used for morphometric analysis; however, of the rats studied for Specific Aims 1 and 3, five were identified as having advanced spleen and liver involvement. It was felt that the effects of the leukemia should not be seen in the bronchi or brouchioles, and they were shown to be extremely focal by Chang and coworkers

(1995). In an examination in their laboratory, only one rat of a possible seven showed histologic changes consistent with leukemia. Nevertheless, the data were analyzed using all animals (n = 32) and excluding any rats with advanced spleen and liver leukemia (n = 27).

RESULTS

Effects of Leukemia

Statistical analysis was carried out both using all animals (n = 32) and excluding animals with liver and spleen leukemia (n = 27). If the rats with leukemia contributed greatly to the variability in the responses, then excluding them could result in more statistically significant results. On the other hand, excluding five animals may result in an appreciable loss of statistical power and some loss of statistical significance. The results of MANOVA and univariate ANOVA using both sample sizes were compared for all variables analyzed. Few significant differences, particularly with respect to the effects of ozone concentrations, were found between the two sets of analyses. None of the changes in statistical significance would change the overall interpretation of the results. On the other hand, loss of power from the smaller sample size was much more noticeable when examining the patterns of significance in the t tests with the Bonferroni adjustment. Therefore, only the results obtained from the analysis performed with all rats are reported.

Multivariate Analysis

The statistical significances observed in the multivariate and univariate analyses for the tracheobronchial airway data are shown in Table 2. Stored secretory product was significantly affected by ozone exposure and differed significantly between males and females. From the ANOVA, it was observed that there were significant concentration-related effects in the trachea, cranial bronchus, and caudal bronchus, but not in the central bronchus. At all four locations, males had more stored secretory product than females, although this difference was statistically significant only in the central bronchus. At the multivariate level an interaction between ozone concentration aud gender was observed for the nonciliated cell volume density. Statistically significant ANOVA effects were found only in the central bronchus. Despite the significant ANOVA test for ozone concentration, none of the pairwise comparisons of interest were statistically significant. As for stored secretory product, the nonciliated cell volume was greater in males than in females at all four locations but the difference was statistically significant only in the central bronchus.

The changes in nonciliated cell volumes were offset by changes in basal and ciliated cell volumes: a small but significant increase in the basal cell volume in the central bronchus and significant decreases in the ciliated cell volume in both the central and caudal bronchi. The net effect of these changes in cell volume was that the total epithelial thickness in the airways was unchanged following ozone exposure.

Results of the repeated measures analyses for the centriacinar data are shown in Table 3. A statistically significant interaction involving differences between the cranial and caudal sites in both the proximal and terminal airways in male and female rats following ozone exposure was observed for the nonciliated cell volume density. The univariate ANOVA indicated greater nonciliated cell volume densities in female rats than in male rats in the proximal airways (although the difference was not statistically significant), while the values for the males were greater than for the females in the terminal bronchioles. Concentration-gender interactions were found in the cranial proximal bronchiole and in the caudal terminal bronchiole.

These results are discussed in more detail in subsequent sections. Because of the small sample sizes available for these measurements, there was not always adequate statistical power to detect trends that could have biological significance. Such trends are noted despite their lack of statistical significance.

Trachea

Carbohydrate histochemical staining identified AB/PAS-positive material in the epithelium of the trachea (Figure 3). Most of the staining was confined to circular inclusions within tbe apices of nonciliated cells, which ranged in color from a purplish-pink to deep purple. There was little difference in the color range among different exposure groups. The primary intergroup differences were a reduction in the abundance of AB/PAS-positive secretory product within nonciliated cells and a reduction in the number of cells with AB/PAS-positive inclusions. There was approximately one-half as much material in the tracheas of animals exposed to 1.0 ppm ozone as in control animals exposed to filtered air (Table 4; Figure 4). Although there was a consistent decrease in stored secretory product as ozone exposure concentration increased, this difference was statistically significant only at 1.0 ppm. The histologic appearance of epithelial cells lining the distal trachea was not appreciably different in control rats and rats exposed to 0.12 or 0.5 ppm ozone (Figure 5).

Morphometric assessment of the average thickness of the tracheal epithelium indicated some reduction in epithelial thickness in the group exposed to 1.0 ppm ozone, but due

to the variability at different sites in all animals, these differences were not statistically significant (Table 5; Figure 6). There was no significant change in the volume density of nonciliated cells (Table 6).

Intrapulmonary Bronchi

Cranial Bronchus. The bronchus in the cranial portion of the left lung (position A in Figure 1) was chosen for its short path length, small diameter, and large alteration in path angle from the trachea (Table 1). Carbohydrate histochemistry identified very few AB/PAS-positive inclusions in epithelial cells lining this airway in the lungs of control animals. The majority of the positively staining purplish material was observed in nonciliated cells (Figure 3). There was little difference in the distribution of AB/PAS-positive material in this airway generation in animals exposed to 0.12 or 0.5 ppm ozone compared with that in controls (Figure 4). However, in animals exposed to 1.0 ppm ozone, there was a marked increase in the amount of purplish-red to dark purple material observed in spherical and circular inclusions in nonciliated cells and an apparent increase in the number of cells containing AB/PAS-positive material (Figure 3). In this airway, the amount of AB/PAS-positive material stored in epithelial cells, per unit area of basal

Table 2. Statistical Analysis of Tracheobronchial Airway Data of Rats Exposed to Ozone for 20 Months

	Multivariate p Values[a]			Univariate p Values[b]		
Variables	Ozone Concentration	Gender	Concentration × Gender	Ozone Concentration	Gender	Concentration × Gender
Primary						
Stored secretory product	< 0.01[c]	0.02[c]	0.47			
Trachea				0.03[d]	0.43	
Cranial bronchus				< 0.01[d]	0.19	
Central bronchus				0.23	< 0.01[d]	
Caudal bronchus				0.01[d]	0.24	
Nonciliated cell volume	0.11	0.26	0.04[c]			
Trachea				0.91	0.35	0.12
Cranial bronchus				0.08	0.36	0.59
Central bronchus				0.03[d]	0.02[d]	0.23
Caudal bronchus				0.95	0.18	0.79
Total epithelial thickness	0.15	0.47	0.40			
Trachea						
Cranial bronchus						
Central bronchus						
Caudal bronchus						
Confirmatory						
Basal cell volume	< 0.01[c]	0.84	0.34			
Trachea				0.84		
Cranial bronchus				1.0		
Central bronchus				< 0.01[d]		
Caudal bronchus				0.25		
Ciliated cell volume	< 0.01[c]	0.13	0.19			
Trachea				0.17		
Cranial bronchus				0.62		
Central bronchus				< 0.01[d]		
Caudal bronchus				< 0.0[d]		

[a] Multivariate significance was tested by the Hotelling-Lawley trace.

[b] Univariate significance was tested by ANOVA factor F tests. A blank column indicates that the multivariate tests did not permit subtests of that factor at the univariate level.

[c] Statistically significant effect.

[d] Statistically significant effect that was subtested if needed.

Table 3. Statistical Analysis of Centriacinar-Bronchiole Data of Rats Exposed to Ozone for 20 Months

Analysis	Primary Variables		Confirmatory Variable: Ciliated Cell Volume
	Nonciliated Cell Volume	Epithelial Thickness	
Repeated Measures[a]			
Site[b]	0.16	0.14	0.01[c]
Concentration × site	0.15	0.67	0.27
Gender × site	0.07[c]	< 0.01[c]	0.04[c]
Concentration × gender × site	0.51	0.28	0.57
Airway[d]	0.75	< 0.01[c]	< 0.01[c]
Concentration × airway	0.29	0.79	0.99
Gender × airway	< 0.01[c]	0.02[c]	0.77
Concentration × gender × airway	0.02[c]	0.58	0.59
Site × airway	0.62	0.15	0.25
Concentration × site × airway	0.27	0.26	0.48
Gender × site × airway	0.34	0.89	0.49
Concentration × gender × site × airway	0.04[c]	0.39	0.94
Univariate ANOVA[e]			
Cranial proximal bronchiole			
Concentration	0.11		
Gender	0.12		
Concentration × gender	0.02[c]		
Cranial terminal bronchiole			
Concentration	0.38		
Gender	0.08		
Concentration × gender	0.06		
Caudal proximal bronchiole			
Concentration	0.19		
Gender	0.81		
Concentration × gender	0.61		
Caudal terminal bronchiole			
Concentration	< 0.01[c]		
Gender	< 0.01[c]		
Concentration × gender	0.02[c]		
Averaged values			
Concentration		0.65	0.01[c]
Gender		0.58	0.38
Concentration × gender		0.51	0.78

[a] Repeated measures p values were based on the Hotelling-Lawley trace.

[b] Sites were cranial or caudal.

[c] Statistically significant effect.

[d] Airways were proximal or terminal bronchioles.

[e] Univariate ANOVA p values were based on factor F tests. Univariate results are reported by site and airway only for nonciliated cell volume because no statistically significant multivariate effects due to concentration or concentration × gender interactions with the dependent variable were observed for the other variables. Univariate results using averaged values over site and airway are shown for the other variables.

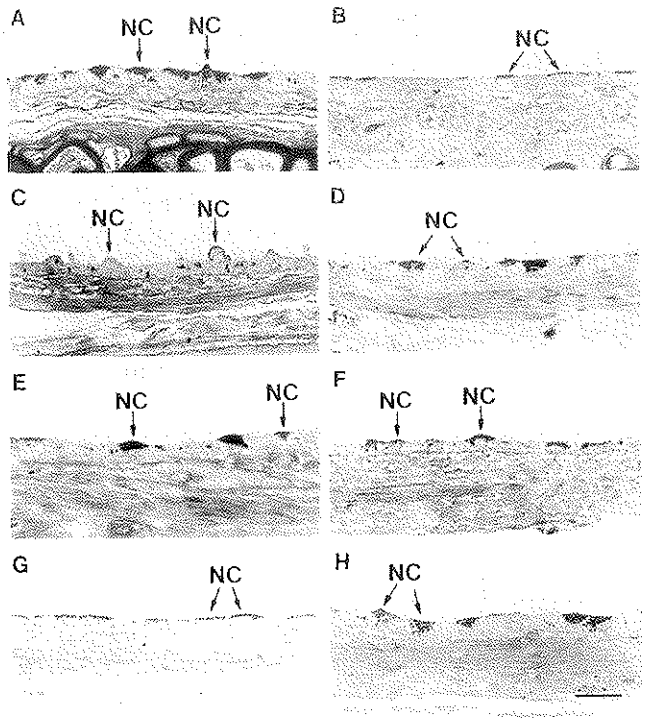

Figure 3. Differences in secretory product stored in nonciliated cells (NC) in the tracheobronchial airways of rats exposed for 20 months to filtered air (left column) or to 1.0 ppm ozone (right column). Alcian blue/periodic acid–Schiff stain was used. Bar = 20 μm. A and B: Trachea. C and D: Cranial bronchus. E and F: Central bronchus. G and H: Caudal bronchus.

lamina, was more than six times greater in animals exposed to 1.0 ppm ozone than it was in animals exposed to filtered air or to lower ozone concentrations (Table 4, Figure 4). The histologic appearance of the epithelial cells lining this airway in all exposure groups did not differ remarkably (Figure 5). There were two categories of cells present: ciliated and nonciliated. There was variability from animal to animal and from region to region within the same airway in an individual animal. Differences in the thickness of the epithelium in exposed groups, in the volume fraction of the epithelium composed of nonciliated cells (Figure 7), and in the volume density of nonciliated cells lining this airway (Table 6; Figure 7) were not statistically significant.

Central Bronchus. The bronchus in the central portion of the left lung (position B in Figure 1) was selected for its short path length, large diameter, and small alteration in path angle from the trachea (Table 1). It was approximately the same path length from the carina as the cranial bronchus, but had a much smaller cumulative branch angle and more than three times the cross-sectional diameter (Table 1). Carbohydrate histochemistry identified substantial amounts of AB/PAS-positive material in the nonciliated cells of this airway (Figure 3). There was approximately one-third as much AB/PAS-positive material stored in the nonciliated cells of this airway as in the trachea of control animals (Table 4; Figure 4), but no significant change in the amount of stored material in ozone-exposed animals. The epithelium lining this airway was composed almost exclusively of nonciliated and ciliated cells varying in shape from cuboidal to low columnar (Figure 5). The thickness of the epithelium (Table 5; Figure 8), the volume fraction of the epithelium composed of nonciliated cells (Figure 8), and the volume density of nonciliated cells (per unit of surface area) were not significantly altered by ozone exposure (Table 6; Figure 8).

Caudal Bronchus. The bronchus isolated from the caudal region (position C in Figure 1) was twice the number of generations of branching from the trachea as were the bronchi isolated from the cranial and central regions. This airway had a much longer path length from the carina, a low cumulative branch angle, and a cross-sectional diameter approximately equal to that of the cranial airway but approximately one-half that of the central airway (Table 1). Carbohydrate histochemistry identified little AB/PAS-positive material in the nonciliated cells lining this airway in

Table 4. Stored Secretory Product in Tracheobronchial Airways of Rats Exposed to Ozone for 20 Months[a]

		Ozone Concentration (ppm)			
Airway	Region	0.0	0.12	0.5	1.0
Distal trachea		0.64 ± 0.07	0.53 ± 0.08	0.42 ± 0.06	0.34 ± 0.06[b]
Bronchus	Cranial	0.04 ± 0.03	0.03 ± 0.03	0.02 ± 0.03	0.25 ± 0.03[b]
Bronchus	Central	0.14 ± 0.03	0.23 ± 0.03	0.18 ± 0.03	0.16 ± 0.03
Bronchus	Caudal	0.06 ± 0.04	0.14 ± 0.05	0.10 ± 0.04	0.26 ± 0.04[b]

[a] Values are least-squares means ± SE expressed in $\mu m^3/\mu m^2$; n = 8 rats (4 male and 4 female) for each concentration group.

[b] $p < 0.05$ compared with the value for animals exposed to 0.0 ppm ozone.

control animals (Figures 3 and 4). However, in ozone-exposed animals, AB/PAS-positive material increased, in terms of both the amount per cell and the number of cells with positive material. In comparison with control animals, the amount of stored intraepithelial AB/PAS-positive material increased with increasing ozone concentration and was significantly ($p < 0.05$) greater in the animals exposed to 1.0 ppm ozone (Table 4; Figure 4). The cellular composition of the epithelium lining this airway was similar to that in the cranial and central airways (Figure 5). The thickness of the epithelium lining the caudal bronchus decreased in relation to rising ozone concentration (Table 5; Figure 9). The volume fraction of the epithelium composed of nonciliated cells (Figure 9) and the volume density of nonciliated cells (per unit surface area) (Table 6; Figure 9) were unchanged by ozone exposure.

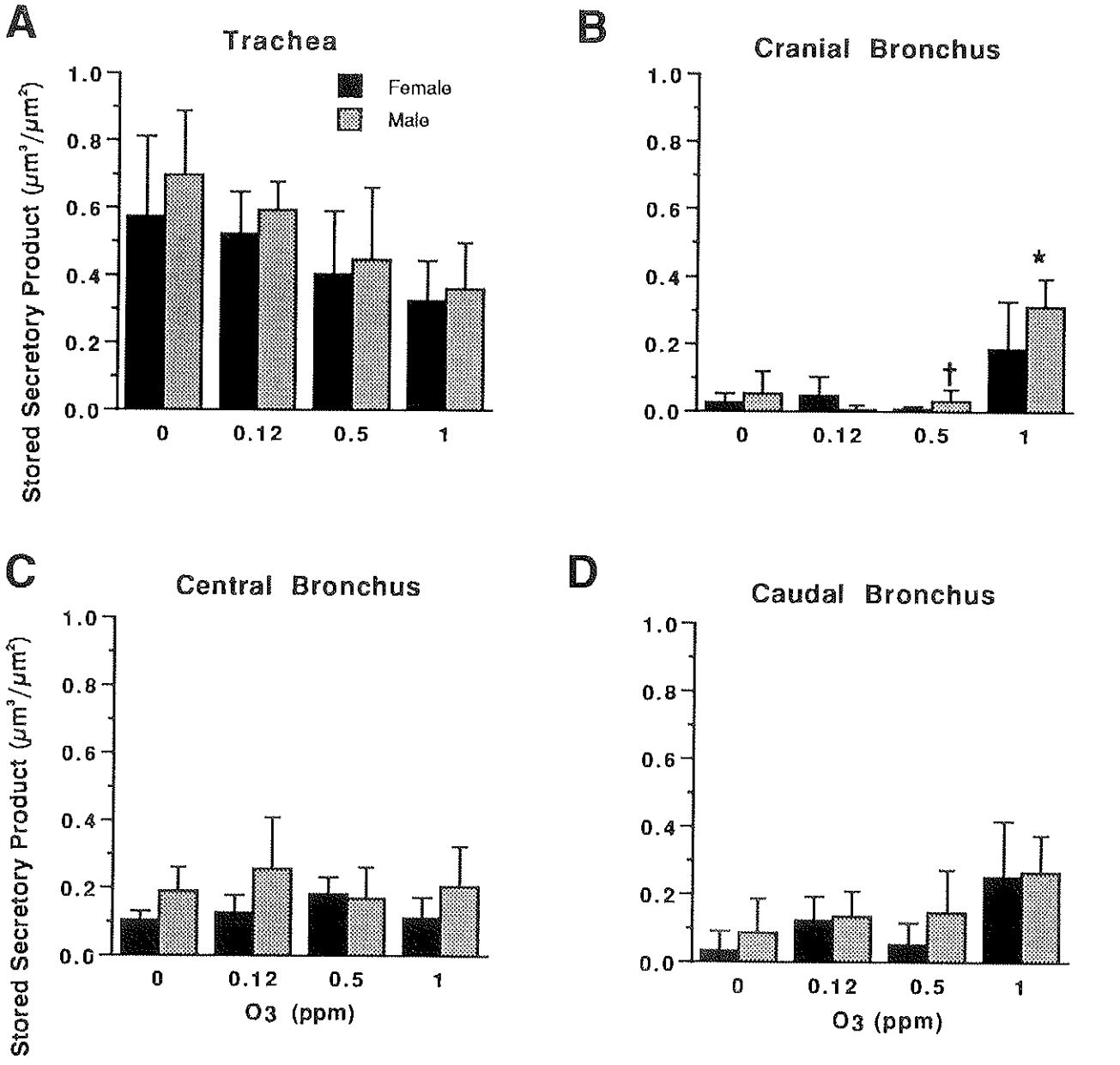

Figure 4. Comparison of stored secretory product in four regions of the tracheobronchial airways of male and female rats exposed for 20 months to filtered air or to 0.12, 0.5, or 1.0 ppm ozone. A: Trachea. Ozone (O_3) exposure resulted in a dose-dependent loss of stored AB/PAS-positive material in the trachea. B: Cranial bronchus. Exposure to 1.0 ppm ozone significantly increased the amount of stored AB/PAS-positive material in the cranial bronchus. C: Central bronchus. Exposure to 1.0 ppm ozone did not result in a change in stored AB/PAS-positive material. D: Caudal bronchus. Exposure to 1.0 ppm ozone resulted in an increase of stored AB/PAS-positive material in the caudal bronchus. * = statistically significant difference ($p < 0.05$) from the control value.

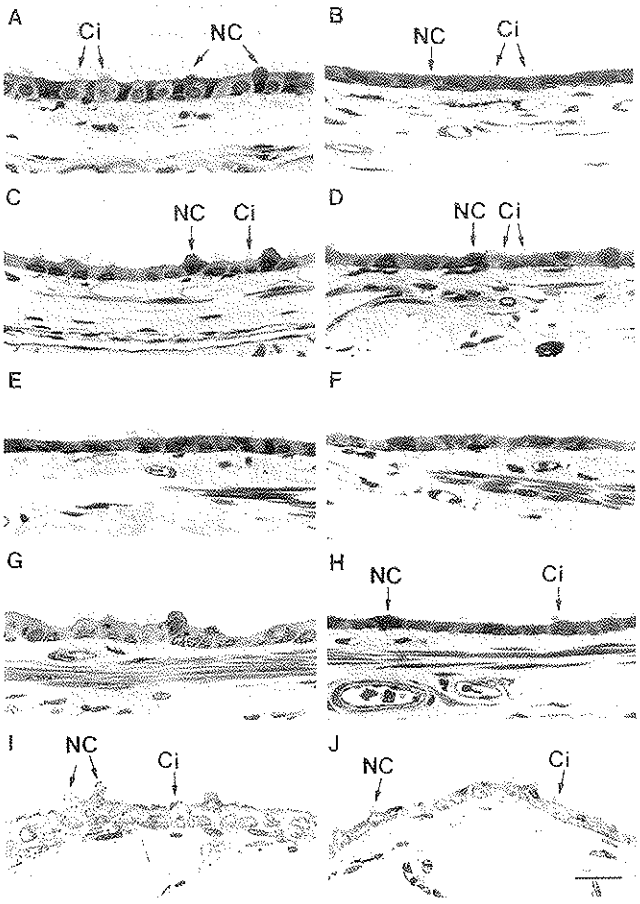

Figure 5. Histopathologic comparison of tracheobronchial epithelium in rats exposed for 20 months to filtered air (left column) or to 1.0 ppm ozone (right column). Toluidine blue stain was used. Bar = 20 μm. A and B: Trachea. C and D: Cranial bronchus. E and F: Central bronchus. G and H: Caudal bronchus. I and J: Terminal bronchiole from the caudal region. NC = nonciliated cells; Ci = ciliated cells.

Centriacinar Airways

Terminal Bronchioles. The epithelium lining the portion of the centriacinar bronchiole that was adjacent to the first alveolar outpocketing, or the terminal bronchiole (Figure 2), was composed of nonciliated cells whose apices often projected into the airway lumen and of ciliated cells with abundant cilia on their luminal surfaces. The two cell types were also distinguished by the presence of cilia and basal bodies in the lightly staining cytoplasm of ciliated cells and by the denser staining cytoplasm of secretory granules in the nonciliated cells (Figure 5). Terminal bronchioles were isolated from two separate regions at different distances from the carina, with different generations of branching from the trachea, and with different cumulative branch angles (Table 1). There were no statistically significant differences in the thickness of this epithelium in any exposure groups (Table 7; Figure 10). The volume density of nonciliated cells in the caudal terminal bronchiole after any ozone exposure was significantly greater than that in control animals (Table 8; Figure 10). This effect was observed only in male rats. There was no detectable AB/PAS-positive material in the nonciliated cells lining this region.

Proximal Bronchioles. The epithelium lining the proximal bronchioles, which was approximately 1 mm closer to the trachea but in the same centriacinar region as the terminal bronchioles, had a cellular composition very similar to that of the terminal bronchioles (Figure 2). The epithelium was thicker than that of the terminal bronchioles (Table 2; Figure 11). The volnme fractions and volume densities of ciliated and nonciliated cells (Figure 11) were approximately the same in exposed and control animals. There was some variability in the histologic composition of this epithelium both within and between animals.

Table 5. Epithelial Thickness in Tracheobronchial Airways of Rats Exposed to Ozone for 20 Months[a]

		Ozone Concentration (ppm)			
Airway	Region	0.0	0.12	0.5	1.0
Distal trachea		7.01 ± 0.69	6.73 ± 0.69	6.90 ± 0.69	5.86 ± 0.69
Bronchus	Cranial	6.52 ± 0.44	6.55 ± 0.44	6.68 ± 0.44	7.04 ± 0.44
Bronchus	Central	5.70 ± 0.42	5.69 ± 0.42	5.38 ± 0.42	4.71 ± 0.42
Bronchus	Candal	7.60 ± 0.55	7.48 ± 0.55	7.33 ± 0.55	5.23 ± 0.55

[a] Values are least-squares means ± SE expressed in μm; n = 8 rats (4 male and 4 female) for each concentration group.

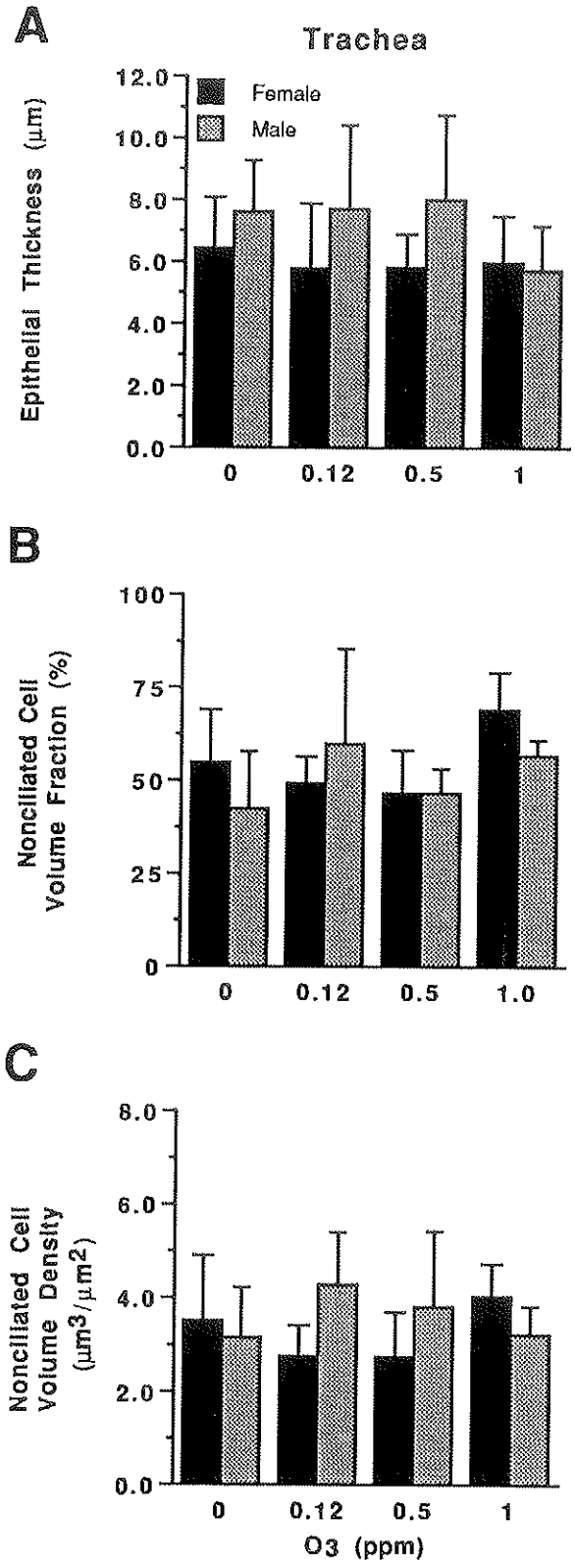

Figure 6. Comparison of epithelial composition in tracheas of male and female rats exposed to ozone for 20 months. A: Epithelial thickness. B: Volume fraction (%) of nonciliated cells. C: Volume density (per unit surface area) of nonciliated cells.

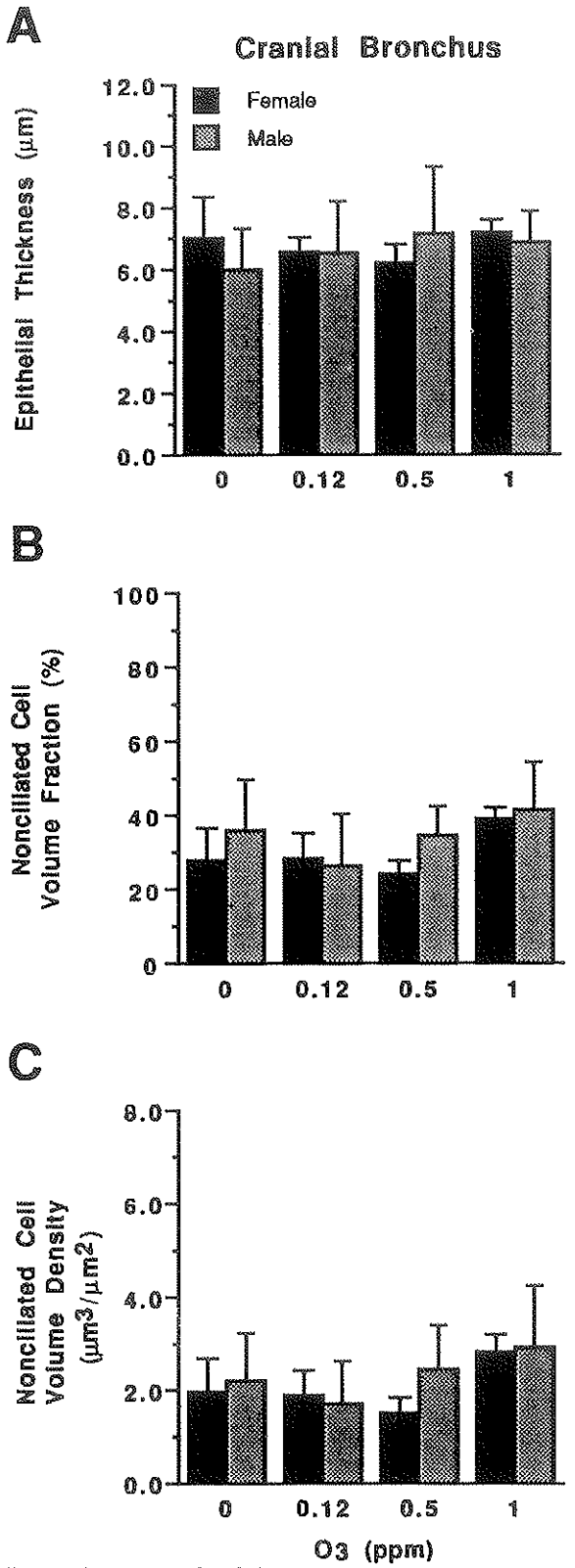

Figure 7. Comparison of epithelial composition in cranial bronchus of male and female rats exposed to ozone for 20 months. A: Epithelial thickness. B. Volume fraction (%) of nonciliated cells. C: Volume density (per unit surface area) of nonciliated cells.

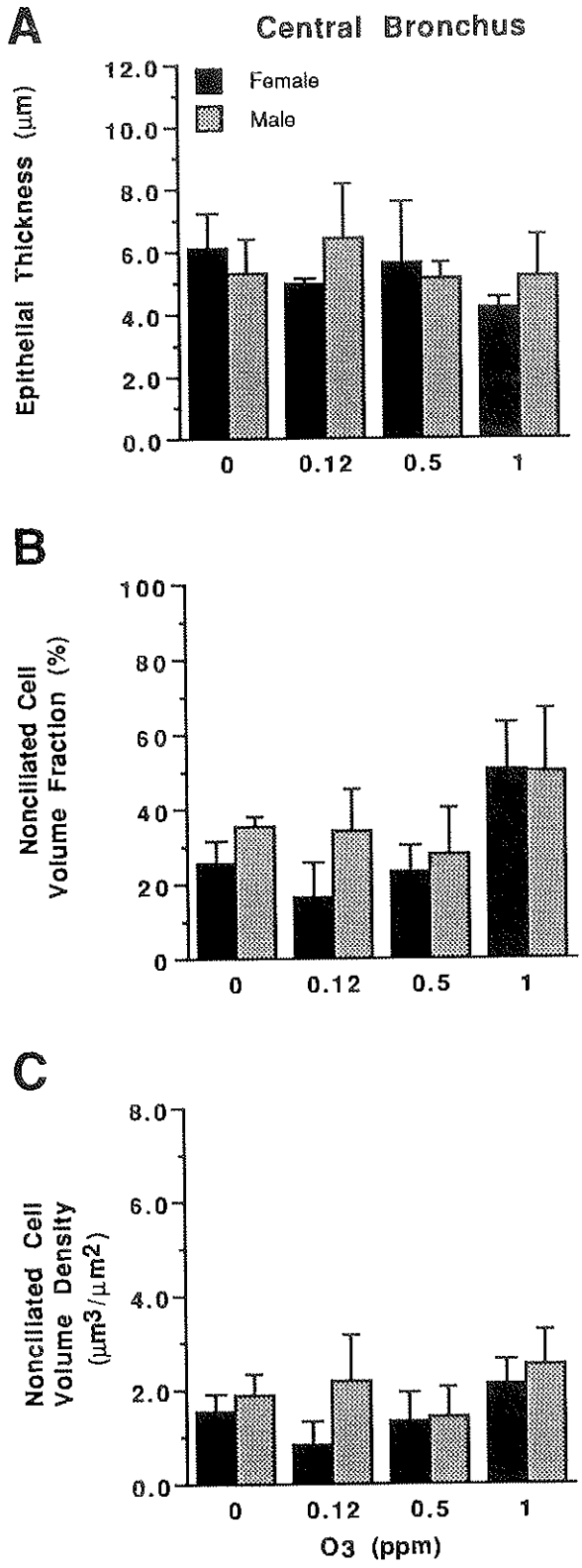

Figure 8. Comparison of epithelial composition in the central bronchus of male and female rats exposed to ozone for 20 months. A: Epithelial thickness. B: Volume fraction (%) of nonciliated cells. C: Volume density (per unit surface area) of nonciliated cells.

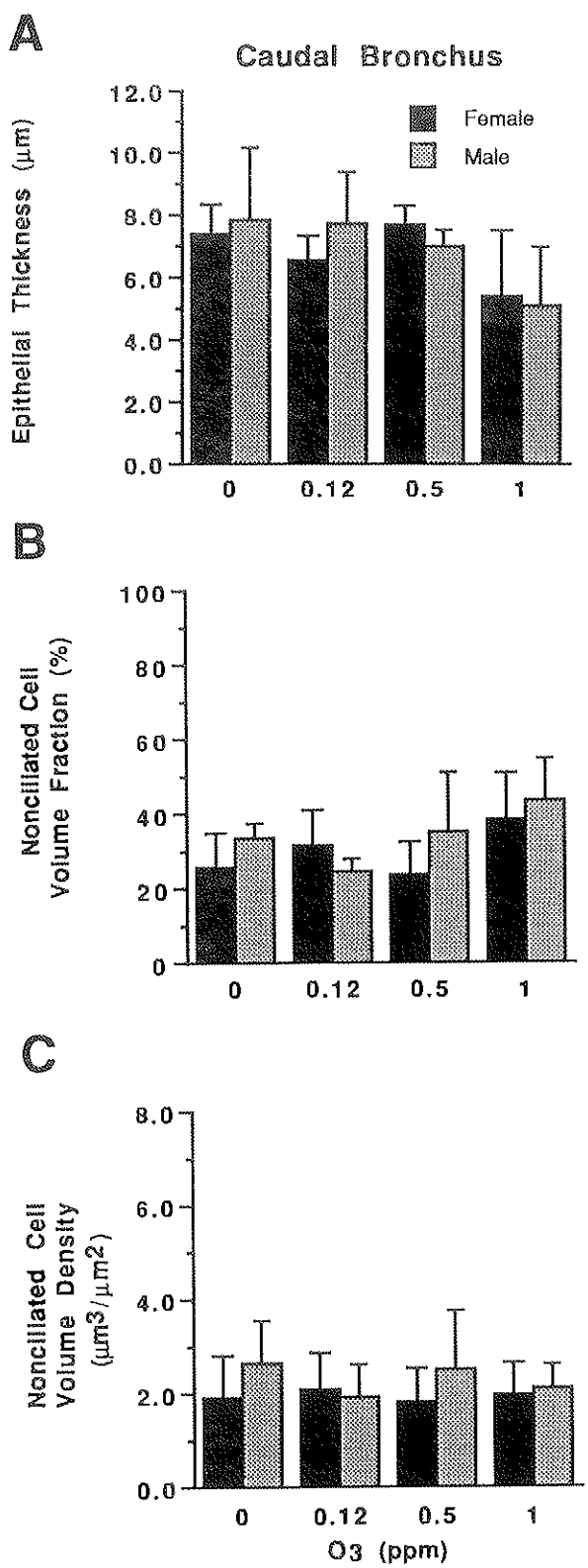

Figure 9. Comparison of epithelial composition in caudal bronchus of male and female rats exposed to ozone for 20 months. A: Epithelial thickness. B: Volume fraction (%) of nonciliated cells. C: Volume density (per unit surface area) of nonciliated cells.

Ozone Response Based on Gender

Tracheobronchial Epithelium

Stored Secretory Product. Comparison of the amounts of AB/PAS-positive material stored in the epithelium of the trachea showed no difference between males and females. In both males and females the decrease in the amount of stored secretory product was dependent on the ozone exposure concentration (Figure 4). The amount of material stored in the tracheal epithelium of males and females exposed to 1.0 ppm ozone was approximately 60% of that stored in tracheas of controls exposed to filtered air. In the cranial bronchus, there was no difference in the amount of AB/PAS-positive material stored in the epithelium of males

Table 6. Volume Density of Nonciliated Epithelial Cells in Tracheobronchial Airways of Rats Exposed to Ozone for 20 Months[a]

		Ozone Concentration (ppm)			
Airway	Region	0.0	0.12	0.5	1.0
Distal trachea		3.33 ± 0.38	3.52 ± 0.38	3.28 ± 0.38	3.63 ± 0.38
Bronchus	Cranial	2.09 ± 0.30	1.80 ± 0.30	1.98 ± 0.30	2.87 ± 0.30
Bronchus	Central	1.71 ± 0.22	1.51 ± 0.22	1.38 ± 0.22	2.33 ± 0.22
Bronchus	Caudal	2.84 ± 0.30	2.13 ± 0.30	2.16 ± 0.30	2.03 ± 0.30

[a] Values are least-squares means ± SE expressed in $\mu m^3/\mu m^2$; $n = 8$ rats (4 male and 4 female) for each concentration group.

Table 7. Epithelial Thickness in Centriacinar Bronchioles of Rats Exposed to Ozone for 20 Months[a]

		Ozone Concentration (ppm)			
Airway	Region	0.0	0.12	0.5	1.0
Terminal bronchiole	Cranial	6.63 ± 0.37	6.76 ± 0.40	6.75 ± 0.40	5.63 ± 0.45
Terminal bronchiole	Caudal	6.38 ± 0.25	6.60 ± 0.27	6.38 ± 0.27	6.36 ± 0.31
Proximal bronchiole	Cranial	7.62 ± 0.61	8.11 ± 0.66	7.03 ± 0.66	7.82 ± 0.75
Proximal bronchiole	Caudal	7.36 ± 0.46	6.53 ± 0.50	7.18 ± 0.50	6.62 ± 0.57

[a] Values are least-squares means ± SE expressed in μm; $n = 8$ rats (4 male and 4 female) for each concentration group.

Table 8. Volume Density of Nonciliated Epithelial Cells in Centriacinar Bronchioles of Rats Exposed to Ozone for 20 Months[a]

		Ozone Concentration (ppm)			
Airway	Region	0.0	0.12	0.5	1.0
Terminal bronchiole	Cranial	2.31 ± 0.21	2.66 ± 0.23	2.80 ± 0.23	2.37 ± 0.26
Terminal bronchiole	Candal	2.28 ± 0.20	2.74 ± 0.21	2.81 ± 0.21	3.48 ± 0.24[b]
Proximal bronchiole	Cranial	2.87 ± 0.24	2.45 ± 0.26	2.18 ± 0.26	3.10 ± 0.29
Proximal bronchiole	Caudal	2.33 ± 0.35	2.45 ± 0.38	2.96 ± 0.38	3.48 ± 0.43

a Values are least-squares means ± SE expressed in $\mu m^3/\mu m^2$; $n = 8$ rats (4 male and 4 female) for each concentration group.

[b] $p < 0.05$ compared with the same area in animals exposed to 0.0 ppm ozone.

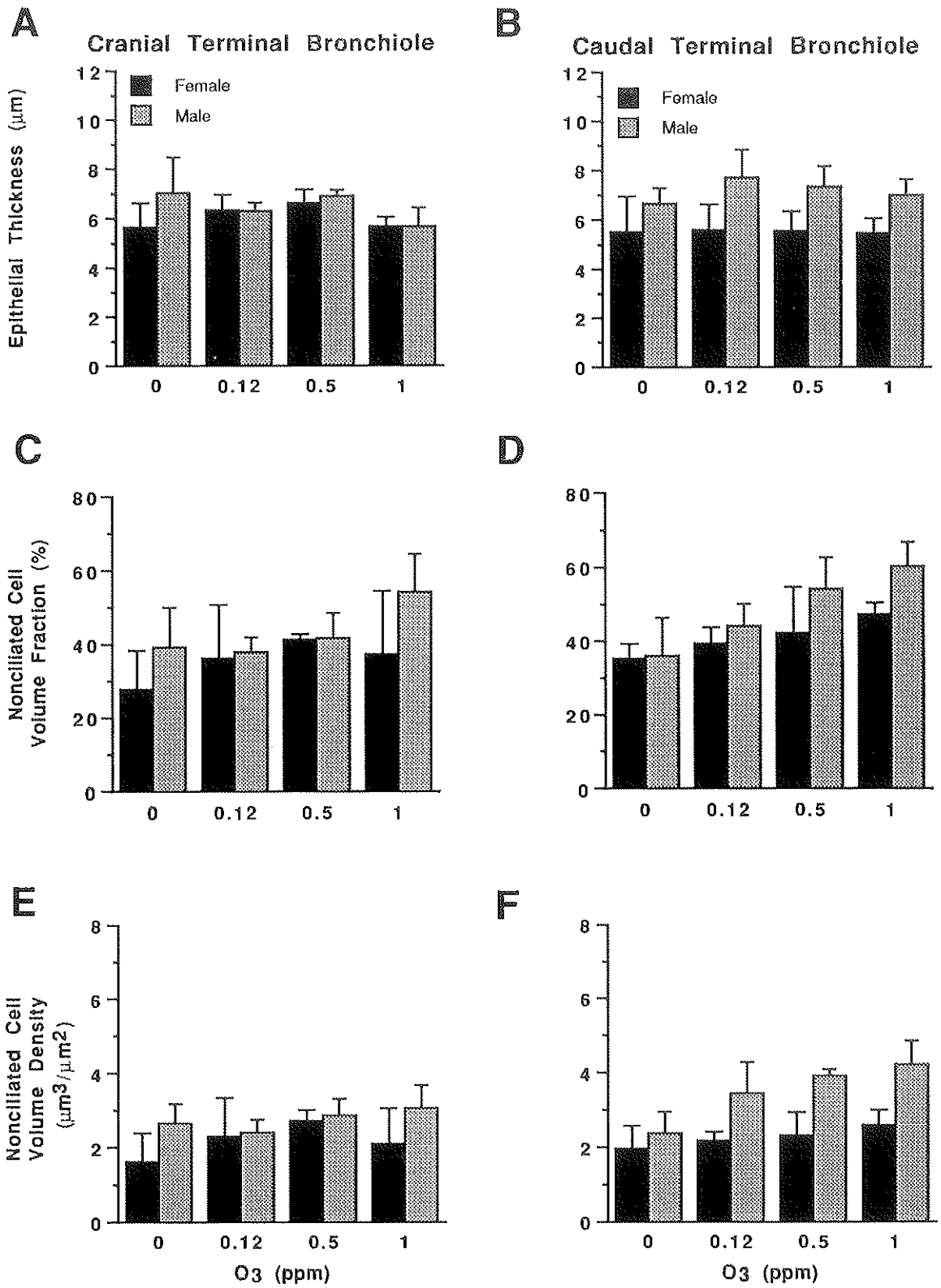

Figure 10. Comparison of epithelial composition in the terminal bronchioles of cranial regions (A, C, E) and caudal regions (B, D, F) of male and female rats exposed to ozone for 20 months. A and B: Epithelial thickness. C and D: Volume fraction (%) of nonciliated cells. E and F: Volume density (per unit surface area) of nonciliated cells.

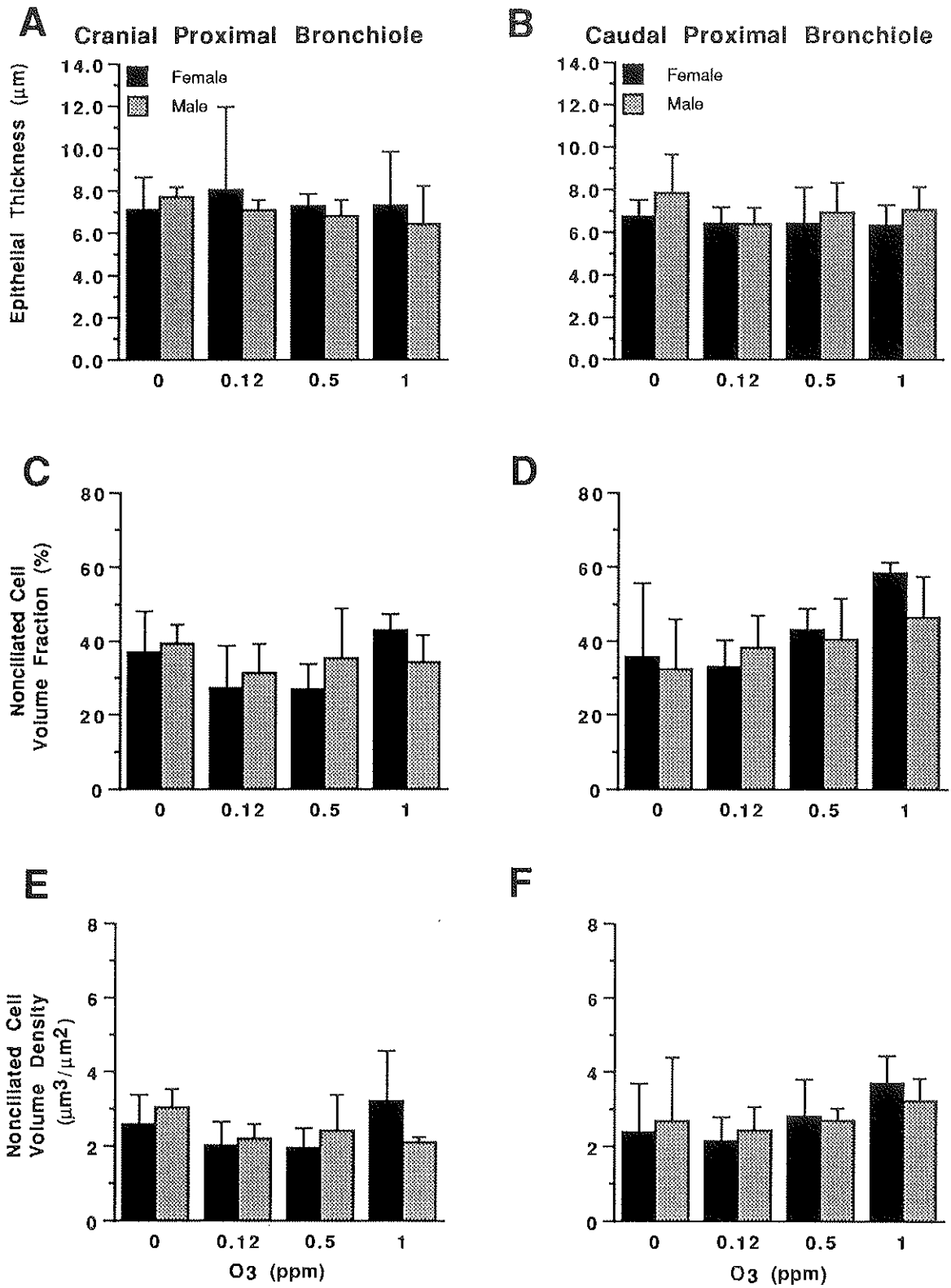

Figure 11. Comparison of epithelial composition in the proximal bronchioles of cranial regions (A, C, E) and caudal regions (B, D, F) of male and female rats exposed to ozone for 20 months. A and B: Epithelial thickness. C and D: Volume fraction (%) of nonciliated cells. E and F: Volume density (per unit surface area) of nonciliated cells.

or females (Figure 4). In the central bronchus, there was significantly less AB/PAS-positive material stored by females. There were no differences in the amount stored as a function of increasing ozone concentration for either gender (Figure 4). In the caudal bronchus there was no significant difference in the amount of AB/PAS-positive material stored in the epithelium of males or females. Although the amount of stored material appeared to increase in a dose-dependent fashion in the males, this was not the case in the females (Figure 4). There was no detectable AB/PAS-positive material in the bronchiolar epithelium.

Epithelial Composition. Comparison between the epithelial composition of the tracheas, cranial bronchi, and caudal bronchi of the males and females indicated that there were no significant differences, based on either gender or ozone exposure concentration, in epithelial thickness, in the volume fraction of the epithelium composed of nonciliated cells, or in the volume density of nonciliated cells (per unit surface area of basal lamina) (Figures 6, 7, and 9).

Centriacinar Bronchioles

Terminal Bronchioles. Comparison of epithelial composition in terminal bronchioles showed there was no significant difference in the thickness of the epitbelium in the cranial or caudal region between males and females associated with ozone exposure concentration. The volume density of nonciliated cells in the caudal terminal bronchioles of male animals increased significantly following exposure to any ozone concentration (Table 3; Figure 10).

Proximal Bronchioles. In proximal bronchioles of both the cranial and caudal regions of males and females, there was no difference in epithelial thickness with ozone exposure (Figure 11). Only in the cranial region of the proximal bronchioles of animals exposed to 1.0 ppm ozone was the volume of nonciliated cells significantly elevated in females relative to that in males.

DISCUSSION

This study tests the hypothesis that respiratory epithelium develops resistance to injury from oxidant air pollutants by reorganizing to favor cell types that are less susceptible to the acute injury that results from initial exposure. We addressed this issue in animals exposed to ozone for nearly their entire life span. Because of the focal nature of tbe acute injury associated with ozone exposure, we attempted to characterize epithelial changes within carefully defined regions and to compare changes in areas known to be highly susceptible to acute injury (target areas) with changes in areas known to be less susceptible (nontarget areas). Our results show that long-term exposure significantly alters the amount of stainable secretory material stored in tracheobronchial epithelium. However, these alterations are site-specific, in terms of both the direction of the change and the extent of the change elicited by the exposure concentration. The cellular composition of the trachea and the proximal intrapulmonary conducting airways remained generally unaltered by ozone exposure. In contrast, in the centriacinar regions, the epithelium was significantly reorganized following ozone exposure. The primary change involved an increase in the volume density of nonciliated cells lining the terminal bronchioles of the caudal site following exposure to any of the ozone concentrations in male rats. No statistically significant changes were observed in female rats. Proximal bronchiolar epithelium, which is not thought to be a major site of acute bronchiolar injury, was altered by the exposure conditions. In female rats there was a statistically significant increase in the volume density of nonciliated cells relative to that in male rats following exposure to 1.0 ppm ozone. The levels were not significantly elevated in ozone-exposed females relative to those in female controls. Further studies would be needed to determine wbether this represented a biological shift of response from the terminal bronchioles (which were approximately the same following 1.0 ppm ozone as in control female rats) to the proximal bronchioles. The terminal broncbiolar epithelium of the centriacinar regions was reorganized in favor of the nonciliated cell population. The bronchiolar epithelium that lined bronchiolarized alveolar ducts in exposed animals exhibited a mixture of characteristics found in the terminal bronchiolar epithelial populations of both control and exposed animals.

From this study, it appears that epithelial reorganization plays a role in the development of tolerance in response to long-term exposure to ozone. The changes vary according to site and are most pronounced in those portions of the tracheobronchial tree tbat are most affected in short-term exposures. Some changes appear to be dose-dependent; others do not. The changes involve alterations in secretory activity as well as in the cellular composition of the epithelial lining.

The variability in epithelial response observed in different regions of the tracheobronchial airways is consistent with predictions of local ozone dose based on computer simulation models (Overton et al. 1987, 1989; Miller et al. 1988). These models, which take into account differences in path length from the trachea to the terminal bronchiole, predict differences in the amount of ozone delivered to different sites within the tracheobronchial airways (Overton et al. 1989). Simplifying the assumptions used with these models, it can be shown that dose depends primarily on transit time and airspace volume distal to the airway.

The sites selected in this study allow qualitative examination of the relative importance of transit time (approximated by path length) and distal volume (estimated by summing the volumes of all the airways along the same path but distal to the airway in question, based on the data of Raabe et al. 1976).

The central and caudal sites are along the same pathway, with the central bronchus having both a shorter transit time and a larger distal volume. A comparison between the central and cranial sites may be used to assess the importance of distal volume as the two sites have similar path lengths but the volume distal to the cranial site is smaller. A comparison between the cranial and caudal sites indicates the importance of transit time as the path length to the caudal site is nearly twice that to the cranial site; however, they are predicted to have similar distal volumes. In addition, the cranial and caudal samples were selected to be representative of the short path (distance from trachea to terminal bronchiole 7 to 8 generations of branching) and the long path (distance from trachea to terminal bronchiole 15 to 17 generations), respectively, used in the model of Overton and colleagues (1989).

The changes in proximal conducting airways were mainly in stored secretory product. The bronchus we chose from the central region corresponds to the fourth- to sixth-generation bronchi in the long path in the ozone model. The dose of ozone to this site is predicted to be somewhat lower than that to the trachea. Correspondingly, this airway showed no epithelial response to the long-term ozone exposure in terms of either altered secretory product storage or reorganized epithelial composition. The model predicted a larger dose of ozone in more distal conducting airways of the same cross-sectional area in the long path (8 to 12 generations) than in the short path (4 to 5 generations). This prediction correlates with the differences in the amount of cellular change we observed in these two zones. The small-diameter bronchus in the caudal zone, or long path, had a dramatic dose-dependent increase in the amount of stored secretory product. In the small-diameter airway in the short path (cranial bronchus), the changes in stored secretory product were not nearly so dramatic and were observed only at the highest ozone concentration. There was no marked change in the thickness of the epithelium, which suggests that the changes in this airway were less severe than those in the airways of the same size but with a longer path from the trachea.

In contrast, the principal change in the trachea, a site where ozone dose is predicted to be higher than in more distal conducting airways, was a concentration-related loss of stored secretory product. Previous studies of long-term (60-day) exposures that focused on the rat trachea did not find the same sorts of changes we observed. In those studies, the secretory cell population and the amount of stored secretory product did not appear to change, nor did the composition of the epithelial cell population (Nikula et al. 1988). There was, however, a loss of ciliated cells, a feature we did not observe after 20 months. Long-term (one-year) exposure of rabbits to ozone at an ambient concentration (0.1 ppm) produced a transient increase in secretory cells (at four months), which was not present after one year (Schlesinger et al. 1992). In that study, analysis of epithelial responses to ambient concentrations of ozone (0.1 ppm) by airway size showed an increase in secretory cells in airways of small and medium diameter, but no change in larger airways. However, the lack of detectable change may be due to the high probability of not knowing the precise airway generation within the airway tree, as is needed for prediction with the model.

Short-term exposure studies have not found alterations in tracheobronchial mucous substances to be a major feature of the injury response in primates (Mellick et al. 1977; Wilson et al. 1984) or in rats (Schwartz et al. 1976). Thus, part of the basic cellular response to chronic oxidant stress produced by long-term exposure to reactive gases, such as ozone, appears to be an alteration in secretory product storage, which depends on location within the conducting airway tree. Epithelial populations in conducting airways also may respond to chronic stress by altering the composition of the epithelium, but again, this response appears to be site-specific and may be closely related to the dose of ozone delivered to each site.

Changes in the centriacinar region of the rat do not correlate as closely with model-based predictions of ozone dose. The model suggests that the terminal bronchioles in the short path will be exposed to higher concentrations of ozone than terminal bronchioles in the long path (Overton et al. 1989). We evaluated terminal bronchiolar epithelium from two sites: one corresponding to the short path (cranial region) and one to the long path (caudal region). They were predicted to have similar distal volumes. We observed no significant changes in epithelial thickness in either region. However, in the caudal region, the volume density of nonciliated cells was significantly elevated in male rats following all of the ozone exposures. This finding suggests that the terminal bronchiole epithelium responds differently to ozone exposure depending on its position within the tracheobronchial tree, but factors other than ozone dose also may be important. For example, in our case, the long path was located in the caudal region, a zone that could receive a larger volume of air, and, hence, ozone during inspiration; or the size of the ventilatory unit (defined as all alveolar ducts and alveoli extending from an airway branch in

which the transition from bronchiolar to alveolar epithelium occurs) could be greater in the caudal region. Either of these factors (Mercer and Crapo 1987; Mercer and Pinkerton 1990; Mercer et al. 1991) would result in a higher ozone dose to that region than was predicted hy Overton and coworkers (1989). The model predicts that, regardless of path, the lowest concentration of ozone throughout the conducting airways will be in the airway one generation proximal to the terminal bronchiole (Overton et al. 1989). We evaluated this site in short-path (cranial) and long-path (caudal) regions. As predicted, we found minimal change as a result of ozone exposure.

In summary, this portion of our study shows that the epithelial populations in conducting airways, which are targets for injury in initial phases of inhalation of reactive oxidant gases, establish a new homeostasis in which cell injury is no longer an obvious result of exposure. Epithelial cell populations establish a variety of new conformations directly associated with the development of tolerance. These conformations involve alterations in secretory product storage as well as shifts in epithelial composition toward cell types that are less susceptible to acute injury. It appears that long-term, essentially lifetime, exposure to injurious oxidant gases causes the epithelium to be redefined. Repeated exposure to nitrogen dioxide also results in nonciliated cell hyperplasia in centriacinar bronchioles (Evans et al. 1986). Long-term exposure to other irritants, including sulfur dioxide, sulfuric acid aerosol, cigarette smoke, and formaldehyde, produces secretory cell hyperplasia in the proximal respiratory tract (Lamb and Reid 1968, 1969; Spicer et al. 1974; Schlesinger et al. 1992). However, as our study shows, this redefinition, at least for ozone, depends on the specific location of the epithelium, and probably also its local microenvironment and preexposure composition. Epithelial cells lining the trachea respond differently to chronic injury than do epithelial cells lining more distal conducting airways. In addition, the response in terminal bronchioles, another major site of injury, differs from that in more proximal airways. Finally, all of the regional differences in the epithelial response correlate closely with the predicted ozone doses at those sites.

PULMONARY ACINUS

METHODS

Lung Fixation and Processing for Microscopy

In general, four male and four female rats from the control group and four male and four female rats from each of the ozone exposure groups were randomly selected for evaluation. Animals were killed with an overdose of sodium pentobarbital. The lungs were collapsed by diaphragmatic puncture and fixed in situ by intratracheal instillation of 2% glutaraldehyde in cacodylate buffer (pH 7.4, 350 mOsm) for 15 minntes at 30 cm of fixative pressure (Plopper 1990). The fixed lungs were removed by thoracotomy and stored in the same fixative until processing for immunohistochemistry, histochemistry, light microscopy, and scanning electron microscopy. The fixed lungs were trimmed of all mediastinal contents, and the lung volumes were measured by fluid displacement. Regions of the left lung lobe were selected for complementary histochemistry and high-resolution light microscopy.

Beginning with the trachea, airways were dissected along their long axes to approximately the level of the terminal bronchiole (Plopper 1990). The dissections were done with the aid of a Wild M8 dissecting microscope and fiber-optic illumination. The areas selected for study were chosen from cranial and caudal regions of the lung at the distal ends of two conducting airway paths, one in which air travels a short path with a large cumulative angle of change in the path direction, and the other selected from a region served by a mnch longer path with a low cumulative angle of deviation (Figure 1). The tissue blocks revealed by microdissection were nsually two to four generations from the terminal bronchioles. After dissection, blocks were removed and embedded again as larger blocks. Tissue slices (approximately 2 × 4 × 6 mm in size) were postfixed in 1% osmium tetroxide in Zetterquist's buffer, followed sequentially by 1% tannic acid and 1% uranyl acetate in maleate buffer, dehydrated in ethanol and propylene oxide, and embedded in either Epon 812 or Araldite 502.

Identification of the Bronchiole–Alveolar Duct Junction

To measure systematically the distribution of tissue changes in ventilatory units of animals exposed to ozone, a strategy is required that ensures the proper identification of the BADJ. If these junctions are not easily identified, then comparisons between control and treated animals may involve inappropriately matched alveolar duct generations. This problem arises with exposures to high levels of ozone, which cause the bronchiolar epithelium to extend from the level of the terminal bronchiole into the proximal alveolar regions of the ventilatory unit (Boorman et al. 1980; Barr et al. 1988). When such a change has occurred, the first alveolar dnct generations in control animals may be inadvertently compared with the second and third alveolar duct generations in the lungs of these ozone-exposed animals. However, if no alveoli are obliterated during the process of epithelial reorganization, the first alveolar outpocketing along the

airway path may serve as a landmark for identifying the original BADJ.

Because of the changes occurring in the BADJ with long-term exposure to ozone, scanning electron microscopy was used to examine the three-dimensional appearance of this region. The distal third of the right middle lung lobe from three animals selected at random from each exposure group was dried to the critical point using ethanol and carbon dioxide (Karrer 1958; Tyler et al. 1985). The distal conducting airways and the BADJs were identified by microdissection of dried specimens (Plopper 1990) to reveal complementary halves of single BADJs (Pinkerton et al. 1993). The dissected lungs were mounted on stubs sputter-coated with gold and were examined with a Phillips 501 scanning electron microscope.

Isolation of Bronchiole–Alveolar Duct Junctions for Light Microscopy

From each embedded tissue block taken from the cranial and caudal sites in the left lung lobe, BADJs were isolated by the methods of Pinkerton and colleagues (1993). Centriacinar regions were isolated by cutting the entire tissue block into slices approximately 0.4 to 0.5 mm thick. Each slice was examined under a dissecting microscope to identify BADJs in longitudinal profile. The criterion for selection was a symmetrical pair of alveolar ducts arising from a single terminal bronchiole. Ventilatory unit isolations meeting this selection criterion consistently contained alveolar duct paths in longitudinal profile that extended two to four generations beyond the BADJ. Selected isolations were remounted on beem blanks and sectioned at a thickness of 0.5 μm with glass knives. Sections were stained with toluidine blue (0.5% in 1% borate buffer).

Morphometric Analysis of Alveolar Septal Tips

Each ventilatory unit isolation was captured as a digital video image on the computer. From a single reference point at the level of the first alveolar outpocketing, a pattern of concentric circles at 100-μm intervals was placed over the isolation (Figure 12). These digital images for each isolation served as guides to identify arc intercepts of each circle with tissues along the ducts of each ventilatory unit. Only those arc intercepts with tissues along open duct paths within a 30° angle incident to either side of a line bisecting the ventilatory unit profile were measured.

The first approach for analyzing each isolation was to measure the intercept length that each arc made with tissue using a Zeiss optical microscope, a cursor with a digitizing pinpoint light source, and a tablet interfaced to an IBM PS/2 computer. A microscope photoextension tube facilitated measurements with the light cursor while directly viewing the tissue under the microscope. A 40 × objective was used to provide better resolution of tissues than that seen on the arc map, thus permitting more accurate visualization of tissue surfaces and distinction of alveolar macrophages from septal tissues. Each intercept measurement followed the precise path of the arc traversing over tissue as it appeared on the "arc map." Exceptions to this rule were intercepts of tissue with the first 100-μm arc. Because of the considerable curvature of this arc, a line perpendicular to the surface at the point where the curve intercepted tissue was measured rather than the actual path of the arc. All measurements were taken through the complete tissue wall including the capillary space. Intercepts that passed through a blood vessel (arterioles and venules) greater than 30 μm in diameter were excluded from measurement. Of note is the observation that the septal capillary diameter rarely exceeded 15 μm in the rats.

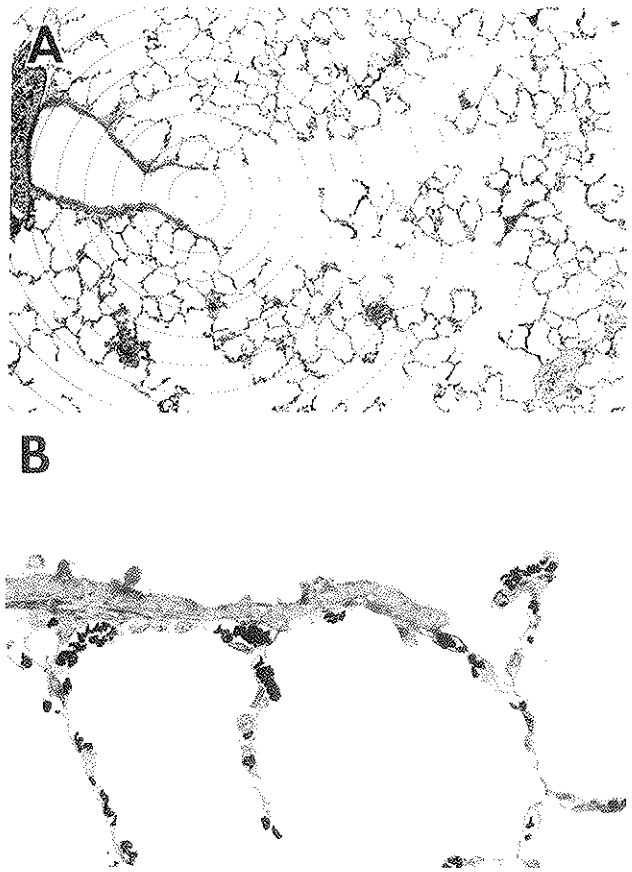

Figure 12. A: Computer video image of a ventilatory unit from the lung of a control rat with the terminal bronchiole, a symmetrical pair of alveolar ducts, and the intervening tissue bifurcation ridge captured in longitudinal profile. A computer-generated "bull's-eye" pattern of 100-μm concentric circles is overlaid on the isolation with the center of the bull's-eye over the geometric center of the airway at the level of the first alveolar outpocketing. B: Enlarged view of the BADJ from panel A. The abrupt transition of bronchiolar to alveolar epithelium from the conducting airway to the alveolar duct is illustrated.

For the initial analysis, only arc intercepts with tissues forming alveolar septal edges (tips) were measured. Alveolar septal tips were distinguished from alveolar walls by drawing a line to separate alveolar airspaces from the alveolar duct lumen. All tissues that touched this line were classified as a part of the alveolar septal tip that forms the mouth opening or crest of each alveolus into the duct. Tissues not touching this line were considered to be part of the alveolar wall (Figure 13). This method provided a simple way to separate these two parameters without any subjective bias on the part of the observer. The actual path of the arc intercept with each alveolar septal tip was used as a measure of alveolar septal tip thickness. When the path of an arc passed through the septal tip and down the alveolar wall parallel to the tissue surface exposed to air, only that length of the arc that intercepted the septal tip was measured. This approach helped to eliminate inappropriately long measurements through septal tissue walls parallel to the alveolar surface.

Epithelial and interstitial thickness were measured in the following manner. Using the map with concentric circles, each region of the arc that intercepted an alveolar septal tip was enlarged to approximately 400× magnification and captured as a computer image. A straight line was drawn to approximate the path over which the arc traversed (Figure 14). Measurements were made based on the path of this line as it crossed over the various tissue compartments composing the septal tip including epithelium, interstitium, and capillary lumen. Cumulative measurements of the epithelium were made across the entire alveolar septal tip because, generally, two epithelial surfaces were traversed by the arc. Interstitial measurements included distances traversing the endothelium. The distance of the arc across the capillary lumen also was recorded.

Morphometric Analysis of the Alveolar Duct Wall

The same images that were captured at 400× magnification for alveolar septal tip thickness measurements based on arc intercept lengths were reanalyzed using a test lattice overlay (21 lines) to count points and intercepts in order to derive volume densities. All volume density measurements were normalized to the area of the alveolar surface. In this study, the surface area was defined as the alveolar tissue–air interface. In total, four to eight isolations per animal were used for this analysis. These measurements were made for each 100-μm interval down the alveolar duct. The measurements per 100-μm interval down the alveolar duct were averaged and expressed as epithelial, interstitial, and capillary density. Tissue density was derived by counting points and intercepts from each field analyzed. All counts were compiled and moved to a spreadsheet, the data were organized, and calculations were made to determine volume densities for the epithelium, interstitium, and capillary lumen. In addition, alveolar macrophages, although not part of the septal wall, were measured as a volume density normalized to the alveolar surface within each 100-μm interval in which these cells were found.

Extent of Bronchiolar Epithelium Down Alveolar Duct Paths

To measure the extension of bronchiolar epithelium into alveolar ducts, the same rigid sampling scheme for each ventilatory unit isolation was employed. Using the same

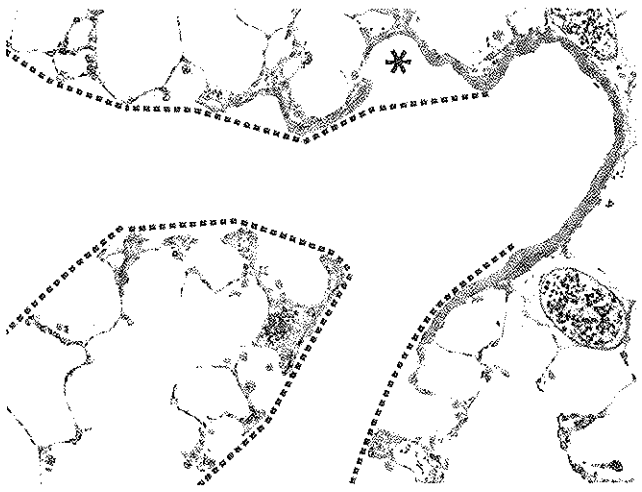

Figure 13. Proximal alveolar region from the lung of a rat exposed to 1.0 ppm ozone. An outpocketing of an alveolus lined with cuboidal and bronchiolar epithelial cells (*) is present within the wall of this isolated tissue. Dashed lines that separate alveoli from alveolar duct lumina serve to define alveolar tips (edges) for analysis in this study. Magnification: is ×115

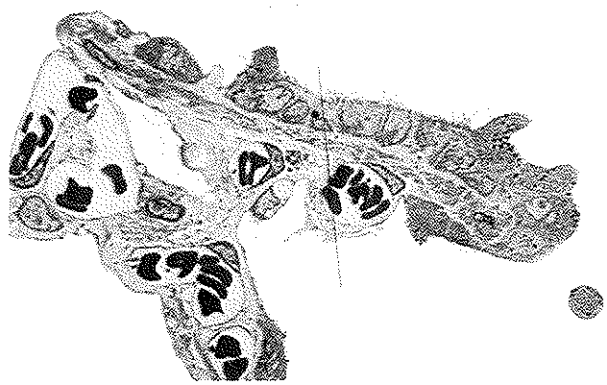

Figure 14. Computer image of a septal edge 400 μm into an alveolar duct in the lung of an animal exposed to 1.0 ppm ozone. The intercept of the concentric circle with tissue is shown by the vertical line crossing the epithelial, interstitial, and capillary compartments. Each compartment is measured individually to determine its contribution to the overall thickening of the septal wall.

concentric circle grid at 100-μm intervals, we generated a map of each ventilatory unit. At high magnification (40×), the most distal ciliated and nonciliated bronchiolar cells within the ventilatory units were identified. The extension within the ventilatory unit was determined using the concentric circle pattern as a measure of distance from the central reference point. Figure 12 illustrates the organization of this concentric circle overlay.

Lung Modeling and Determination of Dose-Versus-Distance Curves for Multiple Ozone Exposures

The distribution of dose versus distance in the acinus was determined for each of the three exposure concentrations using previously described methods (Pinkerton et al. 1992). Modeling of the uptake of a reactive gas inspired into the lungs was used to predict the amount of ozone delivered to the ventilatory unit as a function of distance from the BADJ (Mercer et al. 1991). For the modeling, structural parameters affecting gas uptake, such as volume and the surface area for gas exchange, were determined along with factors influencing deadspace volume contributed by the proximal tracheobronchial tree. These structural parameters were obtained by serial section analysis methods previously described (Mercer and Crapo 1987; Mercer et al. 1991). The average ventilatory unit volume was 0.53 ± 0.03 mm^3, and surface area was 18.1 ± 0.7 mm^2. Previously reported dimensions of the tracheobronchial tree (Mercer et al. 1991) were used to describe the deadspace volume and surface area of airways proximal to the BADJ defining entry into the ventilatory unit.

Data Reduction for Statistical Analysis

A block of tissue was taken from each of the regions identified as cranial and caudal in each rat. From this block, several isolations were made for potential analysis. An isolation was accepted for analysis if there was a complete vertical sectioning of a ventilatory unit beginning at the approximate center of a terminal bronchiole and leading into approximately symmetric alveolar ducts. As described above, a septal tip was identified as a field and selected for analysis if it intersected a concentric circle grid overlay. Because there would not necessarily be any intersections with an arc, there were not always reported values for each distance down a path even though there might be multiple isolations and fields for that animal.

The data could be aggregated into appropriate units of analysis in several ways. In the morphometric measurements, the points on a grid of specific size (42 points in this case) falling in defined regions (for example, epithelium or interstitium) were manipulated mathematically to estimate tissue volume density. The first decision was whether to calculate the volume density individually for each combination of isolation, field, and distance down a path and then obtain an average value for each animal at each distance, or to sum the points for all the isolation-field combinations and calculate a single distance value for each animal. The calculations were performed both ways, and we found somewhat less variability in means across animals when summing the points and calculating a single value per animal for each distance. Therefore, single values were calculated for each animal at each distance down each path by summing all the points first.

In further testing, it was found that if an animal only had one field and only one isolation at any distance, then this value contributed significantly to overall variability in the mean (for all animals at that distance along that path) and was frequently identified as an outlier by the Wilcoxon signed-rank test (Snedecor and Cochran 1967). Accordingly, these observations were deleted. In no case did this result in losing all data for an animal along either path; however, as described subsequently, some animals had to be excluded from specific statistical analyses because of the amount of missing data resulting from these deletions.

Statistical Methods

The measurements of epithelial, interstitial, and capillary volume density were analyzed independently although there is clearly a multivariate correlation structure that could be of interest. Measurements were made in the caudal and cranial paths, and these were treated as the multivariate dimension as discussed for Specific Aim 1. To take advantage of longitudinal information within the same ventilatory unit in an animal, a multiple-stage statistical analysis strategy was developed. First, linear regression models were fit for each of the dependent variables (that is, epithelial, interstitial, and capillary volume density) for each path for each animal. From visual observation of all of the data, it was evident that interstitial and capillary volume density could be fit to a linear regression but that the epithelial volume density behaved differently. The regression models are discussed in more detail below. Once the appropriate model was fit, the regression parameters were analyzed by MANOVA with gender and ozone exposure concentration as the independent variables. If the appropriate regression model included only a single parameter (the mean), then a multivariate analysis with path as the multivariate vector was used to compare differences between the cranial and caudal tissue volume densities. Univariate analyses were used to examine the effects of gender and ozone concentration on the individual paths (if the MANOVA indicated a significant difference [Hotelling-Lawley trace

value of $p < 0.05$] between the two paths) or to determine the average of the two paths (if the MANOVA indicated no difference between the paths). Significant ANOVA effects associated with ozone concentration or the concentration-gender interaction were subtested using t tests with a Bonferroni adjustment. If the appropriate regression included more than one parameter (for example, intercept and slope), then the MANOVA was used only to control for the correlations between the parameter estimates within each animal. A separate MANOVA was run for each path. A two-way MANOVA (including tests for path and parameter differences) would be an appropriate way to analyze these data; however, there were not adequate degrees of freedom to construct the tests. The same step-down process as described above was used. For all analyses, significant ANOVA effects ($p < 0.05$) were required before performing subtests to examine effects of concentration or the concentration-gender interaction.

From visual inspection, it appeared that the data for the three variables, epithelial, interstitial, and capillary volume densities, would be best described by a flat line as a function of distance, that is, the mean. Individual regressions were fit for each animal and each path of each animal assuming a flat line, a linear model, a quadratic model (linear and square term), and a square term only. The models were compared based on mean square error (MSE), and it was found, in general, that a flat line described the data well. The variables for which some kind of trend was significant were examined more closely. The regressions between the two paths were compared for all three variables to determine if there was any consistent shift from a flat line relation to some kind of trend in that rat. Nothing was observed for any of the cases with the significant trends. It appeared that the flat line was a fair approximation over the range of data available for the variables with some statistical trend, so we felt that the flat line approximation would not be inappropriate. In doing these regressions or even the simple means that were ultimately selected, it was found that the rats with volume density data for only one or two distances of the possible eight contributed substantially to the variability in the animal means. As a result the records for four rats were excluded from the analysis: H45 (male, 0.0 ppm ozone, cranial path), H124 (female, 1.0 ppm ozone, cranial path), H67 (female, 0.5 ppm ozone, caudal path), and H52 (female, 1.0 ppm ozone, caudal path).

Epithelial volume density declined as a function of distance according to one of two stylized patterns (Figure 15). To model this relation, three linear segments were fit using a nonlinear iterative least-squares regression procedure.

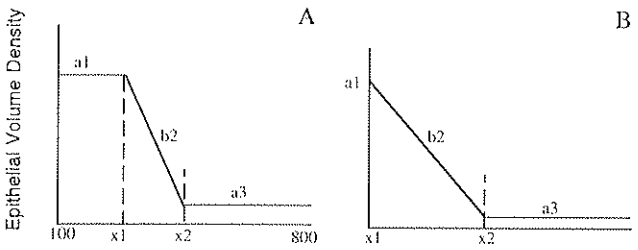

Figure 15. Five parameters were fit to describe the epithelial volume density for (A) three linear segments or (B) two linear segments. For some rats an initial "plateau" in thickness ($a1$) was observed from 100 to $x1$ µm in distance down an acinus. For rats without this plateau, $a1$ is the y intercept for the linearly declining segment and $x1 = 100$ µm. Following a linearly declining segment described by its slope, $b2$, a lower flat segment was observed ($a3$). It began at $x2$ µm distal from the terminal bronchiole and continued through 800 µm.

The two-segment model shown in panel B of Figure 15 is a subset of the three-segment model with the length of the first segment heing zero. The interpretation of the parameters follows. There is an epithelial volume density at the entrance of the ventilatory unit ($a1$) that declines linearly ($b2$) until it reaches some minimum volume density ($a3$) that appears to be a constant for the remainder of the length of the ventilatory unit. The initial volume density is maintained for some distance ($x1$), and the minimum volume density begins at some distance ($x2$). If the linear decline in volume density begins immediately, then $x1$ is equal to the distance of the first measurement, 100 µm in tbis study. Effects of pollutant exposure could affect this relation in several ways. The initial volume density could be increased or decreased ($a1_{exposed} \neq a1_{control}$), the distance that the initial volume density is maintained could be increased ($x1_{exposed} > 100$), the rate at which the initial volume density declines to the minimum volume density could be changed ($b2_{exposed} \neq b2_{control}$), the distance at which the minimum volume density is achieved could be changed — probably increased ($x2_{exposed} > x2_{control}$) — or the minimum volume density could be changed ($a3_{exposed} \neq a3_{control}$).

In fitting the data to this model (one curve was fit for each path for each animal), some observations had to be deleted because of missing values at different distances. Models were not fit if four or more of the possible eight values were missing, if two or more values were missing in the first 400 µm, or if two or more values were missing in the last 300 µm (this condition was required only for the ventilatory unit at the end of the caudal path, which was more variable than the cranial path). In addition to the 4 animals (from one path or the other) that were excluded from the analysis of the other variahles, 15 other animals (from one path or the other) also had to be excluded from the analysis.

RESULTS

Scanning Electron Microscopy

To obtain a three-dimensional perspective on the centriacinar epithelial reorganization occurring with long-term ozone exposure, scanning electron microscopy was performed on complementary halves of BADJs. As illustrated in Figure 16, by using the tilt function on the scanning electron microscope, it was possible to view all sides of the walls in this region. In animals exposed to air (Figures 16A and 16B) or to ozone (Figures 16C through 16E), the most proximal alveolar outpocketings were within 100 μm of the BADJ. In both control and ozone-exposed animals, the epithelial surface of the airway proximal to the first alveolar outpocketing was a mixture of ciliated cells and nonciliated cells, most of which had apical projections into the airway lumen. In control animals, the surface pattern of epithelial cells characteristic of those in the terminal bronchiole was observed to extend a variable distance beyond the most proximal alveolar outpocketing. This variation was observed from animal to animal, and from BADJ to BADJ within the same animal. Bronchiolar epitbelial cells, identified by their surface features, were occasionally found as far distally as the first bifurcation point of the alveolar duct. In animals exposed to ozone, the three-dimensional perspective on all portions of the airway wall indicated that the bronchiolar epithelium extended several generations into the alveolar ducts, well beyond the first alveolar dnct hifurcation ridge (Figure 16C through 16E). These cells within alveolar ducts appeared to have surface characteristics similar to those of the terminal bronchiole cells, although occasionally small regions within some alveolar duct generations contained squamous epithelial cells on the surfaces of alveolar mouth openings as well as in the alveolar outpockets (Figure 16D). The extent of bronchiolarization varied from animal to animal and from BADJ to BADJ. However, the surface pattern of bronchiolar epithelial cell types was relatively equal in extent around the entire circumference of affected alveolar ducts. Preferential location of the bronchiolar epithelium in relation to the position of the pulmonary arteriole or to the number of generations of branching of alveolar ducts in whicb the epithelium was ohserved was not apparent. In both control and ozone-exposed animals, when cuboidal cells with apical projections were observed in groups, ciliated cells also were present.

Exposure to 0.12 or 0.5 ppm ozone also was associated with significant changes in the pattern of epithelial interdigitation of the terminal bronchiole with the alveolar duct. In contrast to the abrupt transition from bronchiolar to alveolar epithelium at BADJs in the lnngs of control animals, bronchiolar epithelial cells extended for two to three alveoli into the alveolar duct in animals exposed to 0.12 ppm ozone (Figure 17A and 17B) and to greater depths in the lungs of animals exposed to 0.5 ppm ozone (Figure 18A and 18B). Unlike the epithelium in animals exposed to 1.0 ppm ozone, the bronchiolar epithelium within alveolar ducts of animals exposed to 0.12 or 0.5 ppm ozone appeared to be limited to surfaces forming the mouth openings of each alveolus in the central acinus.

Morphometric Analysis of the Alveolar Duct Wall and Septal Tips

To define the extent of epithelial and interstitial changes within the lungs, tissue changes of the septal tip and of the alveolar wall in proximity to the septal tip were examined. Measurements of this nature are more representative of changes occurring within the alveolus at various distances into the ventilatory unit. These measurements are illustrated in Figures 19 to 23 for the epithelium, interstitium, and capillary.

Epithelium. A mathematical model (Overton et al. 1987; Mercer et al. 1991) was used to estimate delivered dose as a function of distance within a ventilatory unit. Assuming that different alveoli at different distances from the BADJ respond similarly to ozone, the curves shown in Figure 24 can he used to predict isoresponse points hetween the different ozone exposures, that is, distances from the BADJ which should produce similar responses at different exposures. For example, the relative predicted dose of ozone at 200 μm in the group exposed to 0.12 ppm ozone is the same as the predicted dose at 400 μm in the group exposed to 0.5 ppm ozone and at 600 μm in the group exposed to 1.0 ppm ozone (Figure 24). Epithelial changes within ventilatory units arising from short (cranial) and long (caudal) airway paths in male and female rats were fit to a linear segment model with a high asymptote ($a1$), a slope segment ($b2$), a low asymptote ($a3$), and the two breakpoints for the beginning ($x1$) and end ($x2$) of the sloped segment, as illustrated schematically in Figure 15. The data for tbe individual rats are shown in Appendix A, Figures A.1 through A.4. The predicted curves are shown in Figure 25. This model was fit separately for ventilatory units of the cranial region and for ventilatory units of the caudal region.

As described above in the Statistical Methods section, some of the sample sizes for this analysis were quite small (n = 2 to 5 per gender and ozone concentration group). Despite this small size, several statistically significant effects were observed. At the multivariate level, there was a significant concentration-gender interaction for the cranial path, but no significant differences at all for the caudal path (Table 9).

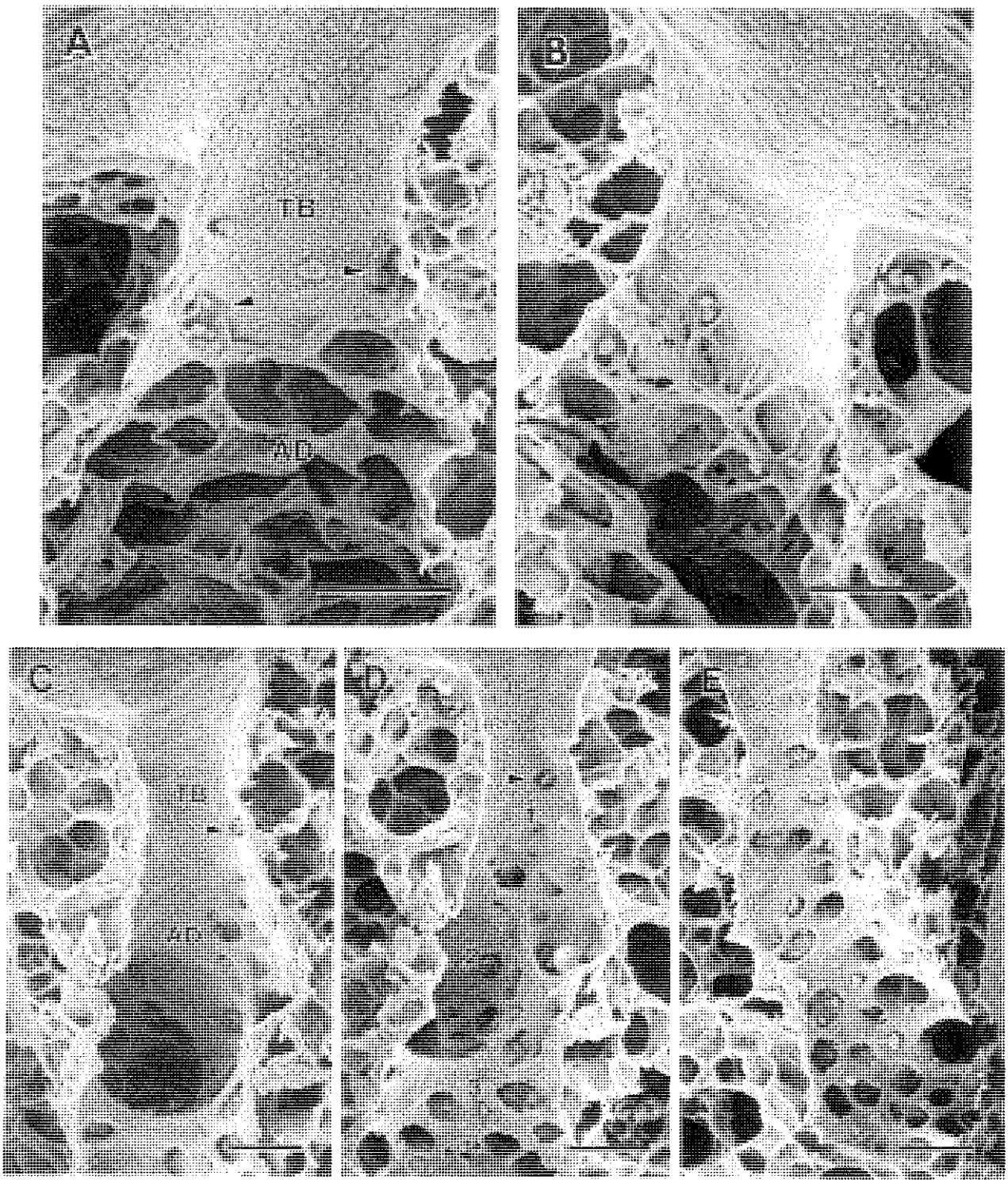

Figure 16. Scanning electron micrographs of complementary halves of a single BADJ from the lungs of a control rat (A and B) and a rat exposed to 1.0 ppm ozone (C, D, and E). Two alveolar outpocketings are present near the level of the abrupt transition of the BADJ in the lungs of the control animal (arrowheads in panel A). The most proximal alveolar outpocketing is still evident in the animal exposed to ozone for 20 months (arrowhead in panels C and D), but ciliated cells and cells with prominent apical protrusions have extended well beyond this level into three alveolar duct generations.(1, 2, and 3 in panel D). The asterisk in panel D denotes regions of squamous alveolar epithelium. TB = terminal bronchiole; AD = alveolar duct. Bar = 100 μm.

For the cranial site, the $a1$ value (the epithelial volume density at the entrance to the ventilatory unit) was significantly smaller in female than in male rats.

There were no statistically significant differences in the minimum epithelial volume density ($a3$) between the genders or associated with ozone exposure, although the concentration-gender interaction was marginally significant. The low asymptote ($a3$) for the females exposed to 1.0 ppm ozone was the highest value and could perhaps be interpreted as suggesting that there was a general thickening of the epithelium in response to high levels of ozone exposure (Figure 25). An alternative interpretation is that, because the analysis was based only on measurements reported through 800 μm, the estimate of the low epithelial volume density is based on too few measurements (perhaps one or two) if the declining linear segment extends far down the ventilatory unit (as happened in the group exposed to 1.0 ppm ozone).

In the sloped segment ($b2$), there was a statistically significant concentration-gender interaction. In the female rats, there were no differences in slope (rate of decrease of thickness) at any ozone concentration. In male rats, the slope of the control rats was steeper than the slope following any of the three ozone exposure concentrations and also steeper than the slope in the female control rats. In contrast, in rats exposed to 0.12 ppm ozone, the decline in epithelial volume density was steeper in females than in males. This variability is probably due to the small sample sizes. It is difficult to say whether these differences are real (that is, whether they have biological plausibility or not) given the small sample sizes. By simply qualitatively examining the slopes as a function of ozone exposure concentration (averaging over males and females), it does appear as though there is a concentration-related flattening of the slope—that is, the thickened epithelium extends farther into the ventilatory unit with increasing ozone exposure. Although no

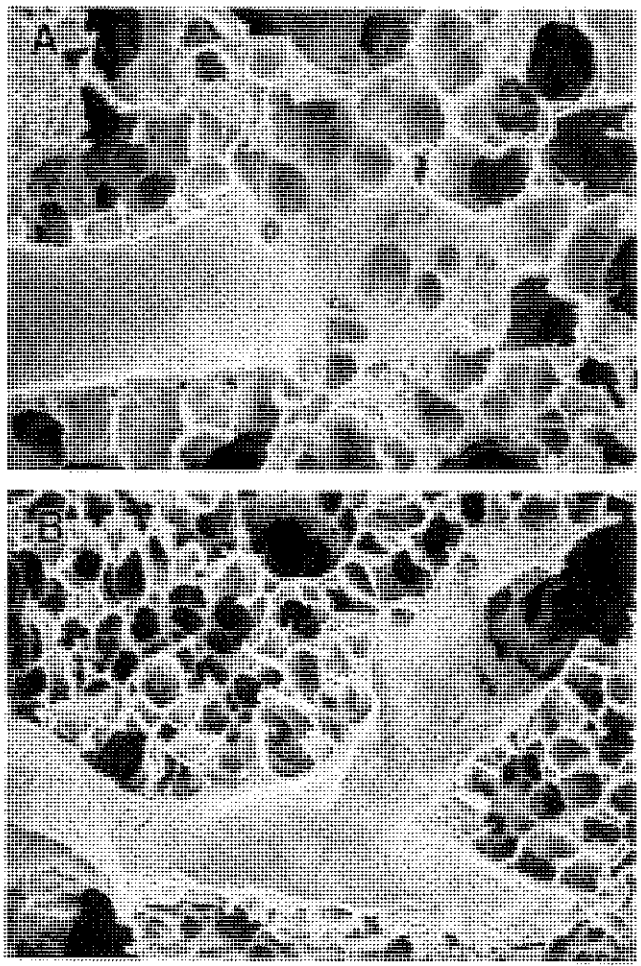

Figure 17. Scanning electron micrographs of two BADJs (A and B) from the lungs of a rat exposed to 0.12 ppm ozone for 20 months. Bronchiolar epithelium extends beyond the terminal bronchiole into the proximal portions of the alveolar duct. Bar = 100 μm.

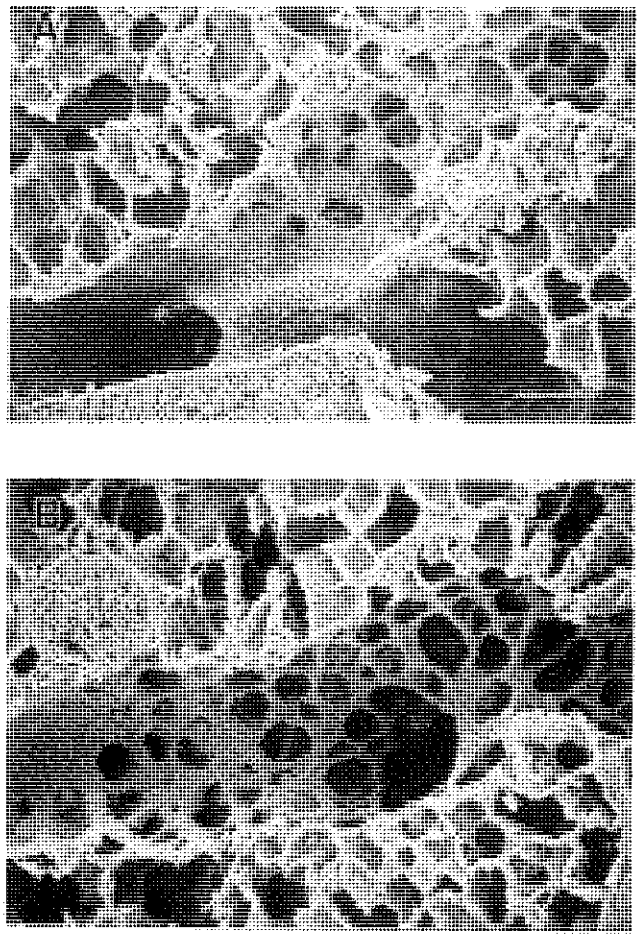

Figure 18. Scanning electron micrographs of two BADJs (A and B) from the lungs of a rat exposed to 0.5 ppm ozone for 20 months. Bronchiolar epithelium extends beyond the terminal bronchiole farther into the alveolar duct than noted in animals exposed to 0.12 ppm ozone. Bar = 100 μm.

significant effects in the caudal location were observed, a similar decreasing trend in slopes is present.

A concentration difference was observed in the distance down the ventilatory unit (x1) that the initial epithelial volume density was maintained before beginning the decrease described by the sloped segment. In control rats and those exposed to 0.12 ppm ozone, this distance was estimated as approximately 130 µm. Following exposure to 0.5 ppm ozone, the initial epithelial volume density was maintained for about 200 µm before beginning to decline, although this difference was not significantly greater than in the control animals. Following 1.0 ppm ozone exposure, the plateau region extended for approximately 400 µm and was significantly different from the region in the control rats.

The distance down the ventilatory unit at which the "background" (that is, some minimum level that is maintained normally throughout the ventilatory unit) epithelial volume density was achieved (x2) differed significantly between males and females and was affected by ozone exposure. In female rats, there was an approximately monotonic increase in distance to the background epithelial volume density as a function of ozone concentration. In control rats, this level was attained at a distance of about 240 µm, which decreased slightly (but not significantly) to 185 µm following exposure to 0.12 ppm ozone, increased to 345 µm following exposure to 0.5 ppm ozone, and increased significantly to 563 µm following exposure to 1.0 ppm ozone. In male rats, the trend was similar but statistical significances were observed at all ozone concentrations when compared with controls. Qualitatively, the distance to the background level was greater in the males relative to the females at all ozone exposure levels, although statisti-

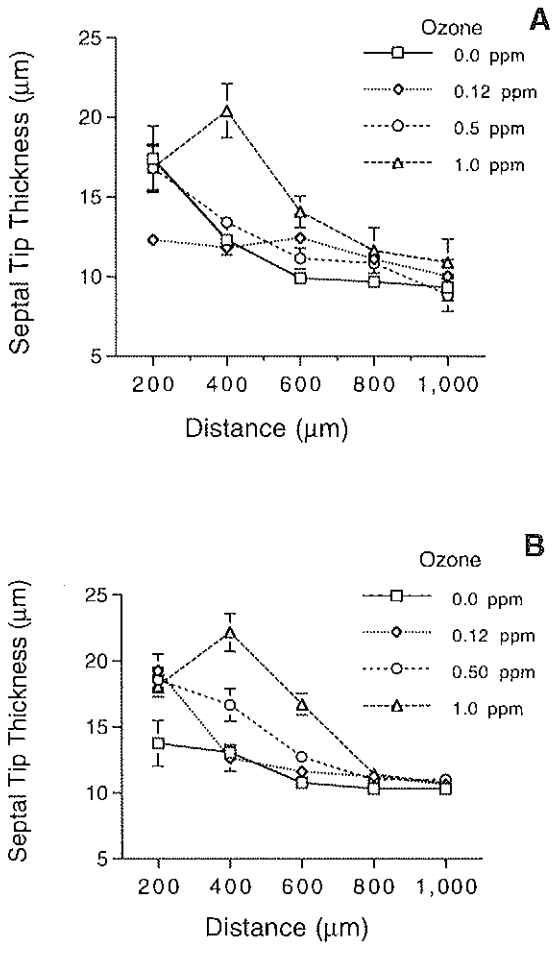

Figure 19. Changes in alveolar septal tip thickness with increasing distance into the alveolar duct for female (A) and male (B) rats. At 200 µm into the alveolar duct, all concentrations of ozone resulted in similar changes in septal tip thickness from the control value. Significant septal tip thickening was noted as deep as 600 µm into the alveolar duct with 20 months of exposure to 1.0 ppm ozone. Values are for cranial and caudal regions combined.

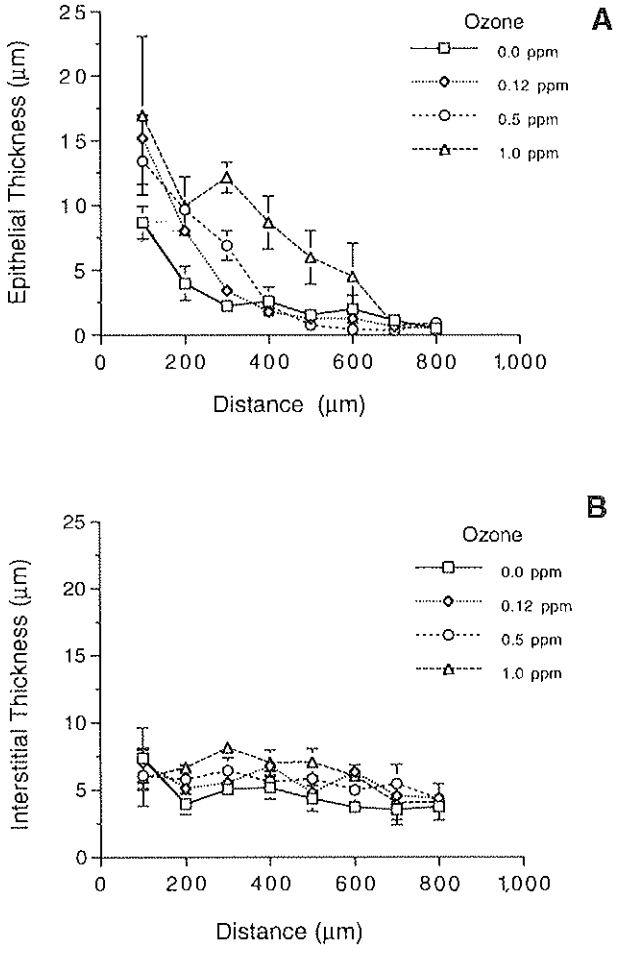

Figure 20. Thickness of epithelial (A) and interstitial (B) compartments of alveolar septal tips as a function of distance down the alveolar duct after 20 months of exposure to 0.0, 0.12, 0.5, or 1.0 ppm ozone in male rats. Epithelial changes are more marked than interstitial changes, although both tissue compartments contribute to the overall thickening of septal edges. Values are for cranial and caudal regions combined.

cally significant differences between males and females were observed only in rats exposed to 0.12 or 1.0 ppm ozone.

Epithelial volume density differed between the two sites: statistically significant effects due to both gender and concentration were observed in the cranial but not the caudal location (although the trends were similar). The epithelial volume density at the entrance of the cranial ventilatory unit was greater in males than in females, although there were no gender differences in the distal minimum volume density. The volume density itself was not affected by ozone exposure.

Interstitium. Data on interstitial volume density as a function of distance into the ventilatory unit were analyzed in a MANOVA comparing the cranial and caudal sites. Because there were no distance-related trends in volume density (Appendix A, Figures A.5 through A.8), a single average value for each site was used for each animal. Based on the MANOVA, there were no statistically significant differences between the cranial and caudal sites. The data from the two sites were averaged and reanalyzed. Significant gender and concentration effects were found (Table 10). The males had significantly greater interstitial volume densities than the females among rats exposed to 0.12 or 0.5 ppm ozone. Although the values for males were still elevated relative to those for females following 1.0 ppm ozone exposure, the difference was no longer statistically significant. Within each gender, there was a trend of increasing interstitial volume density with increasing ozone concentrations; however, volume density was significantly elevated relative to the control value only following exposure to 1.0 ppm ozone for both the male and female rats.

Capillaries. Longitudinal data on capillary volume density were averaged to produce a single value in each of the two sites (cranial and caudal) for each animal and subjected to a MANOVA. According to the MANOVA, there was a significant difference between the cranial and caudal sites in capillary volume density, with the density generally greater in the caudal site. Comparison of the gender- and concentration-specific means between these two sites (Table 11) suggested significant differences in the cranial versus caudal locations for females exposed to 1.0 ppm ozone

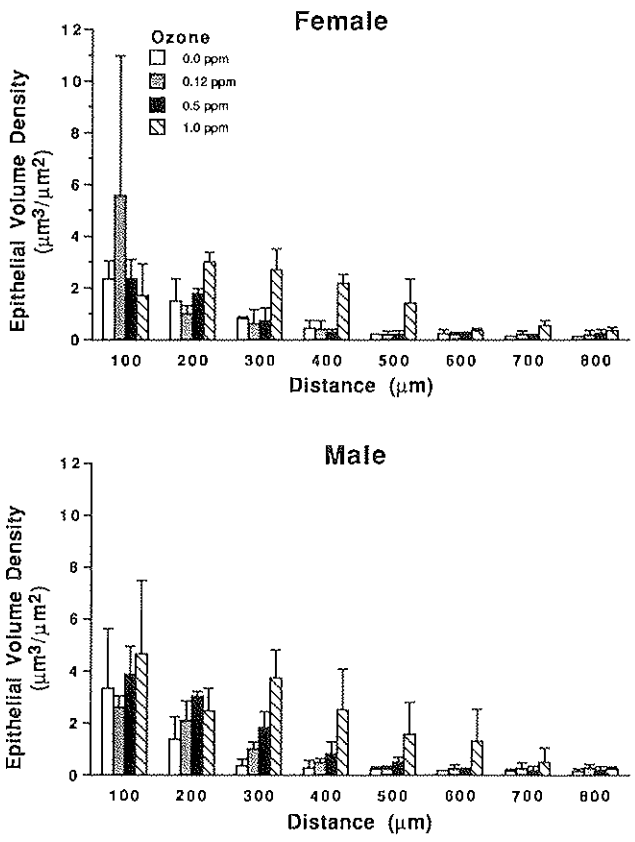

Figure 21. Comparison of epithelial volume density in female and male rats as a function of distance down the alveolar duct with exposure to 0.0, 0.12, 0.5, or 1.0 ppm ozone. Values are for cranial and caudal regions combined.

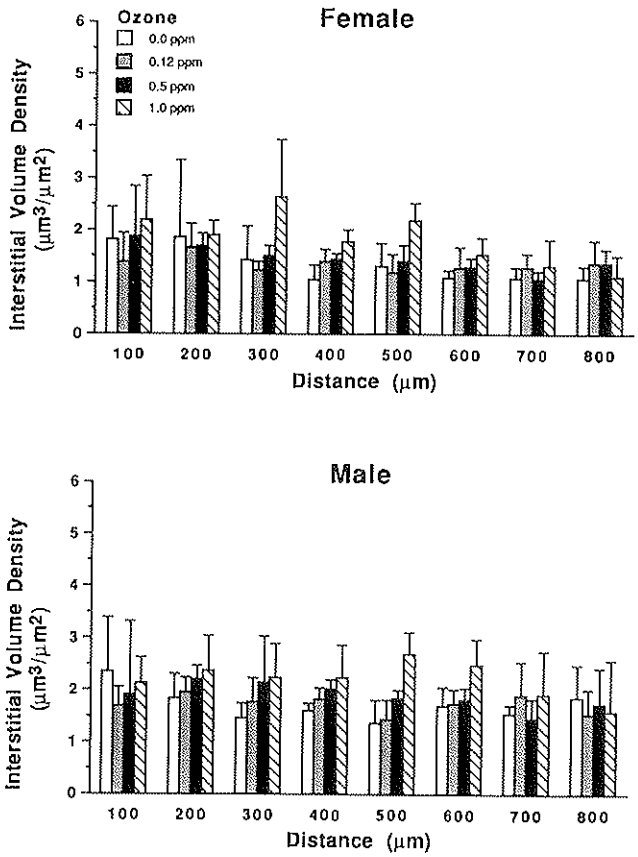

Figure 22. Comparison of interstitial volume density in female and male rats as a function of distance down the alveolar duct with exposure to 0.0, 0.12, 0.5, or 1.0 ppm ozone. Values are for cranial and caudal regions combined.

and for the males exposed to 0.12 ppm ozone. These significances were attributable more to smaller standard errors in these groups than to extreme values in the means. Accordingly, the site differences must be interpreted with caution because of the small sample sizes. When the ANOVA results were examined separately for each site, a significant gender effect in the cranial location (males greater than females) and a marginally significant concentration effect wre observed (Table 3). Examining the cell means (without corrections for multiple comparisons) indicated a significant difference between male and female control animals and a significant elevation in capillary volume density in females exposed to 0.5 ppm ozone relative to the female controls (but not in females exposed to 1.0 ppm ozone). In the caudal location, significant gender and concentration effects were observed. The density volumes for males were significantly greater than those for females in both the control rats and tbose exposed to 0.12 ppm ozone, and were qualitatively higher in the other two exposure groups. In male animals, the capillary volume density was significantly depressed in those exposed to 1.0 ppm ozone relative to control values. Despite these different statistical significances, these results should be interpreted with caution because of the small sample sizes and the lack of monotonic trends in the responses.

In summary, capillary volume density differed between the two sites and was greater in male than in female rats. An ozone-related effect was observed in the caudal location in male animals (a decrease in volume density following 1.0 ppm ozone exposure). It is difficult to know if this is a biologically meaningful difference. Similarly, the differences between the two locations did not show any consistent trends.

As a further assessment of these epithelial changes, and to better define the effect of airway path length on changes within the ventilatory unit, we examined the extent of bronchiolar epithelium within two different regions: first, a short airway path leading to the cranial aspects of the lung, a distance of approximately eight airway generations; and second, a longer airway path leading to the gas-exchange regions in the caudal portion of the left lobe, a distance of approximately 17 airway generations before reaching the level of the pulmonary acinus. These studies demonstrated that the extent of bronchiolar epithelium was approximately the same for the control animals and for those auimals exposed to 0.12 or 0.5 ppm ozone, regardless of airway path length. However, it was clear that exposure to ozone, even at the lowest concentrations, did lead to a significant extension of bronchiolar epithelium into the

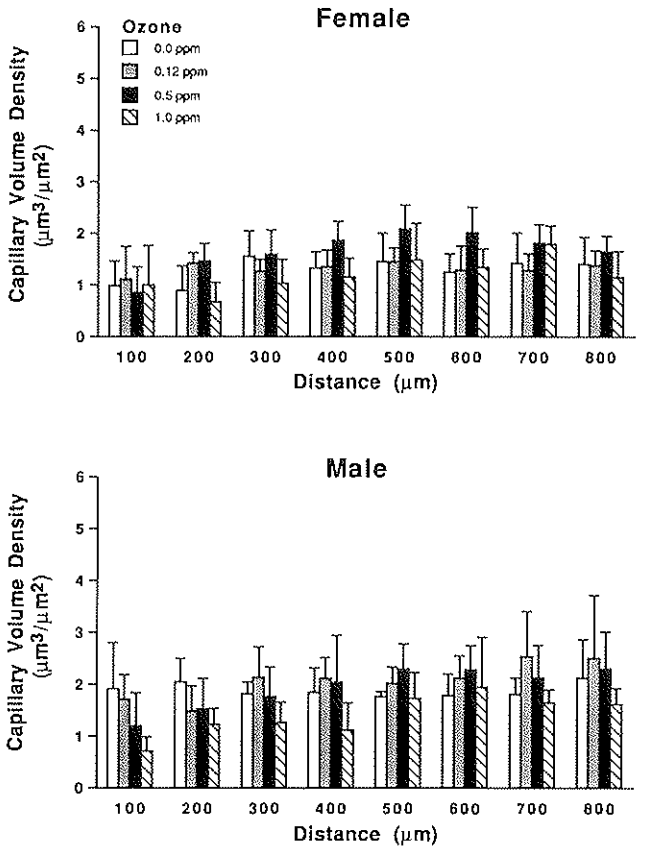

Figure 23. Comparison of capillary volume density in female and male rats as a function of distance down the alveolar duct with exposure to 0.0, 0.12, 0.5, or 1.0 ppm ozone. Values are for cranial and caudal regions combined.

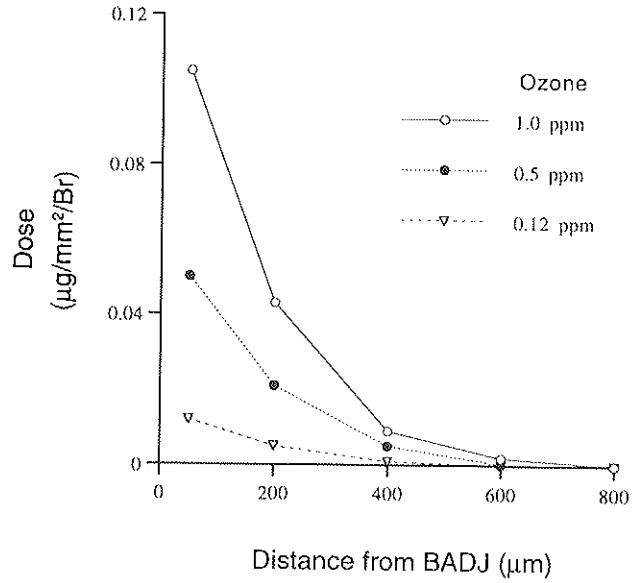

Figure 24. A mathematical model used to predict the uptake of ozone in the ventilatory unit. More than 90% of the relative effective dose of ozone initially present at the BADJ has been taken up into tissues approximately 500 μm into the ventilatory unit. The rapid uptake with increasing distance from the BADJ reflects a tremendous increase in the alveolar surface area on which the gas can be absorbed. Br = breath.

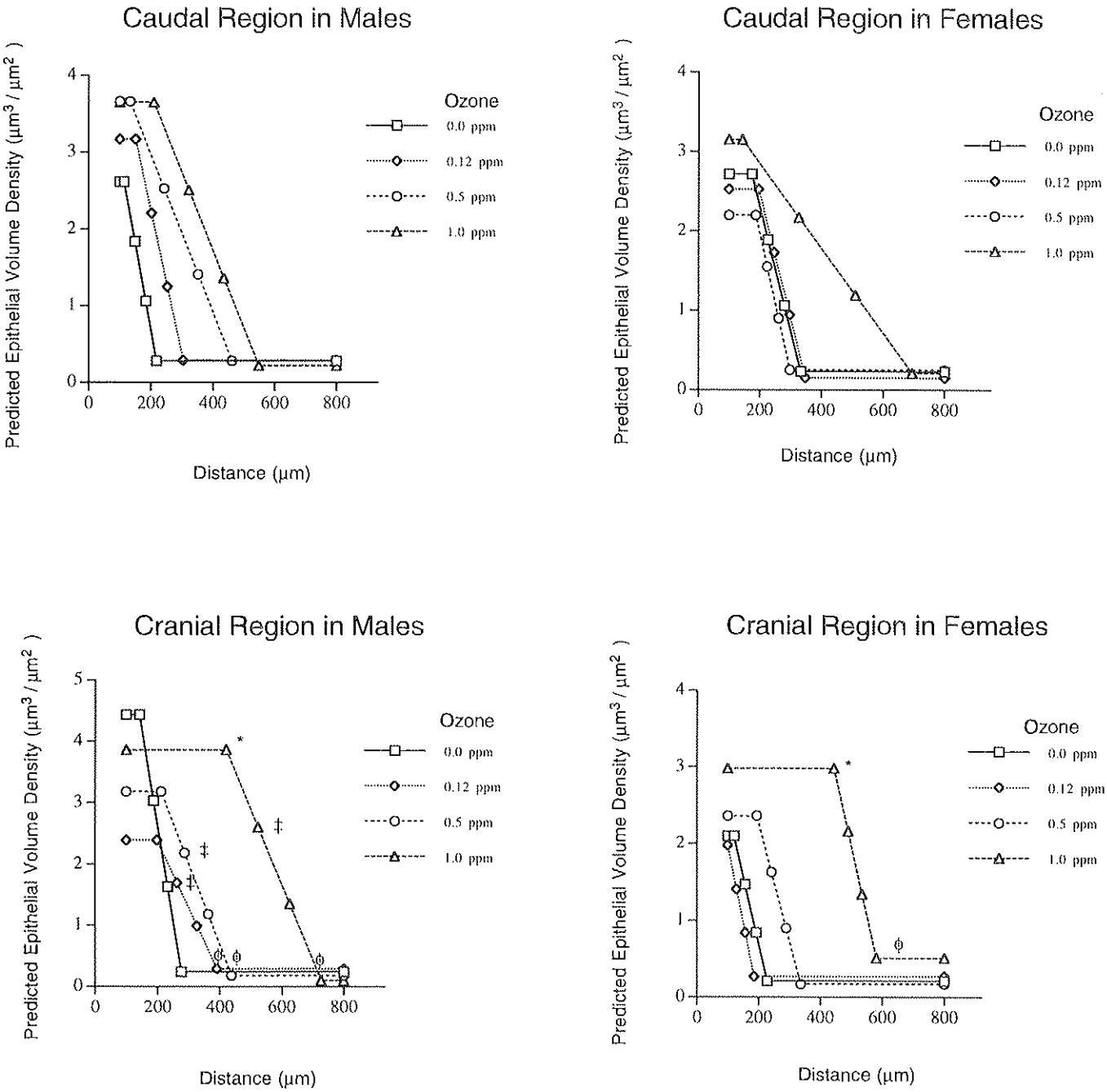

Figure 25. Means of the linear segments model for predicted epithelial volume density in individual rats are shown for the two regions (cranial and caudal) in male and female animals. Sample sizes were two to five per group. An asterisk (*) indicates $p < 0.05$ comparing the value of $x1$ (the distance into the ventilatory unit that the initial volume density is maintained) in exposed animals to that in the control group; ‡ indicates $p < 0.05$ comparing the value of $b2$ (the rate of decline in volume from the initial value to the minimum value) in exposed animals to that in the control group; ϕ indicates $p < 0.05$ comparing the value of $x2$ (the distance beyond which a constant, minimum epithelial volume density was observed) in exposed rats to that in the control group. Because no multivariate significances were detected, no pairwise comparisons were considered in the caudal region.

alveolar duct. Only at the highest concentration of 1.0 ppm ozone was there a significant difference in the extension of bronchiolar epithelium into the alveolar duct. In the cranial region, bronchiolar epithelium extended 200 μm deeper into the alveolar duct than it did in the caudal region of the lung.

Distribution and Extent of Ciliated and Nonciliated Cells Down Alveolar Ducts

In 1-μm sections stained with toluidine blue, the bronchiolar epithelium was characterized by a dense staining pattern (Figure 2). The heterogeneity of bronchiolar epithelial extension into alveolar ducts also was discernible. Bronchiolar epithelium occupied a variable extent of the alveolar ducts down different pathways in the same pulmonary acinus. At higher magnification, the densely staining epithelium in these distal regions could be seen to contain cuboidal cells with identifiable cilia and nonciliated cells with apical projections (Figure 2). Using these criteria, we observed a significant difference in the average distance ciliated and nonciliated cells extended into alveolar ducts (Figure 2b). In control animals, ciliated cells were found an average of 106 ± 23 μm into the alveolar duct. In contrast, ciliated cells in animals exposed to 1.0 ppm ozone extended

Table 9. Statistical Significance of Parameters Describing Epithelial Volume Density of the Pulmonary Acinus

	Multivariate p Values[a]			Univariate p Values[b]		
Parameter	Concentration	Gender	Concentration × Gender	Concentration	Gender	Concentration × Gender
Cranial Region	< 0.01[c]	0.02[c]	< 0.01[c]			
*a*1				0.24	0.02[d]	0.32
*x*1				< 0.01[d]	0.34	0.73
*b*2				0.01[d]	0.71	0.01[d]
*x*2				< 0.01[d]	< 0.01[d]	0.08
*a*3				0.33	0.14	0.08
Caudal Region	0.22	0.26	0.33			
*a*1						
*x*1						
*b*2						
*x*2						
*a*3						

[a] Multivariate significance was tested by the Hotelling-Lawley trace.

[b] Univariate significance was tested by ANOVA factor F tests. A blank column indicates that the multivariate tests did not permit subtests of that factor at the univariate level.

[c] Statistically significant effect.

[d] Statistically significant effect that was subtested if needed.

Table 10. Interstitial Volume Density of the Pulmonary Acinus for Cranial and Caudal Regions Combined[a]

	Ozone Concentration (ppm)			
Gender	0.0	0.12	0.5	1.0
Females	1.32 ± 0.11 (5)	1.41 ± 0.09 (6)	1.50 ± 0.06 (5)	1.92 ± 0.03[b] (4)
Males	1.66 ± .014 (4)	1.80 ± 0.15[c] (4)	1.92 ± 0.06[c] (4)	2.25 ± 0.22[b] (4)

[a] Values are means ± SE. Sample size is given in parentheses on the line below the data.

[b] Significantly different from the control group at a level of $p < 0.05$.

[c] Airways from male rats were significantly different from airways from female rats ($p < 0.05$).

an average of four times deeper (476 ± 34 μm). Animals exposed to 0.12 or 0.5 ppm ozone had proportionally less extension of bronchiolar epithelium into alveolar ducts.

Nonciliated cells in control animals extended slightly farther down alveolar duct paths (122 ± 23 μm) than did ciliated cells. In animals exposed to 1.0 ppm ozone, nonciliated cells were observed four times deeper down alveolar duct paths (481 ± 34 μm) than they were in control animals. As with ciliated cells, the extent of nonciliated cell distribution into alveolar ducts differed significantly between control animals and animals exposed to 1.0 ppm ozone, and to a lesser degree between control animals and animals exposed to 0.12 or 0.5 ppm ozone.

Gender Differences in Ozone-Induced Alveolar Duct Organization

Comparing of the epithelium in the alveolar ducts of male and female rats, a significant increase in the density of the

Table 11. Capillary Volume Density of the Pulmonary Acinus[a]

	Ozone Concentration (ppm)			
Gender	0.0	0.12	0.5	1.0
Cranial Region				
Females	1.17 ± 0.19 (4)	1.53 ± 0.12 (6)	1.78 ± 0.19[b] (5)	1.19 ± 0.10 (3)
Males	1.90 ± 0.17[c] (3)	1.89 ± 0.19 (4)	1.95 ± 0.19 (4)	1.37 ± 0.23 (3)
Caudal Region				
Females	1.41 ± 0.05 (5)	1.65 ± 0.18 (6)	1.67 ± 0.16 (4)	1.24 ± 0.02 (3)
Males	2.06 ± 0.20[c] (4)	2.16 ± 0.14[c] (4)	2.05 ± 0.14 (4)	1.51 ± 0.09[b] (4)

[a] Values are means ± SE. Sample size is given in parentheses on the line below the data.

[b] Significantly different from the control group at a level of $p < 0.05$.

[c] Airways from male rats were significantly different from airways from female rats at a particular site ($p < 0.05$).

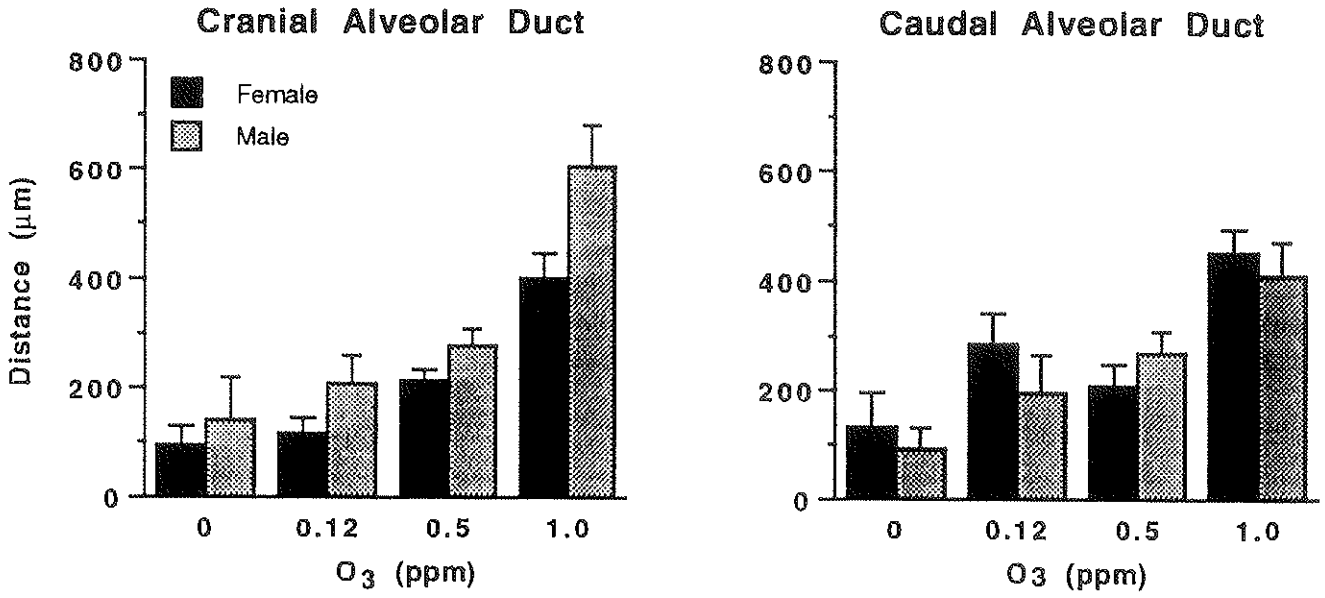

Figure 26. Effects of ozone on the extension of nonciliated bronchiolar epithelium into alveolar ducts in the cranial and caudal regions of female and male rats.

epithelium in males from all three exposure groups was evident at 200, 300, and 400 μm into the alveolar duct (Figure 21). In females exposed to 1.0 ppm ozone, there was a significant elevation in density at 200 to 500 μm into the alveolar duct. In males exposed to 1.0 ppm ozone, there was a significant increase as far as 600 μm into the alveolar duct. In all cases, the volume density of the interstitium was similar in males and females except at 100 μm (Figure 22). The volume density of interstitial tissue lining alveolar ducts was elevated as far as 700 μm into the alveolar duct in male animals exposed to 1.0 ppm ozone. This elevation was found only at 600 μm into the alveolar duct in females exposed to 1.0 ppm ozone. There were no major differences in capillary lumen volume density between males and females (Figure 23).

DISCUSSION

The reorganization of the centriacinar regions of the lung is a well-recognized result of continued inhalation of toxic oxidant gases at high ambient levels. Previous work has shown that exposure to oxidant air pollutants such as ozone and nitrogen dioxide for a reasonably long term (two to three months) alters the mixture of epithelial cell populations that occupy the proximal gas-exchange areas of pulmonary acini in species with short or nonexistent respiratory bronchioles (Boorman et al. 1980; Barr et al. 1988, 1990). The present study addresses some of the questions raised by these previous investigations. What is the extent of the reorganization in proximal alveolar ducts at different concentrations of ozone? How heterogeneous is the extent of this reorganization within the centriacinar regions of the same animal or in different animals at different concentrations of ozone? What is the degree of differentiation of the bronchiolar epithelium that becomes associated with alveolar gas-exchange areas? Does extended exposure, up to essentially a lifetime, alter the degree of reorganization?

Chronic exposure to ozone leads to significant changes within the lung. The unique sampling strategy designed for this study allows us to examine the heterogeneity of response to ozone within the pulmonary acinus as a function of distance into the same ventilatory unit of the lungs. Evaluation of multiple ventilatory units of animals from each ozone concentration group permits us to define, in detail, the changes occurring within each tissue compartment of the alveolar duct or ventilatory unit as oxidant gases proceed deeper into the gas-exchange regions of the lung. Dividing the ventilatory unit into 100-μm intervals facilitates the measurement of changes within the alveolar duct as a function of distance. Using a simple but crude measnre of thickness, we examined the septal tip as a specific target of injury and remodeling. To further define these changes, the contributions of individual components within the septal tip were subsequently determined by measuring the epithelial, interstitial, and capillary volume densities.

The sampling process applied in this study allowed us to examine changes within specifically defined microdomains of the pulmonary acinus. These microdomains were based on a linear distance into the alveolar duct taken from isolations in which the terminal bronchiole, the first alveolar outpocketing along the plane of the terminal bronchiole, could be clearly defined. The criterion of a symmetrical pair of alveolar ducts with an intervening ridge of tissue bifurcation between them also increased the likelihood that a true linear path within the ventilatory unit was followed. The placement of the center of the concentric circles, or bull's-eye, beginning with the geometric center at the level of the first alveolar outpocketing, allowed us to divide the isolation systematically but completely, in an objective manner, into specific 100-μm intervals for analysis and to analyze these changes by strictly objective criteria. One of the most powerful uses of this approach is the ability to compare biological changes associated with different predicted ozone concentrations at different levels of the pulmonary acinus. Equivalent doses of ozone, based on location within the ventilatory unit, could be analyzed for animals exposed to different concentrations of ozone. In addition, the concentric circle analysis allowed us to correlate the biological response to ozone of the pulmonary acinus to models of ozone dosimetry based on predicted gradients of ozone dose that would be found along a known distance into each ventilatory unit.

The findings of this study demonstrate that chronic exposure to ozone is dependent on dose, site-specific, and a function of distance from the BADJ. All changes were associated with significant alterations in all tissue compartments, but particularly in the epithelium. Many of these changes were associated with the replacement of alveolar epithelium in alveolar ducts by a well-differentiated bronchiolar epithelium consisting of ciliated bronchiolar cells and nonciliated bronchiolar Clara cells. Alterations in the type of epithelium lining the most proximal portion of the alveolar duct were independent of ozone concentration. Even at the lowest ozone concentration of 0.12 ppm, we found well-differentiated bronchiolar epithelium beyond the BADJ (Figure 21). A rigid sampling strategy for the ventilatory unit clearly defined subtle changes.

Our study has shown that BADJ reorganization can extend for as many as five generations of branching into the pulmonary acinus. The remodeling is not polarized and involves all sides of an alveolar duct branch. The alterations

in epithelial populations not only occur on the epithelial surfaces lining the alveolar duct lumen, but also extend down into alveolar outpocketings at the highest concentration of ozone (1.0 ppm). However, a large degree of heterogeneity was noted in this response even in different alveolar duct pathways arising from the same terminal bronchiole.

In the control animals, we also found bronchiolar epithelium extending into alveolar duct branches to varying degrees. In some cases, bronchiolar epithelium was present on a wall of an alveolar duct that also contained gas-exchange regions. In other cases, the junction between the terminal bronchiole and the first alveolar duct generation was clearly delineated. However, exposure to ozone concentrations as low as 0.12 ppm for 20 months was associated with significant remodeling of the epithelium at the BADJ. Although the changes were highly heterogeneous, the differences in the distribution of bronchiolar epithelium and in the thickening of the epithelium within the first 200 μm of the alveolar duct were significant.

When our findings in this study are compared with those of previous studies, it appears that the inhalation of toxic oxidant gases over essentially a lifetime (that is, 20 months) does not mitigate the extent or the nature of the remodeling that occurs with a shorter exposure to ozone (2 to 3 months). In fact, our findings suggest that with repetitive exposure up to 20 months, the epithelial cell populations in remodeled airways achieve a higher degree of differentiated function than is observed with shorter exposures (of 2 to 3 months) (Boorman et al. 1980; Barr et al. 1988, 1990).

The centriacinar region is a prominent site in the lungs where many inhaled toxic agents have a significant impact, and is also the location where contrasting epithelial cell populations lining the conducting airways and the gas-exchange areas interdigitate. This transition zone between two epithelial cell populations with different compositions and functions varies greatly from species to species, even in normal adult animals. In many species, including small rodents like the rat and mouse and some larger species such as sheep and cattle, the transition from one epithelial population to the other is reasonably abrupt (Plopper et al. 1991b). The extent of interdigitation between epithelial populations that express differentiated functions characteristic of epithelium in more proximal airways and epithelial populations that express functions characteristic of gas-exchange areas is minimized, and generally occurs at the branch point between airway generations or within the length of one airway generation. In many other species, including primates and most carnivores, this interdigitation and interaction is extensive and can include the epithelial lining of a large number of airway generations that contain extensive areas of alveolar outpocketings. Therefore, in these regions, bronchiolar and alveolar epithelial cells coexist in a mixed population. The response of this critical region to ozone may be different in humans and primates than in rodents. It is known that the epithelial cell composition of respiratory bronchioles in nonhuman primates can be significantly altered by exposure to ozone, with the extension of bronchiolar epithelium into alveolar ducts and an increase in the surface area of respiratory bronchioles covered by nonalveolar epithelial cells (Fujinaka et al. 1985).

When the gas-exchange area of rodent lungs is evaluated on the basis of ventilatory units as described by Mercer and colleagues (Mercer and Pinkerton 1990; Mercer and Crapo 1991; Mercer et al. 1991), the heterogeneity in the extension of bronchiolar cells down alveolar duct paths becomes more apparent. Because of the extensive remodeling of the most proximal alveolar ducts arising from the terminal bronchiole, we used the most proximal alveolar outpocketing along an airway as the point of reference to define the beginning of a ventilatory unit in rats. Mercer and coworkers have demonstrated that the ventilatory unit volume in the lungs of rats is highly heterogeneous (Mercer and Crapo 1987, 1991; Mercer and Pinkerton 1990; Mercer et al. 1991). Ventilatory unit size has a significant effect on the volume of toxic gas that will pass through the BADJ of that anatomical unit during an exposure. Whether the heterogeneity and degree of bronchiolar cell extension down alveolar duct paths can be explained in direct relation to the dose of ozone and to the amount of injury that occurs in a location cannot he determined from our study. However, the existence of ventilatory units with widely varying degrees of bronchiolarization, when combined with previous observations that the volume of a ventilatory unit can vary by a factor of 3 to 10 (Mercer and Crapo 1991; Mercer et al. 1991), would suggest that ventilatory unit size may be a major factor. The results of our study emphasize the need to explore more thoroughly the impact that ventilatory unit size can have on the response of epithelial populations within the target zone of oxidant air pollutants.

Transformation of the epithelial cell populations lining proximal alveolar ducts as a result of exposure to oxidant gases has been observed under a wide variety of exposure conditions. Proliferation and hyperplasia of cuboidal epithelial cells in zones previously occupied by squamous, alveolar type I cells occurs as little as three days after initiation of exposure (Plopper et al. 1979). With extended exposures of up to three months, this population appears to be altered from what would be expected for a hyperplastic population of alveolar type II cells (Barr et al. 1988; Johnson et al. 1990). To the best of our knowledge, this is

the first study to address directly the extent of this epithelial transformation within the target zone. We observed that this cuboidal population extends as far as 1,000 μm into the gas-exchange area with long-term exposure. We also demonstrated that the extension is highly variable. Using the criteria for differentiation that we have applied would suggest that the longer the exposure, the more differentiated this epithelial cell population will become. We base this suggestion primarily on the observation of cells with full-length cilia well into alveolar duct regions. Previous studies have not clearly demonstrated the presence of well-ciliated cells in bronchiolar populations lining the target zone in animals exposed to approximately the same concentration of ozone but for shorter periods of time (Boorman et al. 1980; Barr et al. 1988). Using another marker of differentiation, the presence of a secretory protein, our findings suggest that the nonciliated cells occupying these cuboidal cell populations in distal alveolar ducts are reasonably well differentiated. Whether this is the case for shorter exposures has not been evaluated.

The fact that bronchiolar epithelial cells can maintain a differentiated state over a long period of time in a zone where unexposed animals would have a completely different mixture of cells opens a number of questions concerning the regulation of differentiation and the control of epithelial cell homeostasis in the respiratory system. The presence of epithelial cells expressing differentiated functions that they would normally express in a different zone suggests that several factors in the local microenvironment must be altered to produce this type of differentiation. Some of the factors that could be explored are changes in the interactions between interstitial cells and the epithelial population; alterations in the extracellular matrix, including composition of the basal lamina; and changes in mediators, such as cytokines, that regulate epithelial functions in inflammatory responses.

ANTIOXIDANT ENZYME ACTIVITY

One of the fundamental characteristics of the respiratory system's response to the inhalation of reactive oxidant air pollutants such as ozone is that the cell populations that are injured during the initial phases of the exposure become resistant to further injury as exposure progresses. In the short term (two weeks or less), the acute injury and epithelial cell death that characterize the beginning of exposure are followed by a proliferative response of more resistant types of lung epithelial cells, which results in epithelial hyperplasia and metaplasia (Stephens et al. 1974; Schwartz et al. 1976; Gordon and Lane 1977; Mellick et al. 1977). The epithelial cells in regions that are most severely injured during initial exposure develop resistance to further injury (Boorman et al. 1980; Barr et al. 1988, 1990).

The mechanisms accounting for the increased tolerance of oxidant injury are poorly understood. A number of studies have observed elevations in the activities of enzyme systems that are involved in protecting cells from injury by oxidant radicals after short-term exposure (seven days or less). As early as three to four days after short-term exposure, GPx and glutathione reductase activities increase significantly (Clark et al. 1978; Rietjens et al. 1985; van Bree et al. 1992). With longer exposures (up to two weeks), both GPx and SOD increase substantially (Heng et al. 1987; Elsayed et al. 1988; Ichinose and Sagai 1989). Some studies have suggested that one basis for the increased tolerance of target cells to ozone-induced injury may be the elevation in antioxidant enzymes (Jackson and Frank 1984). It also has been suggested that the elevation of activity with short-term exposnre is directly related to the hyperplastic increase of cells in target zones (Bassett et al. 1988). Increased expression of messenger RNA during short-term exposure precedes the pattern of elevated enzyme activity for SOD, catalase, and GPx (Rahman et al. 1991).

Repeated exposure for longer periods produces a somewhat reorganized respiratory system with virtually no detectable cellular injury (Boorman et al. 1980; Barr et al. 1988, 1990). The role antioxidant enzymes may play in protecting reorganized epithelium during long-term exposure has not been well studied. Exposure for 12 months resulted in increased GPx and glutathione reductase activities, but no change in SOD (Grose et al. 1989). On the other hand, exposures for nearly a lifetime (22 months) resulted in SOD, GPx, glutathione reductase, and GST activities similar to those found in control animals (Sagai and Ichinose 1991).

Another characteristic of the lung's cellular response to inhaled reactive oxidant air pollutants is that the injury is not uniform throughout the respiratory tree. Not only does the degree of acute injury vary by location within the tracheobronchial airways, but the pattern of the injury repair also varies (Hyde et al. 1992a). This heterogeneous response also is found in the cellular reorganization that occurs with long-term exposure (Barr et al. 1988; Nikula et al. 1988). The nature of the cellular response varies not only by position within the airway tree, but also by path length from the trachea to the gas-exchange area. We recently observed that antioxidant enzyme activities at specific sites within the airway tree of normal animals varied substantially from the activities measured from whole-lung homogenates, which further complicates our understanding. The four different antioxidant enzymes measured were SOD, GPx, catalase, and GST (Duan et al. 1993). Whether the

cellular reorganization that occurs in response to long-term exposure to reactive oxidant gases is associated with alterations in the activities of antioxidant enzymes at these sites is not known.

The purpose of this portion of our study was to answer the following questions: (1) Are there changes in antioxidant enzymes as a result of long-term exposure to ozone? (2) Do these changes vary by site within the respiratory tree? (3) Are there differences between the activities of antioxidant enzymes at target sites within the respiratory system, those at nontarget sites, and those taken from the whole lung? (4) Does the length of exposure or the concentration of toxic gas modify the extent of the metabolic response? To address these questions, we evaluated the activities of three antioxidant enzymes, SOD, GPx, and GST, on a site-specific basis within the lower respiratory tree of rats exposed for either 90 days or 20 months to ozone concentrations ranging from 0.12 to 1.0 ppm.

METHODS

Chemicals

Waymouth's medium 752/1, containing 25 mM *N*-2-hydroxyethyl-piperazine-*N*-2-ethanesulfonic acid (HEPES), was obtained from Gibco Labs (Green Island, NY). Low-gelling-temperature agarose (Sea Plaque GTG) was purchased from FMC Bio Products (Rockland, ME). Glutathione (reduced form), nitroblue tetrazolium (NBT, grade 3), xanthine (grade 3), glutathione reductase (type 3, from baker's yeast), catalase (from *Aspergillus niger*), and xanthine oxidase (grade 4, from milk) were purchased from Sigma Chemical Co. (St. Louis, MO). Diethylenetriamine-pentaacetic acid (98%) (DETAPAC) and potassium periodate (American Chemical Society grade) were purchased from Aldrich Chemical Company (Milwaukee, WI) or Fisher Scientific (Fair Lawn, NJ).

Preparation of Tissue Specimens for Activity Determinations

The procedure for obtaining defined specimens of the lung by blunt dissection has been described in detail (Plopper et al. 1991a; Duan et al. 1993). Briefly, the animal was killed by an overdose of pentobarbital and exsanguinated, and the trachea was exposed and cannulated. The lungs were perfused with 20 mL of phosphate-buffered saline (PBS), pH 7.4, via the pulmonary artery, and 12 mL of low-temperature agarose (1% in Waymouth's medium) was injected via a tracheal cannula. The lung was immersed in Waymouth's medium for 30 minutes at 4°C. Beginning at the hilum of the left lobe, we removed the pulmonary vessels and tracheobronchial tree by blunt dissection under a dual viewing stereomicroscope (Wild M8). The following subcompartments were obtained: distal trachea, lobar bronchi, the axial pathway of the largest (major daughter) branch, the pathways of the first and second of the largest daughter branches from the major axial pathway (minor daughters), the most distal three to four generations (distal bronchioles–central acinus) of conducting airway and the proximal acinus, and lung parenchyma that was free of all of the other components. Before dissection, the caudal one-quarter of the left lobe was removed and homogenized for estimating activity in the whole lung. The distal one-third of the trachea also was removed and placed in Waymouth's medium (4°C). All dissections were completed within 90 minutes of the animal's death. As pieces were removed, they were homogenized in 300 to 1,000 µL of phosphate buffer (50 mM, pH 7.4, 4°C) with microglass homogenizers; the resulting homogenate was centrifuged at 9,000 × *g* for 10 minutes. Either activities were measured immediately after centrifugation, or supernatants were stored at –80°C for up to one week. (Comparison of aliquots assayed before and after freezing indicated no alteration in activity for this storage period.) In the 90-day exposure, lungs from four rats from each exposure group were used. For the 20-month study, lungs from three males and two females from each exposure group were used.

The total amount of protein in the supernatant from the distal bronchiole, lobar bronchus, and minor daughter segments (mean of 111, 119, and 124 µg, respectively) was relatively lower than that in the supernatant from the distal trachea, major daughter, and parenchyma (213, 177, and 417 µg, respectively).

Enzyme Activity Assays

Total SOD activity was measured by the xanthine oxidase–NBT assay first described by Beauchamp and Fridovich (1971), and modified for small samples by Oberley and Spitz (1984). Xanthine–xanthine oxidase was utilized to generate a superoxide flux, and NBT was used as an indicator of superoxide production. The percentage that NBT reduction was inhibited served as a measure of the amount of SOD present. In a total volume of 700 µL, the assay mixture contained catalase (0.7 units, to remove hydrogen peroxide), DETAPAC (1.0 mM, to chelate metal ions), xanthine (0.16 mM), xanthine oxidase, NBT (0.06 mM), and 4 to 10 µg supernatant protein centrifuged at 9,000 × *g*. Duplicate assays from the same sample differed by less than 10%.

Selenium-dependent GPx was measured by a modification of the method of Paglia and Valentine (1967) using hydrogen peroxide as a substrate. This assay couples the reduction of hydrogen peroxide to the oxidation of nicoti-

namide adenine dinucleotide phosphate (NADPH) by glutathione reductase, and was monitored at 340 nm using a microplate reader. Incubations contained the following in a total volume of 150 µL: 9,000 × *g* supernatant (8 to 20 µg of protein), 0.075 mM hydrogen peroxide, 0.28 mM NADPH, and 0.05 units of glutathione reductase. One unit of GPx is defined as the amount required to oxidize 1 µmol of NADPH per minute.

Glutathione S–transferase activity was assayed using 1-chloro-2,4-dinitrobenzene (CDNB) as a substrate. Incubations contained 6 to 15 µg of protein in a final volume of 650 µL (Habig et al. 1974). One unit represents the formation of 1 µmol of product per minute.

DNA Content

DNA content was determined using 4′-6-diamidino-2-phenylindole (DAPI) as a derivatizing agent (Meyer and Grundmann 1984). Samples were freeze-dried and beated to 95°C in 0.2 M sodium hydroxide solution for 40 minutes and combined with DAPI solution (0.2 µg/mL). Fluorescence emission was measured at 453 nm with excitation at 360 nm.

Statistical Methods

Results of antioxidant enzyme assays are expressed as units of enzyme activity per milligram of DNA and are presented as means ± 1 SD. Assays for each subcompartment were cnnducted in duplicate or triplicate from a minimum of four animals. Activity levels were compared by ozone exposure groups and by age for each lung subcompartment using ANOVA. Post hoc tests were performed using Dunnett's method to test for significant differences between control and exposed groups. Tests for concentration-dependent differences were performed using regression analysis (Glantz 1992). A value of $p < 0.05$ was considered statistically significant.

For the purposes of integration, MANOVA was used to evaluate concentration, gender, and path location only for animals exposed for 20 months. Regression models were used to estimate and test the main effects of ozone concentration, gender, and sampling location. Linear trend tests for ozone concentration were used to examine the dose-response relation along with pairwise tests of control versns 0.5 ppm ozone and control versus 1.0 ppm ozone. Gender-concentration and location-concentration interactions also were investigated. Analyses were conducted using generalized estimating equations to account for repeated measnres across location. All reported p values are two-tailed without adjustment. The path followed consisted of proximal trachea, distal trachea, lobar bronchus, cranial bronchus, distal bronchiole, and parenchyma.

RESULTS

Superoxide Dismutase

Exposure of rats to ozone for 90 days produced a concentration-dependent elevation in SOD activity at both 0.12 and 1.0 ppm, with the subcompartment showing the greatest increase being the distal bronchiole–central acinus (Table 12). Activity of SOD in this compartment was twice as high in the rats exposed to 1.0 ppm ozone as in control animals exposed to filtered air. The minor daughter broncbi also showed a concentration-dependent elevation in SOD activity, although the more proximal (major) daughter bronchi exhibited a concentration-dependent decrease. There were minor variations in SOD activity in other lung compartments, but these differences were not statistically significant. In whole-lung homogenates, there was a small concentration-dependent increase in activity.

Exposure of rats to ozone for 20 months produced significant elevations in SOD activity in two subcompartments, the distal trachea and the distal bronchiole–central acinus (Table 12). The activity in the distal bronchiole–central acinus in animals exposed to 1.0 ppm ozone was 1.7 times that in control animals; exposure to 0.5 ppm ozone elevated SOD levels by 1.5 times. The distal trachea showed a concentration-dependent increase in SOD activity; however, there were no significant differences in SOD activity in samples derived from whole-lung homogenates.

A comparison of control animals aged 22 months with those aged 20 weeks indicated that there were significant age-related differences in SOD activity in three snbcompartments: distal trachea, lobar bronchus, and distal bronchiole–central acinus. In the distal tracheas and distal bronchioles of 22-montb-old animals, the activity level was approximately 50% (46% and 64%, respectively) of tbat observed in the same compartment in 20-week-old animals. For the lobar bronchus, the activity in the 22-month-old animals was 1.8 times that in the 20-week-old animals. There were no other significant differences in activity in samples derived from whole-lung homogenates.

Glutathione Peroxidase

Exposure to ozone for 90 days produced significant concentration-dependent changes in the activity of GPx in only two lung subcompartments, the major daughter bronchi and distal bronchiole–central acinus (Table 13). In animals exposed to 1.0 ppm ozone, GPx activity was 1.2 times greater than that of controls in the distal bronchiole–central acinus, yet it was only 0.67 times that of controls in major

daughter bronchi. There were no differences among other subcompartments or in the whole-lung homogenates.

Exposure of rats to ozone for 20 months produced concentration-dependent elevations in GPx activity in two subcompartments: minor daughter bronchus and distal bronchiole–central acinus (Table 13). Glutathione peroxidase activity of animals exposed to 1.0 ppm ozone was approximately 50% greater in the distal bronchiole and minor daughter bronchus than in the corresponding sites in control animals. After exposure to 0.5 ppm ozone, activity

Table 12. Superoxide Dismutase Activity in Lung Subcompartments of Rats Exposed to Ozone for 90 Days or 20 Months[a]

	90-Day Exposure[b]			20-Month Exposure		
Compartment	0.0 ppm	0.12 ppm	1.0 ppm	0.0 ppm	0.5 ppm	1.0 ppm
Distal trachea	295.2 ± 64.3	395.0 ± 88.7	394.4 ± 136.0	136.8 ± 40.7[c,d]	238.5 ± 80.7[d]	311.3 ± 140.8[d]
Lobar bronchus	239.5 ± 49.5	514.1 ± 161.8	397.8 ± 101.2	449.5 ± 108.1[c]	369.2 ± 194.5	370.3 ± 138.8
Major daughter bronchus	379.5 ± 59.9[d]	409.1 ± 70.8[d]	255.9 ± 76.9[d]	292.6 ± 68.7	308.0 ± 95.3	215.5 ± 44.1
Minor daughter broncbus	619.1 ± 179.2[d]	954.8 ± 84.1[d]	1,235.6 ± 276.2[d]	398.1 ± 115.4	489.2 ± 173.0	517.6 ± 183.6
Distal bronchiole–central acinus	550.3 ± 55.9[d]	641.4 ± 43.2[d,e]	1,113.0 ± 238.9[d,e]	353.8 ± 53.3[c,d]	543.3 ± 131.4[d,e]	590.9 ± 200.1[d,e]
Parenchyma	452.9 ± 37.2	514.0 ± 130.1	604.3 ± 148.9	452.2 ± 149.1	417.9 ± 217.9	409.2 ± 173.8
Whole lung homogenate	573.2 ± 23.8[d]	575.5 ± 58.7[d]	741.3 ± 103.1[d]	397.7 ± 144.5	406.8 ± 172.3	367.5 ± 169.5

[a] Values are expressed in units/mg of DNA.

[b] The 90-day exposure was conducted at the University of California at Davis under conditions identical to those for the 20-month exposure (Plopper et al. 1994b).

[c] Significant ($p < 0.05$) compared with the group exposed to 0.0 ppm ozone for 90 days.

[d] Significance was found to be dependent on concentration; $p < 0.05$ by regression analysis.

[e] Significant ($p < 0.05$) compared with control group exposed to 0.0 ppm ozone from the same study.

Table 13. Glutathione Peroxidase Activity in Lung Subcompartments of Rats Exposed to Ozone for 90 Days or 20 Months[a]

	90-Day Exposure[b]			20-Month Exposure		
Compartment	0.0 ppm	0.12 ppm	1.0 ppm	0.0 ppm	0.5 ppm	1.0 ppm
Distal trachea	0.330 ± 0.059	0.413 ± 0.110	0.425 ± 0.165	0.379 ± 0.197	0.466 ± 0.139	0.512 ± 0.043
Lobar bronchus	0.315 ± 0.107	0.528 ± 0.166	0.455 ± 0.151	0.609 ± 0.214	0.597 ± 0.295	0.643 ± 0.117
Major daughter bronchus	0.544 ± 0.065[c]	0.525 ± 0.141[c]	0.367 ± 0.074[c]	0.775 ± 0.238[c]	0.597 ± 0.245[c]	0.436 ± 0.128[c]
Minor daughter bronchus	0.692 ± 0.107	0.794 ± 0.122	0.850 ± 0.100	0.691 ± 0.184[c]	0.684 0.097[c]	1.055 ± 0.275[c]
Distal bronchiole–central acinus	0.583 ± 0.073[c]	0.545 ± 0.101[c]	0.712 ± 0.099[c]	0.612 ± 0.145[c]	0.947 ± 0.327[c]	1.000 ± 0.172[c]
Parenchyma	0.829 ± 0.149	0.966 ± 0.221	0.819 ± 0.208	0.787 ± 0.249	0.787 ± 0.301	0.691 ± 0.073
Whole lung homogenate	0.981 ± 0.079	0.961 ± 0.212	0.958 ± 0.083	0.865 ± 0.257	0.915 ± 0.241	1.016 ± 0.383

[a] Values are expressed in units/mg of DNA.

[b] The 90-day exposure was conducted at the University of California at Davis under conditions identical to those for the 20-month exposure (Plopper et al. 1994b).

[c] Significance was found to be dependent on concentration; $p < 0.05$ by regression analysis.

was also approximately 1.5 times the control values in the distal bronchiole. There was a significant concentration-dependent decrease in GPx activity in the major daughter bronchus. The value after exposure to 1.0 ppm ozone was approximately 60% of that for filtered air controls. There were no differences in other subcompartments or in the whole-lung homogenates.

There was no significant difference in the activity of GPx in any subcompartment or in whole-lung homogenates between control animals aged 20 weeks and those aged 22 months (Table 13).

Glutathione S–Transferase

Exposure of rats to ozone for 90 days produced concentration-dependent changes in GST activity in two subcompartments: the minor daughter bronchus and the distal bronchiole–central acinus (Table 14). In animals exposed to 1.0 ppm ozone, GST activity was elevated by 50% over that in controls. There were no other significant changes in animals exposed to 1.0 or 0.12 ppm ozone in any subcompartment or in samples derived from homogenates of whole lung.

Twenty-month exposure to ozone produced no concentration-dependent changes in GST activity in any lung subcompartments (Table 14). There were significant differences in GST activity in the lungs of 22-month-old control rats when compared with 20-week-old control rats in two subcompartments: lobar bronchus and distal bronchiole–central acinus (Table 14). In the lobar bronchus of the older rats, GST activity was 2.4 times that of the 20-week-old animals, although in the distal bronchiole, GST activity was only 0.7 times that of 20-week-old animals.

The integration of antioxidant enzyme activity levels observed through the tracheobronchial tree and lung parenchyma is presented in Table 15. Gender, ozone concentration, and path location along the respiratory tract were evaluated. Significant concentration effects were noted for both SOD and GPx. Glutathione S–transferase was significantly higher in males than in females, but demonstrated no significant concentration effects. Figure 27 illustrates the relative levels of SOD, GST, and GPx along specific sites of the respiratory tract after 20 months of exposure to 0.0, 0.5, and 1.0 ppm ozone.

DISCUSSION

This study was designed to determine whether long-term exposure to oxidant air pollutants such as ozone alters the antioxidant enzyme capabilities of regions within the respiratory system that exhibit different degrees of injury. Chronic exposure resulted in changes in the activity of all three enzymes examined: SOD, GPx, and GST. These changes varied by site within the airway tree and were not reflected in samples derived from whole-lung homogenates. The region of the lung showing the most striking and consistent change was the site identified as being the most susceptible to acute lung injury from ozone exposure: the junction of

Table 14. Glutathione S–Transferase Activity in Lung Subcompartments of Rats Exposed to Ozone for 90 Days or 20 Months[a]

	90-Day Exposure[b]			20-Month Exposure		
Compartment	0.0 ppm	0.12 ppm	1.0 ppm	0.0 ppm	0.5 ppm	1.0 ppm
Distal trachea	0.130 ± 0.027	0.179 ± 0.048	0.179 ± 0.038	1.047 ± 0.028	0.179 ± 0.033	0.168 ± 0.032
Lobar bronchus	0.121 ± 0.029	0.213 ± 0.064	0.183 ± 0.053	0.294 ± 0.074[c]	0.322 ± 0.172	0.232 ± 0.193
Major daughter bronchus	0.173 ± 0.017	0.203 ± 0.074	0.142 ± 0.015	0.210 ± 0.049	0.182 ± 0.056	0.126 ± 0.050
Minor daughter bronchus	0.433 ± 0.130	0.711 ± 0.049[d]	0.742 ± 0.056[d]	0.392 ± 0.068	0.453 ± 0.049	0.427 ± 0.137
Distal bronchiole–central acinus	0.430 ± 0.063[e]	0.453 ± 0.078[e]	0.648 ± 0.135[d,e]	0.321 ± 0.021[c]	0.490 ± 0.158	0.470 ± 0.065
Parenchyma	0.272 ± 0.050	0.284 ± 0.032	0.302 ± 0.077	0.330 ± 0.102	0.302 ± 0.093	0.308 ± 0.074
Whole lung homogenate	0.355 ± 0.023	0.357 ± 0.071	0.492 ± 0.079	0.294 ± 0.071	0.335 ± 0.076	0.307 ± 0.072

[a] Values are expressed in units/mg of DNA.

[b] The 90-day exposure was conducted at the University of California at Davis under conditions identical to those for the 20-month exposure (Plopper et al. 1994b).

[c] Significant ($p < 0.05$) compared with the control group exposed to 0.0 ppm ozone for 90 days.

[d] Significant ($p < 0.05$) compared with the control group exposed to 0.0 ppm ozone.

[e] Significance was found to be dependent on concentration; $p < 0.05$ by regression analysis.

the terminal bronchiole with alveolar ducts (the distal bronchiole–central acinus zone). Other areas affected on a variable basis included major and minor daughter intrapulmonary bronchi. Changes observed in most regions were concentration-dependent. There was considerable variability in the response, depending on the length of exposure, with animals exposed for nearly a lifetime (20 months) showing a wider variety of changes in enzymatic activity than animals exposed for a shorter time (90 days). Another observation from this study is that there are significant age-related changes in activities of two of these enzymes: SOD and GST. These changes were site-specific, with decreases in the distal bronchiole and elevations in the lobar bronchus in older animals.

Elevation in the antioxidant enzyme activities is a consistent response of the respiratory system of rats to short-term exposure to the reactive air pollutant ozone. The SOD activity level is substantially elevated after seven days of exposure to the ozone concentrations used in our study (1.0 ppm and lower) (Jackson and Frank 1984; Heng et al. 1987; Elsayed et al. 1988). The level of GPx activity is also substantially elevated by exposures ranging from three days (van Bree et al. 1992) to seven days (Jackson and Frank 1984; Heng et al. 1987; Elsayed et al. 1988; Ichinose et al. 1988; Ichinose and Sagai 1989). Whether a similar elevation of GST activity occurs in the acute phase of response to ozone has not been evaluated. There are fewer studies of long-term exposures, but they suggest that elevations in the early phases of the response may not be preserved over the long term. A twelve-month exposure to low ambient concentrations of ozone produces elevations in GPx and glutathione reductase, but not in SOD (Grose et al. 1989). Near-lifetime (22-month) exposure results in no changes in SOD, GPx, or GST (Sagai and Ichinose 1991).

All of these studies are based on assessing antioxidant enzyme activity in samples from whole-lung homogenates. As Bassett and colleagues (1988) suggested, caution must be exercised in evaluating these changes if consideration is not given to the differences in cellular organization that are part of the response to oxidant injury. In that study, the authors accounted for these potential differences by standardizing their activities in relation to DNA content. We have taken a similar approach and extended it by also evaluating activities on a site-specific basis, which allows us to separate areas where considerable ozone injury is known to occur from areas where little injury has been identified. When our results were corrected for differences in the responsiveness of sites, as well as differences in cell abundance, we still found significant local variability in these enzyme systems as a result of lifetime exposure. All three of the enzyme systems we evaluated showed these types of site-specific changes. Although most changes involved elevations in activity over control values, some involved decreases, as in the major daughter bronchus. We also observed that both the concentration of ozone and the length of long-term exposure produce differences in the nature of the response in some portions of the respiratory system but not others. For example, the distal bronchiole–central acinus responded consistently to all concentrations of ozone and both lengths of exposure. In contrast, the responses of the trachea and large and small intrapulmonary bronchi varied substantially with differences in exposure length.

Table 15. Multivariate Analysis of Antioxidant Enzyme Activity[a]

Enzyme	Ozone Linear Trend	Control Group vs. Group Exposed to 0.5 ppm Ozone	Control Group vs. Group Exposed to 1.0 ppm Ozone	Gender
Superoxide dismutase[b,c]	0.023	NS[d]	0.025	NS
Glutathione peroxidase[e]	0.030	NS	0.030	0.016
Glutathione S–transferase[f,g,h]	NS	NS	NS	0.034

[a] Data are presented as two-tailed p values.

[b] Although the analysis was primarily interested in estimating the main effect of ozone across sites, supplementary analysis of the location × concentration effects revealed (via a trend test) a significant decrease in superoxide dismutase in the lobar region ($p = 0.016$), and a suggestion of a decrease in superoxide dismutase in the parenchymal region ($p = 0.11$).

[c] No main effect of gender was present for superoxide dismutase in either the short or long path.

[d] NS = not significant.

[e] Overall glutathione peroxidase was significantly higher in males (by 0.14 units/mg of DNA).

[f] Overall glutathione S–transferase was significantly higher in males (by 0.047 units/mg of DNA).

[g] The distal bronchiole was the only region to show a significant location × concentration interaction ($p = 0.0015$).

[h] Throughout the analysis, no gender × concentration trend tests were significant. The only gender interactions for GST occurred in the group exposed to 0.5 ppm ozone compared with the control group, in which there was a significant increase for males ($p = 0.0038$). Note that this interaction was not present when values for the group exposed to 1.0 ppm ozone were compared with control values.

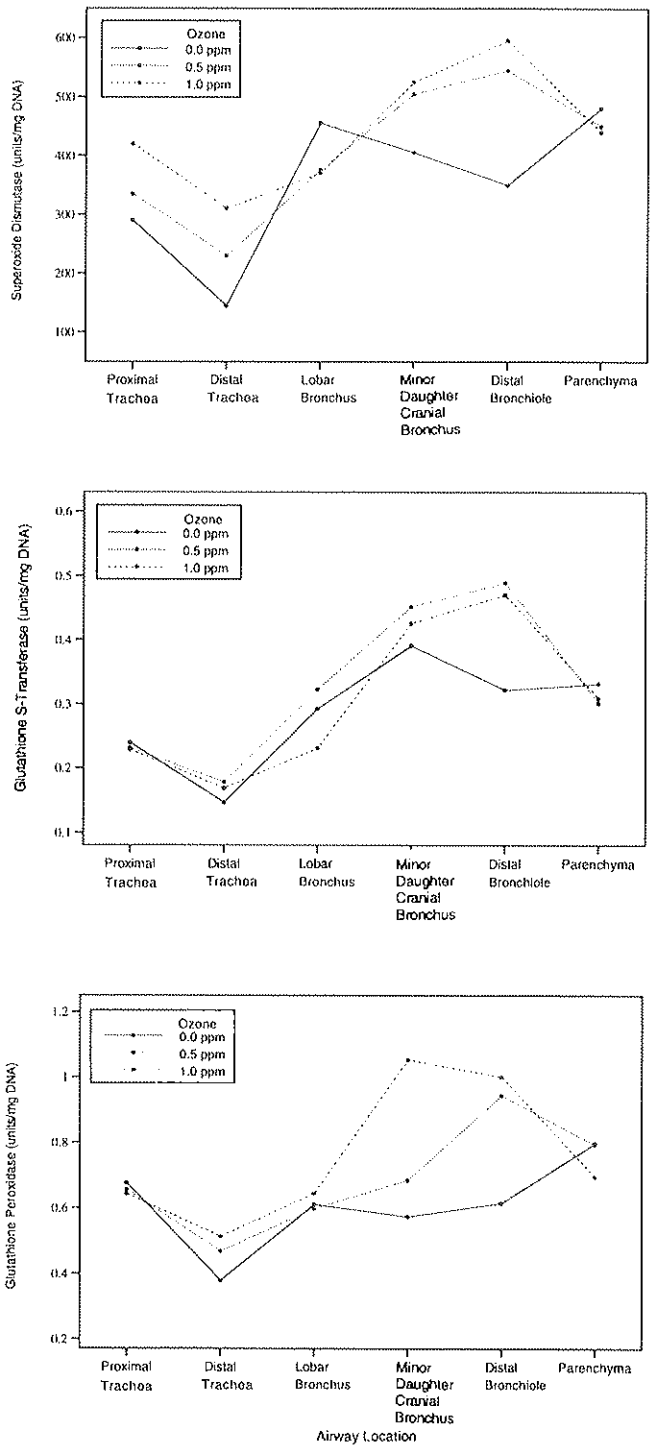

Figure 27. Antioxidant enzyme activity levels of the respiratory tract following 20 months of exposure to 0.0, 0.5, or 1.0 ppm ozone. Antioxidant enzyme activity is expressed in units per milligram of DNA for SOD, GST, and GPx. Activity levels are shown for the proximal and distal trachea, lobar bronchus, minor daughter (cranial) bronchus, distal bronchiole, and lung parenchyma.

The mechanisms involved in establishing tolerance to repeated ozone exposure involve a number of potential factors. In the initial phases of the injury response, elevations in antioxidant enzymes are closely associated with proliferation of type II alveolar cells in the centriacinar region (Jackson and Frank 1984). Corrections for DNA content indicate that these elevations are the result of increases in epithelial cell density and the number of interstitial cell infiltrates in the target zone, the centriacinar region (Bassett et al. 1988). Whether antioxidant enzyme activities increase in the lungs of animals whose tolerance to oxidant injury has developed from long-term exposure and whether these elevations are secondary manifestations of cellular proliferative and reorganizational responses was the focus of the present study. To address these issues more precisely, we evaluated activities on a site-specific basis to facilitate association with the cellular reorganization determined in companion pathologic studies (Dodge et al. 1994; Plopper et al. 1994a).

The tracheal epithelium of the rat does not develop complete tolerance at the end of 60 days of exposure to ozone (Nikula et al. 1988). There is a reorganization of the epithelium, which includes changes in cell density and epithelial composition, but there is no frank cellular necrosis. The only characteristic pathologic alteration is a shortening of the cilia compared with the cells of control animals. After 90 days, respiratory bronchioles with cuboidal epithelial cells form, lining the alveolar ducts and extending a substantial distance into the gas-exchange area (Barr et al. 1988). The cells are poorly differentiated, and at the distal end of the bronchiolarized airways there is still evidence of alveolar epithelial cell necrosis. The condition of airways corresponding to the large intrapulmonary (or major daughter) and small intrapulmonary (minor daughter) bronchi in our study is not known. Correlation of our findings with histopathologic observations for two of the main target sites, the distal trachea and the distal bronchiole–central acinus, indicates that after 90 days of exposure, reorganization in the trachea is not associated with an elevation in the activity of SOD, as we reported previously (Nikula et al. 1988), or of GST or GPx. Conversely, in the distal bronchiole–central acinus, cellular reorganization and the formation of bronchiolar epithelial cells, albeit only partially differentiated ones, does result in a dose-dependent elevation of activity for all three of these enzymes. Whether cellular reorganization of intrapulmonary conducting airways occurs within the 60-day and 90-day exposure time frame and whether it is associated with elevations of antioxidant enzyme activity has not been evaluated. However, our

study shows that at least two of these enzyme systems, SOD and GPx, are responding to oxidant stress in intrapulmonary conducting airways.

In companion studies designed to define cellular responses to near-lifetime (20-month) exposure to ozone within the National Ambient Air Quality Standard concentration (0.12 ppm), we observed a variety of cellular responses in different regions of the respiratory tract (Dodge et al. 1994; Plopper et al. 1994a). In the proximal respiratory tract, including the distal trachea, a large-diameter central bronchus, and small bronchi of short and long path lengths, the principal change was in the volume density of stored secretory product. In only one airway, the small bronchus in the long path, was there any indication of an alteration in cellular organization. This alteration involved a decrease in overall epithelial cell volume without an increase either in the proportion of nonciliated cells or in the total volume of nonciliated cells per unit area (Plopper et al. 1994a). In the present study, there was a dose-dependent increase in the activity of SOD in the trachea without any significant reorganization of the epithelium. The minor daughter and major daughter bronchi showed concentration-dependent, yet opposite, alterations in GPx and GST activities (Plopper et al. 1994b). These airways were the same airway paths as the companion studies' large-diameter central bronchus and the small-diameter (short-path) bronchus, neither of which showed any significant epithelial reorganization. The major daughter bronchus also showed a drop in GST activity, which again was not associated with any alteration in the cellular composition of that airway level. In the centriacinar region, there was significant reorganization of the terminal bronchiole and the bronchiolar epithelium in alveolar ducts to favor an increase in the proportion (volume fraction) and, in some cases, the volume density of nonciliated bronchiolar cells (Plopper et al. 1994a). We also observed an increase in the amount of stored secretory product (Clara cell 10-kilodalton protein) produced by nonciliated bronchiolar cells in the centriacinar region (Dodge et al. 1994). These changes in the centriacinar region are closely associated with ozone concentration–dependent increases in SOD, GPx, and GST activities (Plopper et al. 1994a,b). We found no significant changes in the activity of any of these enzymes in the majority of the lung tissue, the gas-exchange area, or the parenchyma, which is unaltered by ozone exposure (Dodge et al. 1994; Pinkerton et al. 1993; Plopper et al. 1994a, b). It should also be noted that SOD was the only enzyme studied that, after 90 days of exposure, showed any significant alterations in activity in whole-lung homogenates. This observation closely matches the findings of a long-term study of similar duration (22 months) (Sagai and Ichinose 1991), though not those of a study using somewhat shorter exposures (12 months) (Grose et al. 1989).

In summary, the current study indicates that long-term exposure to oxidant air pollutants such as ozone at ambient concentrations significantly alters the antioxidant enzyme activities of the lungs. The changes appear to be site-specific and to vary with exposure duration. When the cellular pathology of the same regions is considered, these shifts in antioxidant enzyme activities in some cases appear to be associated with alterations in the cellular populations, and in other cases not. These shifts are observed even when measurements are corrected for DNA content. Another factor is the shift in the abundance of secretory product stored in airway epithelium. This secretory product is primarily AB/PAS-positive material in distal conducting airways and Clara cell secretory protein in the centriacinar region. At least three factors appear to be involved in establishing the new, more tolerant, steady state that characterizes epithelial resistance to oxidant injury from air pollutants. One is an elevation in the local activity of antioxidant enzymes. The second is a shift in the composition of the epithelial population in favor of more resistant cell types. The third is an alteration in the process by which cells store, and possibly synthesize, cellular secretory products. The manner in which these three factors combine to produce a resistant cellular population appears to depend on the location of the cells within the respiratory tract. The sites that exhibit the greatest acute injury appear to have the most changes.

INTEGRATED ANALYSIS

STRUCTURAL AND BIOCHEMICAL CHANGES

The combined findings from each specific aim in this study can be used to examine whether increases in response are observed at sites predicted to receive greater ozone doses and how those responses might vary as a function of changing ozone concentration. Ozone absorption is a complex process that depends on many factors. We simplified the process to show that absorption depends on transit time and airspace volume distal to the airway. The path length to the site of absorption was used to approximate transit time, and an estimate of terminal bronchioles below the anatomical site, determined from the data of Raabe and coworkers (1976), was used to approximate distal volume.

It is now well recognized that exposure to the oxidant air pollutant ozone is toxic to the epithelial cells of the respiratory system. Most of the injury to the cell and the accom-

panying inflammation occur during the initial phases of exposure. The severity and nature of both the acute necrosis and the associated inflammatory response are not uniform throughout the respiratory tract. Injury occurs even at ambient ozone concentrations. By contrast, continual exposure to ozone, even at concentrations that initially produce epithelial necrosis and acute inflammation, is associated with epithelial populations exhibiting little cell death and minimal inflammation. The overall purpose of the present study was to define the cellular and enzymatic changes in the respiratory system that are associated with the lack of necrosis and inflammation characteristic of mammals exposed to ambient levels of ozone for near-lifetime periods. We evaluated sites within the respiratory system that are recognized as either sensitive or resistant to the acute effects of initial exposure. The sensitive sites we evaluated included the trachea, the lobar bronchus, the distal conducting airways (terminal bronchioles), and alveolar ducts of the central pulmonary acinus. Areas we examined that are considered to be less susceptible to acute injury and inflammation included the intrapulmonary bronchial airways and the distal lung parenchyma. Our findings suggest that the long-term response of the respiratory system to continual oxidant insult from air pollutants is heterogeneous in terms of location within the respiratory tract, pollutant concentration, and the nature of the response.

For this study, we defined the cellular organization of the epithelium, and in some cases the composition of the interstitium, and evaluated the potential for protection against oxidant injury via three antioxidant, or phase II, enzymes: SOD, GPx, and GST. The response of the tracheobronchial airways was highly heterogeneous. The ability of conducting airways to store a secretory product decreased in a dose-dependent fashion in the trachea. This absolute amount, but not the dose-response relation, differed in males and females. Female control animals had less stored AB/PAS-positive material and female exposed animals had a lesser degree of change, compared with males. However, there was no obvious reorganization of the epithelium in terms of either epithelial thickness or the volume fraction of the cell population recognized as being most resistant, the nonciliated epithelial cells. Of the three antioxidant enzymes examined, only SOD activity was elevated in the trachea. In the longer, less deviant path through the conducting airways, which included the central and the caudal bronchi, there were marked changes in the smaller, more peripheral of the two airways (the caudal), but not in the proximal airway. There was no change in storage of AB/PAS-positive material centrally, but there was an elevation caudally in both males and females, although to a lesser extent in females. What epithelial reorganization did occur was in male rats, but not in the females. Antioxidant enzyme activity in this portion of the airways including these two airway generations (major daughter pathways) was actually reduced for both GPx and GST. There was no change in SOD activity in exposed animals. In contrast, in the shortest path (cranial bronchus), epithelial storage of AB/PAS-positive material was elevated in both males and females. The proportion of nonciliated cells within the epithelium was increased only in the females. There were no changes in epithelial composition of any significance in males. In contrast, the activity of two of the antioxidant enzymes, SOD and GPx, increased significantly in a dose-dependent fashion in the portion of the airway tree that included the cranial bronchus (minor daughter bronchi).

As would be expected from previous studies, the airways of the centriacinar region were the most responsive to continual oxidant stress. We evaluated the epithelial composition in three of these zones: the terminal bronchiole, which was the most distal conducting airway generation; the bronchiole one generation proximal to it; and the alveolar ducts extending at least 800 μm distal from the junction with the terminal bronchiole. The terminal bronchiolar epithelial organization was most varied in the caudal region, with changes primarily in the composition of the epithelial cell types in favor of nonciliated cells and, in the case of males, an increase in the total cell volume, which did not occur in the females. In the terminal bronchiole from the cranial region, epithelial changes occurred only in males. By contrast, in the proximal bronchiole, the only change was a reorganization in the composition of the epithelium in favor of nonciliated cells. This finding was present only in the caudal region and only in females. There was a proximal-to-distal bronchiolarization extending a significant distance into the alveolar duct in exposed animals. This epithelium was similar in cellular organization to that found in terminal bronchioles of control and treated animals. Bronchiolarization extended farther into the alveolar ducts in the cranial regions in males than it did in females, but in the caudal region the extent was greater in females than in males. The epithelium contained a greater proportion of nonciliated cells than in terminal bronchioles of control animals. This was true for females at the high dose (1.0 ppm ozone) in the cranial region and for males at 0.5 and 1.0 ppm ozone in both the caudal and cranial regions. There were dose-related elevations in the activities of SOD, GPx, and GST in the distal bronchiole–central acinus.

When the data are examined as a pathway by which ozone travels, we see the heterogeneity of the response in the lower respiratory tract. The antioxidant enzyme activities following a pathway from the trachea to the alveolus

are summarized in Figure 27. The heterogeneity of response from site to site is further emphasized in Figure 28.

Several factors may result in differences in the response of the respiratory epithelium to chronic oxidant stress. Metabolic differences, including alterations both in stored secretory product and in antioxidant enzymes, would in most cases tend to favor increased resistance. Gender differences in the overall pattern of response appear to be minimal, but a slightly lower level of response in females was observed. Epithelial reorganization in favor of less sensitive cell types, nonciliated cells, is the predominant response of epithelium throughout the conducting airways. However, this response is not uniform, is definitely site-specific, and occurs to a much greater extent in males than in females. This includes reorganization not only in conducting airways but also in the bronchiolarized epithelium of alveolar ducts. The primary target site, the central acinus, where modeling studies indicate some of the highest local concentrations of ozone would be expected, has the greatest degree of epithelial change and exhibits the most elevated response in terms of increased antioxidant enzymes.

HIGHLIGHTS OF FINDINGS

Airways

- The amount of stored epithelial mucosubstances was significantly reduced in the trachea, was unchanged in the central bronchus, increased six-fold in the cranial bronchus, and increased three-fold in the caudal bronchus with ozone exposure.
- The epithelial composition of the airways was unchanged in the trachea and bronchi. Nonciliated bronchiolar cell volume density was significantly increased in a dose-dependent manner in terminal bronchioles in the caudal left lung arising from a long airway path relative to the trachea.
- The extension of bronchiolarized epithelium into alveolar ducts was greater in cranial regions than in caudal regions.

Pulmonary Acinus

- The predominant changes in the ventilatory units of the lungs following exposure to ozone were extension of bronchiolar epithelium (ciliated and nonciliated cells) into alveolar ducts and increase in interstitial volume density. The depth to which bronchiolar epithelium extended beyond the BADJ was concentration-dependent and site-specific. The most prominent changes were noted in male rats in ventilatory units arising form a short airway path (cranial region of the left lung), rather than ventilatory units arising from a long airway path (caudal region of the left lung).
- Change in the ventilatory units of animals exposed to 0.12 ppm ozone consisted of the extension of bronchiolar epithelium 200 to 300 μm beyond the BADJ, but this alteration was significant only in male animals and was most evident in ventilatory units arising from a short airway path (cranial region of the left lung).

Antioxidant Enzymes

- Glutathione S–transferase, glutathione peroxide, and superoxide dismutase significantly increased in a concentration-dependent fashion in the distal bronchiole–central acinus.
- Superoxide dismutase increased in a concentration-dependent fashion in the distal trachea.
- Antioxidant enzyme activity responded differently in different lung subcompartments.
- Antioxidant enzyme activities for the whole lung do not reflect changes in lung subcompartments.

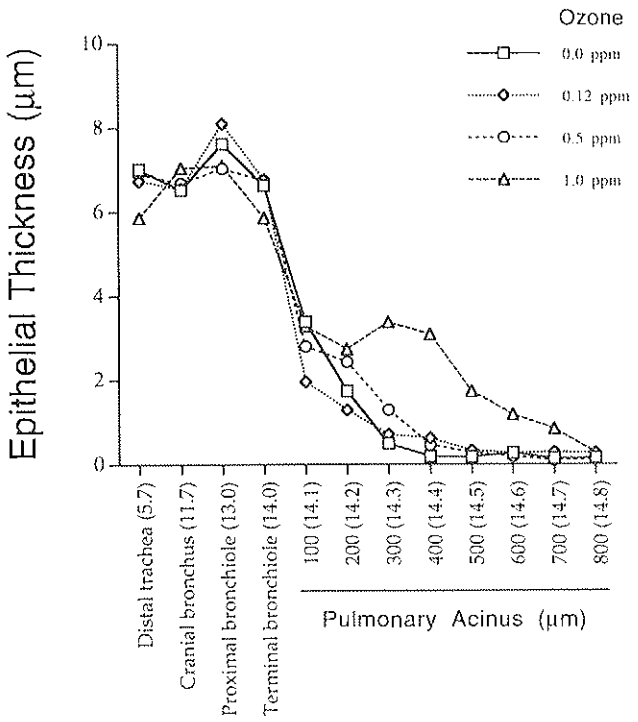

Figure 28. Epithelial thickness (μm) of the lower respiratory tract after 20 months of exposure to 0.0, 0.12, 0.5, or 1.0 ppm ozone. The estimated distance (mm) of each anatomical site from the larynx to the cranial pulmonary acinus is given in parentheses. Values presented are the average of the combined data for both males and females.

ACKNOWLEDGMENTS

The authors appreciate the coordination and planning efforts of Dr. Debra A. Kaden of HEI and Dr. Gary A. Boorman of NTP during the course of this study. Several collaborators played key roles in the completion of this study. For morphometric analysis of the tracheobronchial tree, Fung-Ping Chu, Carole J. Haselton, Janice Peake, and James Wu provided expert technical assistance. For morphometric studies of the pulmonary acinus, Janice Peake, Jane Cederdahl-Demmler, John T. Gallen, and Viviana J. Wong worked many long hours to complete this work. Expert statistical analysis and insightful discussions of ozone dosimetry were provided by Robert R. Mercer, Frederick J. Miller, Paul J. Catalano, and Louise M. Ryan. Antioxidant enzyme activity measurements were performed by Xiuzhen Duan and Alan R. Buckpitt from the Department of Molecular Biosciences in the School of Veterinary Medicine, University of California at Davis.

REFERENCES

Barr BC, Hyde DM, Plopper CG, Dungworth DL. 1988. Distal airway remodeling in rats chronically exposed to ozone. Am Rev Respir Dis 137:924–938.

Barr BC, Hyde DM, Plopper CG, Dungworth DL. 1990. A comparison of terminal airway remodeling in chronic daily versus episodic ozone exposure. Toxicol Appl Pharmacol 106:384–407.

Bassett DJP, Bowen-Kelly E, Elbon CL, Reichenbaugh SS. 1988. Rat lung recovery from three days of continuous exposure to 0.75 ppm ozone. J Toxicol Environ Health 25:329–347.

Beauchamp C, Fridovich I. 1971. Superoxide dismutase: Improved assays and an assay applicable to acrylamide gels. Anal Biochem 44:276–287.

Boorman GA, Schwartz LW, Dungworth DL. 1980. Pulmonary effects of prolonged ozone insult in rats: Morphometric evaluation of the central acinus. Lab Invest 43(2):108–115.

Castleman WL, Dungworth DL, Schwartz LW, Tyler WS. 1980. Acute respiratory bronchitis: An ultrastructural and autoradiographical study of epithelial cell injury and renewal in Rhesus monkeys exposed to ozone. Am J Pathol 98:811–827.

Chang, L-Y, Stockstill B, Menache MG, Mercer RR, Crapo JD. 1995. Consequences of Prolonged Inhalation of Ozone on F344/N Rats: Collaborative Studies, Part VIII, Morphometric Analysis of Structural Alterations in Alveolar Regions. Research Report Number 65. Health Effects Institutes, Cambridge, MA.

Chow CK, Plopper CG, Chiu M, Dungworth DL. 1981. Dietary vitamin E and pulmonary biochemical and morphological alterations of rats exposed to 0.1 ppm ozone. Environ Res 24:315–324.

Clark K, Posin C, Buckley R. 1978. Biochemical response of squirrel monkeys to ozone. J Toxicol Environ Health 4:741–753.

Dodge DE, Rucker RB, Pinkerton KE, Haselton CJ, Plopper CG. 1994. Dose-dependent tolerance to ozone: III. Elevation of intracellular Clara cell 10 kDa protein in central acini of rats exposed for 20 months. Toxicol Appl Pharmacol 127:109–123.

Duan X, Buckpitt AR, Plopper CG. 1993. Variation in antioxidant enzyme activities in anatomic subcompartments within rat and rhesus monkey lungs. Toxicol Appl Pharmacol 123:73–82.

Elsayed NM, Kass R, Mustafa MG, Hacker AD, Ospital JJ, Chow CK, Cross CE. 1988. Effect of dietary vitamin E level on the biochemical response of rat lung to ozone inhalation. Drug Nutr Interact 5:373–386.

Eustis SL, Schwartz LW, Kosch PC, Dungworth DL. 1981. Chronic bronchiolitis in nonhuman primates after prolonged ozone exposure. Am J Pathol 105:121–137.

Evans MJ, Shami SG, Cabral-Anderson LJ, Dekker NP. 1986. Role of nonciliated cells in renewal of the bronchial epithelium of rats exposed to NO_2. Am J Pathol 123:126–133.

Fujinaka LE, Hyde DM, Plopper CG, Tyler WS, Dungworth DL, Lollini LO. 1985. Respiratory bronchiolitis following long-term ozone exposure in bonnet monkeys: A morphometric study. Exp Lung Res 8:167–190

Glantz SA. 1992. Primer of Biostatistics. McGraw-Hill, New York, NY.

Gordon RE, Lane BP. 1977. Cytokinetics of rat tracheal epithelium stimulated by mechanical trauma. Cell Tissue Kinet 10:171–181.

Grose EC, Stevens MA, Hatch GE, Jaskot RH, Selgrade MJK, Stead AG, Costa DL, Graham JA. 1989. The impact of a 12-month exposure to a diurnal pattern of ozone on pulmonary function, antioxidant biochemistry and immunology. In: Atmospheric Ozone and Its Policy Implications (Schneider T, Lee SD, Wolters GJR, Grant LD, eds.) pp. 535–544. Elsevier Science Publishing Co., New York, NY.

Habig WH, Pabst MJ, Jakoby B. 1974. Glutathione S–transferase: The first step in mercapturic acid formation. J Biol Chem 249:7130–7139.

Harkema JR, Plopper CG, Hyde DM, St George JA, Dungworth DL. 1987a. Effects of ambient levels of ozone on primate nasal epithelial mucosubstances: Quantitative histochemistry. Am J Pathol 127:90–96.

Harkema JR, Plopper CG, Hyde DM, St. George JA, Wilson DW, Dungworth DL. 1987b. Response of the macaque nasal epithelium to ambient levels of ozone: A morphologic and morphometric study of the transitional and respiratory epithelium. Am J Pathol 128:29–44.

Heng H, Rucker RB, Crotty J, Dubick MA. 1987. The effects of ozone on lung, heart, and liver superoxide dismutase and glutathione peroxidase activities in the protein-deficient rat. Toxicol Lett 38:225–237.

Hyde DM, Hubbard WC, Wong V, Wu R, Pinkerton K, Plopper CG. 1992a. Ozone-induced acute tracheobronchial epithelial injury: Relationship to granulocyte emigration in the lung. Am J Respir Cell Mol Biol 6:481–497.

Hyde DM, Magliano DJ, Plopper CG. 1992b. Morphometric assessment of pulmonary toxicity in the rodent lung. Toxicol Pathol 19:428–446.

Hyde DM, Plopper CG, St. George JA, Harkema JR. 1990. Morphometric cell biology of air space epithelium. In: Electron Microscopy of the Lung (Schraufnagel DE, ed.) pp. 71–120. Marcel Dekker, New York, NY.

Ichinose T, Arakawa K, Shimojo N, Sagai M. 1988. Biochemical effects of combined gases of nitrogen dioxide and ozone: II. Species differences in lipid peroxides and antioxidative protective enzymes in the lungs. Toxicol Lett 42:167–176.

Ichinose T, Sagai M. 1989. Biochemical effects of combined gases of nitrogen dioxide and ozone: III. Synergistic effects on lipid peroxidation and antioxidative protective systems in the lungs of rats and guinea pigs. Toxicology 59:259–270.

Jackson RM, Frank L. 1984. Ozone-induced tolerance to hyperoxia in rats. Am Rev Respir Dis 129:425–429.

Johnson DA, Winters RS, Lee KR, Smith CE. 1990. Oxidant Effects on Rat and Human Lung Proteinase Inhibitors. Research Report Number 37. Health Effects Institute, Cambridge, MA.

Karrer HE. 1958. The fine structure of connective tisssue in the tunica propria of bronchioles. J Ultrastruct Res 2:96–121

Lamb D, Reid L. 1968. Mitotic rates, goblet cell increase and histochemical changes in mucus in rat bronchial epithelium during exposure to sulphur dioxide. J Pathol Bacteriol 96:97–111.

Lamb D, Reid L. 1969. Goblet cell increase in rat bronchial epithelium after exposure to cigarette and cigar tobacco smoke. Br Med J 1:33–35.

Lum H, Schwartz LW, Dungworth DL, Tyler WS. 1978. A comparative study of cell renewal after exposure to ozone or oxygen. Response of terminal bronchiolar epithelium in the rat. Am Rev Respir Dis 118:335–345.

Mellick PW, Dungworth DL, Schwartz LW, Tyler WS. 1977. Short-term morphologic effects of high ambient levels of ozone on lungs of rhesus monkeys. Lab Invest 36:82–90.

Mercer RR, Anjilvel S, Miller FJ, Crapo JD. 1991. Inhomogeneity of ventilatory unit volume and its effects on reactive gas uptake. J Appl Physiol 70:2193–2205.

Mercer RR, Crapo JD. 1987. Three-dimensional reconstruction of the rat acinus. J Appl Physiol 63(2):785–794.

Mercer RR, Crapo JD. 1991. Architecture of the acinus. In: Treatise on Pulmonary Toxicology: Comparative Biology of the Normal Lung (Parent RA, ed.) pp. 109–119. CRC Press, Boca Raton, FL.

Mercer RR, Pinkerton KE. 1990. The influence of ventilatory unit size on the distribution and uptake of reactive gases. In: Biofluid Mechanics 3 (Schneck DJ, Lucas CL, eds.) pp. 27–35. New York University Press, New York, NY.

Meyer JC, Grundmann H. 1984. Fluorometric determination of DNA in epidermis and cultured fibroblasts using 4′-6-diamidino-2-phenylindole (DAPI). Arch Dermatol Res 276:52–56.

Miller FJ, Overton JH, Gerrity TR, Graham RC. 1988. Interspecies dosimetry of reactive gases. In: Inhalation Toxicology (Mohr U, Dungworth D, Kimmerle G, Lewkowski J, McClellan R, Stöber W, eds.) pp. 139–155. Springer-Verlag, New York, NY.

Miller FJ, Overton J, Jasket R, Menzel DB. 1985. A model of the regional uptake of gaseous pollutants in the lung: I. The sensitivity of the uptake of ozone in the human lung to lower respiratory tract secretions and exercise. Toxicol Appl Pharmacol 79:11–27.

Moffatt RK, Hyde DM, Plopper CG, Tyler WS, Putney LF. 1987. Ozone-induced adaptive and reactive cellular changes in respiratory bronchioles of bonnet monkeys. Exp Lung Res 12:57–74.

Nikula KJ, Wilson DW, Giri S, Plopper CG, Dungworth DL. 1988. The response of the rat tracheal epithelium to ozone exposure: Injury, adaptation, and repair. Am J Pathol 131:373–384.

Oberley LW, Spitz DR. 1984. Assay of superoxide dismutase activity in tumor tissue. Methods Enzymol 105:457–464.

Overton JH, Barnett AE, Graham RC. 1989. Significances of the variability of tracheobronchial airway paths and their air flow rates to dosimetry model predictions of the absorption of gases. In: Extrapolation of Dosimetric Relationships for Inhaled Particles and Gases (Crapo JD, Smolko ED, Miller FJ, Graham JA, Hayes AW, eds.) pp. 273–291. Academic Press, Orlando, FL.

Overton JH, Graham RC, Miller FJ. 1987. A model of the regional uptake of gaseous pollutants in the lung: II. The sensitivity of ozone uptake in laboratory animal lungs to anatomical and ventilatory parameters. Toxicol Appl Pharmacol 88:418–432.

Paglia DE, Valentine WN. 1967. Studies on the quantitative and qualitative characterization of erythrocyte glutathione peroxidase. J Lab Clin Med 70:58–169.

Patra AL, Gooya A, Menache M. 1986. A morphometric comparison of the nasopharyngeal airway of laboratory animals and humans. Anat Rec 215:42–50.

Phalen RF, Oldham MJ. 1983. Tracheobronchial airway structure as revealed by casting techniques. Am Rev Respir Dis 128:51–53.

Phalen RF, Yeh HC, Schum GM, Raabe OG. 1978. Application of an idealized model to morphometry of the mammalian tracheobronchial tree. Anat Rec 190:167–176.

Pinkerton KE, Mercer RR, Plopper CG, Crapo JD. 1992. Distribution of injury and microdosimetry of ozone in the ventilatory unit of the rat. J Appl Physiol 73:817–824.

Pinkerton KE, Dodge DE, Cederdahl-Demmler J, Wong VJ, Peake J, Haselton CJ, Mellick PW, Singh G, Plopper CG. 1993. Differentiated bronchiolar epithelium in alveolar ducts of rats exposed to ozone for 20 months. Am J Pathol 142:947–956.

Plopper CG. 1990. Structural methods for studying bronchiolar epithelial cells. In: Models of Lung Disease: Microscopy and Structural Methods (Gil J, ed.) pp. 537–559. Marcel Dekker, New York, NY.

Plopper CG, Chang AM, Pang A, Buckpitt AR. 1991a. Use of microdissected airways to define metabolism and cytotoxicity in murine bronchiolar epithelium. Exp Lung Res 17:197–212.

Plopper CG, Chow CK, Dungworth DL, Brummer M, Nemeth TJ. 1979. Effect of low level of ozone on rat lungs: II. Morphological responses during recovery and re-exposure. Exp Mol Pathol 29:400–411

Plopper CG, Chu F, Haselton CJ, Peake J, Wu J, Pinkerton KE. 1994a. Dose-dependent tolerance to ozone: I. Tracheobronchial epithelial reorganization in rats after 20 months exposure. Am J Pathol 144:404–421.

Plopper CG, Duan X, Buckpitt AR, Pinkerton KE. 1994b. Dose-dependent tolerance to ozone: IV. Site-specific elevation in antioxidant enzymes in the lungs of rats exposed for 90 days or 20 months. Toxicol Appl Pharmacol (*in press*). 127:124–131.

Plopper CG, Hyde DM, Buckpitt AR. 1991b. Clara cells. In: The Lung, Scientific Foundations (Crystal RG, West JB, eds.) pp. 215–216. Raven Press, New York, NY.

Plopper CG, Macklin J, Nishio SJ, Hyde DM, Bnckpitt AR. 1992. Relationship of cytochrome P450 activity to Clara cell cytotoxicity: III. Morphometric comparison of changes in the epithelial populations of terminal bronchioles and lobar bronchi in mice, hamsters, and rats after parenteral administration of naphthalene. Lab Invest 67:553–565.

Raabe OG, Yeh HC, Schum GM, Phalen RF. 1976. Tracheobronchial Geometry: Human, Dog, Rat, Hamster. Lovelace Foundation Report Number 53. Lovelace Foundation, Albuquerque, NM.

Rahman IU, Clerch LB, Massaro D. 1991. Rat lung antioxidant enzyme induction by ozone. Am J Physiol 260:L412–L418.

Rietjens IMCM, van Bree L, Marra M, Poelen MCM, Rombout PJA, Alink GM. 1985. Glutathione pathway enzyme activities and the ozone sensitivity of lung cell populations derived from ozone exposed rats. Toxicology 37:205–214.

Sagai M, Ichinose T. 1991. Biochemical effects of combined gases of nitrogen dioxide and ozone: IV. Changes of lipid peroxidation and antioxidative protective systems in rat lungs upon life span exposure. Toxicology 66:121–132.

Schlesinger RB, Gorczynski JE, Dennison J, Richards L, Kinney PL, Bosland MC. 1992. Long-term intermittent exposure to sulfuric acid aerosol, ozone, and their combination: Alterations in tracheobronchial mucociliary clearance and epithelial secretory cells. Exp Lung Res 18:505–534.

Schwartz LW, Dungworth DL, Mustafa MG, Tarkington BK, Tyler WS. 1976. Pulmonary responses of rats to ambient levels of ozone: Effects of 7-day intermittent or continuous exposure. Lab Invest 34:565–578.

Snedecor GW, Cochran WG. 1967. Statistical Methods, 6th ed. Iowa State University Press, Ames, IA.

Spicer SS, Chakrin LW, Wardell JR. 1974. Effect of chronic sulfur dioxide inhalation on the carbohydrate histochemistry and histology of the canine respiratory tract. Am Rev Respir Dis 110:13–24.

Stephens RJ, Sloan MF, Evans MJ, Freeman G. 1974. Early response of lungs to low levels of ozone. Am J Pathol 74:31–58.

Tyler WS, Dungworth DL, Plopper CG, Hyde DM, Tyler NK. 1985. Structural evaluation of the respiratory system. Fundam Appl Toxicol 5:405–422

Tyler WS, Tyler NK, Last JA, Barstow TJ, Magliano DJ, Hinds DM. 1987. Effects of ozone on lung and somatic growth: Pair fed rats after ozone exposure and recovery periods. Toxicology 46:1–20.

van Bree L, Marra M, Rombout PJA. 1992. Differences in pulmonary biochemical and inflammatory responses of rats and guinea pigs resulting from daytime or nighttime, single and repeated exposure to ozone. Toxicol Appl Pharmacol 116:209–216.

Wilson DW, Plopper CG, Dungworth DL. 1984. The response of the macaque tracheobronchial epithelium to acute ozone injury. Am J Pathol 116:193–206.

APPENDIX A. Combined Data from Caudal and Cranial Regions According to Distance Down the Alveolar Duct

Table A.1. Epithelial Tissue Volume Density for Female Rats[a]

Ozone Concentration (ppm)	Distance Down Alveolar Duct (μm)							
	100	200	300	400	500	600	700	800
0.0	2.348 ± 0.707	1.487 ± 0.865	0.805 ± 0.083	0.437 ± 0.304	0.212 ± 0.030	0.22 ± 0.169	0.134 ± 0.049	0.114 ± 0.033
0.12	5.569 ± 5.403	1.003 ± 0.316	0.604 ± 0.565	0.399 ± 0.329	0.187 ± 0.125	0.191 ± 0.094	0.212 ± 0.116	0.178 ± 0.179
0.5	2.356 ± 0.735	1.765 ± 0.203	0.734 ± 0.492	0.296 ± 0.107	0.211 ± 0.127	0.22 ± 0.074	0.139 ± 0.057	0.232 ± 0.158
1.0	1.699 ± 1.238	3.004 ± 0.362	2.689 ± 0.815	2.172 ± 0.352	1.417 ± 0.933	0.344 ± 0.090	0.531 ± 0.194	0.346 ± 0.119

[a] Values reflect combined data for the cranial and caudal regions and are given as means ± SDs expressed in $\mu m^3/\mu m^2$.

Table A.2. Interstitial Tissue Volume Density for Female Rats[a]

Ozone Concentration (ppm)	Distance Down Alveolar Duct (μm)							
	100	200	300	400	500	600	700	800
0.0	1.806 ± 0.636	1.854 ± 0.1.490	1.412 ± 0.662	1.038 ± 0.288	1.3 ± 0.443	1.079 ± 0.141	1.069 ± 0.2	1.058 ± 0.246
0.12	1.383 ± 0.561	1.664 ± 0.453	1.223 ± 0.164	1.387 ± 0.238	1.179 ± 0.3531	1.268 ± 0.396	1.28 ± 0.261	1.365 ± 0.430
0.5	1.872 ± 0.973	1.691 ± 0.235	1.494 ± 0.2	1.428 ± 0.108	1.396 ± 0.305	1.291 ± 0.160	1.06 ± 0.146	1.361 ± 0.269
1.0	2.191 ± 0.847	1.898 ± 0.281	2.628 ± 1.107	1.77 ± 0.229	2.181 ± 0.328	1.523 ± 0.328	1.306 ± 0.508	1.108 ± 0.394

[a] Values reflect combined data for the cranial and caudal regions and are given as means ± SDs expressed in $\mu m^3/\mu m^2$.

Table A.3. Capillary Volume Density for Female Rats[a]

Ozone Concentration (ppm)	Distance Down Alveolar Duct (μm)							
	100	200	300	400	500	600	700	800
0.0	0.985 ± 0.48	0.893 ± 0.470	1.549 ± 0.493	1.324 ± 0.322	1.453 ± 0.555	1.251 ± 0.355	1.421 ± 0.588	1.405 ± 0.530
0.12	1.112 ± 0.630	1.423 ± 0.199	1.268 ± 0.232	1.358 ± 0.320	1.452 ± 0.272	1.289 ± 0.472	1.287 ± 0.317	1.386 ± 0.283
0.5	0.86 ± 0.491	1.463 ± 0.345	1.592 ± 0.473	1.862 ± 0.370	2.086 ± 0.469	2.02 ± 0.491	1.818 ± 0.364	1.653 ± 0.298
1.0	0.997 ± 0.765	0.669 ± 0.380	1.031 ± 0.469	1.149 ± 0.368	1.486 ± 0.715	1.343 ± 0.361	1.79 ± 0.363	1.15 ± 0.509

[a] Values reflect combined data for the cranial and caudal regions and are given as means ± SDs expressed in $\mu m^3/\mu m^2$.

Table A.4. Alveolar Macrophage Volume Density for Female Rats[a]

Ozone Concentration (ppm)	Distance Down Alveolar Duct (μm)							
	100	200	300	400	500	600	700	800
0.0	0.234 ± 0.245	0.115 ± 0.184	0.043 ± 0.059	0.044 ± 0.088	0.056 ± 0.041	0.023 ± 0.027	0.05 ± 0.058	0.054 ± 0.048
0.12	0	0.037 ± 0.031	0.035 ± 0.04	0.033 ± 0.025	0.046 ± 0.062	0.149 ± 0.130	0.045 ± 0.054	0.066 ± 0.071
0.5	0.093 ± 0.111	0.122 ± 0.082	0.064 ± 0.028	0.048 ± 0.082	0.027 ± 0.033	0.044 ± 0.045	0.047 ± 0.052	0.025 ± 0.029
1.0	0.179 ± 0.194	0.238 ± 0.302	0.29 ± 0.272	0.329 ± 0.375	0.158 ± 0.183	0.053 ± 0.094	0.039 ± 0.056	0.034 ± 0.039

[a] Values reflect combined data for the cranial and caudal regions and are given as means ± SDs expressed in $\mu m^3/\mu m^2$.

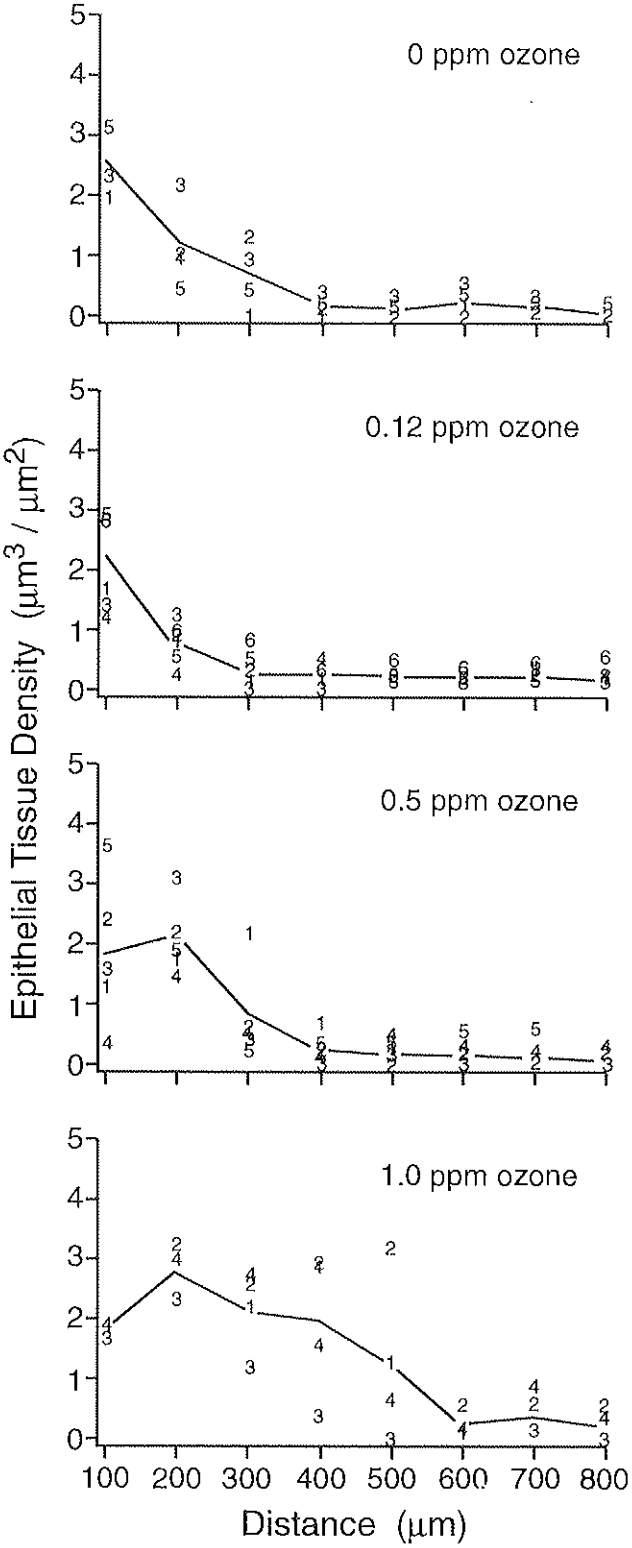

Figure A.1. Epithelial tissue volume density (expressed as a function of distance in ventilatory units) of the cranial region in female rats exposed to 0.0, 0.12, 0.5, or 1.0 ppm ozone.

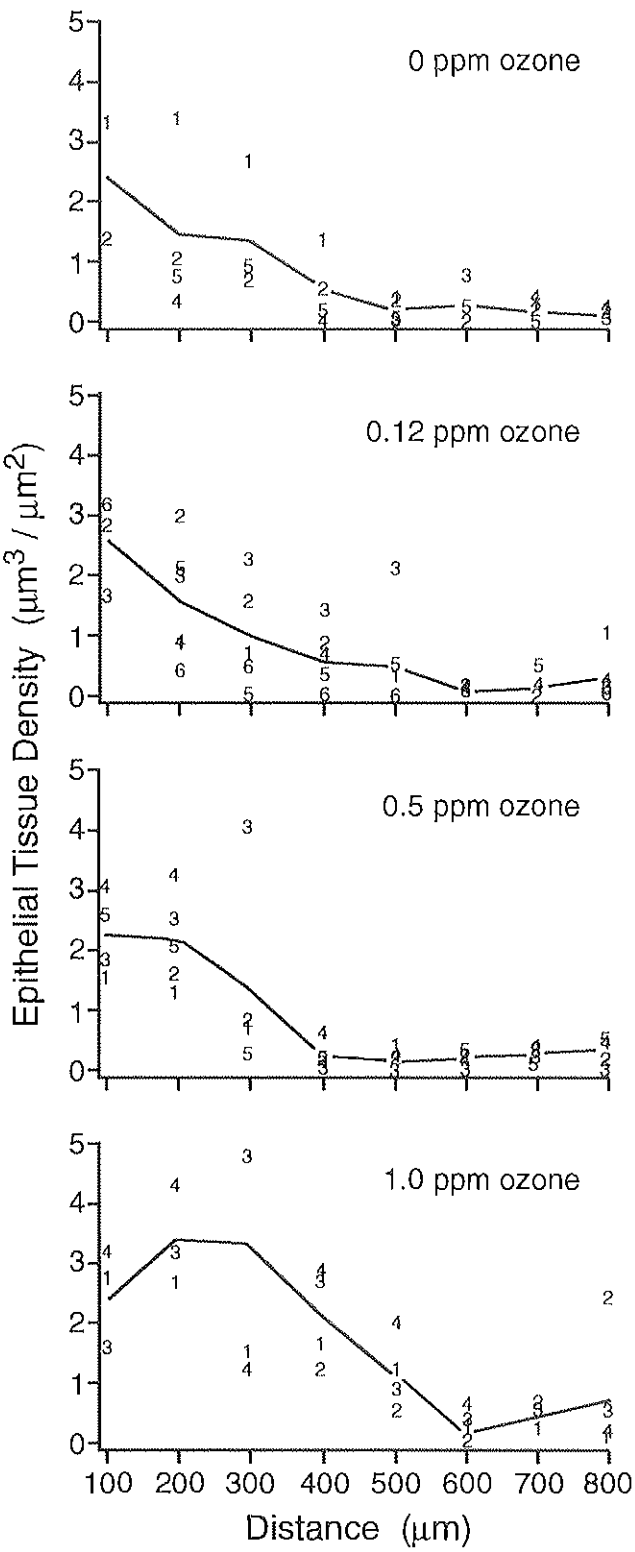

Figure A.2. Epithelial tissue volume density (expressed as a function of distance in ventilatory units) of the caudal region in female rats exposed to 0.0, 0.12, 0.5, or 1.0 ppm ozone.

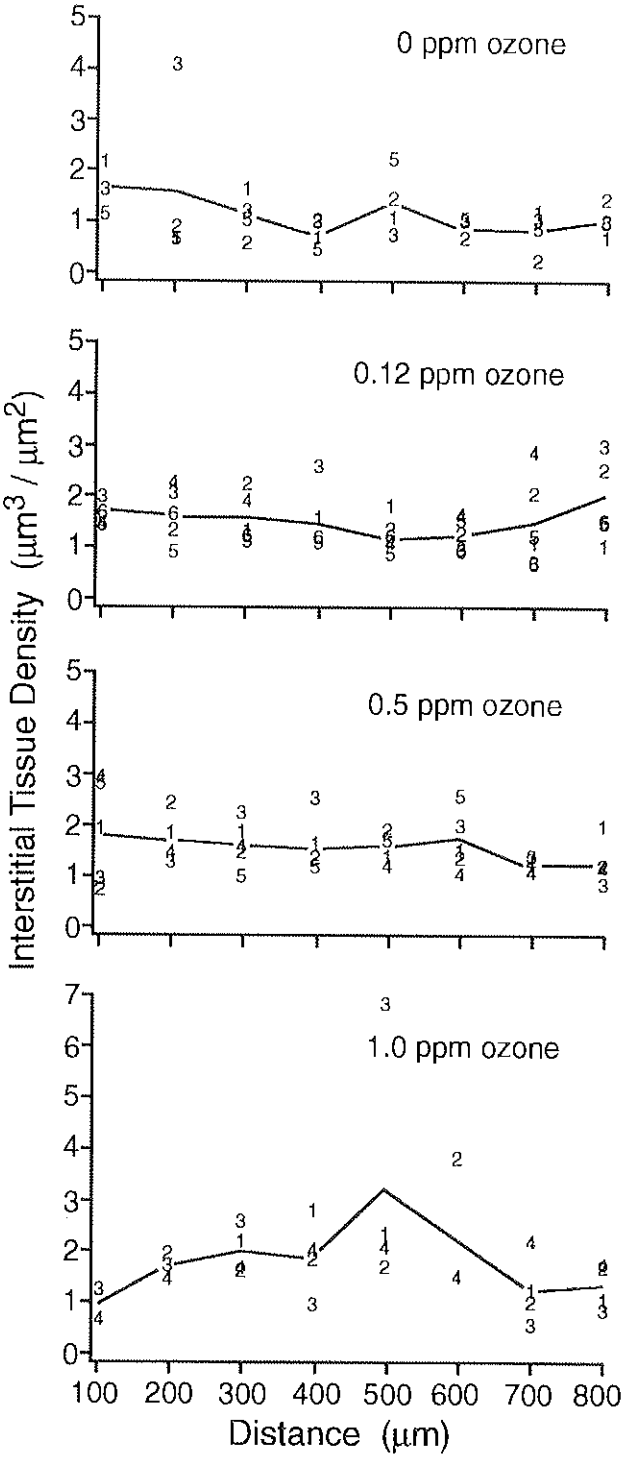

Figure A.3. Interstitial tissue volume density (expressed as a function of distance in ventilatory units) of the cranial region in female rats exposed to 0.0, 0.12, 0.5, or 1.0 ppm ozone.

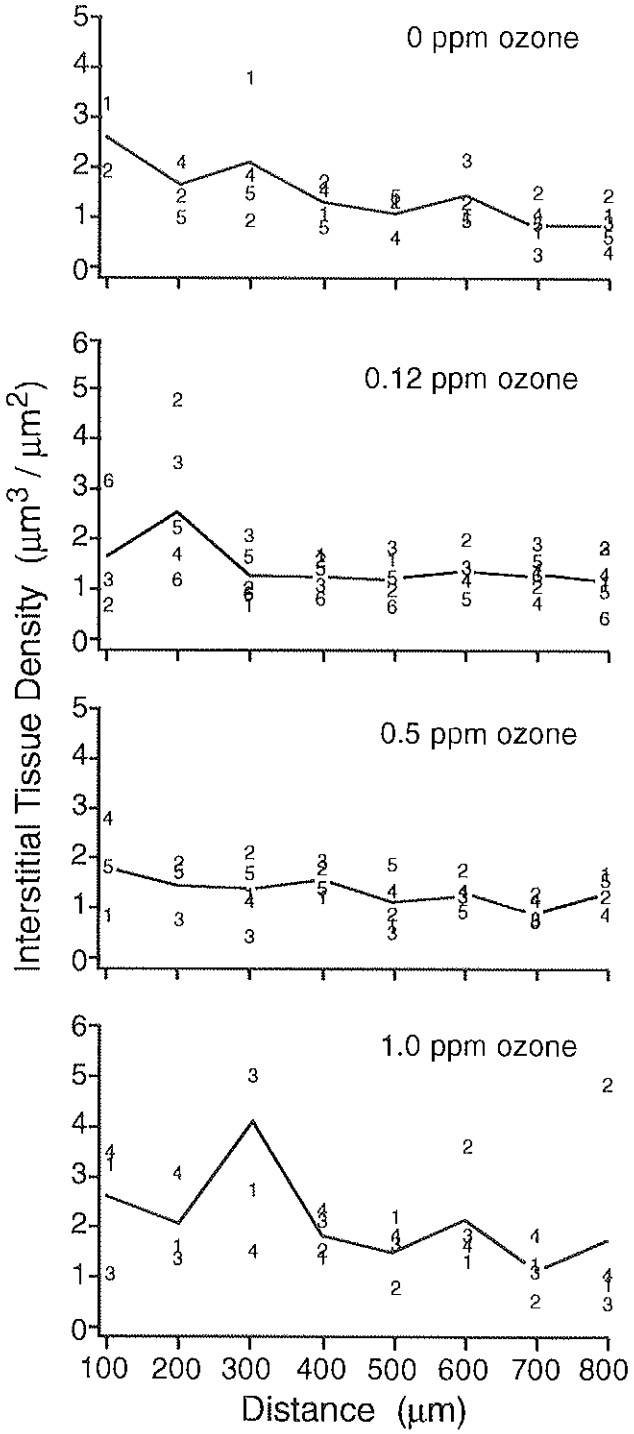

Figure A.4. Interstitial tissue volume density (expressed as a function of distance in ventilatory units) of the caudal region in female rats exposed to 0.0, 0.12, 0.5, or 1.0 ppm ozone.

Table A.5. Epithelial Tissue Volume Density for Male Rats[a]

Ozone Concentration (ppm)	Distance Down Alveolar Duct (μm)							
	100	200	300	400	500	600	700	800
0.0	3.346 ± 2.284	1.389 ± 0.869	0.357 ± 0.272	0.28 ± 0.307	0.236 ± 0.101	0.186 ± 0.036	0.159 ± 0.080	0.144 ± 0.110
0.12	2.635 ± 0.426	2.111 ± 0.762	1.011 ± 0.275	0.51 ± 0.149	0.273 ± 0.091	0.252 ± 0.163	0.285 ± 0.209	0.292 ± 0.136
0.5	3.802 ± 1.074	3.047 ± 0.185	1.639 ± 0.610	0.829 ± 0.464	0.515 ± 0.194	0.168 ± 0.094	0.184 ± 0.188	0.219 ± 0.128
1.0	4.664 ± 2.024	2.485 ± 0.870	3.754 ± 2.824	2.528 ± 1.558	1.57 ± 1.248	1.328 ± 1.238	0.505 ± 0.556	0.237 ± 0.101

[a] Values reflect combined data for the cranial and caudal regions and are given as means ± SDs expressed in $\mu m^3/\mu m^2$.

Table A.6. Interstitial Tissue Volume Density for Male Rats[a]

Ozone Concentration (ppm)	Distance Down Alveolar Duct (μm)							
	100	200	300	400	500	600	700	800
0.0	2.35 ± 1.044	1.637 ± 0.471	1.462 ± 0.286	1.6 ± 0.139	1.365 ± 0.440	1.691 ± 0.362	1.541 ± 0.165	1.853 ± 0.627
0.12	1.693 ± 0.364	1.962 ± 0.276	1.764 ± 0.468	1.828 ± 0.212	1.441 ± 0.373	1.74 ± 0.270	1.899 ± 0.644	1.541 ± 0.463
0.5	1.914 ± 1.408	2.207 ± 0.26	2.148 ± 0.886	2.024 ± 0.178	1.844 ± 0.154	1.811 ± 0.230	1.452 ± 0.376	1.734 ± 0.688
1.0	2.134 ± 0.493	2.371 ± 0.679	2.238 ± 0.657	2.242 ± 0.622	2.696 ± 0.412	2.478 ± 0.494	1.912 ± 0.829	1.588 ± 0.983

[a] Values reflect combined data for the cranial and caudal regions and are given as means ± SDs expressed in $\mu m^3/\mu m^2$.

Table A.7. Capillary Volume Density for Male Rats[a]

Ozone Concentration (ppm)	Distance Down Alveolar Duct (μm)							
	100	200	300	400	500	600	700	800
0.0	1.915 ± 0.883	2.056 ± 0.447	1.813 ± 0.241	1.846 ± 0.477	1.765 ± 0.103	1.783 ± 0.423	1.81 ± 0.326	2.124 ± 0.741
0.12	1.713 ± 0.474	1.485 ± 0.489	2.143 ± 0.587	2.119 ± 0.392	2.025 ± 0.311	2.124 ± 0.432	2.546 ± 0.861	2.515 ± 1.203
0.5	1.199 ± 0.640	1.526 ± 0.593	1.763 ± 0.573	2.045 ± 0.899	2.299 ± 0.481	2.289 ± 0.456	2.132 ± 0.626	2.307 ± 0.713
1.0	0.713 ± 0.276	1.227 ± .0314	1.261 ± 0.401	1.116 ± 0.532	1.73 ± 0.502	1.952 ± 0.961	1.653 ± 0.248	1.629 ± 0.302

[a] Values reflect combined data for the cranial and caudal regions and are given as means ± SDs expressed in $\mu m^3/\mu m^2$.

Table A.8. Alveolar Macrophage Volume Density for Male Rats[a]

Ozone Concentration (ppm)	Distance Down Alveolar Duct (μm)							
	100	200	300	400	500	600	700	800
0.0	0.075 ± 0.150	0.035 ± 0.052	0.025 ± 0.036	0.018 ± 0.022	0.037 ± 0.043	0.058 ± 0.053	0.02 ± 0.04	0.02 ± 0.04
0.12	0	0.055 ± 0.063	0.051 ± 0.058	0.086 ± 0.041	0.105 ± 0.152	0.024 ± 0.048	0.01 ± 0.02	0.053 ± 0.063
0.5	0.129 ± 0.170	0.118 ± 0.090	0.099 ± 0.102	0.066 ± 0.057	0.168 ± 0.109	0.07 ± 0.106	0.026 ± 0.052	0.029 ± 0.058
1.0	0.148 ± 0.172	0.125 ± 0.171	0.267 ± 0.171	0.379 ± 0.405	0.074 ± 0.063	0.113 ± 0.172	0.028 ± 0.056	0.061 ± 0.089

[a] Values reflect combined data for the cranial and caudal regions and are given as means ± SDs expressed in $\mu m^3/\mu m^2$.

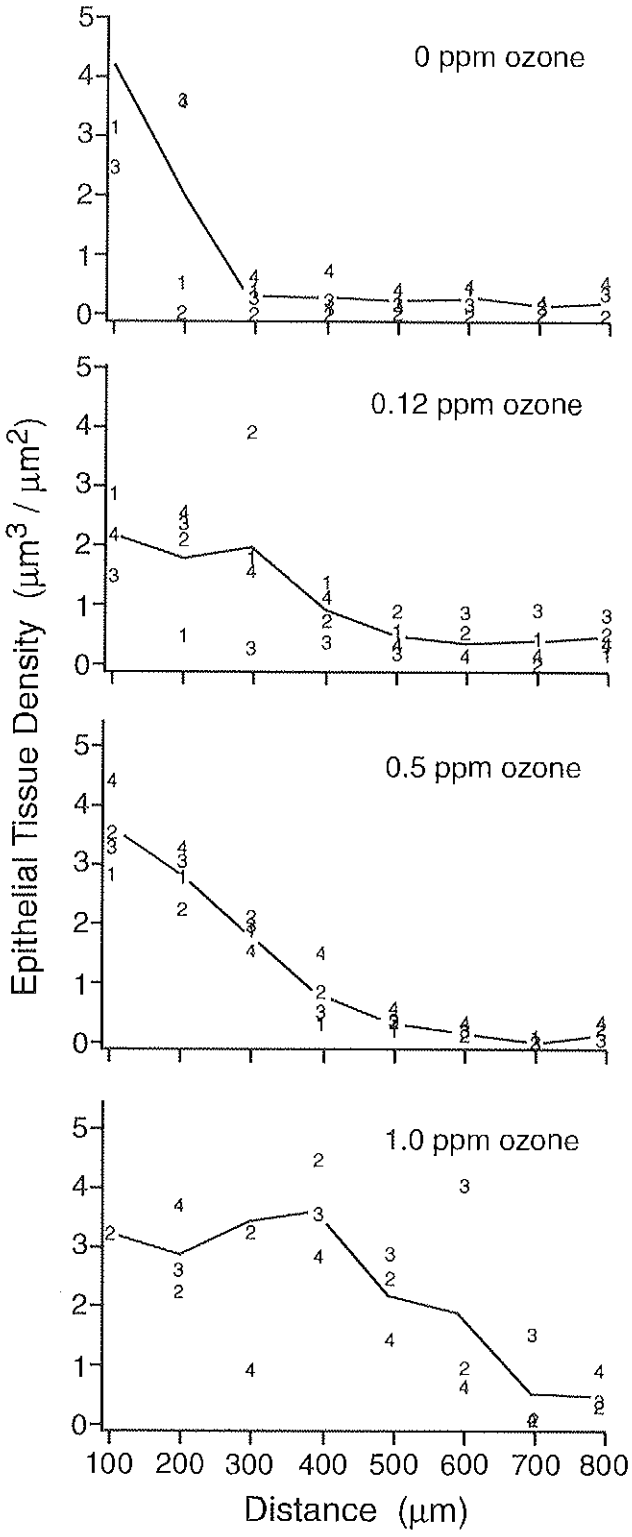

Figure A.5. Epithelial tissue volume density (expressed as a function of distance in ventilatory units) of the cranial region in male rats exposed to 0.0, 0.12, 0.5, or 1.0 ppm ozone.

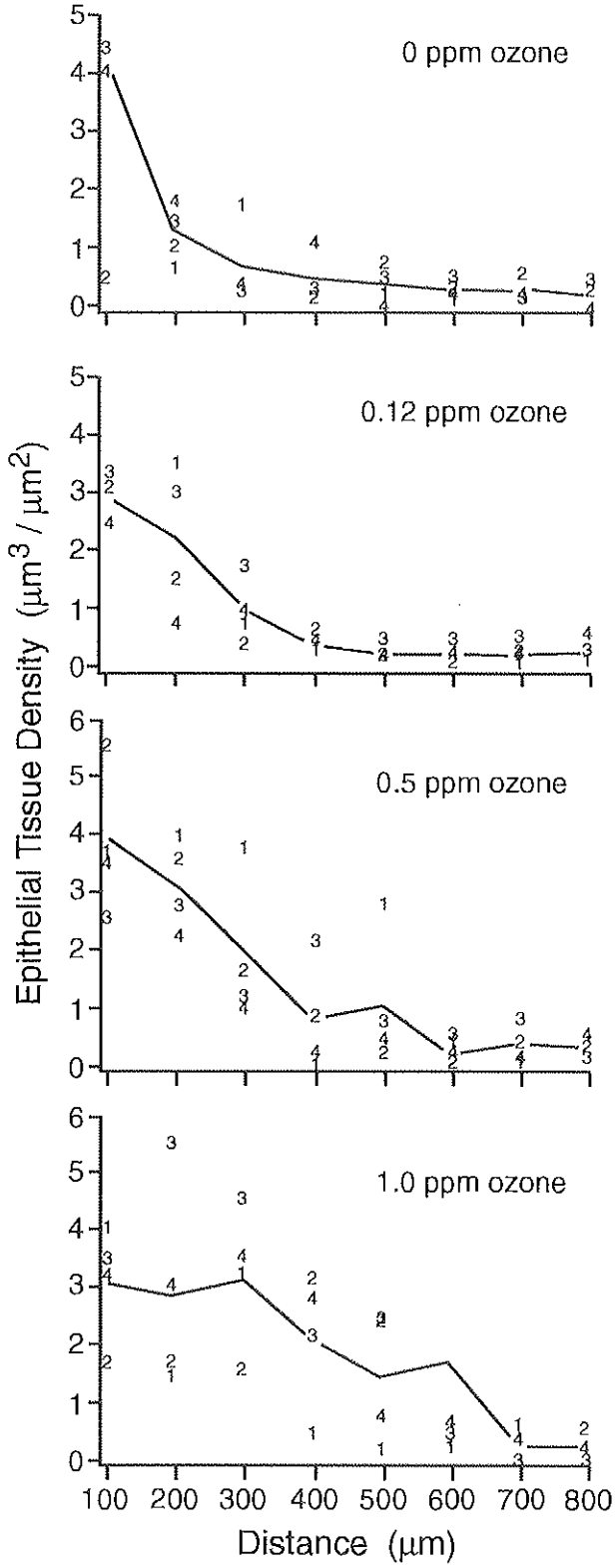

Figure A.6. Epithelial tissue volume density (expressed as a function of distance in ventilatory units) of the caudal region in male rats exposed to 0.0, 0.12, 0.5, or 1.0 ppm ozone.

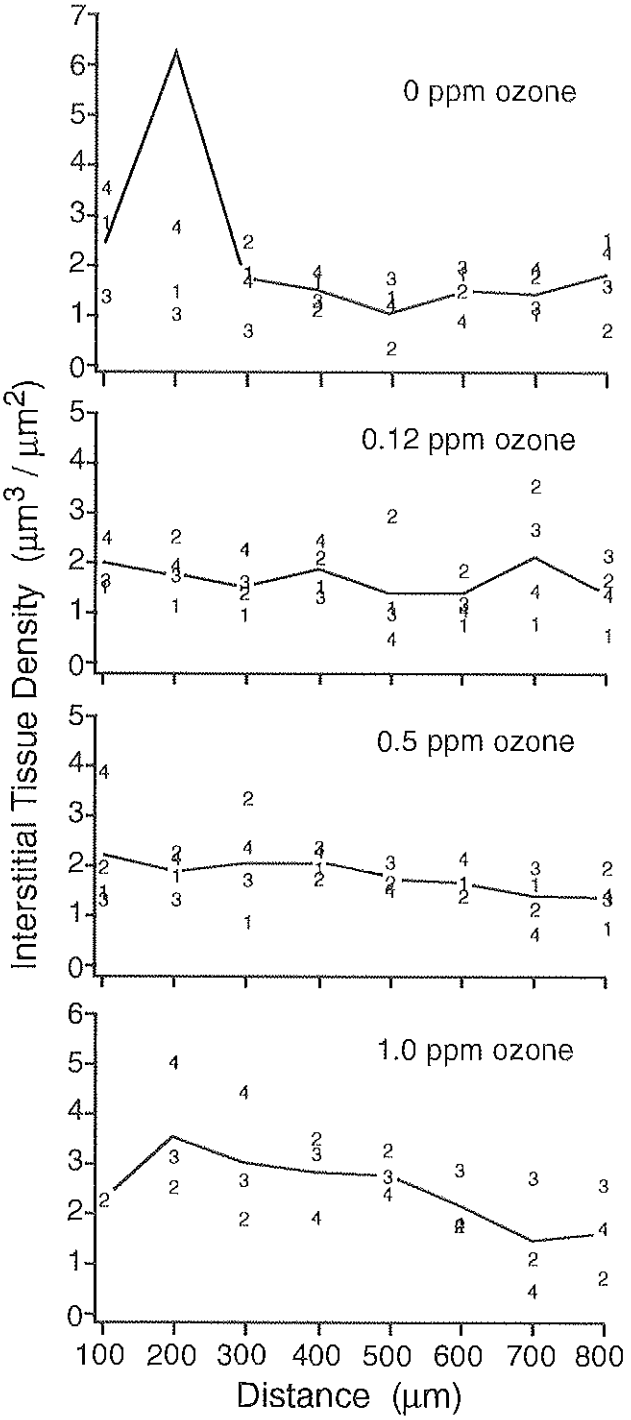

Figure A.7. Interstitial tissue volume density (expressed as a function of distance in ventilatory units) of the cranial region in male rats exposed to 0.0, 0.12, 0.5, or 1.0 ppm ozone.

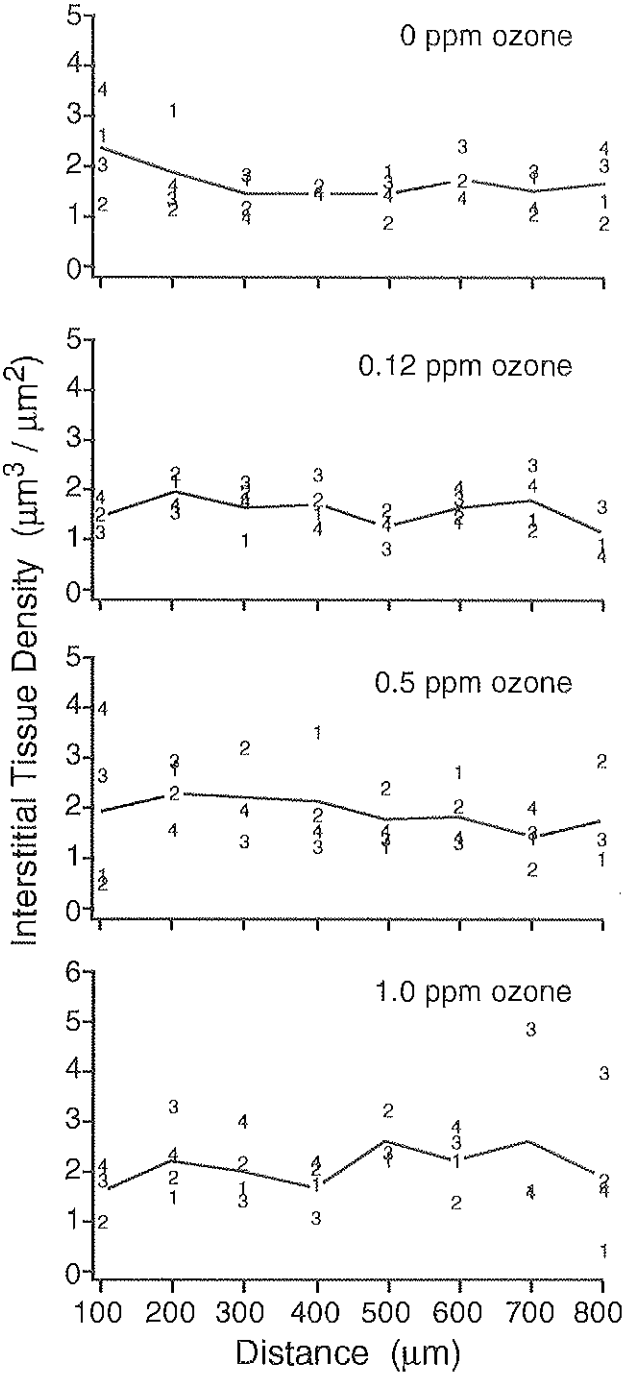

Figure A.8. Interstitial tissue volume density (expressed as a function of distance in ventilatory units) of the caudal region in male rats exposed to 0.0, 0.12, 0.5, or 1.0 ppm ozone.

Table A.9. Distance of Bronchiolar Epithelium Down Alveolar Ducts for Female Rats[a]

Ozone Concentration (ppm)	Cranial Region	Caudal Region	Combined
Ciliated Cells			
0.0	89 ± 32	123 ± 61	106 ± 34
0.12	104 ± 24	282 ± 66	193 ± 43
0.5	223 ± 18	207 ± 44	215 ± 23
1.0	409 ± 26	466 ± 48	437 ± 28
Clara Cells			
0.0	93 ± 36	131 ± 64	112 ± 35
0.12	115 ± 29	284 ± 57	120 ± 40
0.5	214 ± 19	207 ± 40	210 ± 21
1.0	401 ± 45	450 ± 43	426 ± 30

[a] Values are means ± SDs expressed in μm.

Table A.10. Distance of Bronchiolar Epithelium Down Alveolar Ducts for Male Rats[a]

Ozone Concentration (ppm)	Cranial Region	Caudal Region	Combined
Ciliated Cells			
0.0	123 ± 83	82 ± 52	102 ± 67
0.12	200 ± 58	205 ± 76	203 ± 64
0.5	256 ± 29	273 ± 29	265 ± 28
1.0	580 ± 88[b]	410 ± 60	461 ± 43
Clara Cells			
0.0	140 ± 78	91 ± 39	115 ± 63
0.12	207 ± 53	195 ± 69	200 ± 59
0.5	278 ± 31	268 ± 40	273 ± 34
1.0	605 ± 77[b]	410 ± 60	469 ± 45

[a] Values are means ± SDs given in μm.

[b] $p < 0.05$ when compared with caudal ventilatory unit isolations.

Table A.11. Estimated Parameters of Linear Segment Model Used to Describe Epithelial Density[a]

Ozone Concentration (ppm)	n	$a1$ ($\mu m^3/\mu m^2$)	$x1$ (μm)	$b2$ ($[\mu m^3/\mu m^2]/100$ μm)	$x2$ (μm)	$a3$ ($\mu m^3/\mu m^2$)
Cranial Region, Female						
0.0	3	2.1 ± 0.1	128 ± 40	−1.7 ± 0.3	243 ± 61	0.21 ± 0.07
0.12	4	2.2 ± 0.3	90 ± 24	−2.0 ± 0.0	185 ± 25	0.27 ± 0.07
0.5	5	2.4 ± 0.3	196 ± 36	−1.5 ± 0.1	344 ± 31	0.17 ± 0.07
1.0	2	3.0 ± 0.0	388 ± 122	−1.8 ± 0.8	563 ± 40	0.51 ± 0.05
Cranial Region, Male						
0.0	3	4.4 ± 1.4	138 ± 40	−3.0 ± 0.3	271 ± 30	0.24 ± 0.06
0.12	3	2.4 ± 0.3	180 ± 31	−1.1 ± 0.5	476 ± 94	0.29 ± 0.12
0.5	4	3.2 ± 0.4	204 ± 40	−1.3 ± 0.4	441 ± 15	0.18 ± 0.03
1.0	2	3.9 ± 0.5	405 ± 46	−1.2 ± 0.4	774 ± 134	0.10 ± 0.10
Caudal Region, Female						
0.0	2	2.7 ± 0.7	184 ± 33	−1.6 ± 0.4	371 ± 136	0.23 ± 0.06
0.12	2	2.5 ± 0.5	194 ± 6	−1.6 ± 0.5	376 ± 89	0.15 ± 0.11
0.5	4	2.2 ± 0.3	176 ± 19	−1.8 ± 0.4	310 ± 29	0.25 ± 0.04
1.0	2	3.1 ± 0.1	140 ± 59	−0.5 ± 0.0	691 ± 58	0.21 ± 0.01
Caudal Region, Male						
0.0	4	2.6 ± 0.6	118 ± 28	−2.2 ± 0.3	219 ± 33	0.28 ± 0.05
0.12	4	3.2 ± 0.1	146 ± 35	−1.9 ± 0.3	305 ± 38	0.29 ± 0.06
0.5	4	3.7 ± 0.7	125 ± 41	−1.0 ± 0.3	502 ± 69	0.28 ± 0.07
1.0	2	3.7 ± 0.3	198 ± 130	−1.0 ± 0.1	543 ± 66	0.22 ± 0.01

[a] Values are means ± SEs.

APPENDIX B. Identification of Specific Animals in Exposure Groups

Table B.1. Specific Animals Studied

Ozone Exposure (ppm)	Gender	Identification Numbers for Specific Animals
Conducting Airway Secretory Prodnct and Cell Population		
0.0	M	H37, H45[a], H117[a], H125
	F	H41, H49, H121, H129[a]
0.12	M	H38, H46[a], H118, H126
	F	H42, H50, H122, H130
0.5	M	H39, H47, H119, H127
	F	H43, H51, H123, H131[a]
1.0	M	H40, H48, H120, H128
	F	H44, H52, H124, H132
Epithelial Thickness		
Cranial Region		
0.0	M	H37, H117[a], H125
	F	H41, H57, H121
0.12	M	H38, H118, H126
	F	H42, H66, H122, H130
0.5	M	H39, H47, H119, H127[a]
	F	H43, H51, H67, H123, H131[a]
1.0	M	H48, H120
	F	H52, H132
Caudal Region		
0.0	M	H37, H45[a], H117[a], H125
	F	H41, H49
0.12	M	H38, H46[a], H118, H126
	F	H50, H122
0.5	M	H39, H47, H119, H127
	F	H43, H51, H123, H131[a]
1.0	M	H40, H128
	F	H44, H132
Ventilatory Unit Analyses Except Epithelial Thickness		
0.0	M	H37, H45[a], H117[a], H125
	F	H41, H49, H57, H65, H121
0.12	M	H38, H46[a], H118, H126
	F	H42, H50, H58, H66, H122, H130
0.5	M	H39, H47, H119, H127
	F	H43, H51, H67, H123, H131[a]
1.0	M	H40, H48, H120, H128
	F	H44, H52, H124, H132
Biochemistry: Antioxidant Enzyme Activity		
0.0	M	H1, H69, H149
	F	H25, H89, H113
0.5	M	H2, H23, H71
	F	H26, H91, H115
1.0	M	H3, H24, H72
	F	H27, H92, H116

[a] These animals were identified by the pathologist at Battelle Pacific Northwest Laboratories as having advanced leukemia involving the spleen and liver. The data were analyzed both including and excluding these animals. Only the results from the analyses including all rats are presented in the text. (For further explanation, see the Results, Effects of Leukemia section under Tracheobronchial Epithelium.)

ABOUT THE AUTHORS

Kent E. Piukertou, Ph.D., is an Associate Professor in Residence in the Department of Anatomy, Physiology, and Cell Biology in the School of Veterinary Medicine, University of California at Davis. He completed his undergraduate education at Brigham Young University in 1974 and received the M.S. and Ph.D. degrees in pathology from Duke University in 1978 and 1982, respectively. His primary research interests are in respiratory cell biology and environmental air pollutants.

Margaret G. Ménache, M.S., is a biostatistician at the Center for Extrapolation Modeling, Duke University Medical Center, Durham, NC. She completed her undergraduate education at Georgetown University in 1975 and her M.S. degree in hiostatistics at the University of North Carolina, Chapel Hill, in 1991. She is currently pursuing a Ph.D. degree in the School of the Environment at Duke University. Her primary research interests are biostatistical analysis and comparative modeling of the deposition of gases and particles in the respiratory tract of mammalian species.

Charles G. Plopper, Ph.D., is a Professor in the Department of Anatomy, Physiology, and Cell Biology in the School of Veterinary Medicine at the University of California at Davis, where he completed his undergraduate education in 1967 and his Ph.D. degree in anatomy in 1972. His primary research interests are in respiratory cell biology and environmental air pollutants.

PUBLICATIONS RESULTING FROM THIS RESEARCH

Pinkerton KE, Dodge DE, Cederdahl-Demmler J, Wong VJ, Peake J, Haselton CJ, Mellick PW, Singh G, Plopper CG. 1993. Differentiated bronchiolar epithelium in alveolar ducts of rats exposed to ozone for 20 months. Am J Pathol 142:947–956.

Dodge DE, Rucker RB, Pinkerton KE, Haselton CJ, Plopper CG. 1994. Dose-dependent tolerance to ozone: III. Elevation of intracellular Clara cell 10 kDa protein in central acini of rats exposed for 20 months. Toxicol Appl Pharmacol 127:109–123.

Plopper CG, Chu F, Haselton CJ, Peake J, Wu J, Pinkerton KE. 1994. Dose-dependent tolerance to ozone: I. Tracheobronchial epithelial reorganization in rats after 20 months exposure. Am J Pathol 144:404–421.

Plopper CG, Duan X, Buckpitt AR, Pinkerton KE. 1994. Dose-dependent tolerance to ozone: IV. Site-specific elevation in antioxidant enzymes in the lungs of rats exposed for 90 days or 20 months. Toxicol Appl Pharmacol 127:124–131.

ABBREVIATIONS

AB/PAS	Alcian blue/periodic acid–Schiff
ANOVA	analysis of variance
BADJ	bronchiole–alveolar duct junction
CDNB	1-chloro-2,4-dinitrobenzene
DAPI	4′-6-diamidino-2-phenylindole
DETAPAC	diethylenetriamine-pentaacetic acid
GPx	glutathione peroxidase
GST	glutathione S–transferase
I_O	number of intercepts with the object
L_r	total length of test line in the reference volume
MANOVA	multivariate analysis of variance
mOsm	milliosmolal
MSE	mean square error
NADPH	nicotinamide adenine dinucleotide phosphate
NBT	nitroblue tetrazolium
NTP	National Toxicology Program
PBS	phosphate-buffered saline
P_p	point fraction (P_n/P_t)
P_n	number of test points
ppm	parts per million
P_t	total points
SOD	superoxide dismutase
S_v	surface area per reference volume
V_v	volume fraction

INTRODUCTION

Ozone has been known as a powerful lung irritant since the mid-nineteenth century (reviewed by Bates 1989). However, only in recent decades have the potential health effects of exposure to atmospheric oxidants been systematically measured (reviewed by the U.S. Environmental Protection Agency 1986, 1988, 1993; Lippmann 1989, 1992, 1993). In exercising children and young adults, exposure to elevated levels of ozone for relatively short time periods can cause a transient reduction in lung function and the appearance of markers of inflammation in bronchoalveolar lavage fluid from the lungs (Spektor et al. 1988; Lippmann 1989). Whether repeated inhalation of ozone produces long-term effects on lung function, potentially contributing to or aggravating chronic lung disease, is unknown.

In light of widespread exposure to ozone and the great uncertainty regarding the possible health risks of prolonged exposure to this pollutant, the Health Effects Institute and the National Toxicology Program (NTP)* undertook the NTP/HEI Collaborative Ozone Project (described in the Introduction to this Research Report) to evaluate the effects of prolonged exposure to low, medium, and high concentrations of ozone on laboratory animals. In February 1990, HEI solicited proposals for studies by issuing Request for Applications 90-1 on the "Health Effects of Chronic Ozone Inhalation: NTP/HEI Studies, Part B, Structural, Biochemical, and Other Alterations." The proposals submitted in response to this RFA were reviewed by an ad hoc review panel for their scientific merit and by the HEI Research Committee for their contribution to a well-balanced collaborative study.

The Health Effects Institute funded several related studies that evaluated the biochemical, structural, and functional changes in the respiratory tracts of rats caused by prolonged ozone exposure. The two Reports analyzing rat lung structural alterations and antioxidant enzyme activities discussed in this Commentary constitute the pulmonary morphometric component of this multiple-investigator project. The Integrative Summary (Part XI of Research Report Number 65) summarizes the major findings of the eight studies and the statistical analysis in the NTP/HEI Collaborative Ozone Project, and discusses their implications for human health.

The Health Effects Institute funded two investigator groups to conduct detailed analyses of the effects of ozone on the structure of the respiratory tract. Dr. Ling-Yi Chang and her colleagues at Duke University submitted a proposal entitled "Morphometric Analysis of Structural Alterations in Rat Lungs Chronically Exposed to Ozone." The proposed experiments were designed to measure the effects on lung structure dependent on ozone concentration in F344/N rats. Their two-year project began in June 1991 and had total expenditures of $377,744. The Investigators' Report was received for review at HEI in December 1993. A revised report was received in July 1994 and was accepted by the Health Review Committee at that time. Drs. Kent Pinkerton and Charles Plopper of the University of California at Davis submitted a proposal entitled "Health Effects of Chronic Ozone Inhalation." The proposed experiments were designed to measure the ozone concentration–dependent effects on rat lung structure and antioxidant enzyme activities in F344/N rats. Their two-year project, which began in June 1991, had total expenditures of $477,850. The Investigators' Report was received for review at HEI in February 1994. The revised report was accepted by the Health Review Committee in January 1995.

These two structural studies, both discussed in this commentary, were complementary. Dr. Chang and colleagues performed a detailed morphometric analysis of the proximal alveolar region at the electron-microscopic level. Dr. Pinkerton and associates measured changes in airway, bronchiolar, and ductal structure at the light-microscopic level. These investigators correlated the changes in ductal structure with the distance down the alveolar duct from the bronchiole–alveolar duct junction. They also measured antioxidant enzyme activity levels in tissue subcompartments of the lungs.

During the review process, the Review Committee and the investigators had the opportunity to exchange comments and to clarify issues in the Investigators' Reports and in the Review Committee's Commentary. The following Commentary is intended to aid the sponsors of HEI and the public by highlighting both the strengths and limitations of the studies and by placing the Investigators' Reports into scientific and regulatory perspective.

REGULATORY BACKGROUND

The U.S. Environmental Protection Agency (EPA) sets standards for oxidants (and other pollutants) under Section 202 of the Clean Air Act, as amended in 1990. Section 202 (a)(1) directs the Administrator to "prescribe (and from time to time revise) . . . standards applicable to the emission of any air pollutant from any class or classes of new motor vehicles or new motor vehicle engines, which in his judgment cause, or contribute to, air pollution which may reason-

* Lists of abbreviations appear at the ends of the Investigators' Reports for your reference.

ably be anticipated to endanger public health or welfare." Sections 202(a), (b)(1), (g), and (h) and Sections 207(c)(4), (5), and (6) impose specific requirements for reduction in motor vehicle emissions of certain oxidants (and other pollutants) and, in some cases, give EPA limited discretion to modify those requirements.

Section 109 of the Clean Air Act provides for the establishment of National Ambient Air Quality Standards (NAAQS) to protect the public health. The current NAAQS for ozone is 0.12 parts per million (ppm). This standard is exceeded when more than one day per year has a maximum hourly average concentration of ozone above 0.12 ppm. Section 181 of the Act classifies the nonattainment areas according to the degree that they exceed the NAAQS and assigns a standard attainment date for each classification. Section 109 of the Clean Air Act also requires periodic review and, if appropriate, revision of the NAAQS and of the air quality criteria on which they are based.

The EPA completed its last formal review of the air quality criteria for ozone in 1989. Based on that review, it announced a final decision on March 9, 1993, not to revise the existing ozone NAAQS. However, since early 1989, a substantial number of new studies on the health and environmental effects of ozone have appeared in the peer-reviewed literature. As a result of these findings, on February 3, 1994, the EPA announced its intention to undertake an accelerated review of the Air Quality Criteria for Ozone and Other Photochemical Oxidants. The EPA will complete its review of the NAAQS for ozone as soon as possible, consistent with ensuring a sound, scientifically supportable decision concerning any revision of the standard.

The current ozone standard relies heavily on data from controlled studies that have demonstrated lung dysfunction after short-term exposures of humans to ozone at concentrations similar to those found in polluted nrban air. These studies did not address the issue of potential chronic health effects, such as degenerative lung diseases, that might result from long-term ozone exposures. Because the determination of appropriate standards for emissions of oxidants and their precursors depends, in part, on assessing the risks to health that they present, research into the health effects of prolonged exposure of the lung to ozone, such as that described in these Reports, forms the basis of and is essential to the informed regulatory decision-making required by the Clean Air Act.

SCIENTIFIC BACKGROUND

Ozone is a major pollutant in photochemical smog. It is formed by complex photochemical reactions between nitrogen oxides and volatile organic compounds in the presence of sunlight. Motor vehicle and industrial emissions are prominent sources of these compounds (U.S. Environmental Protection Agency 1991b). Peak atmospheric ozone concentrations generally occur during the summer because the photochemical reactions that produce ozone are enhanced by sunlight and high temperature. Exposure to ozone is a major health concern because it is a highly reactive gas that, at sufficiently high concentrations, can injure cells and tissues (U.S. Environmental Protection Agency 1986, 1991b).

Tbe current NAAQS for ozone is 0.12 ppm, a level that is not to be exceeded for more than one hour once a year (U.S. Environmental Protection Agency 1986). This standard is based largely on the results of short-term exposure studies with human subjects. In 1990, daily one-hour maximum ozone levels ranged from 0.06 ppm in less polluted areas of the United States to 0.3 ppm or higher during summer in the Los Angeles hasin (U.S. Environmental Protection Agency 1991a). Peak ozone concentrations of 0.1 ppm and higher, lasting for 8 to 12 hours, have been reported in both the United States and the Netherlands. This exposure pattern can continue for several days during a summer air pollution episode (Rombout et al. 1986; Van Bree et al. 1990). In a 1992 survey, more than 50 million U.S. residents, or 25% of the population, lived in areas where the ozone standard was exceeded (U.S. Environmental Protection Agency 1993).

The overall objective of the NTP/HEI Collaborative Ozone Project was to obtain information that could aid in determining whether prolonged inhalation of ozone produces lasting changes in respiratory tract structure, biochemistry, or function, potentially contributing to or aggravating chronic lung disease. In the studies presented in this Research Report, Drs. Chang and Pinkerton and their colleagues tested the hypothesis that prolonged exposure to ozone affects the microscopic structure and antioxidant enzyme activities in F344/N rat lungs. This work was undertaken to carefully document any lung structural changes and to correlate those changes with the functional and biochemical effects that may be observed in the companion NTP/HEI studies.

The following sections of this scientific background present a brief overview of lung airway structures and review what is known about the effects of ozone on the form and structure of the airways, emphasizing studies of prolonged ozone exposure. The effect of ozone exposure on antioxidant enzyme activities in lung tissue is discussed as well.

AIRWAY STRUCTURE

The lung is a densely branched, tree-like organ in structure. The trachea divides into two major bronchi, which, in

turn, bifurcate repeatedly into smaller and smaller minor bronchi. These ultimately divide into bronchioles. Finally, bronchioles merge into the gas-exchange region of the lung, which contains grape-like clusters of alveoli with minute airspaces that are lined by thin membranes.

The trachea extends from the larynx to the midthorax, where it divides into the left and right primary bronchi. It is partially surrounded by a regular sequence of hyaline cartilage plates interconnected by annular ligaments. Cartilage gaps are bridged by the smooth muscle fibers of the trachealis muscle. The trachea also contains submucosal glands.

The bronchi are the large airways distal to the trachea. Their walls also contain cartilaginous plates, submucosal glands, and smooth muscle. They are lined with ciliated pseudostratified columnar epithelium. The cellular composition of bronchi varies with airway generation and among species.

Bronchioles are continuations of the bronchi; they lack cartilage and submucosal glands, but have a prominent smooth muscle component. Their epithelial lining consists of ciliated and secretory cells that vary from columnar to cuboidal. The terminal bronchioles are the most distal generation of conductive airways. They contain alveolar outpocketings in their walls that are lined with squamous (type I) and cuboidal (type II) epithelial cells (Mariassy 1992).

The centriacinar region is the anatomical site that is the junction of the conducting airways and the gas-exchange region of the lung. It consists of the lung structures supplied by a terminal bronchiole, including respiratory bronchioles when present, the first generation of alveolar ducts, and the alveoli supplied by the terminal bronchiole (Weibel 1963; Weibel 1983; Haefeli-Bleurer and Weibel 1988).

Species differ significantly in the basic structure of the centriacinar region and its epithelial cell lining (Tyler 1983; Plopper 1983; Tyler and Julian 1991). In the centriacinar region of humans, other primates, dogs, cats, and a few other domesticated species, the terminal bronchiole gives rise to several generations of respiratory bronchioles with alveoli that open directly into their lumina and alveolar ducts that branch directly from them. In contrast, the lungs of many other mammals, including those most commonly used for inhalation toxicology such as rats, the respiratory bronchioles are absent or poorly developed and the terminal bronchioles open directly into alveolar ducts.

EFFECTS OF OZONE EXPOSURE ON AIRWAY STRUCTURE

Studies most relevant to evaluating the contribution of ozone to lung disease are those conducted with humans. Field studies and controlled chamber studies provide information only on acute respiratory effects. In general, the results of epidemiologic studies, which entail the evaluation of longer exposures, are complicated by the effects of confounding variables. Also, lung tissue is not available for histologic and biochemical study from human subjects. At present, studies in laboratory animals are still the best source of information on the effects of prolonged exposure to ozone on the respiratory system.

Tracheobronchial Airways

In the trachea, epithelial ciliary cells and cilia were damaged in rats exposed to 0.96 ppm ozone for 60 days (Nikula et al. 1988), and in bonnet monkeys exposed to 0.15 or 0.3 ppm ozone for 90 days (Dimitriadis 1993). In a preliminary report of their study, Dr. Pinkerton and colleagues (Plopper et al. 1993) discussed a dose-dependent decrease in material positively stained with Alcian blue/periodic acid–Schiff in the tracheas of rats exposed to 0.12, 0.5, or 1.0 ppm ozone for six hours per day, five days per week, for 20 months. No differences were found in epithelial cell thickness or cell populations. In addition, this stainable material increased in the caudal bronchi, but not in the cranial or central bronchi.

Centriacinar Region of the Lungs

The region at the junction of the conducting airways and gas-exchange regions of the lungs, called the centriacinar region, has long been recognized to be particularly sensitive to ozone. In fact, the primary site of tissue damage found in animals exposed to ozone is at the acinar entrance (Stephens et al. 1974; Mellick et al. 1977). Interestingly, the highest tissue dose of ozone predicted by mathematical models is in this region (Miller et al. 1985; Overton and Graham 1989; Grotberg et al. 1990).

Boorman and coworkers (1980) were among the first to conduct a thorough morphometric evaluation of the effects of prolonged ozone exposure on the centriacinar region of rats exposed to ozone for up to 90 days. Transmission electron microscopy showed that the air-blood barrier thickened in rats exposed to 0.8 ppm ozone for 20 or 90 days. Also, the relative volume of the lung interstitium (the tissue in alveolar walls) increased, and was characterized by prominent bundles of collagen and increased numbers of fibroblasts.

Exposure to 0.5 or 0.8 ppm ozone also caused respiratory bronchiole segments to form between the terminal bronchioles and the alveolar ducts. Macrophages accumulated in the centriacinar region at these ozone exposure levels. Centriacinar lesions diminished as exposure progressed. However, significant morphologic alterations still persisted

at the end of the 90-day exposure. Other studies using subchronic exposure protocols have reported epithelial thickening and inflammation in the centriacinar region of rats exposed to low levels of ozone (Crapo et al. 1984; Barry et al. 1985).

Chang and colleagues (1992) exposed male F344/N rats to a continuous ozone background level of 0.06 ppm for 22 hours per day, seven days per week. In order to simulate an urban exposure pattern, a nine-hour "ramped spike" (maximum ozone concentration of 0.25 ppm, with an integrated concentration over time of 0.19 ppm) was superimposed on this background for five consecutive days per week for up to 78 weeks. Overall, the responses seen were biphasic, with acute tissue reactions being evident after one week of exposure, then subsiding after three weeks of exposure, and finally increasing progressively with prolonged ozone exposure. In the terminal bronchioles, prolonged exposure to ozone caused structural changes indicative of injury to both ciliated and Clara cells. In the proximal alveolar region, progressive epithelial and interstitial tissue lesions developed during prolonged ozone exposures. These included epithelial hyperplasia, fibroblast proliferation, and the accumulation of interstitial matrix. The content of basement membrane and collagen fibers increased. Most of the interstitial matrix that accumulated during ozone exposure returned to normal levels during recovery in clean air. However, the thickened basement membranes remained. Most other parameters returned to normal during the 17-week recovery period in clean air.

Ozone-induced damage to the centriacinar region has also been studied in primates. Fujinaka and coworkers (1985) reported that the volume of respiratory bronchioles increased and the diameter of the respiratory bronchiolar lumen decreased in bonnet monkeys exposed to 0.64 ppm ozone eight hours per day for one year. The increased volume of respiratory bronchioles is a condition that has been termed respiratory bronchiolitis. Tyler and colleagues (1988) also reported respiratory bronchiolitis in male monkeys exposed to either a daily or "seasonal" regimen of 0.25 ppm ozone for eight hours per day. This seasonal regimen consisted of ozone exposure on alternate months for 18 months.

Bronchiolarization. Bronchiolarization is a process that results in the remodeling of centriacinar airways, and is characterized by an extension of bronchiolar epithelium into the alveolar duct and the formation of respiratory bronchioles in species that normally do not have these structures. New respiratory bronchioles are identified by either scanning electron or light microscopy in lungs from species in which respiratory bronchioles are normally absent or poorly developed (Boorman et al. 1980; Moore and Schwartz 1981). In animal species whose lungs normally have well-developed respiratory bronchioles, the extent of remodeling can be estimated using light-microscopic morphometry (Fujinaka et al. 1985).

Inflammatory Response. The epithelial changes described above may be accompanied by an inflammatory response in the centriacinar region characterized by increased numbers of polymorphonuclear leukocytes in early stages, by increased numbers of alveolar macrophages in lumina and tissues during later stages, by interstitial edema, and by a fibrinous exudate (Stephens et al. 1974; Schwartz et al. 1976; Boorman et al. 1980; Castleman et al. 1980; Fujinaka et al. 1985). As exposure continues, alveolar septae in the centriacinar region thicken owing to an increase in extracellular matrix material, which includes collagen deposition, increased cell numbers due to infiltration of other cells, and hyperplasia of the alveolar epithelium (Boorman et al. 1980; Barry et al. 1983; Crapo et al. 1984; Fujinaka et al. 1985). The inflammatory response seen in rats exposed to 0.5 ppm ozone for 6 or 12 months disappeared after a 6-month recovery period in clean air (Gross and White 1987).

EFFECTS OF OZONE EXPOSURE ON ANTIOXIDANT ENZYME ACTIVITY

One way that ozone damages cells is by its oxidizing activity, which alters cell membranes by the formation of lipid peroxides that inactivate functional groups in proteins and other components of tissue. Ozone also indirectly causes oxidation when the ozone-induced inflammatory reaction causes inflammatory cells to produce oxidants. Protection against pathologic oxidation is provided by a group of enzymes, termed antioxidant enzymes, that inactivate the oxidants either directly or via nonenzymatic reductants such as reduced glutathione.

A number of studies have shown that antioxidant enzyme activities are elevated in lung tissue in response to short-term exposure to ozone. Within three days after short-term ozone exposure, glutathione peroxidase and glutathione reductase activities increased significantly in several species (Clark et al. 1978; Rietjens et al. 1985; Van Bree et al. 1992). In studies of two-week exposures in rats, both glutathione peroxidase and superoxide dismutase activities also increased (Heng et al. 1987; Elsayed et al. 1988; Ichinose and Sagai 1989).

However, the role that antioxidant enzymes play in protecting the reorganized respiratory system during long-term ozone exposure in rats is not completely clear. In one study (Grose et al. 1989), a 12-month exposure to ozone increased glutathione peroxidase and glutathione reductase activities but did not change superoxide dismutase activity in lung

tissue. In another study (Sagai and Ichinose 1991), a 22-month exposure to ozone did not change the activity of these enzymes or that of glutathione S–transferase. In addition to the conflicting results obtained in these long-term exposures, the potential regionality of responses of antioxidant enzyme activities to ozone exposure has not been addressed.

JUSTIFICATION FOR THE STUDIES

The primary objectives of RFA 90-1 were to support biochemical, structural, and functional studies of the respiratory system of F344/N rats to determine whether prolonged inhalation of ozone caused changes that may be related to the health effects of similar exposures in humans. The structural studies funded by HEI were designed to further characterize and elaborate the variety of cellular and extracellular matrix effects that have been found in lungs after exposures to ozone (Plopper et al. 1979; Last et al. 1983; Barry et al. 1988; Chang et al. 1992).

Both investigator groups had extensive experience with the detailed morphometric techniques used to examine and characterize changes in ultrastructure caused by experimental treatments and exposures, including air pollutants. They also have developed methods to evaluate the site-specific nature of ozone effects. In selecting these studies for funding, the HEI Research Committee thought that they would be able to provide benchmark structural data that would complement the other studies in the NTP/HEI Collaborative Ozone Project. As will be discussed below, although both studies addressed changes in airway structure, they were designed to provide complementary information with a minimum of overlap. To further correlate their findings, these two investigator groups shared tissues from the same animals.

TECHNICAL EVALUATION

OVERVIEW OF THE NTP/HEI EXPOSURE PROTOCOL

The protocol established for the NTP/HEI Collaborative Ozone Project exposed rats for six hours daily to concentrations of 0.12, 0.5, or 1.0 ppm ozone for five days per week for 20 months, with a one-week recovery period before their tissues were examined. This protocol is further described in Part VI of Research Report Number 65 (Boorman et al. 1995).

The inhalation component of this project was conducted in compliance with NTP health and safety regulations and the Food and Drug Administration (FDA) Good Laboratory Practice Regulations. Animal care and use were in accordance with the Public Health Service Policy on Humane Care and Use of Animals.

THE CHANG STUDY

Study Objectives

The overall objective of Dr. Chang's study was to conduct a morphometric analysis of the structural alterations in F344/N rat lungs caused by prolonged exposure to ozone. The specific aims were:

- to identify the lowest exposure concentration that resulted in histologic lung injury significantly different from the findings in the control group by using electron-microscopic and morphometric techniques; and
- to characterize the remodeling of interstitial connective tissue using the same morphometric techniques.

The techniques used to attain these goals were electron-microscopic measurement of tissue volumes, surface areas, and cell numbers of major alveolar tissues and cell types in proximal and randomly selected alveolar regions. The epithelial thickness and cell characteristics of the terminal bronchioles also were determined. Finally, changes in the volumes of elastin, collagen, and basement membrane in the interstitium of the proximal alveolar region were quantified.

The investigators analyzed a large number of morphometric parameters with care and precision. This study accumulated a large volume of data and amply fulfilled its goals. The data were meticulously obtained and cautiously interpreted. The methods and data analyses are thoroughly described, and the data are presented clearly. They are internally consistent and in agreement with previous research, and with the morphometric data obtained in the Pinkerton study, which used different methods to analyze tissues from the same rats.

Study Design and Methods

The study design is described in detail in the Methods section of the Investigators' Report. Briefly, the rats were anesthetized, and their lungs were fixed and remained in glutaraldehyde until processing. Once the lungs were processed for electron microscopy, a microdissection technique was used in which sequential sections were examined by light microscopy so that small airways could be followed to the bronchiole–alveolar duct junction. In this way, the investigators were able to identify specific locations, which they divided into sections for electron microscopy, thereby allowing a detailed description of the effects of ozone on lung

microstructures in specific regions. The morphometric parameters studied were the number, surface characteristics, and volume of epithelial cell types, the number of macrophages, and the volume of the interstitium and its subfractions (cells, matrix, and acellular space).

These investigators are highly experienced in the type of morphometric analyses conducted in this study, and their previous work (Chang et al. 1992) provided important background data that were used in the current analysis. The methods of tissue sampling were chosen to ensure that similar sites in the terminal airways and in the proximal alveolar region were selected in each animal.

A potential problem in the analysis of the investigators' data arose as a result of their using a method for obtaining the numerical density of cells, which has since been superseded by the work of Cruz-Orive and Weibel (1990). The method used by Chang and associates required several assumptions; specifically that the nuclei were randomly oriented, and that the ozone exposure had not changed their size, shape, or polarity. The assumption of random orientation of nuclei was checked by the investigators by assessing nuclear profiles in sections of tissue; they, found no difference in the size of nuclei in control animals compared with those in animals exposed to 1.0 ppm ozone, which verified the random orientation of the nuclei. Furthermore, the observed changes in cell number per unit area of basement membrane were found to agree with the observed changes in cell volume per unit area, indicating that cell size and shape had not changed.

Statistical Methods

This study benefitted from a sophisticated statistical analysis. In addition, the conclusions were strengthened because the investigators performed their analyses both with and without the laboratory animals that had contracted leukemia; this procedure confirmed that the inclusion of leukemic animals did not alter their results.

Dr. Chang and colleagues established five categories or types of injury and identified one or two measured parameters as the most sensitive indicators for each injury type. They analyzed their data using a multiple-stage, "step-down" approach in which a multivariate analysis of variance (MANOVA) was performed on the primary variable. If significance was found, then the investigators proceeded to test for significance with a univariate analysis of variance (ANOVA). Also, if the primary variable had a statistically significant factor, then a second MANOVA was performed on the key variables within each injury category. These latter variables provide more information concerning the injury being measured. As with the primary variables, key variables were examined with ANOVA only if the MANOVA results were significant.

Results and Interpretation

Dr. Chang's morphometric analysis focused on the regions of the airways known to be targets for damage induced by ozone, the terminal bronchioles and proximal alveolar regions. Random alveolar regions were studied as well. All results were normalized to the area of epitbelial basal lamina.

The major finding was that exposure to 0.5 or 1.0 ppm ozone caused significant effects in the proximal alveolar region and in the terminal bronchioles. Changes in tbe proximal alveolar region after exposure to 0.5 or 1.0 ppm ozone consisted of epithelial metaplasia, with replacement of squamous (type I) alveolar epithelial cell types by a cuboidal (type II) broncbiolar epithelium, and a thickening of the interstitium due to increases in both cells and extracellular matrix components. Where acinar epithelium remained, squamous cells were smaller, thicker, and more numerous tban in rat lungs from the control group. In the terminal bronchioles after exposure to 1.0 ppm ozone, decreases in cilia and in the volume and number of ciliated cells were noted, with a proportional increase in Clara cells. The number of alveolar macrophages examined also increased at this exposure level. In contrast, no significant changes in any of these parameters were seen in randomly selected alveolar regions. No morphometric effects of exposure to 0.12 ppm ozone were observed in the proximal alveolar region or the terminal bronchioles, and no consistent gender differences were noted in tissue response. These results are important in that they indicate no effect of a 20-month exposure to 0.12 ppm ozone in these lung locations in the animals from this Project. They also add to the database of information that suggests consistent dose-related effects on the centriacinar region during prolonged exposure to ozone concentrations of 0.5 ppm and higher.

THE PINKERTON STUDY

Study Objectives

The overall objective of Dr. Pinkerton's study was to define quantitatively, using morphometric and enzymatic techniques, the structural and biochemical alterations caused by exposure to ozone in target and nontarget sites of the tracheobronchial tree and pulmonary acini in F344/N rat lungs. The specific aims were to:

- to measure changes in cell type and cell volume, and the abundance of secretory product in epithelial cell populations of target and nontarget airway generations of the tracheobronchial tree;
- to describe the architectural remodeling of pulmonary acini and the changes in epithelial, interstitial, and vascular compartments of alveolar septa as a function of distance from the bronchiole–alveolar duct junction; and
- to measure changes in antioxidant enzyme activity levels for superoxide dismutase, glutathione S–transferase, and glutathione peroxidase within selected airway generations.

The specific techniques used to attain these goals were measuring site-specific changes in epithelial cell populations, antioxidant enzyme activities, and intracellular secretory inclusions. Cell type and density were measured in the trachea, bronchus, and terminal bronchiole. Changes in the alveolar septal compartments also were quantified.

The investigators performed their experiments with great precision, being careful and meticulous in their measurement of a large number of parameters. Their study is excellent in that the dosimetry data derived from laboratory research contribute significantly to risk assessment issues. As will he discussed later, however, problems in analyzing the data on the architectural remodeling of pulmonary acini as a function of distance from the bronchiole–alveolar duct junction limit the ability to interpret the results of this study.

Study Design and Methods

The study design is described in detail in the Methods section of the Investigators' Report. Lungs for the morphometric studies were fixed by instillation of fixative, and samples were microdissected in a standardized manner to obtain tissue from identical sites in each animal. The sites studied were the distal trachea, three bronchi from long (caudal) and short (cranial) pathways, and terminal airway alveolar duct units from a short and a long pathway. Activities of three antioxidant enzymes were measured on samples microdissected from similar sites using lungs instilled with agarose. The enzymes studied were superoxide dismutase, glutathione peroxidase, and glutathione S–transferase. Enzyme activities were normalized to lung DNA content.

The dissection method developed by this group of investigators is a particular strength of the study. It permits histologic and biochemical sampling of structures down to the acinar level with knowledge of the complete pathway traversed by the gases that reached them. Hence, they could evaluate the tissue response in terms of the microdosimetry of ozone within specific regions of the lung. By overlaying sections of lung from along the longitudinal axis of alveolar ducts with a series of concentric circles centered on the terminal bronchiole, they were able to map morphologic changes along the alveolar duct and analyze the changes in terms of a model of microdosimetry.

The lung structural changes resulting from ozone exposure were documented in three sections of the Investigators' Report. The first section analyzed the cellular and secretory product changes in the tracheobronchial airways. The second section described the architectural remodeling of pulmonary acini and correlated this remodeling with the distance down the alveolar duct from the bronchiole–alveolar duct junction. The third section presented changes in antioxidant enzyme activity levels within subcompartments of airways. The major findings of the three sections were presented and interpreted in a final summary.

Statistical Methods

As with Dr. Chang's study, statistical comparisons were performed using a similarly sophisticated, multiple-stage, "step-down" analysis. Dr. Pinkerton and colleagues identified primary variables that were analyzed at the multivariate level followed by analysis at the univariate level if significance was found at the multivariate level. However, although this strategy was rigorously followed for the data presented in the first and third sections of the Investigators' Report, for the data reported in the second section of the Report on the architectural modeling of the pulmonary acini, it was used only to analyze the mathematical model.

The statistical analyses of the airway data, the ozone dosimetry model, and the antioxidant enzyme activities all were appropriately conducted. However, the statistical analysis of the data on the architectural remodeling of pulmonary acini does not match the complexity and sophistication of the study design. In performing this analysis, the investigators departed from their multiple-stage analysis.

The investigators' departure from their statistical plan accounts, in large part, for the difficulties in interpreting the remodeling data. Bronchiolarization in the centriacinar region was measured using several approaches, and a large amount of biological data was collected. However, most of it was not statistically analyzed. Only the small portion of the data used to generate the mathematical model was statistically analyzed. Unfortunately, examining of all of the results in this second section leads to the conclusion that the changes seen are not consistent in magnitude or site, particularly at the exposure level of 0.12 ppm ozone. Because no statistical testing was done on the large amount of biological data presented, one is left with only a qualita-

tive impression of the changes seen. As a consequence, the results of these remodeling experiments are not as powerful as they could be.

Results and Interpretation

As presented in the first section of the Investigators' Report, the main findings of Dr. Pinkerton's study on airway structure were a decrease in material positively stained with Alcian blue/periodic acid–Schiff in the distal trachea after exposure to 1.0 ppm ozone, and an increase in the amount of this material in the cranial and caudal bronchi at tbe same ozone concentration. Epithelial composition was unchanged in the trachea and bronchi; but the nonciliated epitbelial cell volume density was increased in the caudal terminal bronchioles at the exposure level of 1.0 ppm ozone.

The effect of ozone exposure on antioxidant enzyme activities in specific lung subcompartments was reported in the third section of Dr. Pinkerton's report. Superoxide dismutase activity increased in the trachea by exposure to all concentrations of ozone. Glutathione peroxidase activitiy increased in the minor daughter bronchi and decreased in the major daughter bronchi. In the distal bronchiole–centriacinar region, both superoxide dismutase and glutathione peroxidase showed increased activities at all ozone exposures. When whole-lung tissue was analyzed, different exposure groups did not show any consistent effects in enzyme activities.

The elegant dissection techniques used by Dr. Pinkerton and his colleagues, enabled them to measure antioxidant enzyme activities in lung subcompartments. They demonstrated that the largest changes occurred in the centriacinar region, the area most affected by ozone exposure, thereby adding significantly to our knowledge of the effect of ozone on these enzymes. These changes in antioxidant enzyme activities, along with the morphologic changes seen in the centriacinar region, are consistent with the idea that prolonged ozone exposure induces replacement of the normal epithelium with epithelial cells having greater antioxidant potential.

Difficulties arise when Dr. Pinkerton and his associates discuss their measurements of bronchiolarization as a function of distance down the alveolar duct in the second section of their report. In agreement with the findings of Dr. Chang and her colleagues, these investigators observed bronchiolarization of the alveolar ducts in rats exposed to 0.5 or 1.0 ppm ozone. In contrast to Dr. Chang's findings, they also reported statistically significant increases in bronchiolarization at the exposure level of 0.12 ppm ozone. These differences were found in areas close to the bronchiole–alveolar duct junction, an area not examined by Dr. Chang and her colleagues. As described above, the regions closer to the bronchiole–alveolar duct junction appear to be more sensitive to ozone exposure than other areas of the lung (Miller et al. 1985; Overton and Graham 1989; Grotberg et al. 1990).

The interpretation of these observations, particularly at the exposure level of 0.12 ppm ozone, is complicated by three issues. First, the conclusion that this level of ozone exposure had an effect on bronchiolarization in alveolar ducts was based on a mathematical model fitted to only a small subset of the data (specifically, epithelial cell density). This model revealed statistically significant increases in epithelial cell density in alveolar ducts from only the cranial region of the lungs of male rats at all levels of ozone exposure. In female rats, a significant difference also was observed in the cranial region, but only at the concentration of 1.0 ppm ozone. Furthermore, the statistically significant effect seen in the cranial region of male rats exposed to 0.12 ppm ozone appears to be influenced by aberrantly high epithelial cell volume density values within the first 200 μm down the alveolar duct in control animals (see Figure 25 in the Investigators' Report). For this first 200 μm of the alveolar duct in the cranial region of male rats, epithelial cell volume density and, therefore, bronchiolarization was greater in the unexposed control group than in the same 200 μm of the cranial alveolar ducts of male rats exposed to ozone (in the lower left panel of Figure 25, compare the data point for 0.0 ppm ozone with the other data points for the first 200 μm). In addition, these values for the cranial region in unexposed male rats were almost twice as high as the control values in the corresponding area for the caudal region in male rats and both the cranial and caudal regions in female rats (compare the control values for the first 200 μm of the alveolar duct in the lower left panel of Figure 25 witb the corresponding control values in the other three panels). These comparisons suggest that the high control values for the first 200 μm of the alveolar duct in the cranial region of male rats may be outliers; however, the investigators did not explore this possibility by applying an appropriate outlier test to the data.

Second, according to the investigator's mathematical model, effects were seen in the alveolar ducts in the cranial, but not the caudal, region of male rats exposed to 0.12 ppm ozone; however effects on nonciliated epithelial cell volume in the terminal bronchioles were seen in the caudal, but not the cranial, region in both genders at 1.0 ppm ozone and only in males at 0.12 ppm ozone. The variability in responses to 0.12 ppm ozone on the basis of site and gender leads one to question the consistency of the effect of ozone at 0.12 ppm.

Third, Dr. Pinkerton and colleagues collected a wealth of biological data for the bronchiolarization endpoints that was not used in their mathematical model or examined

statistically (see Figures 19 through 21 and 26 in the Investigators' Report). A qualitative examination of these data leaves one with the impression that the findings provide weak support for the conclusion that bronchiolarization occurred at the exposure level of 0.12 ppm ozone.

Because of these statistical issues, and the fact that small changes that were inconsistent in location were seen in only a small set of animals, the biological validity of the effects observed at the exposure level of 0.12 ppm ozone is equivocal. In fact, taking into account the multiple testing done on this small set of animals further reduces the likelihood of statistical significance for these results.

INTERPRETATION OF THE COMBINED STUDIES

The major difference between the results of these two studies and those published previously is that the structural changes were less pronounced in the F344/N rats from these studies. For example, although Chang and colleagues did not observe morphologic changes at the level of 0.12 ppm ozone in their study, in earlier studies they had seen definite structural effects in rats at low ozone concentrations (maximum concentration 0.25 ppm, integrated concentration 0.19 ppm) in a protocol for five days per week, with a nine-hour "ramped spike" exposure to ozone (Chang et al. 1992). Also, inflammatory responses have been reported in the centriacinar region of rats exposed to 0.5 ppm ozone for 90 days (Boorman et al. 1980) or 52 weeks (Gross and White 1987). Even at the highest ozone exposure concentrations in the NTP/HEI Collaborative Ozone Project, no signs of inflammation in the lungs of the F344/N rats were identified.

It is possible that the extended exposure period in the NTP/HEI Project allowed sufficient time for adaptation to occur; thus, the ozone-induced structural changes may have been present at 3 or 12 months, but not evident at 20 months. Also, some changes induced by ozone may have regressed during the one-week recovery period. In addition, the animal husbandry conditions may have been an influencing factor. The rats used in the NTP/HEI Project were bred in optimally clean facilities and housed under barrier conditions to eliminate potential pathogens that might affect the study results. In effect, the rats in this Project may have been healthy animals that were consequently more resistant to ozone exposure.

The latter observation could be important in evaluating the human health effects of ozone. It is not at all certain that the type of structural changes observed in rats in the NTP/HEI Collaborative Ozone Project would be severe enough to cause clinically significant disease or to have pathological effects on lung function in healthy humans. However, it is possible that ozone-induced changes may be enough to cause impaired function in humans compromised by other accumulated insults to their lungs.

Clearly, the implications of the results of these studies for human health must be evaluated with caution. Although the investigators have been careful in interpreting their data because the changes they observed were small, their discussion of the structural effects being fibrotic in nature must be assessed cautiously. In fact, profound differences are to be noted between the subtle changes caused by ozone in a limited area of the rat pulmonary acinus and the clinical factors presented in the disease of human idiopathic pulmonary fibrosis. The human clinical condition most characteristic of the changes observed in these studies is respiratory bronchiolitis. This condition is a clinically insignificant, mild lesion arising in response to chronic lung injury that has an uncertain role in for the genesis of chronic lung disease.

IMPLICATIONS FOR FUTURE RESEARCH

Several additional avenues of research suggest themselves as a result of these two studies. First, the possibility of an effect of exposure to 0.12 ppm ozone needs further investigation. Second, further studies that evaluate the permanence of the structural changes by including a period of recovery from ozone exposure are important. Third, investigations of lung clearance and the generation of protective mechanisms would further our understanding of these results.

CONCLUSIONS

After 20 months of exposure to ozone, the centriacinar region of the F344/N rat lung showed the most changes. The extensive architectural remodeling of this region included structural and cytochemical changes in epithelial cells, and increases in interstitial matrix components in rats exposed to 0.5 or 1.0 ppm ozone. Bronchiolarization occurred in the alveolar duct area. Whether this process also occurred at 0.12 ppm ozone is unclear. Dr. Chang and colleagues did not observe any structural alterations in the proximal alveolar region. In a study that included a sampling strategy that allowed systematic investigation of the regions closest to the junction of the terminal bronchiole and the alveolar duct, Dr. Pinkerton and colleagues found some indication

of small changes in the epithelial cells. However, because the effect of exposure to 0.12 ppm ozone was small, inconsistent in terms of site and gender, and of uncertain statistical significance, the effects of this ozone concentration on the structure of the centriacinar region require further study.

Overall, the structural changes observed indicate that, in sites sensitive to ozone exposure, sensitive cell types are replaced with more resistant ones, and changes in antioxidant enzyme activities occur in these same locations. In general, the results of the structural studies agree with earlier observations of the effects of prolonged exposure to ozone on the structure of the small airways of laboratory animals (Fujinaka et al. 1985; Barr et al. 1988; Chang et al. 1992). Specifically, the progressive epithelial and interstitial tissue responses observed, which included epithelial hyperplasia, bronchiolarization of alveolar ductal epithelium, and the accumulation of interstitial matrix constituents, are consistent with previous observations of prolonged exposure to ozone.

Both studies generated a large amount of morphometric information on the structure of rat lungs exposed to ozone. In isolation, the structural changes and the bronchiolarization of ductal epithelium are important observations of the effects of ozone exposure. These results take on more importance when viewed in light of the largely negative results obtained by Drs. Harkema and Mauderly in their study of pulmonary function (HEI Research Report Number 65, Part V). When taken together, these three studies lead to the important conclusion that structural changes induced by ozone occur without correlates detectable by tests of overall lung function.

The lack of functional correlates to lung structural changes is an important observation that agrees with the widely held view that the terminal airways are a relatively silent zone in terms of clinical physiology. The absence of functional changes that correlate with the morphologic changes suggests that the methods of physiological testing are not sensitive enough to detect these morphologic changes. If more sensitive tests of lung function are necessary to demonstrate abnormal function in these rats, it is doubtful that the abnormalities have relevance to lung disease unless they can be shown to be early manifestations of a progressive process. In themselves, such minor physiological abnormalities would not be expected to produce lung disease.

ACKNOWLEDGMENTS

The Health Review Committee wishes to thank the ad hoc reviewers for their help in evaluating the scientific merit of the Investigators' Reports, and is grateful to Drs. Charles Kuhn and Chester Bisbee for assistance in preparing its Commentary. The Committee also acknowledges Virgi Hepner for overseeing the publication of this report, as well as Diane Foster, Valerie Carr, Malti Sharma, and Mary Stilwell for their editorial and administrative support.

REFERENCES

Barr BC, Hyde DM, Plopper CG, Dungworth DL. 1988. Distal airways remodeling in rats chronically exposed to ozone. Am Rev Respir Dis 137:924–938.

Barry BE, Mercer RR, Miller FJ, Crapo JD. 1988. Effects of inhalation of 0.25 ppm ozone on the terminal bronchioles of juvenile and adult rats. Exp Lung Res 14:225–245.

Barry BE, Miller FJ, Crapo JD. 1983. Alveolar epithelial injury caused by inhalation of 0.25 ppm of ozone. In: International Symposium on the Biomedical Effects of Ozone and Related Photochemical Oxidants (Lee SD, Mustafa MG, Mehlman MA, eds.) pp. 299-309. Princeton Scientific Publishers, Princeton, NJ.

Barry BE, Miller FJ, Crapo JD. 1985. Effects of inhalation of 0.12 and 0.25 parts per million ozone on the proximal alveolar region of juvenile and adult rats. Lab Invest 53:692–704.

Bates DV. 1989. Ozone: Myth and reality. Environ Res 50:230–237.

Boorman GA, Catalano PJ, Jacobson BJ, Kaden DA, Mellick PW, Nauss KM, Ryan LM. 1995. Consequences of Prolonged Inhalation of Ozone on F344/N Rats: Collaborative Studies, Part VI, Background and Study Design. Research Report Number 65. Health Effects Institute, Cambridge, MA.

Boorman GA, Schwartz LW, Dungworth DL. 1980. Pulmonary effects of prolonged ozone insult in rats: Morphometric evaluation of the central acinus. Lab Invest 43:108–115.

Castleman WL, Dungworth DL, Schwartz LW, Tyler WS. 1980. Acute respiratory bronchiolitis: An ultrastructural and autoradiographic study of epithelial cell injury and renewal in rhesus monkeys exposed to ozone. Am J Pathol 98:811–840.

Chang L-Y, Huang Y, Stockstill BL, Graham JA, Grose EC, Ménache MG, Miller FJ, Costa DL, Crapo JD. 1992. Epithelial injury and interstitial fibrosis in the proximal alveolar regions of rats chronically exposed to a simulated pattern of urban ambient ozone. Toxicol Appl Pharmacol 115:241–252.

Clark K, Posin C, Buckley R. 1978. Biochemical response of squirrel monkeys to ozone. J Toxicol Environ Health 4:741–753.

Crapo JD, Barry BE, Chang L-Y, Mercer RR. 1984. Alteration in lung structure caused by inhalation of oxidants. J Toxicol Environ Health 13:301–321.

Cruz-Orive LM, Weibel ER. 1990. Recent stereological methods for cell biology: A brief survey. Am J Physiol 258:L148–L156.

Dimitriadis VK. 1993. Tracheal epithelium of bonnet monkey (*Macaca radiaca*) and response to ambient levels of ozone: A cytochemical study. J Submicrosc Cytol Pathol 25:53–61.

Elsayed NM, Kass R, Mustafa MG, Hacker AD, Ospital JJ, Chow CK, Cross CE. 1988. Effect of dietary vitamin E level on the biochemical response of rat lung to ozone inhalation. Drug Nutr Interact 5:373–386.

Fujinaka LE, Hyde DM, Plopper CG, Tyler WS, Dungworth DL, Lollini LO. 1985. Respiratory bronchiolitis following long-term ozone exposure in bonnet monkeys: A morphometric study. Exp Lung Res 8:167–190.

Grose EC, Stevens MA, Hatch GE, Jaskot RH, Selgrade MJK, Stead AG, Costa DL, Graham JA. 1989. The impact of a 12-month exposure to a diurnal pattern of ozone on pulmonary function, antioxidant biochemistry and immunology. In: Atmospheric Ozone Research and Its Policy Implications (Schneider T, Lee SD, Wolters GJR, Grant LD, eds.) pp. 535–544. Elsevier Science Publishing Co., New York, NY.

Gross KB, White HJ. 1987. Functional and pathological consequences of a 52-week exposure to 0.5 ppm ozone followed by a clean air recovery period. Lung 165:283–295.

Grotberg JB, Sheth BV, Mockros LF. 1990. An analysis of pollutant gas transport and absorption in pulmonary airways. J Biomed Eng 112:168–176.

Haefeli-Bleurer B, Weibel ER. 1988. Morphometry of the human pulmonary acinus. Anat Rec 220:401–414.

Heng H, Rucker RB, Crotty J, Dubick MA. 1987. The effects of ozone on lung, heart, and liver superoxide dismutase and glutathione peroxidase activities in the protein-deficient rat. Toxicol Lett 38:225–237.

Ichinose T, Sagai, M. 1989. Biochemical effects of combined gases of nitrogen dioxide and ozone: III. Synergistic effects on lipid peroxidation and antioxidative protective systems in the lungs of rats and guinea pigs. Toxicology 59:259–270.

Last JA, Gerriets JE, Hyde DM. 1983. Synergistic effects on rat lungs of mixtures of oxidant air pollutant (ozone or nitrogen dioxide) and respirable aerosols. Am Rev Respir Dis 128:539–544.

Lippmann M. 1989. Health effects of ozone: A critical review. J Air Pollut Control Assoc 39:672–695.

Lippmann M. 1992. Ozone. In: Environmental Toxicants: Human Exposures and Their Health Effects (Lippmann M, ed) pp. 465–519. Van Nostrand Reinhold, New York, N.Y.

Lippmann M. 1993. Health effects of tropospheric ozone: Review of recent research findings and their implications to ambient air quality standards. J Expos Anal Environ Epidemiol 3:103–129.

Mariassy AT. 1992. Epithelial cells of trachea and bronchi. In: Comparative Biology of the Normal Lung (Parent RA, ed.) pp. 63–76. CRC Press, Boca Raton, FL.

Mellick PW, Dungworth DL, Schwartz LW, Tyler WS. 1977. Short term morphologic effects of high ambient levels of ozone on the lungs of rhesus monkeys. Lab Invest 36:82–90.

Miller FJ, Overton JH Jr, Jaskot RH, Manzel DB. 1985. A model of the regional uptake of gaseous pollutants in the lung: I. The sensitivity of the uptake of ozone in the human to lower respiratory tract secretions and exercise. Toxicol Appl Pharmacol 79:11–27.

Moore PF, Schwartz LW. 1981. morphologic effects of prolonged exposure to ozone and sulfnric acid aerosol on the rat lung. Exp Mol Pathol 35:108–123.

Nikula KJ, Wilson DW, Giri S, Plopper CG, Dungworth DL. 1988. The response of rat tracheal epithelium to ozone exposure: Injury, adaptation, and repair. Am J Pathol 131:373–384.

Overton JH, Graham RC. 1989. Prediction of ozone absorption in humans from newborn to adult. Health Phys (Suppl 1) 57:29–36

Plopper CG. 1983. Comparative morphologic features of bronchiolar epithelial cells: The Clara cell. Am Rev Respir Dis 128:S37–S42.

Plopper CG, Dungworth DL, Tyler WS, Chow CK. 1979. Pulmonary alterations in rats exposed to 0.2 and 0.1 ppm ozone: A correlated morphologic and biochemical study. Arch Environ Health 34:390–395.

Plopper C, Chu F, Haselton C, Pinkerton K. 1993. Tolerance to ozone injury: Tracheobronchial epithelial reorganization in rats after 20-months exposure. Am Rev Respir Dis 147:A391.

Rietjens IU, van Bree L, Marra M, Poelen MCM, Rombout PJA, Alink GM. 1985. Glutathione pathway enzyme activities and the ozone sensitivity of lung cell populations derived from ozone exposed rats. Toxicology 37:205–214.

Rombout PJA, Lioy PJ, Goldstein BD. 1986. Rationale for an eight-hour ozone standard. J Air Pollut Control Assoc 36:913–917.

Sagai M, Ichinose T. 1991. Biochemical effects of combined gases of nitrogen dioxide and ozone: IV. Changes of lipid peroxidation and antioxidative protective systems in rat lungs upon life span exposure. Toxicology 66:121–132.

Schwartz LW, Dungworth DL, Mustafa MG, Tarkington BK, Tyler WS. 1976. Pulmonary responses of rats to ambient levels of ozone: Effects of 7-day intermittent or continuous exposure. Lab Invest 34:565–578.

Spektor DM, Lippmann M, Lioy PJ, Thurston GD, Citak K, James DJ, Bock N, Speizer FE, Hayes C. 1988. Effects of ambient ozone on respiratory function in active, normal children. Am Rev Respir Dis 137:313–320.

Stephens RJ, Sloan MF, Evans MJ, Freeman G. 1974. Early response of lung to low levels of ozone. Am J Pathol 74:31–58.

Tyler WS. 1983. Comparative subgross anatomy of lungs: Pleuras, interlobular septa, and distal airways. Am Rev Respir Dis 128:S32–S36.

Tyler WS, Julian MD. 1991. Gross and subgross anatomy of lungs, pleura, connective tissue septa, distal airways, and structural units. In: Comparative Biology of Normal Lung, Vol 1; Treatise on Pulmonary Toxicology (Parent RA, ed.) pp.37–48. CRC Press, Boca Raton, FL.

Tyler WS, Tyler NK, Last JA, Gillespie MJ, Barstow TJ. 1988. Comparison of daily and seasonal exposures of young monkeys to ozone. Toxicology 50:131–144

U.S. Environmental Protection Agency. 1986. Air Quality Criteria for Ozone and Other Photochemical Oxidants, Vol. I and II. EPA-600/8-84-02aF and EPA 600/8-84-02bF. Environmental Criteria and Assessment Office, Research Triangle Park, NC.

U.S. Environmental Protection Agency. 1988. Review of the National Air Quality Standards for Ozone: Assessment of Scientific and Technical Information. OAQPS draft staff paper. Office of Air Quality Planning and Standards, Research Triangle Park, NC.

U.S. Environmental Protection Agency. 1991a. EPA Aerometric Information Retrieval System: Air Quality Subsystem. National Air Data Branch, Research Triangle Park, NC.

U.S. Environmental Protection Agency. 1991b. National Air Quality and Emissions Trends Report, 1990. EPA 450/4-91-003. Office of Air Quality Planning and Standards, Research Triangle Park, NC.

U.S. Environmental Protection Agency. 1993. National Air Quality and Emissions Trends Report, 1992. EPA 454-R-93-031. Office of Air Quality Planning and Standards, Research Triangle Park, NC.

van Bree L, Lioy PJ, Rombout PJA, Lippmann M. 1990. A more stringent and longer-term standard for tropospheric ozone: Emerging new data on health effects and potential exposure. Toxicol Appl Pharmacol 103:377–382.

van Bree L, Marra M, Rombout PJA. 1992. Differences in pulmonary biochemical and inflammatory responses of rats and guinea pigs resulting from daytime or nighttime, single and repeated exposure to ozone. Toxicol Appl Pharmacol 116:209–216.

Weibel ER. 1963. Morphometry of the Human Lung. Academic Press, Orlando, FL.

Weibel ER. 1983. Is the lung built reasonably? The 1983 J. Burns Amberson lecture. Am Rev Respir Dis 128:752–760.

Report No.	Title	Principal Investigator	Publication Date
Toxicity and Carcinogenesis			
Research Reports			
1	Estimation of Risk of Glucose 6-Phosphate Dehydrogenase-Deficient Red Cells to Ozone and Nitrogen Dioxide	M. Amoruso	1985
6	Effect of Nitrogen Dioxide, Ozone, and Peroxyacetyl Nitrate on Metabolic and Pulmonary Function	D. M. Drechsler-Parks	1987
11	Effects of Ozone and Nitrogen Dioxide on Human Lung Proteinase Inhibitors	D.A. Johnson	1987
14	The Effects of Ozone and Nitrogen Dioxide on Lung Function in Healthy and Asthmatic Adolescents	J.Q. Koenig	1988
22	Detection of Paracrine Factors in Oxidant Lung Injury	A.K. Tanswell	1989
37	Oxidant Effects on Rat and Human Lung Proteinase Inhibitors	D.A. Johnson	1990
38	Synergistic Effects of Air Pollutants: Ozone Plus a Respirable Aerosol	J.A. Last	1991
44	Leukocyte-Mediated Epithelial Injury in Ozone-Exposed Rat Lung	K. Donaldson	1991
45	The Effects of Exercise on Dose and Dose Distribution of Inhaled Automotive Pollutants	M.T. Kleinman	1991
48	Effects of Ozone on Airway Epithelial Permeability and Ion Transport	P.A. Bromberg	1991
50	The Role of Ozone in Tracheal Cell Transformation	D.G. Thomassen	1992
54	Oxidant Injury to the Alveolar Epithelium: Biochemical and Pharmacologic Studies	B.A. Freeman	1993
60	Failure of Ozone and Nitrogen Dioxide to Enhance Lung Tumor Development in Hamsters	H. Witschi	1993
65	Consequences of Prolonged Inhalation of Ozone on F344/N Rats: Collaborative Studies		
	Part I: Content and Cross-Linking of Lung Collagen	J.A. Last	1994
	Part II: Mechanical Properties, Responses to Bronchoactive Stimuli, and Eicosanoid Release in Isolated Large and Small Airways	J.L. Szarek	1994
	Part III: Effects on Complex Carbohydrates of Lung Connective Tissue	B. Radhakrishnamurthy	1994
	Part IV: Effects on Expression of Extracellular Matrix Genes	W.C. Parks	1994
	Part V: Effects on Pulmonary Function	J.R. Harkema	1994
	Part VI: Background and Study Design	G.A. Boorman	1995
	Part VII: Effects on the Nasal Mucociliary Apparatus	J.R. Harkema	1994
	Part X: Robust Composite Scores Based on Median Polish Analysis	P.J. Catalano	1995
	Part XI: Integrative Summary	The Collaborative Ozone Project Group	1995
70	Oxidant and Acid Aerosol Exposure in Healthy Subjects and Subjects with Asthma		1994
	Part I: Effects of Oxidants, Combined with Sulfic or Nitric Acid, on the Pulmonary Function of Adolescents with Asthma	J.Q. Koenig	
	Part II: Effects of Sequential Sulfuric Acid and Ozone Exposures on the Pulmonary Function of Healthy Subjects and Subjects with Asthma	M.J. Utell	

(Continued on next page.)

Report No.	Title	Principal Investigator	Publication Date
HEI Communications Number 1			
	New Methods of Ozone Toxicology: Abstracts of Six Pilot Studies	L-Y.L. Chang R.A. Floyd W.C. Parks K.E. Pinkerton D.A. Uchida R. Vincent	1992

Development of Methods to Measure Exposure

Research Reports

39	Noninvasive Determination of Respiratory Ozone Absorption: Development of a Fast-Responding Ozone Analyzer	J.S. Ultman	1991
63	Development of Samplers for Measuring Human Exposure to Ozone		1994
	Active and Passive Ozone Samplers Based on a Reaction with a Binary Reagent	J. Hackney	
	A Passive Ozone Sampler Based on a Reaction with Nitrate	P. Koutrakis	
	A Passive Ozone Sampler Based on a Reaction with Iodine	Y. Yanagisawa	
69	Noninvasive Determination of Respiratory Ozone Absorption: The Bolus-Response Method	J.S. Ultman	1994

Environmental Epidemiology Planning Project

HEI Communications Number 3 1994

•	Introduction to Working Group on Tropospheric Ozone	I.B. Tager
•	Use of Human Lung Tissue for Studies of Structural Changes Associated with Chronic Ozone Exposure: Opportunities and Critical Issues	M. Lippmann
•	Examining Acute Health Outcomes Due to Ozone Exposure and Their Subsequent Relationship to Chronic Disease Outcomes	B.D. Ostro
•	Detection of Chronic Respiratory Bronchiolitis in Oxidant-Exposed Populations: Analogy to Tobacco Smoke Exposures	D. Bates
•	The Role of Ozone Exposure in the Epidemiology of Asthma	J.R. Balmes
•	Identification of Subpopulations That Are Sensitive to Ozone Exposure: Use of Endpoints Currently Available and Potential Use of Laboratory-Based Endpoints Under Development	R.B. Devlin
•	Design and Analysis of Studies of the Health Effects of Ozone	A. Muñoz
•	Summary of Papers and Research Recommendations of Working Group on Tropospheric Ozone	I.B. Tager

Copies of these reports can be obtained by writing or calling the Health Effects Institute, 141 Portland Street, Suite 7300, Cambridge, MA 02139. Phone (617) 621-0266. FAX (617) 621-0267. Request a Publications and Documents booklet for a complete listing of publications resulting from HEI-sponsored research.

HEI

The Board of Directors

Archibald Cox *Chairman*
Carl M. Loeb University Professor (Emeritus), Harvard Law School

William O. Baker
Chairman (Emeritus), Bell Laboratories

Douglas Costle
Chairman of the Board and Distinguished Senior Fellow, Institute for Sustainable Communities

Donald Kennedy
President (Emeritus) and Bing Professor of Biological Sciences, Stanford University

Walter A. Rosenblith
Institute Professor (Emeritus), Massachusetts Institute of Technology

Health Research Committee

Bernard Goldstein *Chairman*
Director, Environmental and Occupational Health Sciences Institute

Joseph D. Brain
Chairman, Department of Environmental Health, and Cecil K. and Philip Drinker Professor of Environmental Physiology, Harvard University School of Public Health

Glen R. Cass
Professor of Environmental Engineering and Mechanical Engineering, California Institute of Technology

Seymour J. Garte
Professor and Deputy Director, Department of Environmental Medicine, New York University Medical Center

Leon Gordis
Professor and Chairman, Department of Epidemiology, Johns Hopkins University, School of Hygiene and Public Health

Stephen S. Hecht
Director of Research, American Health Foundation

Meryl H. Karol
Professor of Environmental and Occupational Health, University of Pittsburgh, Graduate School of Public Health

Robert F. Sawyer
Class of 1935 Professor of Energy (Emeritus), University of California at Berkeley

Gerald van Belle
Chairman, Department of Environmental Health, School of Public Health and Community Medicine, University of Washington

Health Review Committee

Arthur Upton *Chairman*
Clinical Professor of Pathology, University of New Mexico School of Medicine

A. Sonia Buist
Professor of Medicine and Physiology, Oregon Health Sciences University

Ralph D'Agostino
Professor of Mathematics/Statistics and Public Health, Boston University

Gareth M. Green
Associate Dean for Education, Harvard School of Public Health

Donald J. Reed
Professor and Director, Environmental Health Sciences Center, Oregon State University

David J. Riley
Professor of Medicine, University of Medicine and Dentistry of New Jersey–Robert Wood Johnson Medical School

Herbert Rosenkranz
Chairman, Department of Environmental and Occupational Health, Graduate School of Public Health, University of Pittsburgh

Robert M. Senior
Dorothy R. and Hubert C. Moog Professor of Pulmonary Diseases in Medicine, Washington University School of Medicine

Frederick A. Beland *Special Consultant to the Committee*
Director for the Division of Biochemical Toxicology, National Center for Toxicological Research

Henry A. Feldman *Special Consultant to the Committee*
Senior Research Scientist, New England Research Institute

Edo D. Pellizzari *Special Consultant to the Committee*
Vice President for Analytical and Chemical Sciences, Research Triangle Institute

Officers and Staff

Daniel S. Greenbaum *President*
Richard M. Cooper *Corporate Secretary*
Kathleen M. Nauss *Director for Scientific Review and Evaluation*
Elizabeth J. Story *Director of Finance and Administration*
Jane Warren *Director of Research*
Maria G. Costantini *Senior Staff Scientist*
Chester A. Bisbee *Staff Scientist*
Aaron J. Cohen *Staff Scientist*
Bernard Jacobson *Staff Scientist*
Debra A. Kaden *Staff Scientist*
Martha E. Richmond *Staff Scientist*
Gail V. Allosso *Senior Administrative Assistant*
Valerie Anne Carr *Publications Production Coordinator*
L. Virgi Hepner *Managing Editor*
Teresina McGuire *Accounting Assistant*
Jacqueline C. Rutledge *Controller*
Malti Sharma *Publications Assistant*
Mary L. Stilwell *Administrative Assistant*
Stacy Synan *Administrative Assistant*
Susan J. Walsh *Receptionist*

HEI HEALTH EFFECTS INSTITUTE

141 Portland Street, Cambridge, MA 02139 (617) 621-0266

Research Report Number 65

March 1995